IRON AND THE INTESTINAL MICROBIOTA IN INFLAMMATORY BOWEL DISEASES

Melissa Ellermann

A dissertation submitted to the faculty of the University of North Carolina at Chapel Hill in partial fulfillment of the requirements for the degree of Doctor of Philosophy in the Department of Microbiology and Immunology.

Chapel Hill
2015

Approved by:

R. Balfour Sartor

Rita Tamayo.

John Rawls

Jonathan Hansen

Thomas Kawula

ABSTRACT

Melissa Ellermann: Iron and the intestinal microbiota in inflammatory bowel diseases
(Under the direction of R. Balfour Sartor)

Inflammatory bowel diseases (IBD) are chronic, immune-mediated disorders that are the result of inappropriate immune responses towards a subset of resident intestinal microbes in genetically susceptible individuals. Epidemiological studies have correlated dietary factors with increased risk for disease development, exacerbation and relapse in IBD patients. Iron is of particular interest because of the clinical concern of disease exacerbation upon oral iron supplementation in anemic IBD patients. Moreover, iron can selectively modulate the growth, physiology and function of numerous bacterial taxa, although the precise impact on specific resident intestinal bacteria remains largely unexplored. We therefore hypothesized that intestinal iron availability modulates the ecological structure and proinflammatory potential of the intestinal microbiota. To explore this hypothesis, we investigated how iron availability alters the composition of the intestinal microbiota and impacts the physiology and proinflammatory potential of adherent invasive *Escherichia coli* (AIEC), a distinct pathotype of enteric resident *E. coli* associated with IBD. In inflammation-resistant wild type mice, decreasing luminal iron concentrations during community assembly resulted in compositional changes consistent with a dysbiotic state, including a bloom in endogenous *E. coli*. Aggregation of the resident AIEC strain NC101, which is dependent on both cellulose production and iron availability, influenced subsequent interactions with macrophages. When monoassociated in germ free, inflammation-

susceptible interleukin-10-deficient (*Il10*$^{-/-}$) mice, abrogation of cellulose production in NC101 delayed onset of colitis, suggesting that cellulose may be a novel factor that enhances the proinflammatory potential of AIEC. Consistent with our *in vivo* observations, NC101 cellulose production corresponded with increased resistance against macrophage phagocytosis and enhanced macrophage proinflammatory responses when bacterial iron availability was restricted. When colonized with a complex microbiota, dietary iron supplementation also limited colitis development in *Il10*$^{-/-}$ mice. Taken together, these studies suggest that decreasing iron availability enhances the proinflammatory potential of the intestinal microbiota and highlight the complex interplay between host, microbial and environmental factors in the development of IBD.

To my parents, Maria and Siegfried

ACKNOWLEDGEMENTS

To my thesis advisor, Balfour Sartor, I am deeply grateful for the opportunity to complete my dissertation in your laboratory in an exciting area of research that has simply exploded throughout my time as a graduate student. I am also grateful for the freedom and independence to direct my own research and for your guidance in developing my translational focus towards biomedical research. It is through your mentorship that I feel truly prepared in embarking on the next chapter of my research career.

To the members of my thesis committee, I want to extend my heartfelt gratitude for your guidance and wisdom throughout my journey as a graduate student. Your diverse expertise has taught me to approach scientific problems and experimental design in novel and creative ways, to appreciate the importance of interdisciplinary research and has ultimately shaped me into a well-rounded scientist. To my thesis committee chair, Rita Tamayo, I am deeply grateful for your time and guidance with the microbiological aspects of my dissertation. Your mentorship has undoubtedly solidified my passion for microbiology – a passion I plan to follow through the next stages of my research career.

To Ian Carroll and Janelle Arthur, I cannot begin to express my appreciation and gratitude for your time and mentorship. You saw me as a successful scientist long before I even considered that a possibility and pushed me towards new opportunities that were met with successes when I initially resisted. You are the research scientists I hope to become one day - conducting exciting research that you are truly passionate about and spreading that passion to

others; showing resilience and perseverance in the face of challenges, both the expected and the unexpected, while also serving as compassionate and inspiring mentors for your trainees. I am incredibly fortunate to have been mentored by you both, and it is because of you that I continue my path towards a research career in academia.

To all my friends, I would not be where I am today without your unwavering support and encouragement. To Pharm Club – Ernesto Chanona-Pérez, Rebecca Bauer, Kimberly Maxfield, Tikvah Hayes and Kenton Woodward - I thank you all for your friendship throughout graduate school. You reminded me to have fun, to laugh and to develop new, non-science related passions (running!) when fear of failure could just have easily turned me into a hermit in the lab! To my seventh floor peeps – Erin Steinbach, Shehzad Sheikh, Ernesto Chanona-Pérez and Alexi Schoenborn – I am so grateful for your daily friendship and support that endures through this day. I know you all are going excel in whatever you do and your imminent successes have kept me motivated in striving for my own dreams. I hope that we continue to be friends and colleagues as we progress further in our careers! To my best friend and fellow art major, Merrilee Barton, I cannot begin to express in words how grateful I am for your ability to listen to my rants and fears when the obstacles in front of me seemed insurmountable and your earnest enthusiasm when I raved about my successes. I am incredibly grateful that our friendship remains as strong as ever as we both transition into new and exciting chapters in our lives.

TABLE OF CONTENTS

LIST OF FIGURES

LIST OF TABLES

LIST OF ABBREVIATIONS

AIEC, adherent invasive *Escherichia coli*

APC, antigen presenting cell

BMDM, bone marrow-derived macrophage

BPD, 2,2-bipyridyl

CEACAM6, carcinoembryonic antigen-related cell adhesion molecule 6

CD, Crohn's disease

CF, calcofluor

CFU, colony forming unit

DTPA, diethylene triamine pentaacetic acid

ECM, extracellular matrix

EHEC, enterohemorrhagic *Escherichia coli*

EIEC, enteroinvasive *Escherichia coli*

ELISA, enzyme-linked immunosorbent assay

EPEC, enteropathogenic *Escherichia coli*

ExPEC, extraintestinal pathogenic *Escherichia coli*

GF, germ free

GFP, green fluorescent protein

GI, gastrointestinal

IBD, inflammatory bowel disease

IEC, intestinal epithelial cell

IDA, iron deficiency anemia

IFN, interferon

Ig, immunoglobulin

IL, interleukin

IP, intraperitoneal

IV, intravenous

LP, lamina propria

LPS, lipopolysaccharide

MLN, mesenteric lymph node

MPO, myeloperoxidase

OD, optical density

OMP, outer membrane protein

OMV, outer membrane vesicle

OTU, operational taxonomic unit

PAMP, pathogen-associated molecular pattern

PRR, pattern recognition receptor

qPCR, quantitative polymerase chain reaction

RDAR, red dry and rough

ROS, reactive oxygen species

rRNA, ribosomal ribonucleic acid

SEM, standard error of the mean

SPF, specific pathogen free

Th, $CD4^+$ T helper cell

TLR, Toll-like receptor

TNBS, 2,4,6-trinitrobenzenesulfonic acid

TNF, tumor necrosis factor

UC, ulcerative colitis

UPEC, uropathogenic *Escherichia coli*

UTI, urinary tract infection

WT, wild type

CHAPTER 1

INTRODUCTION

1.1 Inflammatory bowel diseases

Inflammatory bowel diseases (IBD), including Crohn's disease (CD) and ulcerative colitis (UC), are characterized by chronic and relapsing intestinal inflammation that are the result of inappropriate immune responses to a subset of luminal bacteria and their products (Sartor, 2008). The development of IBD is complex, involving incompletely understood interactions between host genetics, the mucosal immune system, the intestinal microbiota and environmental factors. Approximately 1.2 million individuals in the United States have IBD (Kappelman et al., 2012), which corresponds with a heavy economic burden estimated at $6.3 billion annually (Kappelman et al., 2008). Current IBD therapies include immune suppression and surgical resections of inflamed tissues designed to induce remission. Nonetheless, many patients experience incomplete remission, reactivation of disease following initial response and adverse side effects from immunosuppressive drugs, thus necessitating the development of safer, more efficacious and longer lasting treatments.

1.1.1 Iron and IBD

Epidemiological studies have introduced the potential role of several dietary macronutrients as protective or risk factors in the development of IBD (Ananthakrishnan, 2015).

However, as these epidemiological studies have mainly focused on identifying links between dietary macromolecules and IBD, the potential role of dietary micronutrients in the pathogenesis of IBD remains poorly understood. Dietary iron is of particular clinical interest, given that iron homeostasis is often dysregulated in IBD patients and host iron status can impact immune function. Indeed, anemia is the most common extraintestinal complication within the IBD population that further reduces overall quality of life for many patients (Wells et al., 2006) (Gisbert et al., 2009). Iron deficiency is the most frequent cause of anemia and is estimated to affect 36-90% of IBD patients (Kulnigg and Gasche, 2006). Decreased dietary iron intake as a result of overall reduced appetite and exclusion of iron-rich foods as well as intestinal bleeding during periods of active disease and iron malabsorption in patients with proximal small bowel disease are all likely factors that contribute to iron deficiency anemia (IDA) in IBD (Hwang et al., 2012).

IDA is treated through oral or intravenous (IV) iron supplementation in order to replenish depleted iron stores and increase blood hemoglobin levels. Although both routes of iron administration are effective in increasing hemoglobin levels, oral iron supplementation is less expensive (Rizvi and Schoen, 2011) and can be administered at home and, as a result, is often the first choice of treatment (Hwang et al., 2012). However, oral iron supplementation is not as well tolerated; 5-25% of IBD patients receiving oral iron supplements report adverse side effects such as abdominal pain, diarrhea and constipation, resulting in discontinuation of treatment (de Silva et al., 2005) (Gisbert et al., 2009) (Lee et al., 2012) (Goodhand et al., 2011). Moreover, exacerbation of intestinal inflammation and disease activity have been observed with increased dietary iron consumption in numerous rodent models of experimental colitis (Kulnigg and Gasche, 2006) (Werner et al., 2011) (Chua et al., 2013), further raising concerns regarding the

safety of oral iron supplementation in IBD patients. Interestingly, in some non-IBD infant populations, dietary iron fortification increases diarrhea, intestinal pathogen burden and fecal calprotectin, a biomarker of intestinal inflammation (Zimmermann et al., 2010) (Jaeggi et al., 2014). However in an older population of children (6-11 years) with low initial enteropathogen burden, treatment of iron deficiency through oral iron supplementation was effective and was not associated with increased fecal calprotectin or diarrhea (Dostal et al., 2014a). These contrasting results suggest that other factors such as age, environment or the intestinal microbiota may influence the risk of adverse side effects such as enhanced intestinal inflammation in response to oral iron supplementation. Identifying host and microbial factors that promote iron-induced exacerbation of intestinal inflammation could enable the development of prognostic tools that predict which IBD patient subsets are at risk for disease relapse in response to oral iron supplementation. Ultimately, establishing more definitive and mechanistic links between dietary factors and intestinal inflammation that transcends correlative, epidemiological studies could enable the incorporation of dietary interventions as part of safe, efficacious and long-lasting treatment regimens for IBD.

1.2 Host iron homeostasis

1.2.1 Host iron requirements

Iron is an essential micronutrient for nearly all life forms, serving as a cofactor for numerous cellular proteins involved in diverse processes including DNA synthesis and repair, cellular respiration, biodegradation and biosynthetic pathways and transcriptional regulation (Evstatiev and Gasche, 2012). However, free iron can also participate in Fenton chemistry, a redox reaction that generates toxic reactive oxygen species (ROS) that can damage cellular

lipids, proteins and DNA. As a result, free intracellular iron is tightly regulated through various complex mechanisms both at a systemic and cellular level.

The human body contains about 3.5 g of stored iron, the majority of which is collectively located within erythrocytes (2.5 g), macrophages and monocytes (0.5 g) and hepatocytes (0.2 g) (Stein et al., 2010). Approximately 1-2 mg of iron is lost daily through sloughed off intestinal epithelial cells (IEC), hair loss and perspiration and is replenished through absorption of heme and non-heme iron from the diet (Stein et al., 2010). The remaining daily requirements for iron are met through the recycling of heme from senescent erythrocytes phagocytosed by macrophages of the reticuloendothelial system (Stein et al., 2010).

1.2.2 Regulation of host iron homeostasis

Dietary non-heme iron, either in the form of ferric or ferrous iron, is absorbed by enterocytes in the duodenum. Approximately 5-15% of dietary non-heme iron is absorbed, the bioavailability of which depends on numerous factors including other interacting dietary components, pharmaceuticals, inflammation and host iron status (Hurrell and Egli, 2010). Luminal ferric iron is reduced to ferrous iron by either gastric acid from the stomach or by the apically localized enzyme duodenal cytochrome B (DCYTB) and is subsequently transported into enterocytes via DMT1 (Stein et al., 2010). If systemic iron demands are low, iron binds to the intracellular protein ferritin and is eventually excreted when the enterocyte is sloughed off into the lumen. However, when systemic iron stores are depleted, ferrous iron is exported from the enterocyte via the basally located transporter ferroportin. Ferrous iron is then released into the bloodstream and oxidized by hephaestin before binding to the plasma iron binding protein transferrin (Anderson et al., 2009) (Stein et al., 2010). Once bound to transferrin, iron can be

transported throughout the body, where it can enter cells by binding to the ubiquitiously expressed transferrin receptor 1 (TFR1) (Stein et al., 2010).

The liver peptide hormone hepcidin plays a central role in regulating systemic iron homeostasis. When systemic iron stores are replete, iron-bound transferrin binds TFR1 on hepatocytes (Cherayil et al., 2011). This liberates high-Fe hemochromatosis protein (HFE), which then complexes with transferrin receptor 2 (TFR2) and stimulates an intracellular signaling cascade that results in enhanced transcription of *HAMP* encoding hepcidin (Knutson, 2010). The hormone hepcidin then binds ferroportin on enterocytes and induces its endocytosis (Nemeth et al., 2004b), thus preventing additional duodenal absorption of dietary iron. Hepcidin also regulates systemic iron levels by preventing export of ferrous iron from reticuloendothelial macrophages through a similar mechanism (Theurl et al., 2008). In contrast, when iron is limiting, production of hepcidin is reduced, enabling enhanced membrane localization of ferroportin in both enterocytes and macrophages and increased release of iron into systemic circulation (Cherayil et al., 2011).

1.2.3 Host iron homeostasis and inflammation

Infection and inflammatory processes are intricately linked with host iron homeostasis. Inflammatory mediators such as the proinflammatory cytokine IL-6 can stimulate hepatocyte production of hepcidin, thus perturbing host iron homeostasis by limiting dietary iron absorption and increasing intracellular retention of iron within the reticuloendothelial system (Nemeth et al., 2004a). Chronic production of hepcidin as a result of inflammation or infection can lead to a type of anemia known as anemia of inflammation, which is a frequent cause of anemia within the IBD population (Stein et al., 2010) (Bager et al., 2013). Other proinflammatory processes including

activation of Toll-like receptors (TLRs) by microbial ligands and endoplasmic reticulum (ER) stress have also been linked with increased hepcidin production (Drakesmith and Prentice, 2012). Interestingly, the intestinal microbiota also influences cellular iron homeostasis within enterocytes. In contrast to conventionally housed animals, germ free (GF) mice exhibit an altered profile of proteins involved in intestinal iron absorption and storage that is consistent with an iron deficient state (Deschemin et al., 2015).

Dysregulated iron homeostasis has been observed clinically in IBD patients and in numerous experimental models of colitis and ileitis. Development of intestinal inflammation is associated with increased liver hepcidin expression and decreased systemic iron stores in the TNFΔARE mouse model of ileitis and with *Salmonella*-induced colitis (Wang et al., 2009) (Schümann et al., 2010). Increased hepcidin has also been reported in a T-cell transfer model of colitis and in several chemically-induced models of colitis (Wang et al., 2009) (Wang et al., 2012) (Shanmugam et al., 2014). Reduction of liver hepcidin expression through pharmacological inhibition of BMP signaling results in decreased colonic expression of proinflammatory cytokines and less severe histopathology (Wang et al., 2009) (Wang et al., 2012). Moreover, proinflammatory cytokine production is decreased in iron-depleted macrophages cultured with *Salmonella enterica* serovar Typhimurium or challenged with lipopolysaccharide (LPS) (Wang et al., 2008) (Wang et al., 2009). Interestingly, clinical studies have also demonstrated a positive correlation between serum hepcidin levels and both serum markers of inflammation including IL-6 and C-reactive protein (CRP) and disease activity in IBD patients (Oustamanolakis et al., 2011) (Basseri et al., 2013) (Bergamaschi et al., 2013), although this has not been consistently observed (Mecklenburg et al., 2014). Taken together, intestinal inflammation can perturb host iron homeostasis through modulation of hepcidin

expression. Enhanced hepcidin production in turn promotes iron retention within reticuloendothelial cells such as macrophages and thus can modulate innate immune responses that may further impact the development of inflammation.

1.2.4. Dietary iron and inflammation

The impact of dietary iron supplementation on intestinal inflammation remains controversial, especially considering the inconsistent effects observed in animal models of experimental colitis. As only 5-15% of dietary non-heme iron is absorbed, it is no surprise that consumption of an iron-fortified diet increases total and free non-heme iron concentrations in the feces in a dose dependent manner (Lund et al., 1999) (Carrier et al., 2001). Increased dietary iron intake is also associated with enhanced fecal ROS production (Lund et al., 1999), likely through the participation of free iron in Fenton chemistry. Increased dietary iron and fecal ROS also promotes lipid peroxidation within colonic tissues, indicating a shift towards a more pro-oxidant environment within the colonic mucosa (Lund et al., 1999) (Lund et al., 2001). In models of chemically-induced colitis, increased dietary iron consumption results in more severe histopathology, proinflammatory cytokine production and disease activity that is also associated with increased oxidative stress within colonic tissues (Kulnigg and Gasche, 2006) (Chua et al., 2013). Consistent with these findings, administration of an oral iron chelator in rats fed a control diet ameliorates chemically-induced colitis and reduces colonic markers of oxidative stress (Ablin et al., 1999). Dietary iron restriction also limits the development of ileitis in the TNFΔARE mouse model and is associated with decreased ileal TNF-α production and reduced ER stress (Werner et al., 2011). Taken together, these studies support the hypothesis that increased luminal iron as a result of oral iron supplementation can exacerbate intestinal

inflammation, potentially by enhancing ROS production and consequent oxidative stress within the mucosal environment.

However, more recent studies have demonstrated that oral iron supplementation may also protect against the development of colitis. In one study, mice and rats that received daily oral boluses of ferric or ferrous iron for 6 weeks developed less severe inflammation and exhibited reduced colonic myeloperoxidase (MPO) activity when administered 2,4,6-trinitrobenzenesulfonic acid (TNBS) to induce colitis (Ettreiki, 2012). Dostal and colleagues also demonstrated a similar protective effect with dietary iron supplementation in GF rats colonized with a human microbiota in the absence of any chemical treatment to induce colitis (Dostal et al., 2014b). Interestingly, dietary iron restriction in these rats also resulted in reduced colonic and ileal histopathology. These findings suggest that iron may have a bimodal effect in modulating intestinal inflammation, thus potentially explaining the inconsistent findings observed in animal studies to date. Moreover, the impact of oral iron supplementation on intestinal inflammation may depend on dose, length and frequency of iron supplementation and the colitis model utilized, all of which vary between these different studies.

1.3 Intestinal microbiota

The gastrointestinal (GI) tract is home to a collection of microbial communities collectively known as the intestinal microbiota. At birth, the GI tract becomes rapidly colonized with microbes. Over the first two years of life, the intestinal microbiota increases in complexity and stability through ecological succession before maturation into an adult state (Koenig et al., 2011) (Subramanian et al., 2014). The bacterial phyla Firmicutes and Bacteroidetes comprise the majority of the normal adult enteric microbiota, with Actinobacteria, Proteobacteria and

Verrucomicrobia present in lesser abundance (Eckburg et al., 2005). At lower taxonomical levels, the composition of the intestinal microbiota exhibits high interindividual variability (Costello et al., 2009). Temporal variations in community composition also occur within an individual as a result of dietary changes and other environmental exposures (David et al., 2013) (Carmody et al., 2015). Finally, the biogeography of the intestines further influences community composition, where distinct microbial niches can be found at mucosal surfaces versus the lumen or proximally versus distally along the GI tract (Zoetendal et al., 2002) (Eckburg et al., 2005) (Zhang et al., 2014).

The intestinal microbiota, in symbiosis with the host, is integral to numerous host processes including immune system development and nutrient metabolism (Cummings and Macfarlane, 1997) (Chow et al., 2010). The intestinal microbiota is physically separated from the underlying mucosal immune system by a single layer of epithelial cells, a thick layer of mucus and host secretions including antimicrobial peptides and soluble IgA antibodies that collectively make up the intestinal barrier. The mucosal immune system is tasked with remaining tolerant of endogenous microbes while selectively responding to pathogens and other microbes that breach the intestinal barrier (Manichanh et al., 2012). Interestingly, select members of the intestinal microbiota promote tolerogenic responses by the mucosal immune system, including the production of anti-inflammatory cytokines and the induction of T-regulatory cells that dampen effector T-cell responses (Sokol et al., 2008) (Llopis et al., 2009) (Atarashi et al., 2011). Conversely, other resident intestinal bacteria promote the establishment of a more proinflammatory intestinal microenvironment (Llopis et al., 2009) (Eun et al., 2014). A bloom of resident bacteria that harbor greater proinflammatory capabilities can potentially promote dysfunctional immune responses and compromise the symbiotic relationship between the

intestinal microbiota and the host. Indeed, numerous chronic diseases including malnutrition, obesity and IBD correlate with such unfavorable compositional and functional changes to the intestinal microbiota (Turnbaugh et al., 2006) (Turnbaugh et al., 2008) (Morgan et al., 2012) (Subramanian et al., 2014) (Gevers et al., 2014), a state known as dysbiosis.

1.3.1 The intestinal microbiota in IBD

Dysregulated mucosal immune responses to luminal resident bacteria and their products are central to IBD pathogenesis. Indeed, several clinical studies have provided evidence for the involvement of resident intestinal microbes in either instigating or perpetuating intestinal inflammation in IBD patients. For example, diversion of the fecal stream in CD patients can promote mucosal healing and remission (D'Haens et al., 1998). Moreover, when exposed to microbial antigens, mucosal T-cells isolated from inflamed tissue segments in CD patients become activated, whereas mucosal T-cells from non-inflamed tissue segments from the same patient remain unresponsive (Pirzer et al., 1991).

The intestinal microbiome, which encompasses all resident microbes and their genes, is significantly altered in IBD patients relative to healthy controls. Community-wide ecological changes frequently observed in IBD patients include decreased microbial biodiversity and richness, decreased compositional stability and a bloom of Enterobacteriaceae family members such as *Escherichia coli* within the mucosa (Martinez et al., 2008) (Morgan et al., 2012) (Gevers et al., 2014). Even within the same individual, reduced microbial biodiversity was observed in inflamed regions of the intestines compared to uninvolved regions (Kostic et al., 2014), suggesting that active inflammatory processes may help drive these compositional changes. In contrast, increased Enterobactericeae abundance and decreased abundance of several families

within the Firmicutes was observed within the uninflamed ileum of colonic CD patients, suggesting that some compositional shifts to the microbiota occurring independently of local inflammation severity (Haberman et al., 2014). An expansion of *E. coli* has also been observed during the onset of intestinal inflammation in several experimental models of colitis (Lupp et al., 2007) (Winter et al., 2013) including the interleukin-10-deficient (*Il10*$^{-/-}$) mouse model (Arthur et al., 2012) and is dependent on the capability of *E. coli* to acquire and utilize nutrients uniquely available within the inflamed environment (Winter et al., 2013). However, as compositional changes to the intestinal microbiota are simply correlated with IBD status, it has been difficult to discern whether compositional changes observed in IBD patients precede or occur as a result of intestinal inflammation, and consequently, whether more abundant microbes in the inflamed environment instigate or perpetuate disease activity or serve as opportunistic bystanders.

1.3.2 The Il10$^{-/-}$ *mouse model of chronic, immune-mediated colitis*

IL-10 is a potent anti-inflammatory cytokine that limits both innate and adaptive immune responses and is therefore a key player in maintaining mucosal homeostasis. Mice deficient in IL-10 develop chronic intestinal inflammation characterized by mucosal and submucosal infiltration of immune cells and distortion of crypt architecture (Kühn et al., 1993) and is driven by effector T-helper-(Th)-1 and Th-17 immune responses (Davidson et al., 1996) (Yen et al., 2006). The central role of resident intestinal microbes in driving pathology in this animal model was demonstrated through the use of GF mice that are completely devoid of microbes (Sellon et al., 1998). In contrast to conventionally housed animals, *Il10*$^{-/-}$ mice raised in GF isolators remain free of inflammation as assessed by histology and subclinical markers, thus demonstrating the necessity of endogenous microbes in initiating and perpetuating disease in this

model (Sellon et al., 1998). Selective colonization of defined bacterial strains, known as gnotobiotics, has demonstrated that specific resident microbes uniquely exhibit the capacity to induce proinflammatory mucosal immune responses. For example, GF *Il10*$^{-/-}$ mice develop colitis when colonized with *E. coli* isolates belonging to a specific functional subset known as adherent invasive *E. coli* (AIEC) (Kim et al., 2005). In contrast, GF *Il10*$^{-/-}$ mice colonized with nonpathogenic intestinal *E. coli* strains do not exhibit pathology (Kim et al., 2008) (Schumann et al., 2013). GF *Il10*$^{-/-}$ mice also develop colitis when colonized with a defined consortium of seven bacterial species that include representatives from predominant phyla present within the human intestinal microbiota (Eun et al., 2014). Interestingly, unfractionated mesenteric lymph node (MLN) cells differentially secrete proinflammatory cytokines when restimulated *ex vivo* with cellular lysates from one of these seven bacteria (Eun et al., 2014). The highest production of the Th-1-associated cytokine interferon gamma (IFN-γ) was observed in response to *E. coli* lysates, whereas *Ruminococcus gnavus* lysates induced the greatest production of the Th-17-associated cytokine IL-17 (Eun et al., 2014). Importantly, GF WT mice do not develop histopathology or exhibit subclinical markers of colitis when colonized with AIEC or this defined consortium of bacteria (Kim et al., 2005) (Eun et al., 2014). Taken together, these studies highlight the differential capacity exhibited by resident intestinal bacterial strains in promoting proinflammatory mucosal immune responses within genetically susceptible hosts. Identifying the environmental and host factors that modulate the proinflammatory potential of specific resident bacteria could provide further mechanistic insight into how a state of dysbiosis is established and maintained. This could ultimately lead to the identification of novel anti-microbial targets that can be utilized to restore the symbiotic relationship between the intestinal microbiota and the host during disease states such as IBD.

1.3.3 Dietary iron and the intestinal microbiota

Both short- and long-term dietary patterns heavily influence the composition of the intestinal microbiota, likely by modulating nutrient availability, microbial metabolic activity and consequent microbial growth (Wu et al., 2011) (Muegge et al., 2011) (David et al., 2013) (Carmody et al., 2015). Iron is an important co-factor for numerous enzymes involved in microbial metabolism and biosynthetic pathways and thus serves as a growth limiting nutrient for many bacterial taxa (Andrews et al., 2003). In the intestinal environment, dietary iron likely serves as a predominant source of iron for resident bacteria, as only a fraction of dietary iron is absorbed in the duodenum. Host processes such as the cyclic shedding of ferritin-laden enterocytes during steady-state conditions and processes associated with inflammation may also modulate iron availability for the microbiota. For example, in chemically-induced models of colitis, luminal heme iron concentrations increase with inflammation, likely as a result of intestinal bleeding (Carrier et al., 2001) (Carrier et al., 2002). Moreover, in the inflamed intestinal environment, acceleration of epithelial cell turnover and decreased absorption of dietary iron as a result of inflammation-mediated upregulation of hepcidin may also increase luminal iron concentrations (Nemeth et al., 2004a). Conversely, host secretion of antimicrobial peptides such as lactoferrin and lipocalin-2 limit bacterial iron availability as part of the innate immune response (Flo et al., 2004) (Raffatellu et al., 2009) (Yen et al., 2011). Indeed, inflammation confers a fitness advantage to *Salmonella* and the probiotic strain *E. coli* Nissle that is in part due to their enhanced ability to scavenge iron from the host, an advantage that is lost in *lipocalin-2*-deficient (*Lcn2*$^{-/-}$) mice (Raffatellu et al., 2009) (Deriu et al., 2013). More broadly, resident bacteria within the intestinal community harbor differential capacities for

acquiring iron, which may consequently play a role in bacterial niche selection within the intestines. Taken together, although the precise bioavailability of iron for specific resident bacteria remains unclear, it is likely that dietary and host factors as well as the functional capacity of the microbiome collectively modulate microbial iron availability throughout the intestines.

Total non-heme iron in the feces can be dramatically reduced through dietary iron restriction and enhanced with dietary iron supplementation (Lund et al., 1999) (Carrier et al., 2001), which likely modulates luminal iron availability for resident bacteria. Indeed, numerous studies have demonstrated that altering dietary iron consumption results in compositional changes to the luminal microbiota in humans (Zimmermann et al., 2010) (Krebs et al., 2013) (Jaeggi et al., 2014) and in rodent models (Werner et al., 2011) (Dostal et al., 2012a) (Dostal et al., 2014b). Interestingly, dietary iron restriction results in similar compositional changes to the luminal microbiota observed with intestinal inflammation. Dietary iron restriction reduces the biodiversity and microbial richness of the fecal community (Dostal et al., 2012a) (Pereira et al., 2014), which was not fully recovered with subsequent dietary iron repletion (Pereira et al., 2014). Dietary iron restriction has also been associated with a bloom of Enterobacteriaceae in rodents (Dostal et al., 2012a) and in an *in vitro* colonic fermentation model in the absence of host-specific factors (Dostal et al., 2012b). Intriguingly, dietary iron repletion following a period of restriction reversed the bloom of Enterobacteriaceae (Dostal et al., 2012a), suggesting that dietary iron modulates the abundance of Enterobacteriaceae within the intestinal lumen. Similarly, decreased relative abundances of Enterobacteriaceae were observed in infants with low initial pathogen burden following administration of iron-fortified foods (Krebs et al., 2013). In contrast, iron supplementation in infants with high initial pathogen burden including

Salmonella and pathogenic *E. coli* resulted in an expansion of Enterobacteriaceae that correlated with increased fecal markers of intestinal inflammation (Jaeggi et al., 2014), suggesting that the compositional features of the existing microbiota influences the impact dietary iron has on microbial ecology within the intestines.

1.4 Adherent invasive *E. coli*

Adherent invasive *E. coli* (AIEC) are a functionally distinct group of resident intestinal *E. coli* clinically associated with CD. AIEC are recovered more frequently and in higher abundance from ileal and colonic biopsies from CD patients compared to non-CD controls (Darfeuille-Michaud et al., 2004) (Martin et al., 2004) (Sasaki et al., 2007) (Martinez-Medina et al., 2009a). Phylogenetic analyses have demonstrated that AIEC strains do not cluster within a unique clade, but rather cluster separately with other extraintestinal pathogenic *E. coli* (ExPEC) strains (Sepehri et al., 2009) (Dogan et al., 2014). Thus, in the absence of common identifying genetic markers or established invasive determinants, AIEC are currently distinguished through *in vitro* functional assays that demonstrate an enhanced ability to adhere to and invade intestinal epithelial cells and to survive and replicate within macrophages (Boudeau et al., 1999) (Glasser et al., 2001) (Darfeuille-Michaud et al., 2004) (Sasaki et al., 2007). Nonetheless, certain putative virulence genes and specific alleles of genes ubiquitously present in *E. coli* are over-represented in mucosally-associated *E. coli* strains recovered from IBD patients (Sepehri et al., 2009) (Iebba et al., 2012). Indeed, a recent report demonstrated that genes involved in propanediol utilization, iron acquisition and adhesion to host cells are over-represented in AIEC strains (Dogan et al., 2014). Interestingly, some of these genes and genetic polymorphisms in AIEC have been linked to the enhanced epithelial invasive capabilities and intramacrophagic survival characteristic of

these strains (Dreux et al., 2013) (Dogan et al., 2014). Thus, the identification of a common genetic signature shared by most AIEC strains may be forthcoming and could provide further insight into the molecular mechanisms that underlie the defining functional features of AIEC.

1.4.1 Interactions with IECs

The intestinal epithelium provides a physical barrier between luminal bacteria and the underlying mucosa immune system, thus limiting inappropriate immune stimulation. However, AIEC strains exhibit enhanced epithelial invasive capabilities that are comparable to enteroinvasive *E. coli* (EIEC) and enteropathogenic *E. coli* (EPEC) and that exceed those of other pathogenic and nonpathogenic *E. coli* strains (Boudeau et al., 1999). AIEC invasion of IECs occurs through macropinocytosis (Boudeau et al., 1999) and requires the expression of the type I pilus FimA and the associated FimH adhesin for maximal adherence and invasion (Boudeau et al., 2001). Interactions between type 1 pili and host-derived glycosylated receptor carcinoembryonic antigen-related cell adhesion molecule 6 (CEACAM6) mediate AIEC adhesion and invasion of IECs and its enhanced mucosal association (Barnich et al., 2007) (Denizot et al., 2011). CEACAM6 is also upregulated on the intestinal epithelium of CD patients (Barnich et al., 2007) (Denizot et al., 2011), which may further perpetuate unfavorable interactions between AIEC and the host. Interestingly, FimH alleles more frequently harbored by AIEC strains (Iebba et al., 2012) (Dreux et al., 2013) promote increased intestinal colonization and proinflammatory cytokine production in transgenic CEABAC10 mice expressing human CEACAMs (Dreux et al., 2013). Other AIEC factors have also been linked to enhanced adhesion or invasion of IECs, including flagella (Boudeau et al., 2001), several outer membrane proteins (Rolhion et al., 2007) (Rolhion et al., 2010), the chitinase ChiA (Low et al., 2013) and the

lipoprotein YfgL (Rolhion et al., 2005). Finally, expression of long polar fimbriae (Lpf) enable increased AIEC translocation across M-cells, a specialized IEC located adjacent to immune cell aggregates known as Peyer's patches, and consequently promote enhanced AIEC mucosal association (Chassaing et al., 2011).

1.4.2 Interactions with macrophages

Macrophages are central components of host immune defense in the intestines. Resident macrophages limit microbial stimulation of the mucosal immune system and systemic dissemination of intestinal microbes by phagocytosing and destroying bacterial invaders and their products that breach the epithelial barrier (Steinbach and Plevy, 2014). AIEC strains exhibit an enhanced ability to survive within the phagolysosomes of macrophages relative to nonpathogenic *E. coli* strains without inducing host cell death (Glasser et al., 2001) (Bringer et al., 2006). Indeed, intracellular bacteria within macrophages are evident when AIEC are co-cultured *ex vivo* with human colonic tissues (Jarry et al., 2015). Moreover, increased intracellular *E. coli* are recovered from mucosal biopsies from CD patients versus non-CD controls (Martin et al., 2004) and are present within mucosal macrophages in granulomatous colitis (Simpson et al., 2006). Several genes linked to bacterial resistance against stressors likely present within the phagolysosomal environmental, including peroxide and acid stress and nutrient starvation, contribute to the enhanced ability of AIEC to survive within macrophages (Bringer et al., 2005) (Bringer et al., 2007). In contrast, deletion of the heat shock proteins IbpA and IbpB in an AIEC strain enhances intramacrophagic survival (Patwa et al., 2011), which corresponds with increased proinflammatory cytokine production and more severe colitis when monoassociated in GF *Il10*$^{-/-}$ mice. Thus the precise mechanisms that enable enhanced AIEC survival within macrophages

remain incompletely understood. Moreover, little is known about the AIEC factors that potentially modulate initial interactions with macrophages and consequent proinflammatory responses.

1.4.3 Biofilm formation

In addition to their distinct interactions with host cells, AIEC strains also form more robust *in vitro* biofilms in comparison to other non-AIEC strains (Martinez-Medina et al., 2009b). Strong biofilm formation in AIEC strains positively correlates with an enhanced ability to adhere to and invade IECs (Martinez-Medina et al., 2009b), suggesting that extracellular structures and matrix components synthesized within AIEC biofilms may also serve as important adhesion and invasion determinants. Indeed, disruption of biofilm formation in an AIEC strain reduced its competitive advantage at the mucosa relative to the parental strain in a murine ileal loop model (Chassaing and Darfeuille-Michaud, 2012). However, the extracellular matrix components present within AIEC biofilms have not been identified, although there is some evidence for the involvement of type 1 pili (Chassaing and Darfeuille-Michaud, 2012).

Numerous factors including nutrient availability and environmental stressors induce biofilm formation and other multicellular behaviors by *E. coli* strains (Gerstel and Römling, 2001) (Yoo and Chen, 2009) (Rowe et al., 2010) (Medeiros et al., 2014) (Depas et al., 2013). In AIEC, increased osmolarity and contact with IECs enhance the expression of factors required for biofilm formation (Chassaing and Darfeuille-Michaud, 2012). However, additional environmental factors including iron availability that modulate biofilm formation in other *E. coli* strains may also promote AIEC biofilm formation.

1.4.4 Induction of colitis in rodent models

AIEC strains are capable of inducing and perpetuating intestinal inflammation in various rodent models of experimental colitis. In the presence or absence of an established complex microbial community, colonization of WT mice with AIEC does not induce colitis (Kim et al., 2005) (Carvalho et al., 2009) (Denizot et al., 2011) (Chassaing et al., 2014), therefore highlighting the opportunistic nature of these strains. Indeed, perturbations to the intestinal microbiota through antibiotic treatment or through diet-induced dysbiosis prior to AIEC colonization results in the development of mild histopathology in the colon and increased production of proinflammatory cytokines in WT and CEABAC10 mice (Martinez-Medina et al., 2013) (Small et al., 2013). AIEC colonization in chemically-induced models of colitis also exacerbates clinical disease activity, histopathology and proinflammatory cytokine production in comparison to vehicle controls or colonization with *E. coli* K12 strains or AIEC strains lacking established invasive determinants (Carvalho et al., 2008) (Drouet et al., 2012) (Low et al., 2013). In the absence of an intestinal microbiota, colonization of AIEC in genetically susceptible GF hosts including Toll-like receptor 5-deficient (*Tlr5*$^{-/-}$) mice and *Il10*$^{-/-}$ mice results in the development of immune-mediated colitis (Kim et al., 2005) (Carvalho et al., 2012). Interestingly, initial colonization of GF *Tlr5*$^{-/-}$ mice with AIEC prior to establishment of a complex microbiota also results in the development of colitis. In contrast, GF *Tlr5*$^{-/-}$ mice colonized with a flagella-deficient AIEC mutant and subsequently with a complex microbiota do not develop colitis, which coincided with enhanced clearance of the mutant (Carvalho et al., 2012). Taken together, in conjunction with increased epithelial invasive capabilities, environmental factors that alter the intestinal microbiota or that compromise host barrier or immune function also influences the proinflammatory potential of AIEC strains.

Although the precise contribution of AIEC to CD pathology remains unclear, the enhanced mucosal presence of AIEC likely provides the physically opportunity for continual stimulation of the mucosal immune system, thus perpetuating a state of chronic inflammation. The invasive capabilities of AIEC and their resistance to microbial killing by macrophages, in conjunction with host genetic factors including reduced function polymorphisms in genetic loci involved in microbial clearance, potentially enable enhanced mucosal association by AIEC (Lapaquette et al., 2010) (Sadaghian Sadabad et al., 2014). However, little is known about the putative environmental factors such as iron availability encountered by AIEC within the intestines that potentially facilitate these more unfavorable interactions with the host. Interestingly, exposure to bile salts has been recently shown to increase AIEC expression of Lpf and promote enhanced translocation across M-cells (Chassaing et al., 2012). Thus, identifying the environmental factors that promote enhanced mucosal association of AIEC and consequent inappropriate immune stimulation is clearly warranted.

1.5 Iron homeostasis in *E. coli*

1.5.1 Sensing of iron availability

Iron is an essential micronutrient for most bacteria including *E. coli*. However, as excess free iron can be highly toxic, acquisition and intracellular utilization of iron must be tightly regulated. In *E. coli*, the ferric uptake regulator (Fur) senses changes in free intracellular iron concentrations by its ability to bind ferrous iron and consequently regulates the expression of genes involved in maintaining iron homeostasis (Andrews et al., 2003). When intracellular iron is replete, the Fur-Fe^{2+} complex inhibits the transcription of genes involved in iron acquisition, thus preventing excess iron import into the cell (McHugh et al., 2003) (Seo et al., 2014). Holo-

Fur also mediates the incorporation of free iron into iron binding proteins by directly activating the transcription of genes involved in intracellular iron storage (Seo et al., 2014). Through transcriptional repression of the small RNA (sRNA) ryhB, Fur-Fe^{2+} indirectly regulates additional iron storage proteins and iron-dependent enzymes such as superoxide dismutase and enzymes involved in cellular respiration (Massé and Gottesman, 2002). Under iron limiting conditions, apo-Fur predominates in the cell, resulting in the derepression of iron acquisition genes and consequent iron transport into the cell (McHugh et al., 2003) (Seo et al., 2014).

1.5.2 Iron acquisition

In *E. coli*, iron import into the cell occurs either through siderophore-mediated transport or directly through divalent metal and heme iron transporters. Siderophores are small molecules with a high affinity for ferric iron that are synthesized and secreted by bacteria in order to scavenge iron when availability is limited. Siderophore-bound iron is transported through cognate outer membrane receptors that require energy transduction by the TonB-ExbB-ExbD complex (Letain and Postle, 1997) (Andrews et al., 2003). In the periplasm, a chaperone protein binds the iron-chelate and delivers the complex to cognate ABC permeases on the inner membrane (Köster, 2001). Finally, once in the cell, iron is released from the siderophore and reduced to its ferrous form for cellular use (Andrews et al., 2003). Ferrous iron on the other hand is directly transported into *E. coli* cells through inner membrane permeases such as FeoB or through inner membrane ABC transporters such as SitABCD (Kammler et al., 1993) (Sabri et al., 2006). Some *E. coli* strains are also capable of directly importing heme iron through the TonB-dependent hemin transporter ChuA (Nagy et al., 2001).

In the *E. coli* genome, diverse siderophore-mediated iron acquisition systems are encoded. Although laboratory *E. coli* K12 strains harbor at least six outer membrane receptors that recognize at least eight different iron-siderophore complexes, only the siderophore enterobactin is endogenously produced in these strains (Andrews et al., 2003). Enterobactin is a catecholate siderophore that is ubiquitously present among Entorobacteriaceae family members including *E. coli.* With its extremely high affinity for ferric iron, enterobactin can outcompete host iron binding proteins such as transferrin for iron, thus enabling the potential for *E. coli* to effectively scavenge iron within the host (Fischbach et al., 2006a). However, as part of the innate immune response, the host produces the antimicrobial peptide lipocalin-2 that can sequester enterobactin (Goetz et al., 2002) and limit *E. coli* growth and *in vivo* virulence (Flo et al., 2004).

To counteract this host immune response, some pathogenic and resident intestinal *E. coli* produce additional siderophores such as salmochelin and yersiniabactin that are resistant to lipocalin-2 binding. Glycosylation of enterobactin by enzymes encoded by the *iro* gene cluster results in the production of salmochelin (Fischbach et al., 2006b). *E. coli* strains that harbor the *iro* gene cluster are more virulent in an I.P. infection mouse model, an enhanced virulence that is lost in *Lcn2*$^{-/-}$ mice (Fischbach et al., 2006b). Because of its phenolate structure, yersiniabactin is also not recognized by lipocalin-2 (Bachman et al., 2011). Intact biosynthesis and import of yersiniabactin is required for virulence in numerous Enterobacteriaceae pathogens including *Yersinia pestis* (Perry and Fetherston, 2011) and *Klebsiella pneuomoneae* (Bachman et al., 2011). Moreover, in contrast to catecholate siderophores, yersiniabactin uniquely confers a fitness advantage for uropathogeneic *E. coli* strains in the urinary tract (Garcia et al., 2011).

The contribution of this heavy genomic investment in iron acquisition systems to *E. coli* fitness in the intestinal environment has not been fully studied. Ferrous iron import through the

permease FeoB, and not ferric iron scavenging by enterobactin, is essential for intestinal colonization of an *E. coli* K12 strain (Stojiljkovic et al., 1993), suggesting that in the non-inflamed and anaerobic intestinal environment, ferrous iron may be the predominant form of available iron. However, inactivation of TonB-dependent iron transport decreases the competitive advantage of the intestinal *E. coli* strain Nissle over *S.* Typhimurium in the inflamed intestinal environment, a growth advantage that is dependent on host secretion of lipocalin-2 (Deriu et al., 2013). Similarly, the creation of a quadruple mutant unable to import salmochelin, yersiniabactin, the siderophore aerobactin and heme also produced similar results (Deriu et al., 2013), suggesting that ferric and heme iron may be the predominant form of available iron in the inflamed intestines. Interestingly, distinct *in vitro* growth conditions promote maximal expression of different iron uptake genes (Valdebenito et al., 2006), suggesting that encoding seemingly redundant iron uptake systems may actually enable effective colonization and adaptability within diverse niches throughout the intestines. Although the precise contribution of each of these iron acquisition systems to *E. coli* fitness throughout the GI tract has not been explored, it is interesting to note that the yersiniabactin biosynthetic and transport genes are overrepresented in fecal versus environmental *E. coli* isolates and in AIEC versus other *E. coli* pathotypes (Dogan et al., 2014) (Searle et al., 2015). Similarly, the heme acquisition and utilization genes *chu* and the ferrous iron and manganese permease *sitABCD* are also overrepresented in AIEC strains (Dogan et al., 2014) and may therefore contribute to AIEC fitness within the intestines. Finally, when a K-12-like *E. coli* strain was monoassociated in a WT mouse, transcriptional expression of genes involved in enterobactin biosynthesis were upregulated in the mucus relative to the lumen (Li et al., 2015). This suggests that redundant iron acquisition systems in *E. coli*, particularly those that are able to evade innate immune responses,

may be important for mucosal colonization. Indeed, total iron concentrations in the absence of inflammation was approximately 5-6 fold lower in the mucus versus the lumen (Li et al., 2015).

1.5.3 Functional responses to iron availability

In addition to regulating the expression of iron metabolism genes, Fur-Fe^{2+} and apo-Fur also regulate genes involved in other cellular processes including metabolism, stress response, motility and biofilm formation (McHugh et al., 2003) (Seo et al., 2014). Microbial iron exposure can also alter the intracellular redox state of the cell that is sensed by iron-sulfur cluster transcription factors including IscR and Fnr (Kiley and Beinert, 2003), which further modulates the global transcriptome and consequent bacterial physiology and function (Giel et al., 2006) (Fink et al., 2007) (Wu and Outten, 2009). Moreover, the generation of intracellular ROS as a result of the Fenton reaction is sensed by additional transcription factors including OxyR, further impacting microbial function including phase variable colony morphology and aggregation and peroxide stress responses (Kullik et al., 1995) (Henderson and Owen, 1999) (Zheng et al., 1999). Finally, the basRS two-component system in *E. coli* senses extracellular ferric iron, which can result in the altered expression of genes involved in shaping the outer membrane landscape of the cell (Hagiwara et al., 2004) (Ogasawara et al., 2012).

In response to various environmental stimuli including iron availability, *E. coli* forms multicellular sessile communities such as biofilms and cellular aggregates. When iron availability is decreased, some *E. coli* strains respond by reducing biofilm (Wu and Outten, 2009) (Alves et al., 2010) and rugose colony formation (Depas et al., 2013), a colony morphotype associated with several multicellular behaviors (Römling et al., 1998) (Zogaj et al., 2001). In contrast, under iron replete conditions, biofilm and aggregate formation by other *E. coli*

strains is limited (Alves et al., 2010) (Rowe et al., 2010), demonstrating the heterogeneity of responses to iron availability exhibited by distinct *E. coli* strains. Iron also modulates *E. coli* interactions with host cells. For example, iron enhances the susceptibility of a bovine *E. coli* strain to phagocytosis by neutrophils (Wise et al., 2002) and adherence of enteric pathogenic *E. coli* to IECs (Alves et al., 2010) (Kortman et al., 2012). Similarly, the host antimicrobial and iron binding protein lactoferrin limits the epithelial invasiveness of AIEC (Bertuccini et al., 2014). The formation of multicellular communities and interactions with host cells are dependent on *E. coli* production of extracellular structures including flagella, fimbriae, and the exopolysaccharide cellulose. Interestingly, iron can directly and indirectly modulate the expression of some of these extracellular structures in certain *E. coli* strains (Guzzo et al., 1991) (Brombacher et al., 2006) (Wu and Outten, 2009) (Wu et al., 2013), therefore providing a putative mechanism by which iron may influence *E. coli* physiology and subsequent host-bacterial interactions. However, although there is evidence that iron availability influences *E. coli* multicellular behaviors and interactions with distinct host cell types *in vitro*, the precise impact of iron on AIEC-host interactions remains unclear.

1.6 Bacterial cellulose

Cellulose is a polysaccharide consisting of β(1→4)-linked D-glucose monomers. Bacteria including some *Salmonella* and *E. coli* strains synthesize cellulose as part of the ECM within biofilms and other multicellular structures (Zogaj et al., 2001) (Da Re and Ghigo, 2006) (Gualdi et al., 2008) (Ma and Wood, 2009) (Serra et al., 2013). In *Salmonella* and *E. coli*, genes involved in cellulose biosynthesis are divergently encoded by the *bcsQABZD* and *bcsEFG* gene clusters (Zogaj et al., 2001) (Solano et al., 2002) (Le Quéré and Ghigo, 2009). The catalytic subunit of

cellulose synthase, BcsA, is located on the inner membrane and polymerizes UDP-glucose onto the growing cellulose chain (Römling, 2002) (Omadjela et al., 2013). The bacterial second messenger cyclic-di-guanosine monophosphate (c-di-GMP) is required for cellulose synthase activity (Omadjela et al., 2013). Intracellular c-di-GMP levels are modulated by the biosynthetic and degradative activity of two opposing enzymes, diguanylate cyclase (DGC) and phosphodiesterase (PDE). Within the *E. coli* genome, there is an estimated 20 to 30 enzymes with predicted DGC and/or PDE activity (Weber et al., 2006) (Spurbeck et al., 2012) that can potentially modulate intracellular c-di-GMP concentrations, several of which have been implicated in regulating cellulose production in *Salmonella* and *E. coli* (Zogaj et al., 2001) (García et al., 2004) (Da Re and Ghigo, 2006) (Monteiro et al., 2009) (Spurbeck et al., 2012). The presence of numerous putative DGCs and PDEs in *E. coli* provides the potential for distinct environmental stimuli to modulate cellulose production and cellulose-dependent multicellular behaviors through transcriptional regulation of these enzymes.

1.6.1 Fitness, virulence and interactions with host cells

The impact of bacterial cellulose on *E. coli* interactions with host cells has largely been investigated with IECs *in vitro*. Cellulose production by the intestinal *E. coli* strain Nissle and by EPEC and enterohemorrhagic *E. coli* (EHEC) strains was associated with enhanced adherence to IECs (Monteiro et al., 2009) (Saldaña et al., 2009) and promoted increased epithelial production of the proinflammatory cytokine IL-8 (Monteiro et al., 2009). In contrast, abrogation of cellulose production in a different resident intestinal *E. coli* isolate reduced adhesion and invasion of IECs and subsequent IL-8 production (Wang et al., 2006). In an AIEC strain, cellulose production had

no impact on epithelial adhesion and invasion (Claret et al., 2007). Thus the influence of cellulose on *E. coli* interactions with IECs is complex and varies depending on the *E. coli* strain.

The impact of cellulose production on *E. coli* interactions with macrophages to our knowledge has not been previously studied. In a recent study by Pontes and colleagues, intracellular production of cellulose by *Salmonella* was demonstrated within the phagolysosome of macrophages (Pontes et al., 2015). Intriguingly, inactivation of cellulose production in *Salmonella* enhanced intramacrophagic survival and *in vivo* pathogenicity in an I.P. murine infection model (Pontes et al., 2015), suggesting that cellulose production may limit the virulence potential of *Salmonella* at extraintestinal sites. Similarly, deletion of the DGC regulator YfiR in an UPEC strain increased production of cellulose and curli fimbriae and corresponded with reduced fitness in the urinary tract (Raterman et al., 2013). Abrogation of both curli and cellulose biosynthesis in the YfiR-deficient mutant restored its *in vivo* fitness (Raterman et al., 2013), suggesting that production of both extracellular structures may limit the growth advantage of UPEC strains in the urinary tract.

In contrast, another group demonstrated that cellulose-deficient UPEC mutants were more readily cleared from the kidneys in a urinary tract infection (UTI) mouse model in a neutrophil-dependent manner (Kai-Larsen et al., 2010). Moreover, production of cellulose or cellulose-dependent multicellular structures is triggered or enhanced by stressors likely present within the host, including iron deprivation, iron exposure, peroxide stress and soluble IgA (Rowe et al., 2010) (Depas et al., 2013) (Amarasinghe et al., 2013). Therefore, cellulose may serve as a bacterial resistance factor against environmental stressors and has indeed been shown to enhance bacterial survival with chlorine exposure and ethanol stress (Solano et al., 2002) (Yoo and Chen, 2009). However, the precise mechanisms by which these environmental factors such as iron

availability modulate cellulose production and cellulose-dependent behaviors are not well understood and likely vary by *E. coli* strain, especially considering that different stimuli induce cellulose production and cellulose-dependent behaviors in different strains. Taken together, the contribution of cellulose production to the fitness and virulence potential of *E. coli* remains unclear and likely depends on the genetic background of the strain and environmental factors. Interestingly, when screening for cellulose-positive intestinal and UPEC isolates, Bokranz and colleagues demonstrated that more intestinal *E. coli* isolates produce cellulose at the physiological temperature of 37°C compared to UPEC isolates that only produced cellulose at 28°C (Bokranz, 2005). Thus, it is tempting to speculate that resident intestinal *E. coli* may have retained the ability produce cellulose at physiological temperatures as a potential fitness advantage within the intestinal environment.

1.7 Iron and the proinflammatory potential of the intestinal microbiota

The prevailing hypothesis explaining how oral iron supplementation may exacerbate intestinal inflammation is through the increased production of oxygen radicals as a byproduct of the Fenton reaction. However, it has been well documented that some members of the intestinal microbiota, such as AIEC, can drive and perpetuate intestinal inflammation in genetically susceptible hosts. Given that iron selectively modulates bacterial growth, physiology and function, another conceivable and largely unexplored mechanism explaining the link between increased oral iron intake and intestinal inflammation is the iron-mediated induction of a more proinflammatory intestinal microbiota. However, studies investigating the impact of iron on host-microbial interactions have primarily focused on pathogens, and thus, little is known about

the functional impact of iron on resident intestinal bacteria such as AIEC and subsequent host responses.

We first investigated how intestinal iron availability shapes the ecological structure of the microbial community. In inflammation-resistant WT mice, decreasing luminal iron concentrations through dietary manipulations resulted in compositional changes consistent with a dysbiotic state. This included the relative expansion of Enterobacteriaceae family members including the siderophilic resident bacterium *E. coli* and an increase in the predicted abundance of iron acquisition genes. When iron availability was restricted, inactivation of TonB-dependent iron transport in *E. coli* reduced its relative abundance when grown in competition with a non-siderophilic intestinal bacterium, suggesting that harboring numerous iron acquisition systems may confer a fitness advantage for *E. coli* in the intestines under iron limiting conditions.

To investigate the impact of iron availability on the proinflammatory potential of the intestinal microbiota, we utilized the AIEC strain NC101 as a model organism to assess how iron influences bacterial physiology and subsequent host-microbial interactions. The physiological state of NC101 (i.e. aggregate versus non-aggregate) is dependent on both cellulose production and iron availability and influenced subsequent interactions with macrophages. Specifically, under iron limiting conditions, cellulose production by NC101 was associated with enhanced resistance against macrophage clearance and macrophage production of cytokines that promote Th-1/Th-17 immune responses. Abrogation of cellulose production in NC101 also delayed onset of chronic, immune-mediated colitis when monoassociated in germ free *Il10*$^{-/-}$ mice, further demonstrating the contribution of cellulose to the proinflammatory potential of NC101.

Finally, dietary iron supplementation limited colitis development in *Il10*$^{-/-}$ mice when colonized with a complex microbiota. However, this was not associated with distinct

compositional changes to the luminal microbial community in comparison to the control diet, where colitis development was most severe. Nonetheless, these results do not exclude the possibility that iron supplementation functionally alters the intestinal microbiome in a manner that limits colitis development. Moreover, differences in inflammation severity between the two diet groups were associated with minor compositional changes to the mucosal microbiota, which may also contribute to the protective effect of dietary iron supplementation. Taken together, our results suggest that decreasing microbial iron availability may enhance the proinflammatory potential of the intestinal microbiota and highlight the complex interplay between host, microbial and environmental factors in the development of IBD.

REFERENCES

Ablin, J., Shalev, O., Okon, E., Karmeli, F., and Rachmilewitz, D. (1999). Deferiprone, an oral iron chelator, ameliorates experimental colitis and gastric ulceration in rats. Inflamm Bowel Dis *5*, 253–261.

Alves, J.R., Pereira, A.C.M., Souza, M.C., Costa, S.B., Pinto, A.S., Mattos-Guaraldi, A.L., Hirata-Júnior, R., Rosa, A.C.P., and Asad, L.M.B.O. (2010). Iron-limited condition modulates biofilm formation and interaction with human epithelial cells of enteroaggregative Escherichia coli (EAEC). Journal of Applied Microbiology *108*, 246–255.

Amarasinghe, J.J., D'Hondt, R.E., Waters, C.M., and Mantis, N.J. (2013). Exposure of Salmonella enterica Serovar Typhimurium to a Protective Monoclonal IgA Triggers Exopolysaccharide Production via a Diguanylate Cyclase-Dependent Pathway. Infect Immun *81*, 653–664.

Ananthakrishnan, A.N. (2015). Epidemiology and risk factors for IBD. Nat Rev Gastroenterol Hepatol *12*, 205–217.

Anderson, G.J., Frazer, D.M., and McLaren, G.D. (2009). Iron absorption and metabolism. Curr Opin Gastroenterol *25*, 129–135.

Andrews, S.C., Robinson, A.K., and Rodrã guez-Quiã Ones, F. (2003). Bacterial iron homeostasis. FEMS Microbiology Reviews *27*, 215–237.

Arthur, J.C., Perez-Chanona, E., Muhlbauer, M., Tomkovich, S., Uronis, J.M., Fan, T.J., Campbell, B.J., Abujamel, T., Dogan, B., Rogers, A.B., et al. (2012). Intestinal Inflammation Targets Cancer-Inducing Activity of the Microbiota. Science *338*, 120–123.

Atarashi, K., Tanoue, T., Shima, T., Imaoka, A., Kuwahara, T., Momose, Y., Cheng, G., Yamasaki, S., Saito, T., Ohba, Y., et al. (2011). Induction of Colonic Regulatory T Cells by Indigenous Clostridium Species. Science *331*, 337–341.

Bachman, M.A., Oyler, J.E., Burns, S.H., Caza, M., Lépine, F., Dozois, C.M., and Weiser, J.N. (2011). Klebsiella pneumoniae yersiniabactin promotes respiratory tract infection through evasion of lipocalin 2. Infect Immun *79*, 3309–3316.

Bager, P., Befrits, R., Wikman, O., Lindgren, S., Moum, B., Hjortswang, H., and Dahlerup, J.F. (2013). High burden of iron deficiency and different types of anemia in inflammatory bowel disease outpatients in Scandinavia: a longitudinal 2-year follow-up study. Scand J Gastroenterol *48*, 1286–1293.

Barnich, N., Carvalho, F.A., Glasser, A.-L., Darcha, C., Jantscheff, P., Allez, M., Peeters, H., Bommelaer, G., Desreumaux, P., Colombel, J.-F., et al. (2007). CEACAM6 acts as a receptor for adherent-invasive E. coli, supporting ileal mucosa colonization in Crohn disease. J Clin Invest *117*, 1566–1574.

Basseri, R.J., Nemeth, E., Vassilaki, M.E., Basseri, B., Enayati, P., Shaye, O., Bourikas, L.A., Ganz, T., and Papadakis, K.A. (2013). Hepcidin is a key mediator of anemia of inflammation in Crohn's disease. Journal of Crohn's and Colitis *7*, e286–e291.

Bergamaschi, G., Di Sabatino, A., Albertini, R., Costanzo, F., Guerci, M., Masotti, M., Pasini, A., Massari, A., Campostrini, N., Corbella, M., et al. (2013). Serum Hepcidin in Inflammatory Bowel Diseases. Inflamm Bowel Dis *19*, 2166–2172.

Bertuccini, L., Costanzo, M., Iosi, F., Tinari, A., Terruzzi, F., Stronati, L., Aloi, M., Cucchiara, S., and Superti, F. (2014). Lactoferrin prevents invasion and inflammatory response following E. coli strain LF82 infection in experimental model of Crohn's disease. Dig Liver Dis *46*, 496–504.

Bokranz, W. (2005). Expression of cellulose and curli fimbriae by Escherichia coli isolated from the gastrointestinal tract. Journal of Medical Microbiology *54*, 1171–1182.

Boudeau, J., Barnich, N., and Darfeuille-Michaud, A. (2001). Type 1 pili-mediated adherence of Escherichia coli strain LF82 isolated from Crohn's disease is involved in bacterial invasion of intestinal epithelial cells. Mol Microbiol *39*, 1272–1284.

Boudeau, J., Glasser, A.L., Masseret, E., Joly, B., and Darfeuille-Michaud, A. (1999). Invasive ability of an Escherichia coli strain isolated from the ileal mucosa of a patient with Crohn's disease. Infect Immun *67*, 4499–4509.

Bringer, M.-A., Barnich, N., Glasser, A.-L., Bardot, O., and Darfeuille-Michaud, A. (2005). HtrA stress protein is involved in intramacrophagic replication of adherent and invasive Escherichia coli strain LF82 isolated from a patient with Crohn's disease. Infect Immun *73*, 712–721.

Bringer, M.-A., Glasser, A.-L., Tung, C.-H., Méresse, S., and Darfeuille-Michaud, A. (2006). The Crohn's disease-associated adherent-invasive Escherichia coli strain LF82 replicates in mature phagolysosomes within J774 macrophages. Cell. Microbiol. *8*, 471–484.

Bringer, M.-A., Rolhion, N., Glasser, A.-L., and Darfeuille-Michaud, A. (2007). The oxidoreductase DsbA plays a key role in the ability of the Crohn's disease-associated adherent-invasive Escherichia coli strain LF82 to resist macrophage killing. J Bacteriol *189*, 4860–4871.

Brombacher, E., Baratto, A., Dorel, C., and Landini, P. (2006). Gene expression regulation by the Curli activator CsgD protein: modulation of cellulose biosynthesis and control of negative determinants for microbial adhesion. J Bacteriol *188*, 2027–2037.

Carmody, R.N., Gerber, G.K., Luevano, J.M., Jr, Gatti, D.M., Somes, L., Svenson, K.L., and Turnbaugh, P.J. (2015). Diet Dominates Host Genotypein Shaping the Murine Gut Microbiota. Cell Host Microbe *17*, 72–84.

Carrier, J., Aghdassi, E., Platt, I., Cullen, J., and Allard, J.P. (2001). Effect of oral iron supplementation on oxidative stress and colonic inflammation in rats with induced colitis. Aliment Pharmacol Ther *15*, 1989–1999.

Carrier, J., Aghdassi, E., Cullen, J., and Allard, J.P. (2002). Iron supplementation increases disease activity and vitamin E ameliorates the effect in rats with dextran sulfate sodium-induced colitis. J. Nutr. *132*, 3146–3150.

Carvalho, F.A., Barnich, N., Sauvanet, P., Darcha, C., Gelot, A., and Darfeuille-Michaud, A. (2008). Crohn's disease-associated Escherichia coli LF82 aggravates colitis in injured mouse colon via signaling by flagellin. Inflamm Bowel Dis *14*, 1051–1060.

Carvalho, F.A., Barnich, N., Sivignon, A., Darcha, C., Chan, C.H.F., Stanners, C.P., and Darfeuille-Michaud, A. (2009). Crohn's disease adherent-invasive Escherichia coli colonize and induce strong gut inflammation in transgenic mice expressing human CEACAM. J. Exp. Med. *206*, 2179–2189.

Carvalho, F.A., Koren, O., Goodrich, J.K., Johansson, M.E.V., Nalbantoglu, I., Aitken, J.D., Su, Y., Chassaing, B., Walters, W.A., González, A., et al. (2012). Transient inability to manage proteobacteria promotes chronic gut inflammation in TLR5-deficient mice. Cell Host Microbe *12*, 139–152.

Chassaing, B., and Darfeuille-Michaud, A. (2012). The E Pathway Is Involved in Biofilm Formation by Crohn's Disease-Associated Adherent-Invasive Escherichia coli. J Bacteriol *195*, 76–84.

Chassaing, B., Etienne-Mesmin, L., Bonnet, R., and Darfeuille-Michaud, A. (2012). Bile salts induce long polar fimbriae expression favouring Crohn“s disease-associated adherent-invasive Escherichia coliinteraction with Peyer”s patches. Environmental Microbiology *15*, 355–371.

Chassaing, B., Koren, O., Carvalho, F.A., Ley, R.E., and Gewirtz, A.T. (2014). AIEC pathobiont instigates chronic colitis in susceptible hosts by altering microbiota composition. Gut *63*, 1069–1080.

Chassaing, B., Rolhion, N., de Vallée, A., Salim, S.Y., Prorok-Hamon, M., Neut, C., Campbell, B.J., Söderholm, J.D., Hugot, J.-P., Colombel, J.-F., et al. (2011). Crohn disease--associated adherent-invasive E. coli bacteria target mouse and human Peyer's patches via long polar fimbriae. J Clin Invest *121*, 966–975.

Cherayil, B.J., Ellenbogen, S., and Shanmugam, N.N. (2011). Iron and intestinal immunity. Curr Opin Gastroenterol *27*, 523–528.

Chow, J., Lee, S.M., Shen, Y., Khosravi, A., and Mazmanian, S.K. (2010). Host–Bacterial Symbiosis in Health and Disease. In Advances in Immunology, (Elsevier), pp. 243–274.

Chua, A.C.G., Klopcic, B.R.S., Ho, D.S., Fu, S.K., Forrest, C.H., Croft, K.D., Olynyk, J.K., Lawrance, I.C., and Trinder, D. (2013). Dietary Iron Enhances Colonic Inflammation and IL-6/IL-11-Stat3 Signaling Promoting Colonic Tumor Development in Mice. PLoS ONE *8*, e78850.

Claret, L., Miquel, S., Vieille, N., Ryjenkov, D.A., Gomelsky, M., and Darfeuille-Michaud, A. (2007). The flagellar sigma factor FliA regulates adhesion and invasion of Crohn disease-associated Escherichia coli via a cyclic dimeric GMP-dependent pathway. J Biol Chem *282*,

33275–33283.

Costello, E.K., Lauber, C.L., Hamady, M., Fierer, N., Gordon, J.I., and Knight, R. (2009). Bacterial community variation in human body habitats across space and time. Science *326*, 1694–1697.

Cummings, J.H., and Macfarlane, G.T. (1997). Role of intestinal bacteria in nutrient metabolism. JPEN J Parenter Enteral Nutr *21*, 357–365.

D'Haens, G.R., Geboes, K., Peeters, M., Baert, F., Penninck, F., and Rutgeerts, P. (1998). Early lesions of recurrent Crohn's disease caused by infusion of intestinal contents in excluded ileum. *114*, 262–267.

Da Re, S., and Ghigo, J.M. (2006). A CsgD-Independent Pathway for Cellulose Production and Biofilm Formation in Escherichia coli. J Bacteriol *188*, 3073–3087.

Darfeuille-Michaud, A., Boudeau, J., Bulois, P., Neut, C., Glasser, A.-L., Barnich, N., Bringer, M.-A., Swidsinski, A., Beaugerie, L., and Colombel, J.-F. (2004). High prevalence of adherent-invasive Escherichia coli associated with ileal mucosa in Crohn's disease. Gastroenterology *127*, 412–421.

David, L.A., Maurice, C.F., Carmody, R.N., Gootenberg, D.B., Button, J.E., Wolfe, B.E., Ling, A.V., Devlin, A.S., Varma, Y., Fischbach, M.A., et al. (2013). Diet rapidly and reproducibly alters the human gut microbiome. Nature *505*, 559–563.

Davidson, N.J., Leach, M.W., Fort, M.M., Thompson-Snipes, L., Kühn, R., Müller, W., Berg, D.J., and Rennick, D.M. (1996). T helper cell 1-type CD4+ T cells, but not B cells, mediate colitis in interleukin 10-deficient mice. J. Exp. Med. *184*, 241–251.

de Silva, A.D., Tsironi, E., Feakins, R.M., and Rampton, D.S. (2005). Efficacy and tolerability of oral iron therapy in inflammatory bowel disease: a prospective, comparative trial. Aliment Pharmacol Ther *22*, 1097–1105.

Denizot, J., Sivignon, A., Barreau, F., Darcha, C., Chan, H.F.C., Stanners, C.P., Hofman, P., Darfeuille-Michaud, A., and Barnich, N. (2011). Adherent-invasive Escherichia coli induce claudin-2 expression and barrier defect in CEABAC10 mice and crohn's disease patients. Inflamm Bowel Dis.

Depas, W.H., Hufnagel, D.A., Lee, J.S., Blanco, L.P., Bernstein, H.C., Fisher, S.T., James, G.A., Stewart, P.S., and Chapman, M.R. (2013). Iron induces bimodal population development by Escherichia coli. Proceedings of the National Academy of Sciences *110*, 2629–2634.

Deriu, E., Liu, J.Z., Pezeshki, M., Edwards, R.A., Ochoa, R.J., Contreras, H., Libby, S.J., Fang, F.C., and Raffatellu, M. (2013). Probiotic Bacteria Reduce Salmonella Typhimurium Intestinal Colonization by Competing for Iron. Cell Host Microbe *14*, 26–37.

Deschemin, J.C., Noordine, M.L., Remot, A., Willemetz, A., Afif, C., Canonne-Hergaux, F., Langella, P., Karim, Z., Vaulont, S., Thomas, M., et al. (2015). The microbiota shifts the iron

sensing of intestinal cells. The FASEB Journal.

Dogan, B., Suzuki, H., Herlekar, D., Sartor, R.B., Campbell, B.J., Roberts, C.L., Stewart, K., Scherl, E.J., Araz, Y., Bitar, P.P., et al. (2014). Inflammation-associated adherent-invasive Escherichia coli are enriched in pathways for use of propanediol and iron and M-cell translocation. Inflamm Bowel Dis *20*, 1919–1932.

Dostal, A., Baumgartner, J., Riesen, N., Chassard, C., Smuts, C.M., Zimmermann, M.B., and Lacroix, C. (2014a). Effects of iron supplementation on dominant bacterial groups in the gut, faecal SCFA and gut inflammation: a randomised, placebo-controlled intervention trial in South African children. Br J Nutr *112*, 547–556.

Dostal, A., Chassard, C., Hilty, F.M., Zimmermann, M.B., Jaeggi, T., Rossi, S., and Lacroix, C. (2012a). Iron depletion and repletion with ferrous sulfate or electrolytic iron modifies the composition and metabolic activity of the gut microbiota in rats. Journal of Nutrition *142*, 271–277.

Dostal, A., Fehlbaum, S., Chassard, C., Zimmermann, M.B., and Lacroix, C. (2012b). Low iron availability in continuous in vitrocolonic fermentations induces strong dysbiosis of the child gut microbial consortium and a decrease in main metabolites. FEMS Microbiol. Ecol. *83*, 161–175.

Dostal, A., Lacroix, C., Pham, V.T., Zimmermann, M.B., Del'homme, C., Bernalier-Donadille, A., and Chassard, C. (2014b). Iron supplementation promotes gut microbiota metabolic activity but not colitis markers in human gut microbiota-associated rats. Br J Nutr *111*, 2135–2145.

Drakesmith, H., and Prentice, A.M. (2012). Hepcidin and the Iron-Infection Axis. Science *338*, 768–772.

Dreux, N., Denizot, J., Martinez-Medina, M., Mellmann, A., Billig, M., Kisiela, D., Chattopadhyay, S., Sokurenko, E., Neut, C., Gower-Rousseau, C., et al. (2013). Point Mutations in FimH Adhesin of Crohn's Disease-Associated Adherent-Invasive Escherichia coli Enhance Intestinal Inflammatory Response. PLoS Pathog. *9*, e1003141.

Drouet, M., Vignal, C., Singer, E., Djouina, M., Dubreuil, L., Cortot, A., Desreumaux, P., and Neut, C. (2012). AIEC colonization and pathogenicity: influence of previous antibiotic treatment and preexisting inflammation. Inflamm Bowel Dis *18*, 1923–1931.

Eckburg, P.B., Bik, E.M., Bernstein, C.N., Purdom, E., Dethlefsen, L., Sargent, M., Gill, S.R., Nelson, K.E., and Relman, D.A. (2005). Diversity of the human intestinal microbial flora. Science *308*, 1635–1638.

Ettreiki, C. (2012). Juvenile ferric iron prevents microbiota dysbiosis and colitis in adult rodents. World J. Gastroenterol. *18*, 2619.

Eun, C.S., Mishima, Y., Wohlgemuth, S., Liu, B., Bower, M., Carroll, I.M., and Sartor, R.B. (2014). Induction of Bacterial Antigen-Specific Colitis by a Simplified Human Microbiota Consortium in Gnotobiotic IL-10-/- Mice. Infect Immun.

Evstatiev, R., and Gasche, C. (2012). Iron sensing and signalling. Gut *61*, 933–952.

Fink, R.C., Evans, M.R., Porwollik, S., Vazquez-Torres, A., Jones-Carson, J., Troxell, B., Libby, S.J., McClelland, M., and Hassan, H.M. (2007). FNR Is a Global Regulator of Virulence and Anaerobic Metabolism in Salmonella enterica Serovar Typhimurium (ATCC 14028s). J Bacteriol *189*, 2262–2273.

Fischbach, M.A., Lin, H., Liu, D.R., and Walsh, C.T. (2006a). How pathogenic bacteria evade mammalian sabotage in the battle for iron. Nat Chem Biol *2*, 132–138.

Fischbach, M.A., Lin, H., Zhou, L., Yu, Y., Abergel, R.J., Liu, D.R., Raymond, K.N., Wanner, B.L., Strong, R.K., Walsh, C.T., et al. (2006b). The pathogen-associated iroA gene cluster mediates bacterial evasion of lipocalin 2. Proc Natl Acad Sci USA *103*, 16502–16507.

Flo, T.H., Smith, K.D., Sato, S., Rodriguez, D.J., Holmes, M.A., Strong, R.K., Akira, S., and Aderem, A. (2004). Lipocalin 2 mediates an innate immune response to bacterial infection by sequestrating iron. Nature *432*, 917–921.

Garcia, E.C., Brumbaugh, A.R., and Mobley, H.L.T. (2011). Redundancy and specificity of Escherichia coli iron acquisition systems during urinary tract infection. Infect Immun *79*, 1225–1235.

García, B., Latasa, C., Solano, C., Portillo, F.G.-D., Gamazo, C., and Lasa, I. (2004). Role of the GGDEF protein family in Salmonella cellulose biosynthesis and biofilm formation. Mol Microbiol *54*, 264–277.

Gerstel, U., and Römling, U. (2001). Oxygen tension and nutrient starvation are major signals that regulate agfD promoter activity and expression of the multicellular morphotype in Salmonella typhimurium. Environmental Microbiology *3*, 638–648.

Gevers, D., Kugathasan, S., Denson, L.A., Vázquez-Baeza, Y., Van Treuren, W., Ren, B., Schwager, E., Knights, D., Song, S.J., Yassour, M., et al. (2014). The Treatment-Naive Microbiome in New-Onset Crohn's Disease. Cell Host Microbe *15*, 382–392.

Giel, J.L., Rodionov, D., Liu, M., Blattner, F.R., and Kiley, P.J. (2006). IscR-dependent gene expression links iron-sulphur cluster assembly to the control of O2-regulated genes in Escherichia coli. Mol Microbiol *60*, 1058–1075.

Gisbert, J.P., Bermejo, F., Pajares, R., Pérez-Calle, J.-L., Rodríguez, M., Algaba, A., Mancenido, N., La Morena, De, F., Carneros, J.A., Mcnicholl, A.G., et al. (2009). Oral and intravenous iron treatment in inflammatory bowel disease: hematological response and quality of life improvement. Inflamm Bowel Dis *15*, 1485–1491.

Glasser, A.L., Boudeau, J., Barnich, N., Perruchot, M.H., Colombel, J.F., and Darfeuille-Michaud, A. (2001). Adherent invasive Escherichia coli strains from patients with Crohn's disease survive and replicate within macrophages without inducing host cell death. Infect Immun *69*, 5529–5537.

Goetz, D.H., Holmes, M.A., Borregaard, N., Bluhm, M.E., Raymond, K.N., and Strong, R.K. (2002). The neutrophil lipocalin NGAL is a bacteriostatic agent that interferes with siderophore-mediated iron acquisition. Mol. Cell *10*, 1033–1043.

Goodhand, J.R., Kamperidis, N., Rao, A., Laskaratos, F., McDermott, A., Wahed, M., Naik, S., Croft, N.M., Lindsay, J.O., Sanderson, I.R., et al. (2011). Prevalence and management of anemia in children, adolescents, and adults with inflammatory bowel disease. Inflamm Bowel Dis *18*, 513–519.

Gualdi, L., Tagliabue, L., Bertagnoli, S., Ierano, T., De Castro, C., and Landini, P. (2008). Cellulose modulates biofilm formation by counteracting curli-mediated colonization of solid surfaces in Escherichia coli. Microbiology (Reading, Engl.) *154*, 2017–2024.

Guzzo, A., Diorio, C., and DuBow, M.S. (1991). Transcription of the Escherichia coli fliC gene is regulated by metal ions. Appl Environ Microbiol *57*, 2255–2259.

Haberman, Y., Tickle, T.L., Dexheimer, P.J., Kim, M.-O., Tang, D., Karns, R., Baldassano, R.N., Noe, J.D., Rosh, J., Markowitz, J., et al. (2014). Pediatric Crohn disease patients exhibit specific ileal transcriptome and microbiome signature. J Clin Invest *124*, 3617–3633.

Hagiwara, M., Yamashino, T., and Mizuno, T. (2004). A Genome-wide view of the Escherichia coli BasS-BasR two-component system implicated in iron-responses. Biosci. Biotechnol. Biochem. *68*, 1758–1767.

Henderson, I.R., and Owen, P. (1999). The major phase-variable outer membrane protein of Escherichia coli structurally resembles the immunoglobulin A1 protease class of exported protein and is regulated by a novel mechanism involving Dam and oxyR. J Bacteriol *181*, 2132–2141.

Hurrell, R., and Egli, I. (2010). Iron bioavailability and dietary reference values. American Journal of Clinical Nutrition *91*, 1461S–1467S.

Hwang, C., Ross, V., and Mahadevan, U. (2012). Micronutrient deficiencies in inflammatory bowel disease: From A to zinc. Inflamm Bowel Dis *18*, 1961–1981.

Iebba, V., Conte, M.P., Lepanto, M.S., Di Nardo, G., Santangelo, F., Aloi, M., Totino, V., Checchi, M.P., Longhi, C., Cucchiara, S., et al. (2012). Microevolution in fimH Gene of Mucosa-Associated Escherichia coli Strains Isolated from Pediatric Patients with Inflammatory Bowel Disease. Infect Immun *80*, 1408–1417.

Jaeggi, T., Kortman, G.A.M., Moretti, D., Chassard, C., Holding, P., Dostal, A., Boekhorst, J., Timmerman, H.M., Swinkels, D.W., Tjalsma, H., et al. (2014). Iron fortification adversely affects the gut microbiome, increases pathogen abundance and induces intestinal inflammation in Kenyan infants. Gut.

Jarry, A., Crémet, L., Caroff, N., Bou-Hanna, C., Mussini, J.M., Reynaud, A., Servin, A.L., Mosnier, J.F., Liévin-Le Moal, V., and Laboisse, C.L. (2015). Subversion of human intestinal mucosa innate immunity by a Crohn's disease-associated E. coli. Mucosal Immunology *8*, 572–

581.

Kai-Larsen, Y., Lüthje, P., Chromek, M., Peters, V., Wang, X., Holm, Å., Kádas, L., Hedlund, K.-O., Johansson, J., Chapman, M.R., et al. (2010). Uropathogenic Escherichia coli Modulates Immune Responses and Its Curli Fimbriae Interact with the Antimicrobial Peptide LL-37. PLoS Pathog. *6*, e1001010.

Kammler, M., Schön, C., and Hantke, K. (1993). Characterization of the ferrous iron uptake system of Escherichia coli. J Bacteriol *175*, 6212–6219.

Kappelman, M.D., Moore, K.R., Allen, J.K., and Cook, S.F. (2012). Recent Trends in the Prevalence of Crohn's Disease and Ulcerative Colitis in a Commercially Insured US Population. Dig. Dis. Sci. *58*, 519–525.

Kappelman, M.D., Rifas Shiman, S.L., Porter, C.Q., Ollendorf, D.A., Sandler, R.S., Galanko, J.A., and Finkelstein, J.A. (2008). Direct Health Care Costs of Crohn's Disease and Ulcerative Colitis in US Children and Adults. Gastroenterology *135*, 1907–1913.

Kiley, P.J., and Beinert, H. (2003). The role of Fe–S proteins in sensing and regulation in bacteria. Current Opinion in Microbiology *6*, 181–185.

Kim, S.C., Tonkonogy, S.L., Albright, C.A., Tsang, J., Balish, E.J., Braun, J., Huycke, M.M., and Sartor, R.B. (2005). Variable phenotypes of enterocolitis in interleukin 10-deficient mice monoassociated with two different commensal bacteria. Gastroenterology *128*, 891–906.

Kim, S.C., Tonkonogy, S.L., Jarvis, H.W., Darfeuille-Michaud, A., and Sartor, R.B. (2008). Escherichia coli Strains Differentially Induce Colitis in IL-10 Gene Deficient Mice. Gastroenterology *134*, A–23.

Knutson, M.D. (2010). Iron-Sensing Proteins that Regulate Hepcidin and Enteric Iron Absorption. Annu. Rev. Nutr. *30*, 149–171.

Koenig, J.E., Spor, A., Scalfone, N., Fricker, A.D., Stombaugh, J., Knight, R., Angenent, L.T., and Ley, R.E. (2011). Succession of microbial consortia in the developing infant gut microbiome. Proc Natl Acad Sci USA *108 Suppl 1*, 4578–4585.

Kortman, G.A.M., Boleij, A., Swinkels, D.W., and Tjalsma, H. (2012). Iron Availability Increases the Pathogenic Potential of Salmonella Typhimurium and Other Enteric Pathogens at the Intestinal Epithelial Interface. PLoS ONE *7*, e29968.

Kostic, A.D., Xavier, R.J., and Gevers, D. (2014). The Microbiome in Inflammatory Bowel Disease: Current Status and the Future Ahead. Gastroenterology *146*, 1489–1499.

Köster, W. (2001). ABC transporter-mediated uptake of iron, siderophores, heme and vitamin B12. Research in Microbiologoy *152*, 291–301.

Krebs, N.F., Sherlock, L.G., Westcott, J., Culbertson, D., Hambidge, K.M., Feazel, L.M., Robertson, C.E., and Frank, D.N. (2013). Effects of Different Complementary Feeding

Regimens on Iron Status and Enteric Microbiota in Breastfed Infants. J. Pediatr. *163*, 416–423.e4.

Kullik, I., Toledano, M.B., Tartaglia, L.A., and Storz, G. (1995). Mutational analysis of the redox-sensitive transcriptional regulator OxyR: regions important for oxidation and transcriptional activation. J Bacteriol *177*, 1275–1284.

Kulnigg, S., and Gasche, C. (2006). Systematic review: managing anaemia in Crohn's disease. Aliment Pharmacol Ther *24*, 1507–1523.

Kühn, R., Löhler, J., Rennick, D., Rajewsky, K., and Müller, W. (1993). Interleukin-10-deficient mice develop chronic enterocolitis. Cell *75*, 263–274.

Lapaquette, P., Glasser, A.-L., Huett, A., Xavier, R.J., and Darfeuille-Michaud, A. (2010). Crohn's disease-associated adherent-invasive E. coli are selectively favoured by impaired autophagy to replicate intracellularly. Cell. Microbiol. *12*, 99–113.

Le Quéré, B., and Ghigo, J.-M. (2009). BcsQ is an essential component of the Escherichia colicellulose biosynthesis apparatus that localizes at the bacterial cell pole. Mol Microbiol *72*, 724–740.

Lee, T.W., Kolber, M.R., Fedorak, R.N., and van Zanten, S.V. (2012). Iron replacement therapy in inflammatory bowel disease patients with iron deficiency anemia: A systematic review and meta-analysis. Journal of Crohn's and Colitis *6*, 267–275.

Letain, T.E., and Postle, K. (1997). TonB protein appears to transduce energy by shuttling between the cytoplasmic membrane and the outer membrane in Escherichia coli. Mol Microbiol *24*, 271–283.

Li, H., Limenitakis, J.P., Fuhrer, T., Geuking, M.B., Lawson, M.A., Wyss, M., Brugiroux, S., Keller, I., Macpherson, J.A., Rupp, S., et al. (2015). The outer mucus layer hosts a distinct intestinal microbial niche. Nature Communications *6*, 1–13.

Llopis, M., Antolín, M., Carol, M., Borruel, N., Casellas, F., Martinez, C., Espín-Basany, E., Guarner, F., and Malagelada, J.-R. (2009). Lactobacillus casei downregulates commensals' inflammatory signals in Crohn's disease mucosa. Inflamm Bowel Dis *15*, 275–283.

Low, D., Tran, H.T., Lee, I.-A., Dreux, N., Kamba, A., Reinecker, H.C., Darfeuille-Michaud, A., Barnich, N., and Mizoguchi, E. (2013). Chitin-binding domains of Escherichia coli ChiA mediate interactions with intestinal epithelial cells in mice with colitis. Gastroenterology *145*, 602–12.e609.

Lund, E.K., Fairweather-Tait, S.J., Wharf, S.G., and Johnson, I.T. (2001). Chronic exposure to high levels of dietary iron fortification increases lipid peroxidation in the mucosa of the rat large intestine. J. Nutr. *131*, 2928–2931.

Lund, E.K., Wharf, S.G., Fairweather-Tait, S.J., and Johnson, I.T. (1999). Oral ferrous sulfate supplements increase the free radical-generating capacity of feces from healthy volunteers. Am.

J. Clin. Nutr. *69*, 250–255.

Lupp, C., Robertson, M.L., Wickham, M.E., Sekirov, I., Champion, O.L., Gaynor, E.C., and Finlay, B.B. (2007). Host-Mediated Inflammation Disrupts the Intestinal Microbiota and Promotes the Overgrowth of Enterobacteriaceae. Cell Host Microbe *2*, 119–129.

Ma, Q., and Wood, T.K. (2009). OmpA influences Escherichia colibiofilm formation by repressing cellulose production through the CpxRA two-component system. Environmental Microbiology *11*, 2735–2746.

Manichanh, C., Borruel, N., Casellas, F., and Guarner, F. (2012). The gut microbiota in IBD. Nat Rev Gastroenterol Hepatol *9*, 599–608.

Martin, H.M., Campbell, B.J., Hart, C.A., Mpofu, C., Nayar, M., Singh, R., Englyst, H., Williams, H.F., and Rhodes, J.M. (2004). Enhanced Escherichia coli adherence and invasion in Crohn's disease and colon cancer. Gastroenterology *127*, 80–93.

Martinez, C., Antolín, M., Santos, J., Torrejon, A., Casellas, F., Borruel, N., Guarner, F., and Malagelada, J.-R. (2008). Unstable Composition of the Fecal Microbiota in Ulcerative Colitis During Clinical Remission. Am J Gastroenterology *103*, 643–648.

Martinez-Medina, M., Aldeguer, X., Lopez-Siles, M., González-Huix, F., López-Oliu, C., Dahbi, G., Blanco, J.E., Blanco, J., Garcia-Gil, L.J., and Darfeuille-Michaud, A. (2009a). Molecular diversity of Escherichia coli in the human gut: new ecological evidence supporting the role of adherent-invasive E. coli (AIEC) in Crohn's disease. Inflamm Bowel Dis *15*, 872–882.

Martinez-Medina, M., Denizot, J., Dreux, N., Robin, F., Billard, E., Bonnet, R., Darfeuille-Michaud, A., and Barnich, N. (2013). Western diet induces dysbiosis with increased E coli in CEABAC10 mice, alters host barrier function favouring AIEC colonisation. Gut *63*, 116–124.

Martinez-Medina, M., Naves, P., Blanco, J., Aldeguer, X., Blanco, J.E., Blanco, M., Ponte, C., Soriano, F., Darfeuille-Michaud, A., and Garcia-Gil, L.J. (2009b). Biofilm formation as a novel phenotypic feature of adherent-invasive Escherichia coli (AIEC). BMC Microbiol. *9*, 202.

Massé, E., and Gottesman, S. (2002). A small RNA regulates the expression of genes involved in iron metabolism in Escherichia coli. Proc Natl Acad Sci USA *99*, 4620–4625.

McHugh, J.P., Rodríguez-Quinoñes, F., Abdul-Tehrani, H., Svistunenko, D.A., Poole, R.K., Cooper, C.E., and Andrews, S.C. (2003). Global iron-dependent gene regulation in Escherichia coli. A new mechanism for iron homeostasis. J Biol Chem *278*, 29478–29486.

Mecklenburg, I., Reznik, D., Fasler-Kan, E., Drewe, J., Beglinger, C., and Hruz, P. (2014). Serum hepcidin concentrations correlate with ferritin in patients with inflammatory bowel disease. Journal of Crohn's and Colitis *8*, 1392–1397.

Medeiros, P., Bolick, D.T., Roche, J.K., Noronha, F., Pinheiro, C., Kolling, G.L., Lima, A., and Guerrant, R.L. (2014). The micronutrient zinc inhibits EAEC strain 042 adherence, biofilm formation, virulence gene expression, and epithelial cytokine responses benefiting the infected

host. Virulence *4*, 624–633.

Monteiro, C., Saxena, I., Wang, X., Kader, A., Bokranz, W., Simm, R., Nobles, D., Chromek, M., Brauner, A., Brown, R.M., Jr, et al. (2009). Characterization of cellulose production in Escherichia coliNissle 1917 and its biological consequences. Environmental Microbiology *11*, 1105–1116.

Morgan, X.C., Tickle, T.L., Sokol, H., Gevers, D., Devaney, K.L., Ward, D.V., Reyes, J.A., Shah, S.A., LeLeiko, N., Snapper, S.B., et al. (2012). Dysfunction of the intestinal microbiome in inflammatory bowel disease and treatment. Genome Biology *13*, R79.

Muegge, B.D., Kuczynski, J., Knights, D., Clemente, J.C., González, A., Fontana, L., Henrissat, B., Knight, R., and Gordon, J.I. (2011). Diet drives convergence in gut microbiome functions across mammalian phylogeny and within humans. Science *332*, 970–974.

Nagy, G., Dobrindt, U., Kupfer, M., Emody, L., Karch, H., and Hacker, J. (2001). Expression of Hemin Receptor Molecule ChuA Is Influenced by RfaH in Uropathogenic Escherichia coli Strain 536. Infect Immun *69*, 1924–1928.

Nemeth, E., Rivera, S., Gabayan, V., Keller, C., Taudorf, S., Pedersen, B.K., and Ganz, T. (2004a). IL-6 mediates hypoferremia of inflammation by inducing the synthesis of the iron regulatory hormone hepcidin. J Clin Invest *113*, 1271–1276.

Nemeth, E., Tuttle, M.S., Powelson, J., Vaughn, M.B., Donovan, A., Ward, D.M., Ganz, T., and Kaplan, J. (2004b). Hepcidin regulates cellular iron efflux by binding to ferroportin and inducing its internalization. Science *306*, 2090–2093.

Ogasawara, H., Shinohara, S., Yamamoto, K., and Ishihama, A. (2012). Novel regulation targets of the metal-response BasS-BasR two-component system of Escherichia coli. Microbiology (Reading, Engl.) *158*, 1482–1492.

Omadjela, O., Narahari, A., Strumillo, J., Mélida, H., Mazur, O., Bulone, V., and Zimmer, J. (2013). BcsA and BcsB form the catalytically active core of bacterial cellulose synthase sufficient for in vitro cellulose synthesis. Proceedings of the National Academy of Sciences *110*, 17856–17861.

Oustamanolakis, P., Koutroubakis, I.E., Messaritakis, I., Malliaraki, N., Sfiridaki, A., and Kouroumalis, E.A. (2011). Serum hepcidin and prohepcidin concentrations in inflammatory bowel disease. European Journal of Gastroenterology & Hepatology *23*, 262–268.

Patwa, L.G., Fan, T.-J., Tchaptchet, S., Liu, Y., Lussier, Y.A., Sartor, R.B., and Hansen, J.J. (2011). Chronic intestinal inflammation induces stress-response genes in commensal Escherichia coli. Gastroenterology *141*, 1842–51.e1–10.

Pereira, D.I.A., Aslam, M.F., Frazer, D.M., Schmidt, A., Walton, G.E., McCartney, A.L., Gibson, G.R., Anderson, G.J., and Powell, J.J. (2014). Dietary iron depletion at weaning imprints low microbiome diversity and this is not recovered with oral nano Fe(III). MicrobiologyOpen *4*, 12–27.

Perry, R.D., and Fetherston, J.D. (2011). Yersiniabactin iron uptake: mechanisms and role in Yersinia pestis pathogenesis. Microbes and Infection *13*, 808–817.

Pirzer, U., Schoenhaar, A., Fleischer, B., Hermann, E., and Meyer zum Buschenfelde, K.H. (1991). Reactivity of infiltrating T lymphocytes with microbial antigens in Crohn's disease. *338*, 1238–1129.

Pontes, M.H., Lee, E.-J., Choi, J., and Groisman, E.A. (2015). Salmonella promotes virulence by repressing cellulose production. Proceedings of the National Academy of Sciences *112*, 5183–5188.

Raffatellu, M., George, M.D., Akiyama, Y., Hornsby, M.J., Nuccio, S.-P., Paixao, T.A., Butler, B.P., Chu, H., Santos, R.L., Berger, T., et al. (2009). Lipocalin-2 resistance confers an advantage to Salmonella enterica serotype Typhimurium for growth and survival in the inflamed intestine. Cell Host Microbe *5*, 476–486.

Raterman, E.L., Shapiro, D.D., Stevens, D.J., Schwartz, K.J., and Welch, R.A. (2013). Genetic analysis of the role of yfiR in the ability of Escherichia coli CFT073 to control cellular cyclic dimeric GMP levels and to persist in the urinary tract. Infect Immun *81*, 3089–3098.

Rizvi, S., and Schoen, R.E. (2011). Supplementation with oral vs. intravenous iron for anemia with IBD or gastrointestinal bleeding: is oral iron getting a bad rap? Am J Gastroenterology *106*, 1872–1879.

Rolhion, N., Barnich, N., Bringer, M.-A., Glasser, A.-L., Ranc, J., Hébuterne, X., Hofman, P., and Darfeuille-Michaud, A. (2010). Abnormally expressed ER stress response chaperone Gp96 in CD favours adherent-invasive Escherichia coli invasion. Gut *59*, 1355–1362.

Rolhion, N., Barnich, N., Claret, L., and Darfeuille-Michaud, A. (2005). Strong decrease in invasive ability and outer membrane vesicle release in Crohn's disease-associated adherent-invasive Escherichia coli strain LF82 with the yfgL gene deleted. J Bacteriol *187*, 2286–2296.

Rolhion, N., Carvalho, F.A., and Darfeuille-Michaud, A. (2007). OmpC and the sigma(E) regulatory pathway are involved in adhesion and invasion of the Crohn's disease-associated Escherichia coli strain LF82. Mol Microbiol *63*, 1684–1700.

Rowe, M.C., Withers, H.L., and Swift, S. (2010). Uropathogenic Escherichia coli forms biofilm aggregates under iron restriction that disperse upon the supply of iron. FEMS Microbiol Lett *307*, 102–109.

Römling, U., Sierralta, W.D., Eriksson, K., and Normark, S. (1998). Multicellular and aggregative behaviour of Salmonella typhimurium strains is controlled by mutations in the agfD promoter. Mol Microbiol *28*, 249–264.

Römling, U. (2002). Molecular biology of cellulose production in bacteria. Research in Microbiologoy *153*, 205–212.

Sabri, M., Léveillé, S., and Dozois, C.M. (2006). A SitABCD homologue from an avian

pathogenic Escherichia coli strain mediates transport of iron and manganese and resistance to hydrogen peroxide. Microbiology (Reading, Engl.) *152*, 745–758.

Sadaghian Sadabad, M., Regeling, A., de Goffau, M.C., Blokzijl, T., Weersma, R.K., Penders, J., Faber, K.N., Harmsen, H.J.M., and Dijkstra, G. (2014). The ATG16L1-T300A allele impairs clearance of pathosymbionts in the inflamed ileal mucosa of Crohn's disease patients. Gut.

Saldaña, Z., Xicohtencatl-Cortes, J., Avelino, F., Phillips, A.D., Kaper, J.B., Puente, J.L., and Girón, J.A. (2009). Synergistic role of curli and cellulose in cell adherence and biofilm formation of attaching and effacing Escherichia coliand identification of Fis as a negative regulator of curli. Environmental Microbiology *11*, 992–1006.

Sartor, R.B. (2008). Microbial influences in inflammatory bowel diseases. Gastroenterology *134*, 577–594.

Sasaki, M., Sitaraman, S.V., Babbin, B.A., Gerner-Smidt, P., Ribot, E.M., Garrett, N., Alpern, J.A., Akyildiz, A., Theiss, A.L., Nusrat, A., et al. (2007). Invasive Escherichia coli are a feature of Crohn's disease. Lab. Invest. *87*, 1042–1054.

Schumann, S., Alpert, C., Engst, W., Klopfleisch, R., Loh, G., Bleich, A., and Blaut, M. (2013). Mild gut inflammation modulates the proteome of intestinal Escherichia coli. Environmental Microbiology *16*, 2966–2979.

Schümann, K., Herbach, N., Kerling, C., Seifert, M., Fillebeen, C., Prysch, I., Reich, J., Weiss, G., and Pantopoulos, K. (2010). Iron absorption and distribution in TNFΔARE/+ mice, a model of chronic inflammation. J Trace Elem Med Biol *24*, 58–66.

Searle, L.J., Méric, G., Porcelli, I., Sheppard, S.K., and Lucchini, S. (2015). Variation in siderophore biosynthetic gene distribution and production across environmental and faecal populations of Escherichia coli. PLoS ONE *10*, e0117906.

Sellon, R.K., Tonkonogy, S., Schultz, M., Dieleman, L.A., Grenther, W., Balish, E., Rennick, D.M., and Sartor, R.B. (1998). Resident enteric bacteria are necessary for development of spontaneous colitis and immune system activation in interleukin-10-deficient mice. Infect Immun *66*, 5224–5231.

Seo, S.W., Kim, D., Latif, H., O'Brien, E.J., Szubin, R., and Palsson, B.O. (2014). Deciphering Fur transcriptional regulatory network highlights its complex role beyond iron metabolism in Escherichia coli. Nature Communications *5*, 4910.

Sepehri, S., Kotlowski, R., Bernstein, C.N., and Krause, D.O. (2009). Phylogenetic analysis of inflammatory bowel disease associated Escherichia coli and the fimH virulence determinant. Inflamm Bowel Dis *15*, 1737–1745.

Serra, D.O., Richter, A.M., and Hengge, R. (2013). Cellulose as an architectural element in spatially structured Escherichia coli biofilms. J Bacteriol *195*, 5540–5554.

Shanmugam, N.K.N., Trebicka, E., Fu, L.L., Shi, H.N., and Cherayil, B.J. (2014). Intestinal

Inflammation Modulates Expression of the Iron-Regulating Hormone Hepcidin Depending on Erythropoietic Activity and the Commensal Microbiota. The Journal of Immunology *193*, 1398–1407.

Simpson, K.W., Dogan, B., Rishniw, M., Goldstein, R.E., Klaessig, S., McDonough, P.L., German, A.J., Yates, R.M., Russell, D.G., Johnson, S.E., et al. (2006). Adherent and Invasive Escherichia coli Is Associated with Granulomatous Colitis in Boxer Dogs. Infect Immun *74*, 4778–4792.

Small, C.-L.N., Reid-Yu, S.A., McPhee, J.B., and Coombes, B.K. (2013). Persistent infection with Crohn's disease-associated adherent-invasive Escherichia coli leads to chronic inflammation and intestinal fibrosis. Nature Communications *4*, 1957.

Sokol, H., Pigneur, B., Watterlot, L., Lakhdari, O., Bermu'dez-Humara'n, L.G., Gratadoux, J.-J., Blugeon, S., Bridonneau, C., Furet, J.-P., Corthier, G., et al. (2008). Faecalibacterium prausnitzii is an anti-inflammatory commensal bacterium identified by gut microbiota analysis of Crohn disease patients. Proceedings of the National Academy of Sciences *105*, 16731–16736.

Solano, C., García, B., Valle, J., Berasain, C., Ghigo, J.-M., Gamazo, C., and Lasa, I. (2002). Genetic analysis of Salmonella enteritidis biofilm formation: critical role of cellulose. Mol Microbiol *43*, 793–808.

Spurbeck, R.R., Tarrien, R.J., and Mobley, H.L.T. (2012). Enzymatically active and inactive phosphodiesterases and diguanylate cyclases are involved in regulation of Motility or sessility in Escherichia coli CFT073. mBio *3*.

Stein, J., Hartmann, F., and Dignass, A.U. (2010). Diagnosis and management of iron deficiency anemia in patients with IBD. Nat Rev Gastroenterol Hepatol *7*, 599–610.

Steinbach, E.C., and Plevy, S.E. (2014). The Role of Macrophages and Dendritic Cells in the Initiation of Inflammation in IBD. Inflamm Bowel Dis *20*, 166–175.

Stojiljkovic, I., Cobeljic, M., and Hantke, K. (1993). Escherichia coli K-12 ferrous iron uptake mutants are impaired in their ability to colonize the mouse intestine. FEMS Microbiol Lett *108*, 111–115.

Subramanian, S., Huq, S., Yatsunenko, T., Haque, R., Mahfuz, M., Alam, M.A., Benezra, A., DeStefano, J., Meier, M.F., Muegge, B.D., et al. (2014). Persistent gut microbiota immaturity in malnourished Bangladeshi children. Nature.

Theurl, I., Theurl, M., Seifert, M., Mair, S., Nairz, M., Rumpold, H., Zoller, H., Bellmann-Weiler, R., Niederegger, H., Talasz, H., et al. (2008). Autocrine formation of hepcidin induces iron retention in human monocytes. Blood *111*, 2392–2399.

Turnbaugh, P.J., Bäckhed, F., Fulton, L., and Gordon, J.I. (2008). Diet-induced obesity is linked to marked but reversible alterations in the mouse distal gut microbiome. Cell Host Microbe *3*, 213–223.

Turnbaugh, P.J., Ley, R.E., Mahowald, M.A., Magrini, V., Mardis, E.R., and Gordon, J.I. (2006). An obesity-associated gut microbiome with increased capacity for energy harvest. Nature *444*, 1027–1031.

Valdebenito, M., Crumbliss, A.L., Winkelmann, G., and Hantke, K. (2006). Environmental factors influence the production of enterobactin, salmochelin, aerobactin, and yersiniabactin in Escherichia coli strain Nissle 1917. Int J Med Microbiol *296*, 513–520.

Wang, L., Harrington, L., Trebicka, E., Shi, H.N., Kagan, J.C., Hong, C.C., Lin, H.Y., Babitt, J.L., and Cherayil, B.J. (2009). Selective modulation of TLR4-activated inflammatory responses by altered iron homeostasis in mice. J Clin Invest.

Wang, L., Johnson, E.E., Shi, H.N., Walker, W.A., Wessling-Resnick, M., and Cherayil, B.J. (2008). Attenuated inflammatory responses in hemochromatosis reveal a role for iron in the regulation of macrophage cytokine translation. The Journal of Immunology *181*, 2723–2731.

Wang, L., Trebicka, E., Fu, Y., Ellenbogen, S., Hong, C.C., Babitt, J.L., Lin, H.Y., and Cherayil, B.J. (2012). The bone morphogenetic protein-hepcidin axis as a therapeutic target in inflammatory bowel disease. Inflamm Bowel Dis *18*, 112–119.

Wang, X., Rochon, M., Lamprokostopoulou, A., Lünsdorf, H., Nimtz, M., and Römling, U. (2006). Impact of biofilm matrix components on interaction of commensal Escherichia coli with the gastrointestinal cell line HT-29. CMLS, Cell. Mol. Life Sci. *63*, 2352–2363.

Weber, H., Pesavento, C., Possling, A., Tischendorf, G., and Hengge, R. (2006). Cyclic-di-GMP-mediated signalling within the ? Snetwork of Escherichia coli. Mol Microbiol *62*, 1014–1034.

Wells, C.W., Lewis, S., Barton, J.R., and Corbett, S. (2006). Effects of changes in hemoglobin level on quality of life and cognitive function in inflammatory bowel disease patients. Inflamm Bowel Dis *12*, 123–130.

Werner, T., Wagner, S.J., Martínez, I., Walter, J., Chang, J.-S., Clavel, T., Kisling, S., Schuemann, K., and Haller, D. (2011). Depletion of luminal iron alters the gut microbiota and prevents Crohn's disease-like ileitis. Gut *60*, 325–333.

Winter, S.E., Winter, M.G., Xavier, M.N., Thiennimitr, P., Poon, V., Keestra, A.M., Laughlin, R.C., Gomez, G., Wu, J., Lawhon, S.D., et al. (2013). Host-Derived Nitrate Boosts Growth of E. coli in the Inflamed Gut. Science *339*, 708–711.

Wise, A.J., Hogan, J.S., Cannon, V.B., and Smith, K.L. (2002). Phagocytosis and serum susceptibility of Escherichia coil cultured in iron-deplete and iron-replete media. J Dairy Sci *85*, 1454–1459.

Wu, G.D., Chen, J., Hoffmann, C., Bittinger, K., Chen, Y.-Y., Keilbaugh, S.A., Bewtra, M., Knights, D., Walters, W.A., Knight, R., et al. (2011). Linking long-term dietary patterns with gut microbial enterotypes. Science *334*, 105–108.

Wu, X.-B., Tian, L.-H., Zou, H.-J., Wang, C.-Y., Yu, Z.-Q., Tang, C.-H., Zhao, F.-K., and Pan,

J.-Y. (2013). Outer membrane protein OmpW of Escherichia coli is required for resistance to phagocytosis. Research in Microbiologoy *164*, 848–855.

Wu, Y., and Outten, F.W. (2009). IscR Controls Iron-Dependent Biofilm Formation in Escherichia coli by Regulating Type I Fimbria Expression. J Bacteriol *191*, 1248–1257.

Yen, C.-C., Shen, C.-J., Hsu, W.-H., Chang, Y.-H., Lin, H.-T., Chen, H.-L., and Chen, C.-M. (2011). Lactoferrin: an iron-binding antimicrobial protein against Escherichia coli infection. Biometals *24*, 585–594.

Yen, D., Cheung, J., Scheerens, H., Poulet, F., McClanahan, T., Mckenzie, B., Kleinschek, M.A., Owyang, A., Mattson, J., Blumenschein, W., et al. (2006). IL-23 is essential for T cell–mediated colitis and promotes inflammation via IL-17 and IL-6. J Clin Invest *116*, 1310–1316.

Yoo, B.K., and Chen, J. (2009). Influence of Culture Conditions and Medium Composition on the Production of Cellulose by Shiga Toxin-Producing Escherichia coli Cells. Appl Environ Microbiol *75*, 4630–4632.

Zhang, Z., Geng, J., Tang, X., Fan, H., Xu, J., Wen, X., Ma, Z.S., and Shi, P. (2014). Spatial heterogeneity and co-occurrence patterns of human mucosal-associated intestinal microbiota. Isme J *8*, 881–893.

Zheng, M., Doan, B., Schneider, T.D., and Storz, G. (1999). OxyR and SoxRS regulation of fur. J Bacteriol *181*, 4639–4643.

Zimmermann, M.B., Chassard, C., Rohner, F., N'Goran, E.K., Nindjin, C., Dostal, A., Utzinger, J., Ghattas, H., Lacroix, C., and Hurrell, R.F. (2010). The effects of iron fortification on the gut microbiota in African children: a randomized controlled trial in Cote d'Ivoire. American Journal of Clinical Nutrition *92*, 1406–1415.

Zoetendal, E.G., Wright, von, A., Vilpponen-Salmela, T., Ben-Amor, K., Akkermans, A.D.L., and de Vos, W.M. (2002). Mucosa-Associated Bacteria in the Human Gastrointestinal Tract Are Uniformly Distributed along the Colon and Differ from the Community Recovered from Feces. Appl Environ Microbiol *68*, 3401–3407.

Zogaj, X., Nimtz, M., Rohde, M., Bokranz, W., and Römling, U. (2001). The multicellular morphotypes of Salmonella typhimurium and Escherichia coli produce cellulose as the second component of the extracellular matrix. Mol Microbiol *39*, 1452–1463.

CHAPTER 2

ALTERED ENTERIC MICROBIOTA ECOLOGY IN INTERLEUKIN-10-DEFICIENT MICE DURING DEVELOPMENT AND PROGRESSION OF INTESTINAL INFLAMMATION [1]

2.1 Personal contributions to manuscript

I am a co-author on the manuscript entitled "Altered enteric microbiota ecology in interleukin-10-deficient mice during development and progression of intestinal inflammation," published in *Gut Microbes* in 2013. I contributed to the manuscript by running the animal experiments in which we colonized ex-germ free (GF) mice with a complex microbial community and harvested all necessary samples required for assessment of histopathology, cytokine production and microbiota analysis. I also scored histology sections to assess the severity of inflammation and processed tissue samples to quantify cytokine production, which significantly contributed to the data presented in Figure 1. Additionally, I isolated DNA from fecal samples for 16S rRNA sequencing and subsequent microbiota analysis, the results of which are presented in Figures 2 – 5. Finally, I also assisted in editing the manuscript prior to submission to *Gut Microbes.*

2.2 Overview

[1]Nitsan Maharsak, Christopher D. Packey, Melissa Ellermann, Sayeed Manick, Jennica P. Siddle, Eun Young Huh, Scott Plevy, R. Balfour Sartor and Ian M. Carroll. 2013. Altered enteric microbiota ecology in interleukin-10-deficient mice during development and progression of intestinal inflammation. *Gut Microbes* 4(4):316-324.

Inflammatory bowel diseases (IBD) result from dysregulated immune responses toward microbial and perhaps other luminal antigens in a genetically susceptible host, and are associated with altered composition and diversity of the intestinal microbiota. The interleukin-10-deficient (*Il10*$^{-/-}$) mouse has been widely used to model human IBD; however the specific alterations that occur in the intestinal microbiota of this mouse model during the onset of colonic inflammation have not yet been defined. The aim of our study was to define the changes in diversity and composition that occur in the intestinal microbiota of *Il10*$^{-/-}$ mice during the onset and progression of colonic inflammation. We used high throughput sequencing of the 16S rRNA gene to characterize the diversity and composition of formerly germ-free (GF) wild type (WT) and *Il10*$^{-/-}$ mice associated with the same intestinal microbiota over time. Following two weeks of colonization with a specific pathogen-free (SPF) microbiota, we observed a significant increase in the diversity and richness of the intestinal microbiota of WT mice. In contrast, a progressive decrease in diversity and richness was observed at three and four weeks in *Il10*$^{-/-}$ mice. This decrease in diversity and richness was mirrored by an increase in Proteobacteria and *Escherichia coli* in *Il10*$^{-/-}$ mice. An increase in *E. coli* was also observed in conventionally raised *Il10*$^{-/-}$ mice at the point of colonic inflammation. Our data report the sequential changes in diversity and composition of the intestinal microbiota in an immune-mediated mouse model that may help provide insights into the primary vs. secondary role of dysbiosis in human IBD patients.

2.3 Introduction

Ulcerative colitis (UC) and Crohn disease (CD), collectively known as inflammatory bowel diseases (IBD), are prevalent in the United States (US) affecting 1.4 million individuals

(Xavier and Podolsky, 2007), are associated with reduced quality of life (Cohen, 2002) and a heavy economic burden that is estimated to be $6.3 billion annually in the US (Kappelman et al., 2008). The chronic nature, high rate of recurrence and lack of safe and curative medical treatments for IBD underscore the need for alternate therapeutic approaches for these complex diseases. Although, the precise pathophysiology of IBD remains unclear, it is widely accepted that the pathogenesis of IBD involves dysregulated immune responses toward microbial and other luminal antigens in a genetically susceptible host (Packey and Sartor, 2008) (Packey and Sartor, 2009) (Albenberg et al., 2012) (Shanahan, 2012). Environmental factors also play an important role in the initiation and reactivation of inflammation in IBD (Packey and Sartor, 2008) (Sartor, 2008). An altered composition of the intestinal microbiota (dysbiosis) has been reported for both UC and CD (Frank et al., 2007) (Willing et al., 2010) (Gophna et al., 2006), however this association is not as profound in recent pediatric studies (Kellermayer et al., 2012) (Hansen et al., 2012). Moreover, the primary vs. secondary nature of an intestinal microbial dysbiosis in IBD remains unknown. Thus, more in depth characterization of sequential enteric microbial changes during early and later phases of the inflammatory process may enable the development of better therapeutic strategies for these diseases.

Among the various rodent models for IBD, interleukin-10-deficient (*Il10*$^{-/-}$) mice are widely used for mechanistic studies investigating the pathogenesis of spontaneous, immune-mediated, chronic intestinal inflammation (Büchler et al., 2012) (Barnett et al., 2010) (Hansen et al., 2009). *Il10*$^{-/-}$ mice maintained in germ-free (GF) conditions do not develop intestinal inflammation. However, once colonized with conventional or specific pathogen free (SPF) microbiota, *Il10*$^{-/-}$ mice develop intestinal inflammation as early as one week following colonization with an SPF microbiota (Sellon et al., 1998). Although alterations in the intestinal

microbiota in subsets of IBD patients with established disease compared with healthy controls have been reported (Frank et al., 2007) (Willing et al., 2010) (Sokol et al., 2008), early changes in the composition and diversity of this complex microbial community at the onset of disease cannot be studied in the human intestinal tract, as it is impossible to predict who will develop disease (Sartor, 2008) (Garrett et al., 2010). Currently, little is known about the changes in composition and diversity of the enteric microbiota of *Il10*$^{-/-}$ mice during the onset of intestinal inflammation. Molecular methods are effectively used to characterize the intestinal microbiota due to the limitations of culture-based methods. A study using 16S rRNA-based fingerprinting techniques (denaturing gradient gel electrophoresis [DGGE] and repetitive DNA element-based PCR) reported compositional changes in the intestinal microbiota in *Il10*$^{-/-}$ mice over time (Bibiloni et al., 2005) (Pena et al., 2004); however due to the limitations in technology used for microbiota analysis, these studies provided limited data regarding the abundances of specific taxa and the diversity of the microbiota. Thus, we conducted the current study to characterize the intestinal microbiota of *Il10*$^{-/-}$ mice during the progression of colitis in comparison with wild type (WT) mice. We controlled for variations in the composition of the microbiota using previously GF *Il10*$^{-/-}$ and WT mice colonized with a microbiota from the same donor. We also characterized changes in diversity and composition of the intestinal microbiota in mice from two genetic backgrounds.

2.4 Results

2.4.1 16S rRNA gene sequences

The V1–3 regions of the 16S rRNA gene were amplified from all fecal DNA samples (n = 30). Following high throughput sequencing, four samples (three from week two of the *Il10*$^{-/-}$

group and one from week one of the WT group) yielded sequence numbers that were too low (< 350 16S rRNA sequences per sample) to be included in our analyses. An average of 8012 16S rRNA sequences per sample were obtained from the remaining 26 samples with the following ranges: WT week one (n = 4) 5647–10502 sequences; WT week two (n = 5) 6927–11490 sequences; *Il10*$^{-/-}$ week one (n = 5) 1115–8116 sequences; *Il10*$^{-/-}$ week two (n = 2) 9666–12789 sequences; *Il10*$^{-/-}$ week three (n = 5) 6162–8467 sequences; *Il10*$^{-/-}$ week four (n = 5) 1340–23189 sequences. To determine the numbers and abundances of different bacterial groups in each sample we used 97% similarity between 16S rRNA gene sequences as an indicator of a "species level" operational taxonomic unit (OTU). Using this procedure we found a total of 479 OTUs in our data set.

2.4.2 Intestinal microbial diversity decreases over time in formerly GF Il10$^{-/-}$ *mice*

In our initial investigation we sought to characterize changes in diversity in the intestinal microbiota that arise over time in formerly GF WT and *Il10*$^{-/-}$ mice. The microbiota was characterized in fecal samples collected weekly for two weeks in WT mice and for four weeks in *Il10*$^{-/-}$ mice following association with an SPF microbiota. Based on IL-12 p40 secretion from colonic tissue and composite histology scores, we found that WT mice did not develop significant inflammation whereas *Il10*$^{-/-}$ mice developed moderate intestinal inflammation four weeks following association with an SPF microbiota (Figure 1A and B).

We calculated UniFrac distances for all time points for each group. We found that average weighted and un-weighted UniFrac distances significantly increased (p = 0.003 and p = 8.5 x 10^{-5}, respectively) over the two-week observation period in the WT group (Figure 2C). We investigated the weighted and un-weighted UniFrac distances of the microbiota in fecal samples

obtained one, two, three and four weeks from formerly GF *Il10*$^{-/-}$ mice following association with an SPF microbiota. We found a significant decrease in average weighted UniFrac distances at the three-week ($p = 0.005$) and four-week ($p = 0.005$) time points compared with the 1-week time point (Figure 2A and B).

2.4.3 Intestinal microbial richness decreases over time in formerly GF Il10$^{-/-}$ *mice*

We determined the richness of the intestinal microbiota in all groups using rarefaction analysis. A significant increase ($p = 0.004$) in the number of observed microbial species was found in WT mice two weeks following association with an SPF microbiota when compared with the one-week time point (Figure 3B). In contrast, a significant decrease in the number of observed microbial species was found in *Il10*$^{-/-}$ mice three ($p = 0.02$) and four ($p = 0.009$) weeks following association with an SPF microbiota when compared with the one-week time point (Figure 3A).

2.4.4 Ecological succession of bacterial taxa in formerly GF Il10$^{-/-}$ *mice over time*

In order to determine the dominant bacterial groups that are altered over time in WT and *Il10*$^{-/-}$ mice following colonization with an SPF intestinal microbiota, we summarized the bacterial taxa identified by our 16S rRNA sequences at the phylum level (Figure 4). In WT mice, we found no significant changes in bacterial phyla between one and two weeks post association with an SPF microbiota. In the *Il10*$^{-/-}$ group, we observed a significant decrease in the levels of Bacteroidetes (20.06%–6.30%, false discovery rate [FDR] = 0.01) and Verrucomicrobia (0.74%–0.17%, FDR = 0.02) at three weeks compared with the one-week time point. These changes were further reduced by four weeks: Bacteroidetes (20.06–9.5%, FDR = 0.003) and Verrucomicrobia

(0.74%–0.09%, FDR = 0.02). At four weeks, we observed a significant increase in the levels of Proteobacteria (0.17%–7.71%, FDR = 1.5 Å~ 10−5) and Tenericutes (39.21%–70.66%, FDR = 0.07) compared with the one-week time point. In tandem, at four weeks we observed a decrease in the levels of Actinobacteria (1.27%–0.53%, FDR = 0.07) and Firmicutes (38.48%–11.46%, FDR = 0.03) compared with the one week time point. Additionally, we observed significant changes in the abundances of genus level taxa over time in *Il10*$^{-/-}$ mice (Table 1) and no significant changes in bacterial genera in WT mice over time.

2.4.5 Escherichia coli concentrations increase in formerly GF Il10$^{-/-}$ *mice over time*

Given that *E. coli* is a member of the Proteobacteria phylum and has been established as a proinflammatory microbe in the context of IBD (Darfeuille-Michaud et al., 2004), we used species-specific qPCR to determine the levels of this bacterial species in fecal samples from the *Il10*$^{-/-}$ group of mice. We found that the levels of *E. coli* in the intestinal microbiota of *Il10*$^{-/-}$ mice increased over time and became significantly higher at the four-week time point when compared with the week-one time point (Figure 5). The stepwise increase of *E. coli* over time in the *Il10*$^{-/-}$ group closely paralleled the increase in Proteobacteria in the same mice, confirming results by two different molecular methods (Figure 5).

2.4.6 Alterations in the abundance of E. coli in formerly GF Il10$^{-/-}$ *mice over time are mirrored in SPF Il10*$^{-/-}$ *mice*

In order to determine whether inflammation associated alterations of specific taxa in formerly GF *Il10*$^{-/-}$ mice are also altered in a gut that has developed naturally, we investigated the levels of *E. coli*, *Lactobacillus* species and *Akkermansia muciniphila* in WT and *Il10*$^{-/-}$ mice

raised in an SPF environment. This group of *Il10*$^{-/-}$ mice developed significant intestinal inflammation at 10 weeks of age compared with WT controls that did not develop inflammation (Figure 1C and D). Similarly to formerly GF mice, the abundance of *E. coli* was significantly higher in *Il10*$^{-/-}$ mice at week ten compared with WT mice (Figure 6A). *Akkermansia muciniphila* was significantly higher in *Il10*$^{-/-}$ mice compared with WT mice at both eight and ten weeks (Figure 6B). We did not observe any significant differences in the abundance of *Lactobacillus* species in *Il10*$^{-/-}$ mice compared with WT mice at either time point (Figure 6C).

2.5 Discussion

Based on the established association of the intestinal microbiota with IBD and the frequent use of the *Il10*$^{-/-}$ mouse as a model of spontaneous, immune-mediated colonic inflammation, we characterized the diversity and composition of the intestinal microbiota in this mouse model during the progression of experimental colitis. Previous studies characterizing the intestinal microbiota of *Il10*$^{-/-}$ mice focused on viable bacteria or used molecular techniques that characterize a limited number of bacterial taxa (Bibiloni et al., 2005) (Pena et al., 2004). Our study used a current molecular technique that provided a comprehensive characterization of the changes in microbial composition and diversity in WT and *Il10*$^{-/-}$ mice over time. Additionally, the use of formerly GF WT and *Il10*$^{-/-}$ mice colonized with the same fecal microbiota provided a highly controlled environment to study these changes.

In our investigations we observed an increase in microbial richness (as determined by rarefaction of bacterial species) and diversity (as determined by UniFrac distances) in formerly GF WT mice two weeks following association with an SPF microbiota. This finding suggests that the intestinal microbiota in formerly GF WT mice may still be establishing a homeostatic

balance two weeks after colonization. UniFrac distances can be calculated in a weighted (relative abundance of taxa) or un-weighted (presence or absence of taxa) manner. Low average UniFrac distances indicate higher similarity in the composition of the microbiota within a group of samples, whereas high average UniFrac distances indicate more dissimilarity within a group of samples. We observed an increase in both weighted and un-weighted UniFrac distances two weeks post colonization in WT mice, suggesting that the rise in diversity values at this time point is due to an increase in both high and low abundance bacterial species. A limitation of our study is that we did not investigate the microbial composition and diversity of fecal samples in formerly GF WT mice at three and four weeks following conventionalization with an intestinal microbiota. Thus we cannot conclude whether the intestinal microbiota has reached equilibrium at this point. Interestingly, it has been reported that the microbial composition and diversity of cecal contents in formerly GF WT mice, from a different genetic background (C57BL/6), exhibited stability seven days post-inoculation (Gillilland et al., 2012).

We subsequently characterized the richness and diversity of the intestinal microbiota in formerly GF *Il10*$^{-/-}$ mice up to four weeks following colonization with an SPF microbiota to investigate alterations in the intestinal microbiota during the progression of colitis. Indeed, we observed moderate inflammation at four weeks post colonization in *Il10*$^{-/-}$ mice. A progressive decrease in weighted UniFrac distances was observed three and four weeks post colonization in comparison with one-week values. In addition, the richness of the microbiota was significantly decreased in this cohort of mice at these later time points. Interestingly, we did not observe a significant decrease in un-weighted UniFrac distances at the three and four week time points compared with one week in *Il10*$^{-/-}$ mice. These data suggest that the composition of newly introduced, complex microbial communities in formerly GF *Il10*$^{-/-}$ mice become more alike

during the progression of colonic inflammation and that high abundance taxa are responsible for this change. In the absence of an established fecal marker indicative of intestinal inflammation, we are unable to conclude whether the alterations in the richness and diversity of the enteric microbiota in *Il10*$^{-/-}$ mice occur before, during or after the onset of colonic inflammation. In previous experiments we find that mild inflammation occurs in formerly GF *Il10*$^{-/-}$ mice on a 129 SvEv background two weeks following microbial colonization (Sellon et al., 1998). Our current study shows that enteric microbial richness and diversity dramatically changes at three weeks post association with an SPF microbiota. Thus, we speculate that decreases in enteric microbial richness and diversity in *Il10*$^{-/-}$ mice occur after the onset of colonic inflammation in this mouse model.

In tandem with altered enteric microbial richness and diversity in the intestinal microbiota of *Il10*$^{-/-}$ mice over time, we observed changes in the relative abundances of specific bacterial phyla. Most notable was a step-wise increase in the levels of Proteobacteria that mirrored a significant increase of *E. coli* during the onset of colonic inflammation. Elevated Proteobacteria levels have been reported in UC and CD patients (Frank et al., 2007). Moreover, adherent invasive *E. coli* strains are associated with ileal CD (Darfeuille-Michaud et al., 2004) (Wine et al., 2009). A significant depletion in the concentrations of the Bacteroidetes and Firmicutes phyla were observed over time in *Il10*$^{-/-}$ mice, which also reflect changes reported in the intestinal microbiota of human IBD (Frank et al., 2007) (Willing et al., 2010). Thus, our data demonstrate that the *Il10*$^{-/-}$ mouse model of colitis exhibits alterations in specific members of the intestinal microbiota that parallel those of human IBD. We also observed significant decreases in the levels of Actinobacteria and Verrucomicrobia, which have not been reported for human IBD and may be a consequence of enteric inflammation. It is interesting to note that *Bifidobacterium*

species are encompassed within the Actinobacteria phylum and are considered probiotic microbes. Alterations in the Verrucomicrobia phylum may be yet unreported components of a human IBD dysbiosis, or alternatively, they may be unique to this mouse model. However, it has been reported that *Akkermansia muciniphila* (a member of the Verrucomicrobia phylum) is depleted in the mucus of IBD patients (Png et al., 2010). Indeed, in support of this finding, our 16S rRNA sequence data revealed a significant decrease in the *Akkermansia* genus in *Il10*$^{-/-}$ mice over time. As bacterial richness and diversity decreased in *Il10*$^{-/-}$ mice over time, we observed a profound increase in the levels of the Tenericutes phylum. This phylum encompasses bacteria that lack a cell wall and are thus gram negative. Tenericutes have been reported to be significantly elevated in fecal samples from colonic Crohn's disease patients but decreased in fecal samples from ileal Crohn's disease and ulcerative colitis patients (Willing et al., 2010). From our data set, the dominant genus within the Tenericutes phylum is *Allobaculum*. However, although taxonomies were assigned to our 16S rRNA sequences using the Greengenes database (DeSantis et al., 2006), it is interesting to note that the RDP database (Cole et al., 2007) classifies the *Allobaculum* genus as belonging to the Firmicutes phylum, which would make the Firmicutes the dominant phylum in our data set. Nevertheless, it has been reported that the Greengenes database, which contains the largest and most diverse set of 16S rRNA sequences, is superior to other databases when classifying sequences at the phylum level, particularly with respect to the Tenericutes (Werner et al., 2012). It has been reported that GF mice have abnormal mucosal and immunologic maturation resulting in increased morbidity in the oxazolone-induced mouse model of colitis when compared with SPF mice (Olszak et al., 2012). Thus, we determined the abundances of specific bacterial groups in cohorts of WT and *Il10*$^{-/-}$ mice that were raised with a normal intestinal microbiota. Even though the mice used were of a different genetic background

(C57BL/6) to the mice used in our GF experiments, we observed an increase in the abundance of *E. coli* in *Il10*$^{-/-}$ mice compared with WT mice, suggesting a strong association of this bacterial species with the development of intestinal inflammation in this mouse model over time. We also found that although abundances of *A. muciniphila* and *Lactobacillus* species appeared to decrease over time in *Il10*$^{-/-}$ mice compared with WT mice, these decreases were not significant. Thus, it is possible that the alterations in the enteric microbiota during the development of intestinal inflammation that we observed in formerly GF *Il10*$^{-/-}$ mice are influenced by host genetics and an abnormal gut physiology associated with GF mice.

Our data reports the changes in diversity and composition of the intestinal microbiota in the *Il10*$^{-/-}$ mouse model of spontaneous, immune-mediated colitis over time. The reduction in diversity and most changes in specific bacterial taxa in the intestinal microbiota of this mouse model reflect the changes in this complex microbial community observed in human IBD patients. Thus, our study validates the use of this mouse model for studies relating to the intestinal microbiota and immune-mediated colonic inflammation. The progressive loss of diversity, of dominant commensal microbiota and expansion of Proteobacteria, notably *E. coli*, with increasing experimental inflammation suggests that dysbiosis is secondary to the immune response in this model. Despite the postulated secondary nature of the observed changes, the altered microbiota profiles may still be responsible for perpetuation and amplification of mucosal immune responses and inflammation, since we have documented enteric bacterial specific T-helper (Th)-1 and Th-17 responses in this model (Kim et al., 2005).

2.6 Materials and methods

Mice. Adult WT and *Il10*$^{-/-}$ 129 SvEv mice were maintained in a GF state at the National

Gnotobiotic Rodent Resource Center at UNC-Chapel Hill, NC USA. One group of WT (n = 5) and one group of *Il10*$^{-/-}$ (n = 5) mice were used in this study. Formerly GF mice were inoculated with fecal slurry obtained from a common SPF WT 129 SvEv donor mouse via oral and rectal swabbing (see Figure 7 for a schematic design of the study). Each experimental group (WT and *Il10*$^{-/-}$) consisted of mice from the same litter that were housed in separate cages. Fresh fecal pellets were obtained weekly from all mice. All fecal pellets collected were flash frozen immediately in liquid nitrogen to retain the integrity of the fecal microbiota. In order to translate our findings from GF animals to mice that were raised from birth with a normal microbiota, we investigated WT (n = 8) and *Il10*$^{-/-}$ (n = 9) C57BL/6 mice housed in a specific pathogen-free (SPF) environment. Each experimental group (WT and *Il10*$^{-/-}$) consisted of mice from the same litter that were housed in separate cages. Fecal samples were collected from all mice at eight and 10 weeks of age.

Assessment of intestinal inflammation. Sections of fixed (10% neutral buffered formalin) colons were embedded in paraffin and stained with hematoxylin and eosin. Using a well-validated scale (Sellon et al., 1998) (Veltkamp et al., 2001), the severity of inflammation was blindly assessed. Histological scores (0 to 4) were based on the degree of lamina propria and submucosal mononuclear cellular infiltration, crypt hyperplasia, goblet cell depletion and architectural distortion. A composite histology score was generated by the aggregate scores from the cecum and proximal and distal colon.

Colonic explant cultures were prepared as previously described (Sellon et al., 1998). Briefly, colonic tissue was thoroughly irrigated with phosphate-buffered saline (PBS), shaken at room temperature in Roswell Park Memorial Institute Medium (RPMI) containing 1% penicillin

and streptomycin (GIBCO) for 30 min at 280 rpm, cut into 1-mm fragments and weighed. Intestinal tissue fragments were then distributed (0.05 g per well) into 24-well plates and incubated in 1 mL of RPMI 1640 medium supplemented with 10% fetal bovine serum and 1% antibiotic/antimycotic (penicillin/streptomycin; GIBCO) for 22 h at 37 °C. Supernatants were collected and stored at −20 °C before use for cytokine quantification. Commercially available monoclonal anti-mouse IL-12 p40 capture and detection reagents (BD Biosciences PharMingen) in an enzyme-linked immunosorbent assay (ELISA) were used to measure the levels of IL-12 p40 secreted constitutively in colonic explant cultures (Sellon et al., 1998) (Veltkamp et al., 2001). IL-12 p40 levels were measured in supernatants and compared with standard curves generated by using recombinant murine IL-12 p40.

Isolation of DNA. Bacterial DNA was isolated from all fecal pellets (n = 47) using a phenol/chloroform extraction method combined with physical disruption of bacterial cells and a DNA clean-up kit (Qiagen DNeasy(R) Blood and Tissue extraction kit) as previously described (Gulati et al., 2012). Briefly, 100 mg of frozen feces were suspended in 750 µL of sterile bacterial lysis buffer (200 mM NaCl, 100 mM Tris [pH 8.0], 20 mM EDTA, 20 mg/mL lysozyme) and incubated at 37 °C for 30 min. Next, 40 µL of proteinase K (20 mg/mL) and 85 µL of 10% SDS were added to the mixture and incubated at 65 °C for 30 min. 300 mg of 0.1 mm zirconium beads (BioSpec Products) were then added and the mixture was homogenized in a bead beater (BioSpec Products) for 2 min. The homogenized mixture was cooled on ice and centrifuged at 14,000 rpm for 5 min. The supernatant was transferred to a new 1.5 ml microfuge tube and fecal DNA was further extracted by phenol/chloroform/iso-amyl alcohol (25:24:1) and chloroform/iso-amyl alcohol (24:1). Following extraction the supernatant was precipitated by

absolute ethanol at −20 °C for 1 h. The precipitated DNA was suspended in DNase free H2O and cleaned using the Qiagen DNeasy(R) Blood and Tissue extraction kit per the manufacturer's instructions.

454 pyro-sequencing of 16S rRNA genes. Bacterial community composition in isolated DNA samples was characterized by amplification of the V1–3 (forward, 8f: 5' AGAGTTTGATCMTGGCTCAG-3'; reverse 518r: 5'-ATTACCGCGGCTGCTGG-3') variable regions of the 16S rRNA gene by polymerase chain reaction (PCR) as previously described (Carroll et al., 2012). Forward primers were tagged with 10 bp unique barcode labels at the 5' end along with the adaptor sequence (5'-CCATCTCATCCCTGCGTGTC TCCGACTCAG-3') to allow multiple samples to be included in a single 454 Genome Sequencer (GS) FLX Titanium sequencing plate as previously described (Hamady et al., 2008) (Fierer et al., 2008). 16S rRNA PCR products were quantified, pooled and purified for the sequencing reaction. 454 GS FLX Titanium sequencing was performed on a 454 Life Sciences GS FLX machine (Roche) at the Microbiome Core at UNC-Chapel Hill (http://www.med.unc.edu/microbiome).

Analysis of 16S rRNA sequences using the QIIME pipeline. 16S rRNA sequence data generated by the 454 GS FLX Titanium sequencer were processed by the quantitative insights into microbial ecology (QIIME) pipeline (Caporaso et al., 2010). Briefly, sequences that were less than 200 bp or greater than 1,000 bp in length, contained incorrect primer sequences or contained more than 1 ambiguous base were discarded. The remaining sequences were assigned to WT and *Il10*$^{-/-}$ groups based on their unique nucleotide barcodes, including error-correction (Hamady et al., 2008). Sequences were clustered into OTUs based on 97% sequence similarity

(similar to species level) using BLAST with the Greengenes reference database (McDonald et al., 2012). α-diversity (diversity within samples) was determined with ten iterations at a maximal sequence depth where all samples could be included. β-diversity (diversity between groups of samples) was calculated using weighted and un-weighted UniFrac distances (Lozupone and Knight, 2005) (Lozupone et al., 2011) (Lozupone et al., 2007). UniFrac distances are a β-diversity measure that utilizes phylogenetic information to compare environmental samples (Lozupone and Knight, 2005) (Lozupone et al., 2011).

Quantitative real-time PCR (qPCR). qPCR assays were performed using the SYBR(R) Green PCR Master Mix (Applied Biosystems) with primers that amplify the genes encoding 16S rRNA from *E. coli* (forward, 5'-GTTAATACCT TTGCTCATTG A-3'; reverse, 5'-ACCAGGGTAT CTAATCCTGT T-3'), *Lactobacillus* species (forward, 5'-AGCAGTAGGG AATCTTCCA-3'; reverse, 5'-CACCGCTACA CATGGAG-3'), *A. muciniphila* (forward, 5'-CAGCACGTGA AGGTGGGGAC-3'; reverse, 5'-CCTTGCGGTT GGCTTCAGAT-3') and all bacteria (forward, 5'-TGSTGCAYGG YTGTCGTCA-3'; reverse, 5'-ACGTCRTCCM CACCTTCCTC-3'). qPCR assays were conducted in 96-well plates on an Eppendorf Realplex2 mastercycler thermocycler (Eppendorf). Each PCR was performed in a final volume of 25 µL and contained the following: 1x SYBR Green Master Mix, 0.5 µM of each primer and 10 ng of purified fecal DNA. PCR conditions were as follows: 10 min at 95 °C, followed by 40 cycles of 95 °C for 15 sec, 20 sec at 50 °C and 72 °C for 30 sec. Each plate included duplicate reactions per DNA sample, the appropriate set of standards and a "no template" negative control for each primer set. qPCR standards were generated by PCR amplification of target sequences from genomic DNA of an appropriate positive control strain. Analysis of melting curves confirmed that the fluorescence

signal originated from specific PCR products and not from primer-dimers or other artifacts.

Statistical analyses. Bacterial taxon percentages and average UniFrac value data sets were assessed for normality using the D'Agostino and Pearson omnibus normality test prior to performing statistical analyses. When a data set was identified as not having a normal distribution, it was transformed by log10 (Ramette, 2007) and retested for normality. Normally distributed data sets were compared using a Student's *t*-test. All statistical comparisons were performed using GraphPad Prism software (v4.0a; Prism). We used taxon and phylogenetic-based analyses to compare 16S rRNA gene sequences within WT and *Il10*$^{-/-}$ groups over time. Taxon-based: the means and standard deviations of abundances of bacterial phyla were calculated and compared between all time-points for each group using the Benjamini–Hochberg procedure (Benjamini et al., 2001) to correct for multiple corrections. A *p* value of less than 0.05 and a FDR less than 0.1 was considered significant. Phylogenetic-based: phylogenetic trees for WT and *Il10*$^{-/-}$ groups were generated using the QIIME pipeline (Caporaso et al., 2010). Each tree was subjected to un-weighted and weighted UniFrac analyses (Lozupone and Knight, 2005) (Lozupone et al., 2011) through the QIIME pipeline. UniFrac distances represent the fraction of branch length that is shared by any two samples' communities in a phylogenetic tree built from 16S rRNA sequence data from all samples. Average UniFrac distances, which represent the similarity or dissimilarity of microbial communities within a group, were compared using a Student's *t*-test.

For qPCR assays, the percentage of *E. coli* was determined in all fecal samples ([copies 16S rRNA gene for *E. coli*/copies of 16S rRNA gene for all bacteria] x 100). The concentration of *E. coli* group was expressed as a "fold change" with respect to the concentration in the control

group (WT) at week 1 after colonization. qPCR data were compared between groups using a non-parametric Mann-Whitney test. Similarly, the concentrations of IL-12 p40 secreted by colonic tissue (pg/mL/mg of tissue) were compared between groups using a non-parametric Mann-Whitney test.

2.7 Figures

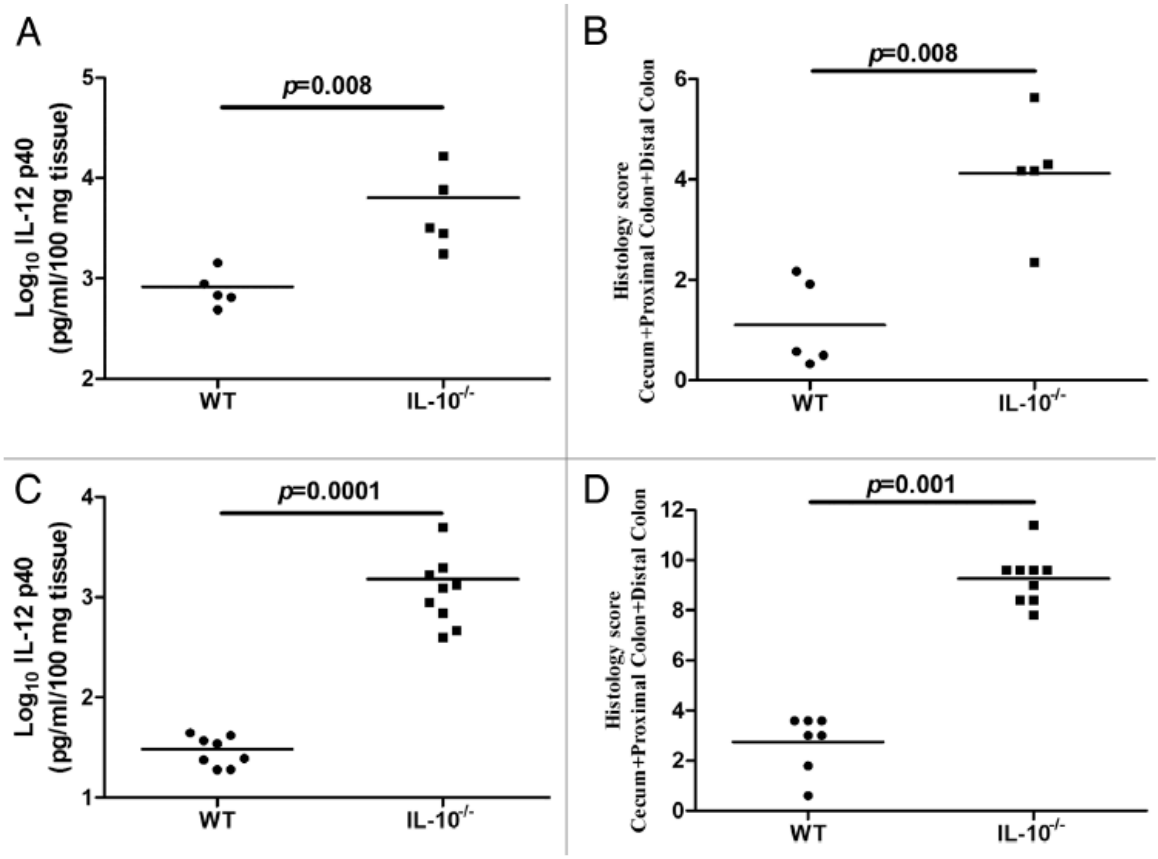

Figure 2.1. Inflammatory changes in the colons of formerly GF mice over time. (A, C) Levels of IL-12 p40 secreted by colonic tissues from formerly GF WT and *Il10*$^{-/-}$ mice (A) and SPF-raised WT and *Il10*$^{-/-}$ mice (C). The levels of IL-12 p40 in *Il10*$^{-/-}$ mice are significantly higher compared with WT mice in both formerly GF ($p = 0.008$) and SPF ($p = 0.0001$) environments. (B, D) Histological scores for formerly GF WT and *Il10*$^{-/-}$ mice (B) and SPF WT ($n = 7$, as one tissue sample degraded during processing) and *Il10*$^{-/-}$ mice (D). The degree of histological inflammation is significantly higher in *Il10*$^{-/-}$ compared with WT mice in formerly GF ($p = 0.008$) and SPF ($p = 0.001$) environments.

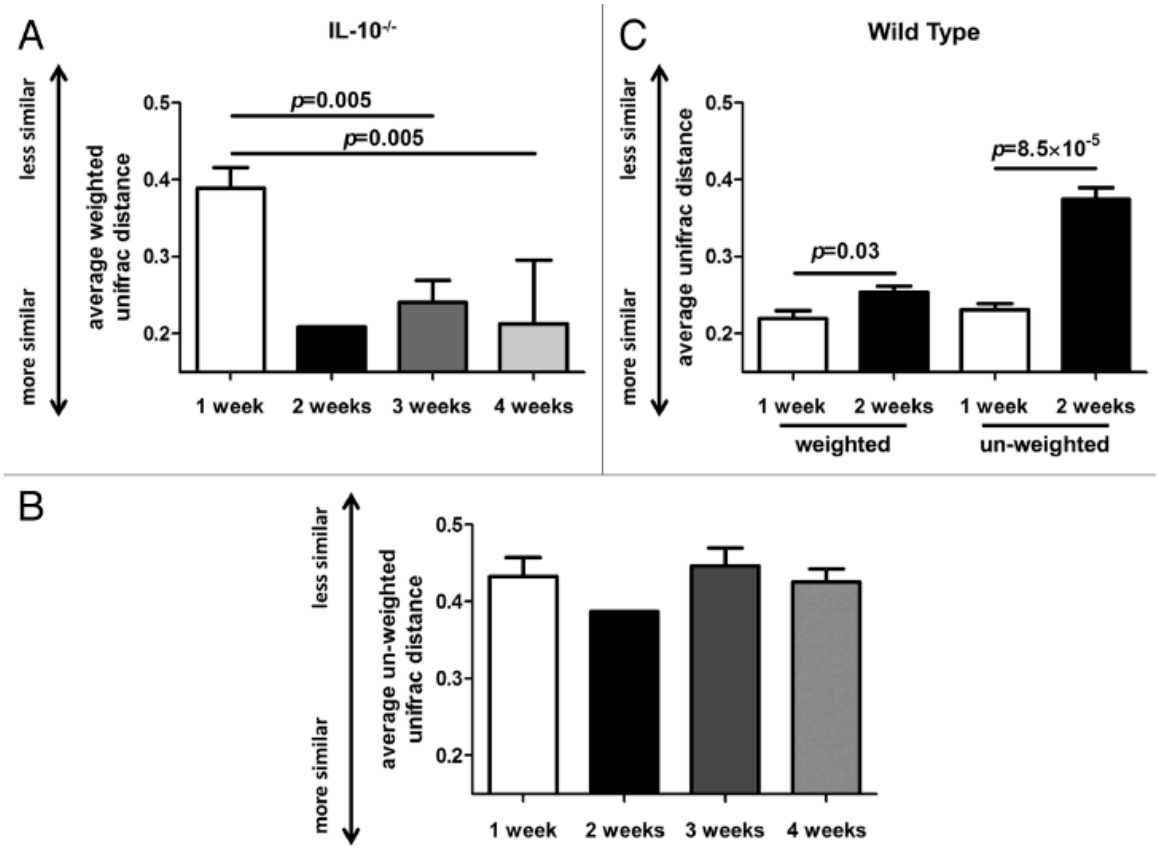

Figure 2.2. Changes in weighted and un-weighted average UniFrac distances in formerly GF WT and *Il10*$^{-/-}$ mice over time. (A) Average weighted UniFrac distances of the intestinal microbiota significantly decrease in *Il10*$^{-/-}$ mice three and four weeks following colonization with a SPF microbiota. (B) Average un-weighted UniFrac distances of the intestinal microbiota do not significantly alter in the *Il10*$^{-/-}$ mice following colonization with an SPF microbiota. (C) Average weighted and un-weighted UniFrac distances significantly increase in WT mice between one and two weeks following colonization with an SPF microbiota.

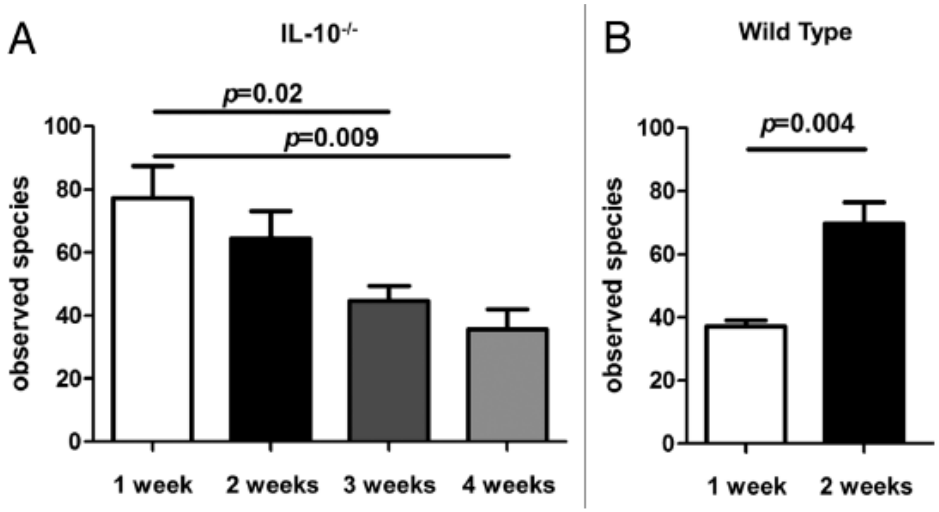

Figure 2.3. Microbial richness of 16S rRNA data. (A) The number of observed bacterial species in formerly GF *Il10*$^{-/-}$ mice decreases between one and four weeks following colonization with an SPF microbiota. (B) The number of observed bacterial species in formerly GF WT mice significantly increases between one and two weeks following colonization with an SPF microbiota.

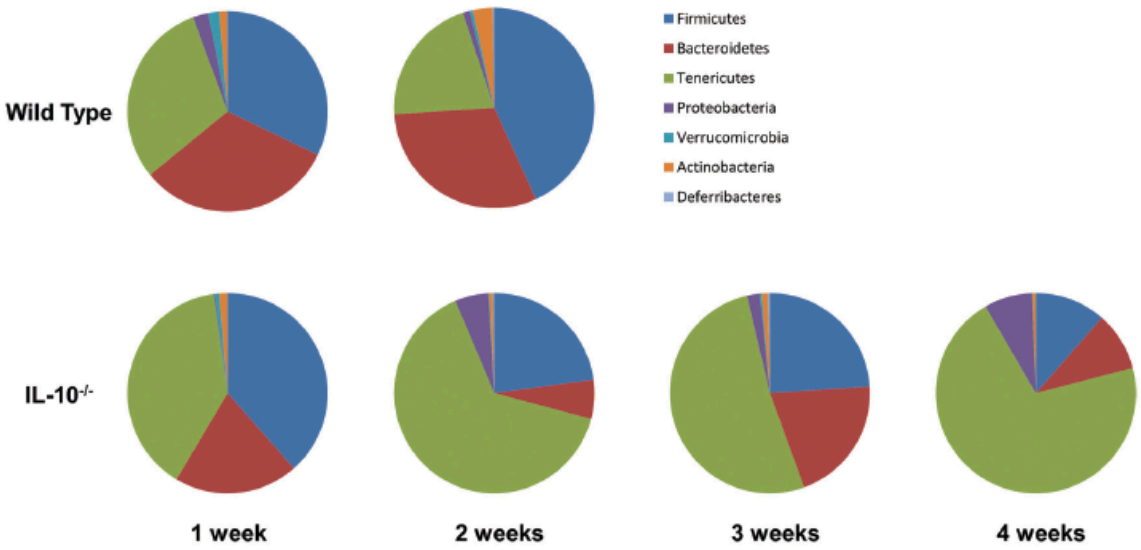

Figure 2.4. Bacterial taxa alterations over time in formerly GF WT and *Il10*$^{-/-}$ mice.

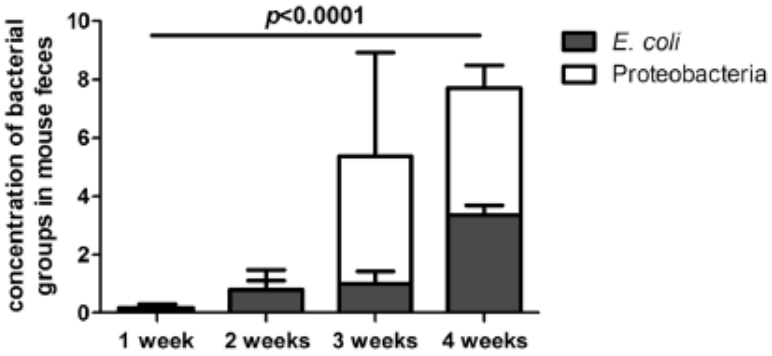

Figure 2.5. Change in levels of Proteobacteria and *E. coli* in formerly GF *Il10*$^{-/-}$ mice over time. Proteobacteria are expressed as the percentage of total 16S rRNA sequences. *E. coli* are expressed as fold increase with respect to baseline (WT at week 1). * The levels of Proteobacteria and *E. coli* are significantly higher at week 4 post colonization compared with week 1 (*E. coli*, $p = 0.0001$; Proteobacteria, FDR = 1.5×10^{-5}).

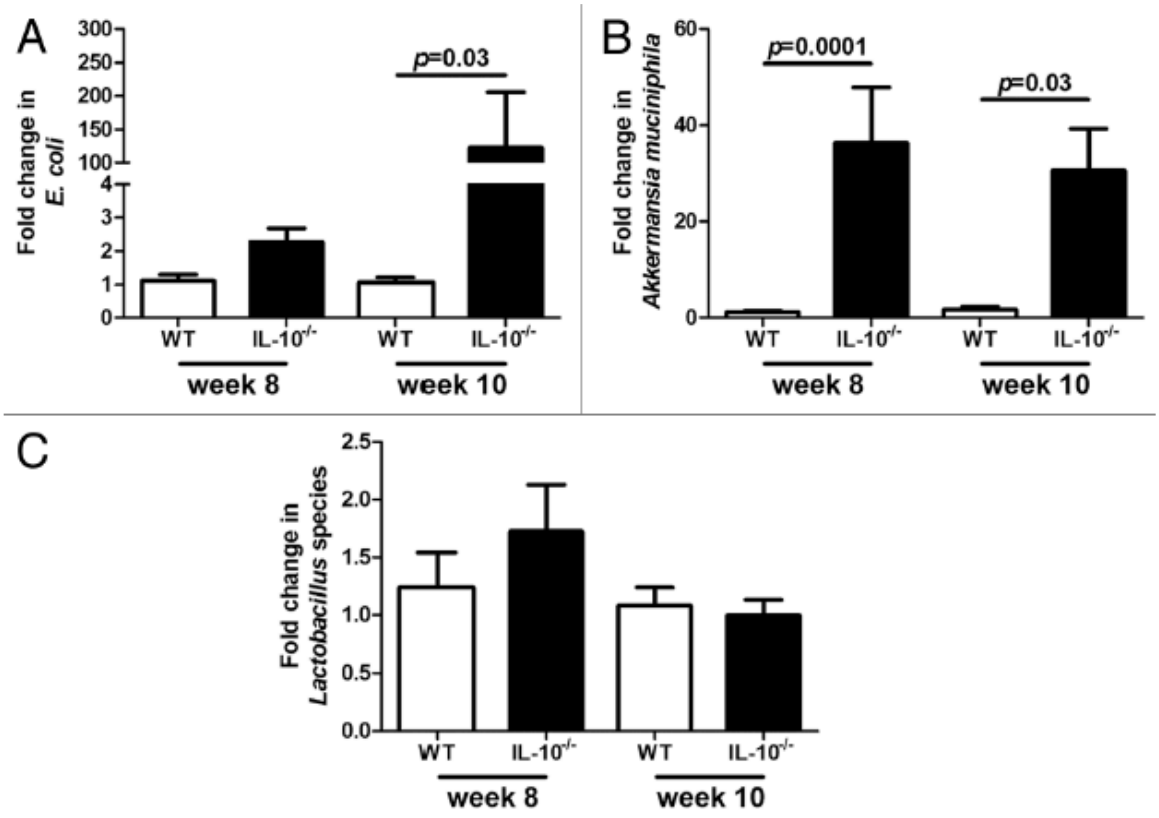

Figure 2.6. Change in levels of *E. coli* (A), *A. muciniphila* (B) and *Lactobacillus* species (C) in SPF WT and *Il10*$^{-/-}$ mice over time.

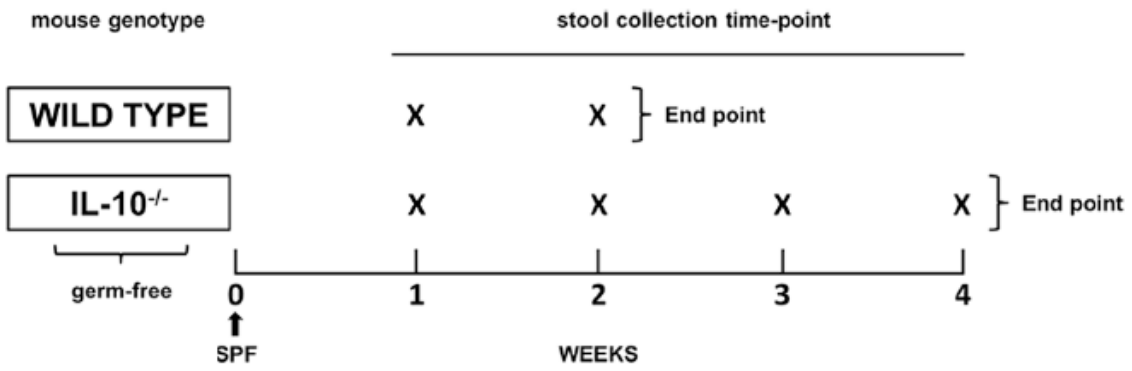

Figure 2.7. Schematic outline of experimental design. Adult WT and *Il10*$^{-/-}$ 129 SvEv GF mice were inoculated with an SPF microbiota from a single donor (black arrow). Fresh fecal pellets were obtained from the WT group (n = 5) at 1 and 2 weeks following SPF inoculation. Fecal pellets were obtained from the *Il10*$^{-/-}$ group (n = 5) at 1, 2, 3 and 4 weeks following association with an SPF intestinal microbiota.

Taxon	% week 1	% week 3	% week 4	*p*	FDR*
Coprobacillus	0.86	0.06		0.004	0.07
Akkermansia	0.75	0.17		0.007	0.06
Lactobacillus	1.20	12.83		0.008	0.05
Staphylococcus	0.50	0.00		0.020	0.10
Parabacteroides	9.15	4.05		0.023	0.10
Raoultella	0.00		0.08	0.002	0.03
Akkermansia	0.75		0.09	0.003	0.02
Clostridium	0.02		0.00	0.006	0.04
Enterobacter	0.10		5.14	0.009	0.04
Oscillospira	0.83		0.04	0.010	0.04

*False discovery rate (FDR) < 0.1 = statistically significant.

Table 2.1. Changes in the abundances of genus level taxa over time in formerly GF *Il10*$^{-/-}$ mice.

REFERENCES

Albenberg, L.G., Lewis, J.D., and Wu, G.D. (2012). Food and the gut microbiota in inflammatory bowel diseases. Curr Opin Gastroenterol *28*, 314–320.

Barnett, M.P., McNabb, W.C., Cookson, A.L., Zhu, S., Davy, M., Knoch, B., Nones, K., Hodgkinson, A.J., and Roy, N.C. (2010). Changes in colon gene expression associated with increased colon inflammation in interleukin-10 gene-deficient mice inoculated with Enterococcus species. BMC Immunol *11*, 39.

Benjamini, Y., Drai, D., Elmer, G., Kafkafi, N., and Golani, I. (2001). Controlling the false discovery rate in behavior genetics research. Behav. Brain Res. *125*, 279–284.

Bibiloni, R., Simon, M.A., Albright, C., Sartor, B., and Tannock, G.W. (2005). Analysis of the large bowel microbiota of colitic mice using PCR/DGGE. Lett. Appl. Microbiol. *41*, 45–51.

Büchler, G., Wos-Oxley, M.L., Smoczek, A., Zschemisch, N.-H., Neumann, D., Pieper, D.H., Hedrich, H.J., and Bleich, A. (2012). Strain-specific colitis susceptibility in IL10-deficient mice depends on complex gut microbiota–host interactions. Inflamm Bowel Dis *18*, 943–954.

Caporaso, J.G., Kuczynski, J., Stombaugh, J., Bittinger, K., Bushman, F.D., Costello, E.K., Fierer, N., Peña, A.G., Goodrich, J.K., Gordon, J.I., et al. (2010). QIIME allows analysis of high-throughput community sequencing data. Nat Meth *7*, 335–336.

Carroll, I.M., Ringel-Kulka, T., Siddle, J.P., and Ringel, Y. (2012). Alterations in composition and diversity of the intestinal microbiota in patients with diarrhea-predominant irritable bowel syndrome. Neurogastroenterology & Motility *24*, 521–e248.

Cohen, R.D. (2002). The quality of life in patients with Crohn's disease. Aliment Pharmacol Ther *16*, 1603–1609.

Cole, J.R., Chai, B., Farris, R.J., Wang, Q., Kulam-Syed-Mohideen, A.S., McGarrell, D.M., Bandela, A.M., Cardenas, E., Garrity, G.M., and Tiedje, J.M. (2007). The ribosomal database project (RDP-II): introducing myRDP space and quality controlled public data. Nucleic Acids Res. *35*, D169–D172.

Darfeuille-Michaud, A., Boudeau, J., Bulois, P., Neut, C., Glasser, A.-L., Barnich, N., Bringer, M.-A., Swidsinski, A., Beaugerie, L., and Colombel, J.-F. (2004). High prevalence of adherent-invasive Escherichia coli associated with ileal mucosa in Crohn's disease. Gastroenterology *127*, 412–421.

DeSantis, T.Z., Hugenholtz, P., Larsen, N., Rojas, M., Brodie, E.L., Keller, K., Huber, T., Dalevi, D., Hu, P., and Andersen, G.L. (2006). Greengenes, a Chimera-Checked 16S rRNA Gene Database and Workbench Compatible with ARB. Appl Environ Microbiol *72*, 5069–5072.

Fierer, N., Hamady, M., Lauber, C.L., and Knight, R. (2008). The influence of sex, handedness,

and washing on the diversity of hand surface bacteria. Proceedings of the National Academy of Sciences *105*, 17994–17999.

Frank, D.N., St Amand, A.L., Feldman, R.A., Boedeker, E.C., Harpaz, N., and Pace, N.R. (2007). Molecular-phylogenetic characterization of microbial community imbalances in human inflammatory bowel diseases. Proc Natl Acad Sci USA *104*, 13780–13785.

Garrett, W.S., Gordon, J.I., and Glimcher, L.H. (2010). Homeostasis and inflammation in the intestine. Cell *140*, 859–870.

Gillilland, M.G., Erb-Downward, J.R., Bassis, C.M., Shen, M.C., Toews, G.B., Young, V.B., and Huffnagle, G.B. (2012). Ecological Succession of Bacterial Communities during Conventionalization of Germ-Free Mice. Appl Environ Microbiol *78*, 2359–2366.

Gophna, U., Sommerfeld, K., Gophna, S., Doolittle, W.F., and Veldhuyzen van Zanten, S.J.O. (2006). Differences between Tissue-Associated Intestinal Microfloras of Patients with Crohn's Disease and Ulcerative Colitis. J. Clin. Microbiol. *44*, 4136–4141.

Gulati, A.S., Shanahan, M.T., Arthur, J.C., Grossniklaus, E., Furstenberg, von, R.J., Kreuk, L., Henning, S.J., Jobin, C., and Sartor, R.B. (2012). Mouse Background Strain Profoundly Influences Paneth Cell Function and Intestinal Microbial Composition. PLoS ONE *7*, e32403.

Hamady, M., Walker, J.J., Harris, J.K., Gold, N.J., and Knight, R. (2008). Error-correcting barcoded primers for pyrosequencing hundreds of samples in multiplex. Nat Meth *5*, 235–237.

Hansen, J.J., Holt, L., and Sartor, B.R. (2009). Gene expression patterns in experimental colitis in IL-10-deficient mice. Inflamm Bowel Dis *15*, 890–899.

Hansen, R., Russell, R.K., Reiff, C., Louis, P., McIntosh, F., Berry, S.H., Mukhopadhya, I., Bisset, W.M., Barclay, A.R., Bishop, J., et al. (2012). Microbiota of De-Novo Pediatric IBD: Increased Faecalibacterium Prausnitzii and Reduced Bacterial Diversity in Crohn's But Not in Ulcerative Colitis. Am J Gastroenterology *107*, 1913–1922.

Kappelman, M.D., Rifas Shiman, S.L., Porter, C.Q., Ollendorf, D.A., Sandler, R.S., Galanko, J.A., and Finkelstein, J.A. (2008). Direct Health Care Costs of Crohn's Disease and Ulcerative Colitis in US Children and Adults. Gastroenterology *135*, 1907–1913.

Kellermayer, R., Mir, S.A.V., Nagy-Szakal, D., Cox, S.B., Dowd, S.E., Kaplan, J.L., Sun, Y., Reddy, S., Bronsky, J., and Winter, H.S. (2012). Microbiota Separation and C-reactive Protein Elevation in Treatment-naïve Pediatric Granulomatous Crohn Disease. Journal of Pediatric Gastroenterology and Nutrition *55*, 243–250.

Kim, S.C., Tonkonogy, S.L., Albright, C.A., Tsang, J., Balish, E.J., Braun, J., Huycke, M.M., and Sartor, R.B. (2005). Variable phenotypes of enterocolitis in interleukin 10-deficient mice monoassociated with two different commensal bacteria. Gastroenterology *128*, 891–906.

Lozupone, C.A., Hamady, M., Kelley, S.T., and Knight, R. (2007). Quantitative and Qualitative Diversity Measures Lead to Different Insights into Factors That Structure Microbial

Communities. Appl Environ Microbiol *73*, 1576–1585.

Lozupone, C., and Knight, R. (2005). UniFrac: a New Phylogenetic Method for Comparing Microbial Communities. Appl Environ Microbiol *71*, 8228–8235.

Lozupone, C., Lladser, M.E., Knights, D., Stombaugh, J., and Knight, R. (2011). UniFrac: an effective distance metric for microbial community comparison. Isme J *5*, 169–172.

McDonald, D., Price, M.N., Goodrich, J., Nawrocki, E.P., DeSantis, T.Z., Probst, A., Andersen, G.L., Knight, R., and Hugenholtz, P. (2012). An improved Greengenes taxonomy with explicit ranks for ecological and evolutionary analyses of bacteria and archaea. Isme J *6*, 610–618.

Olszak, T., An, D., Zeissig, S., Vera, M.P., Richter, J., Franke, A., Glickman, J.N., Siebert, R., Baron, R.M., Kasper, D.L., et al. (2012). Microbial Exposure During Early Life Has Persistent Effects on Natural Killer T Cell Function. Science *336*, 489–493.

Packey, C.D., and Sartor, R.B. (2008). Interplay of commensal and pathogenic bacteria, genetic mutations, and immunoregulatory defects in the pathogenesis of inflammatory bowel diseases. J Intern Med *263*, 597–606.

Packey, C.D., and Sartor, R.B. (2009). Commensal bacteria, traditional and opportunistic pathogens, dysbiosis and bacterial killing in inflammatory bowel diseases. Curr. Opin. Infect. Dis. *22*, 292–301.

Pena, J.A., Li, S.Y., Wilson, P.H., Thibodeau, S.A., Szary, A.J., and Versalovic, J. (2004). Genotypic and phenotypic studies of murine intestinal lactobacilli: species differences in mice with and without colitis. Appl Environ Microbiol *70*, 558–568.

Png, C.W., n, S.K.L.E., Gilshenan, K.S., Zoetendal, E.G., McSweeney, C.S., Sly, L.I., McGuckin, M.A., and Florin, T.H.J. (2010). Mucolytic bacteria with increased prevalence in IBD mucosa augment in vitro utilization of mucin by other bacteria. Am J Gastroenterology *105*, 2420–2428.

Ramette, A. (2007). Multivariate analyses in microbial ecology. FEMS Microbiol. Ecol. *62*, 142–160.

Sartor, R.B. (2008). Microbial influences in inflammatory bowel diseases. Gastroenterology *134*, 577–594.

Sellon, R.K., Tonkonogy, S., Schultz, M., Dieleman, L.A., Grenther, W., Balish, E., Rennick, D.M., and Sartor, R.B. (1998). Resident enteric bacteria are necessary for development of spontaneous colitis and immune system activation in interleukin-10-deficient mice. Infect Immun *66*, 5224–5231.

Shanahan, F. (2012). The microbiota in inflammatory bowel disease: friend, bystander, and sometime-villain. Nutr Rev *70*, S31–S37.

Sokol, H., Pigneur, B., Watterlot, L., Lakhdari, O., Bermu'dez-Humara'n, L.G., Gratadoux, J.-J.,

Blugeon, S., Bridonneau, C., Furet, J.-P., Corthier, G., et al. (2008). Faecalibacterium prausnitzii is an anti-inflammatory commensal bacterium identified by gut microbiota analysis of Crohn disease patients. Proceedings of the National Academy of Sciences *105*, 16731–16736.

Veltkamp, C., Tonkonogy, S.L., De Jong, Y.P., Albright, C., Grenther, W.B., Balish, E., Terhorst, C., and Sartor, R.B. (2001). Continuous stimulation by normal luminal bacteria is essential for the development and perpetuation of colitis in Tg(epsilon26) mice. Gastroenterology *120*, 900–913.

Werner, J.J., Koren, O., Hugenholtz, P., DeSantis, T.Z., Walters, W.A., Caporaso, J.G., Angenent, L.T., Knight, R., and Ley, R.E. (2012). Impact of training sets on classification of high-throughput bacterial 16s rRNA gene surveys. Isme J *6*, 94–103.

Willing, B.P., Dicksved, J., Halfvarson, J., Andersson, A.F., Lucio, M., Zheng, Z., Järnerot, G., Tysk, C., Jansson, J.K., and Engstrand, L. (2010). A pyrosequencing study in twins shows that gastrointestinal microbial profiles vary with inflammatory bowel disease phenotypes. Gastroenterology *139*, 1844–1854.e1.

Wine, E., Ossa, J.C., Gray-Owen, S.D., and Sherman, P.M. (2009). Adherent-invasive Escherichia coli, strain LF82 disrupts apical junctional complexes in polarized epithelia. BMC Microbiol. *9*, 180.

Xavier, R.J., and Podolsky, D.K. (2007). Unravelling the pathogenesis of inflammatory bowel disease. Nature *448*, 427–434.

CHAPTER 3

DIETARY IRON ALTERS THE ECOLOGICAL STRUCTURE OF THE DEVELOPING INTESTINAL MICROBIOTA[2]

3.1 Personal contributions to manuscript

I am the first author on the manuscript entitled "Dietary iron alters the ecological structure of the developing intestinal microbiota" that is in preparation for submission. I contributed to the manuscript by helping run the animal experiments in which we colonized ex-GF mice with a complex microbial community. I helped harvest all necessary samples for assessment of histopathology, cytokine production, iron measurement and microbiota analysis. I scored histology sections to assess the severity of inflammation and prepared and ran samples for measuring iron content by atomic absorption spectophotometry. Additionally, I helped isolate DNA from fecal and tissue samples for 16S rRNA sequencing. I also generated the 16S rRNA libraries for subsequent microbiota analysis and assisted with the analysis and interpretation of the sequencing data. I also conducted all *in vitro* microbiology and tissue culture experiments, conducted and analyzed the bacterial microarrays and constructed the deletion mutants in *E. coli*. Finally, I compiled the figures and wrote the manuscript.

[2] Melissa Ellermann, Raad Z. Gharaibeh, Nitsan Maharshak, Ian M. Carroll, Janelle C. Arthur, Ernesto Peréz-Chanona, Christian Jobin, Scott E. Plevy, Anthony A. Fodor, Cory R. Brouwer and R. Balfour Sartor. 2015. Dietary iron alters the ecological structure of the developing intestinal microbiota. (Manuscript in preparation).

3.2 Overview

Iron deficiency is the most common micronutrient deficiency worldwide. However, the ecological impact of dietary iron supplementation on a developing intestinal microbiota is unclear. Here we demonstrate that altering intestinal iron availability during community assembly impacts the resulting structure of the intestinal microbiota in ex-germ-free WT mice. Dietary iron restriction promoted compositional changes to the luminal community frequently associated with dysbiotic states, including decreased microbial richness and an expansion of Enterobacteriaceae including *Escherichia coli*. *In vitro* growth competitions between *E. coli* and a non-siderophilic bacterium revealed that TonB-dependent iron acquisition in *E. coli* enhanced its relative abundance when iron availability was limited. Although dietary iron restriction in colitis-susceptible interleukin-10-deficient (*Il10*$^{-/-}$) mice resulted in similar ecological changes as observed in WT mice, luminal community composition in *Il10*$^{-/-}$ mice was insensitive to additional iron supplementation over the control diet. Dietary iron supplementation also limited colitis development in the absence of distinct compositional changes to the fecal microbiota. Taken together, iron availability during community assembly influences the ecological structure of the intestinal microbiota that may be driven by differential capabilities for scavenging iron between distinct bacterial taxa and is dependent on the inflammation status of the host.

3.3 Introduction

Iron deficiency anemia (IDA) is the most common micronutrient deficiency, affecting approximately 1 billion individuals worldwide (Berglund and Domellöf, 2014). Although oral iron supplementation regimens can be efficacious in treating IDA (Adu-Afarwuah et al., 2008) (Domellöf et al., 2014), the safety and tolerance of oral iron supplementation within specific

population subsets such as infants and patients with chronic inflammatory diseases remains controversial. Increased diarrhea, enhanced burden of intestinal pathogens and increased fecal markers of inflammation have been reported in iron deficient infants with high pathogen burden receiving iron-supplemented foods (Gera and Sachdev, 2002) (Zimmermann et al., 2010) (Soofi et al., 2013) (Jaeggi et al., 2014) (Abhyankar and Moss, 2015). Increased disease activity and functional GI symptoms with oral iron supplementation have also been observed in some inflammatory bowel diseases (IBD) patients (Erichsen et al., 2005) (Kulnigg and Gasche, 2006) and with increased dietary iron intake in several rodent models of experimental colitis (Werner et al., 2011) (Kulnigg and Gasche, 2006) (Chua et al., 2013). Diet-mediated increases in intestinal iron concentrations can also enhance the luminal production of reactive oxygen species (Lund et al., 1999), a byproduct of the Fenton reaction, which in turn can increase colonic oxidative stress (Kulnigg and Gasche, 2006) and potentially exacerbate the development of intestinal inflammation.

The gastrointestinal (GI) tract is home to a complex community of microbes referred to as the intestinal microbiota. Dietary factors including macronutrient and micronutrient content can alter the composition of the intestinal microbiota (Wu et al., 2011) (Muegge et al., 2011) (Werner et al., 2011) (David et al., 2013), which in turn can impact numerous host processes including metabolism and immune function (Turnbaugh et al., 2006) (Devkota et al., 2012) (Atarashi et al., 2013) (Ojeda et al., 2015). Iron is a necessary cofactor for various bacterial enzymes and therefore serves as an important micronutrient for most members of the intestinal microbiota (Caldwell and Arcand, 1974) (Marcelis et al., 1978) (Imbert and Blondeau, 1998) (Andrews et al., 2003). The iron requirements for different bacterial taxa vary, as does the capacity to acquire iron when availability is limited. An estimated 5-15% of dietary nonheme

iron is absorbed at the duodenum (Hurrell and Egli, 2010), leaving the remaining unabsorbed iron to pass through the GI tract for microbial use. Indeed, changes in luminal iron concentrations through dietary manipulations alter the composition of an established intestinal microbiota (Werner et al., 2011) (Dostal et al., 2014b) (Pereira et al., 2014). Thus the impact of dietary iron on the growth and function of resident intestinal bacteria can conceivably mediate the development of unfavorable side effects that occur with oral iron supplementation in addition to iron-mediated effects on the host.

Studies investigating the impact of dietary iron on the intestinal microbiota have mainly focused on rodent models with an established microbial community. However, population subsets that are most vulnerable to IDA, including the infant and IBD populations, frequently harbor an intestinal microbiota that is either immature or unstable in composition (Martinez et al., 2008) (Koenig et al., 2011) (Pantoja-Feliciano et al., 2013). We therefore sought to determine how dietary iron restriction and supplementation influences the ecological structure of the developing microbiota. Using ex-germ-free (GF) wild type (WT) mice, we show that dietary iron restriction during community assembly resulted in compositional changes that are frequently associated with a dysbiotic state, including an increased relative abundance of Enterobacteriaceae family members including *Escherichia coli*. Moreover, decreased intestinal iron availability corresponded with an enrichment in the presence of genes involved in iron scavenging, including siderophore-mediated iron transport that are redundantly present in some intestinal *Escherichia coli* (Andrews et al., 2003) (Dogan et al., 2014). Consistent with our *in vivo* results, dual-culture growth competitions between *E. coli* and a non-siderophilic bacterium revealed that TonB-dependent iron acquisition in *E. coli* enhanced its relative abundance under iron limiting conditions. In contrast to WT mice, the composition of the developing microbiota in

inflammation-susceptible interleukin-10-deficient (*Il10*$^{-/-}$) mice during the onset of inflammation was insensitive to additional iron supplementation despite its protective effect on colitis development. Taken together, luminal iron availability during community assembly influences the resulting structure of the intestinal microbiota and is dependent on host susceptibility to inflammation and differential capacities for scavenging iron between distinct bacterial taxa.

3.4 Results

3.4.1 Intestinal iron availability during community assembly impacts the resulting structure of the intestinal microbiota

Dietary iron interventions can be administered during infancy when the microbiota is undergoing ecological succession (Koenig et al., 2011) (Pantoja-Feliciano et al., 2013) or during disease states when the microbiota exhibits transient instability (Martinez et al., 2008) (Carvalho et al., 2012). We therefore investigated the impact of dietary iron restriction or supplementation on the developing microbiota. GF WT mice were colonized with the fecal microbiota from a WT donor and were placed on an iron deficient (hereafter referred to as the low iron diet), control or iron supplemented diet (hereafter referred to as the high iron diet). Fecal and cecal tissue samples were collected for 16S rRNA sequencing at 4 weeks following colonization, when the microbiota exhibits initial compositional stability following conventionalization (McCafferty et al., 2013). Because host iron status has been correlated with compositional changes to the intestinal microbiota (Balamurugan et al., 2010) (Shanmugam et al., 2014) (Jaeggi et al., 2014) and consumption of an iron deficient diet can induce a state of iron deficiency as early as 4 weeks (Dostal et al., 2012a) (Pereira et al., 2014), mice maintained on the low iron diet were supplemented with weekly intraperitoneal (IP) iron injections in order to prevent systemic iron

depletion. Following the 4-week dietary intervention and IP injections, liver iron stores were not significantly different between the dietary groups (Fig. S1). Moreover, as described by others (Lund et al., 1999) (Carrier et al., 2001), dietary iron restriction and supplementation significantly altered fecal iron concentrations (Fig. S2), demonstrating that the dietary treatments modulated luminal iron concentrations in the intestines.

Principal coordinate analysis using Bray-Curtis dissimilarity at the operational taxonomic unit (OTU) level revealed compositional differences to the fecal microbiota between the different diets (Fig 1A). The fecal communities in mice maintained on the high iron diet significantly differed from that in mice administered the low iron diet for PCoA axis 1 (FDR-corrected *p* value = $4.4x10^{-9}$) explaining 42.28% of the variance as assessed using a mixed liner model. The composition of the fecal microbiota in mice fed the control diet exhibited the most interindividual variability as assessed by Bray Curtis distances between samples within each diet group (Fig S3), suggesting that supplementation or depletion of dietary iron exerts strong selective pressure in shaping the fecal microbiota. Restriction of dietary iron during community assembly also resulted in a significant reduction in microbial richness relative to iron supplementation as assessed by observed OTUs (Fig 1C) and Shannon diversity (Fig 1E). Taken together, manipulation of intestinal iron availability through dietary interventions during community assembly impacts the ecological structure of the resulting fecal microbiota.

We also examined the impact of dietary iron supplementation and depletion on the structure of the mucosal microbiota. One sample from the low iron diet group was excluded from 16S rRNA sequencing because of low DNA yield. Principal coordinate analysis revealed partial clustering of the mucosal microbiota by dietary treatment, including significant differences between the low and high iron diet groups for PCoA axis 1 (FDR-corrected *p* value = 0.02) (Fig

1B). As in the luminal compartment, dietary iron supplementation increased the microbial richness of the mucosal microbiota (Fig 1D and F). Collectively, these results suggest that although dietary iron influences the biodiversity of the mucosal microbiota, dietary modulation of intestinal iron availability during community assembly has a stronger impact in shaping the resulting luminal versus mucosal microbiota.

3.4.2 Dietary iron supplementation alters the fecal abundances of distinct bacterial taxa

We next evaluated the impact of dietary iron supplementation and depletion on specific taxa within the fecal microbiota. A heat map was generated to highlight OTUs that significantly differed in relative abundance in the feces between at least two diet groups (Fig 2A) (Table S2). Statistical analysis using a mixed linear model revealed that the relative abundances of 59 OTUs (4 Actinobacteria, 5 Bacteroidetes, 57 Firmcutes, 2 Proteobacteria, and 1 Verrucomicrobia) significantly differed between at least two dietary treatments. Iron supplementation during community assembly resulted in the enrichment of 18 OTUs relative to the control diet and 37 OTUs relative to the low iron diet (Fig 2B). In contrast, dietary iron restriction increased the relative abundances of 7 OTUs compared to the control diet and 8 OTUs compared to the high iron diet (Fig 2C). Taken together, these data suggest that increased intestinal iron availability during community assembly corresponds with the enrichment of a greater number of bacterial taxa within the luminal microbial community.

3.4.3 Dietary iron restriction promotes a bloom of Enterobacteriaceae and predicted bacterial iron uptake systems

The impact of dietary iron on the luminal abundance of Enterobacteriaceae is inconsistent, where an enrichment of Enterobacteriaceae with increased dietary iron has been observed in infants (Zimmermann et al., 2010) (Jaeggi et al., 2014), while others have reported the opposite effect in both mice and infants consuming iron-fortified foods (Dostal et al., 2012a) (Krebs et al., 2013). We therefore determined whether the relative abundance of Enterobacteriaceae was altered with dietary iron restriction or supplementation during community assembly. In the control and low iron diet groups, the relative fecal abundances of Proteobacteria and Enterobacteriaceae family members including *Escherichia coli* were significantly increased relative to the high iron diet group (Fig S4, 3A and 3B), suggesting that increased intestinal iron availability during community assembly may accelerate negative selection against Enterobacteriaceae.

Because dietary iron restriction significantly decreases total fecal iron concentrations and presumably bacterial luminal iron availability, we next investigated whether dietary iron restriction also promotes an increase in the presence of genes involved in scavenging iron within the fecal microbiota. Using the metagenomic inference tool PICRUSt, we observed a significant increase in the predicted presence of *tonB* (K03832), *exbB* (K03561) and *exbD* (K03559) in mice maintained on the low iron or control diets (Fig 3C). These three genes are required for bacterial import of various substrates including siderophore-bound iron (Noinaj et al., 2010). The relative abundance of additional genes involved in siderophore-mediated iron acquisition and utilization, including a predicted enterochelin esterase (K07214) required for the hydrolysis of ferric enterobactin (Bryce et al., 1971) and a predicted iron complex outer membrane receptor (K02014), are also increased with the low iron and control diets. Transcript levels of these and other iron acquisition genes in *E. coli* are increased *in vitro* under iron limiting conditions

(McHugh et al., 2003) (Seo et al., 2014), including in a resident intestinal *E. coli* strain (Table S3). Taken together, these data suggest that decreased intestinal iron availability may select for siderophilic bacteria including *E. coli* with a greater capacity to scavenge iron.

3.4.4 TonB-dependent iron acquisition enhances E. coli relative abundance when iron availability is restricted

TonB is an inner membrane protein required for energy transduction that powers import of various nutrients including siderophore-bound iron through cognate receptors in *E. coli* and other siderophilic bacteria (Letain and Postle, 1997) (Noinaj et al., 2010). Because the predicted abundance of *tonB* and other genes involved in siderophore-mediated iron acquisition was increased in the low iron and control diet groups, we determined whether TonB-mediated iron acquisition provides resident intestinal *E. coli* a relative growth advantage when iron availability is restricted. To address this, we created an isogenic *tonB* deletion mutant in *E. coli* to simultaneously inactivate all siderophore-mediated iron import (Braun and Hantke, 2011). Growth of the *tonB* mutant was decreased in the presence of an iron chelator relative to the parental strain (Fig S5A), demonstrating that siderophore-mediated iron scavenging limits the impact of extracellular iron chelation on *E. coli* growth. We then competed the parental and mutant *E. coli* strains with a non-siderophilic bacterium, *Enterococcus faecalis* that exhibits minimal iron requirements (Fig S5B) (Marcelis et al., 1978). Indeed, the relative fecal abundance of *Enterococcaceae* family members remains unchanged as intestinal iron concentrations are altered through the dietary manipulations (Fig 3D). In medium containing the iron chelator, the percent abundance of the parental *E. coli* strain was significantly increased compared to the *tonB* mutant (Fig 4A and 4C), which corresponded with an enrichment of *E. faecalis* in the presence of the *tonB* mutant (Fig 4B and 4D). Addition of exogenous iron in the presence of the iron

chelator restored bacterial growth kinetics observed in the control cultures (Fig 4A-D, Fig S5C-F). Taken together, these data suggest that TonB-dependent iron acquisition may help promote the bloom of *E. coli* observed *in vivo* when dietary iron is restricted by enabling more efficient scavenging of iron through redundant siderophore-mediated iron acquisition systems.

3.4.5 The luminal microbiota in the inflamed environment is insensitive to additional iron supplementation

We previously observed an expansion in Enterobacteriaceae family members including *E. coli* during the onset of colitis in *Il10*$^{-/-}$ mice following conventionalization (Maharshak et al., 2013). Because decreased intestinal iron availability also promotes a bloom of Enterobacteriaceae, we investigated whether administration of a low iron or control diet exacerbates colitis in ex-GF *Il10*$^{-/-}$ mice. At 4 weeks following conventionalization, mice on the high iron diet developed less severe colitis compared to mice on the control diet as assessed by histological inflammation (Fig 5A-D), clinical disease activity (Fig 5E), secretion of the proinflammatory cytokine IL-12 p40 by colonic explant cultures (Fig 5F) and serum levels of IL-12 p40 (Fig 5G). Mice on the low iron diet also developed less severe colitis compared to the control diet group, although this did not achieve statistical significance. Thus, dietary iron restriction and supplementation appear to limit colitis development in *Il10*$^{-/-}$ mice after 4 weeks.

We next determined whether dietary iron restriction or supplementation promoted similar compositional changes to the fecal microbiota in *Il10*$^{-/-}$ mice as in WT mice. Principal coordinate analysis revealed that the composition of the fecal microbiota did not cluster by severity of inflammation (Fig 6A). Instead, consistent with the WT cohort, the communities assembled with dietary iron supplementation significantly differed from those assembled with dietary iron restriction for PCoA axis 1 (FDR-corrected p value = 3.1×10^{-7}). Similarly, microbial richness as

assessed by observed OTUs in the fecal microbiota was reduced (Fig 6B) and the relative abundance of Enterobacteriaceae was enhanced (Fig 6C) with dietary iron restriction. However, in contrast to the WT mice, principal coordinate analysis demonstrated that the fecal communities with the control and high iron diets clustered with each other (Fig 6A). Moreover, 84 bacterial taxa were similarly enriched or depleted in the control and high iron diet groups (Fig. 6C and 6D, Table S4), suggesting that in a state of inflammation, additional iron supplementation does not further alter the structure of the fecal microbiota.

3.4.6 The protective effect of dietary iron supplementation on colitis development may be mediated through host factors

Because increased severity of colitis in *Il10*$^{-/-}$ mice on the control diet did not coincide with distinct structural changes to the fecal microbiota, we investigated whether inflammation corresponded with compositional changes to the mucosal community. One sample from the control diet group was excluded because of low DNA yield. Principle coordinate analysis revealed distinct clustering of the mucosal microbiota by diet, although this did not achieve statistical significance (Fig S6A). In the control group, microbial richness and the relative abundances of numerous OTUs were significantly decreased (Fig S6B and S6C), suggesting that perturbations to the mucosal community may be associated with more severe colitis development. However, this was not associated with an increased relative abundance of mucosal Enterobacteriaceae compared to the low and high iron diet groups (Fig S6D), suggesting that mucosal Enterobacteriaceae abundance may be only be sensitive to the presence rather than the severity of intestinal inflammation. Indeed, the relative abundance of Enterobacteriaceae in the mucosa was consistently higher in *Il10*$^{-/-}$ mice compared to WT mice regardless of diet (Fig S6D and S6E).

The lack of distinct compositional changes to the fecal microbiota with more severe colitis in *Il10*$^{-/-}$ mice on the control diet also suggests the involvement of host factors in mediating the impact of dietary iron on colitis development. Given that iron homeostasis and macrophage function are intimately linked, we tested whether iron impacts *in vitro* macrophage production of IL-12 p40, a proinflammatory cytokine that correlates with colitis severity in *Il10*$^{-/-}$ mice (Kim et al., 2005). As iron concentrations were increased, macrophage production of IL-12 p40 was reduced (Fig 6E) without impacting macrophage viability (Fig 6F). Taken together, these results suggest that the protective effect of dietary iron supplementation on colitis development may in part be mediated through the impact of iron on immune function in the *Il10*$^{-/-}$ mouse model.

3.5 Discussion

Iron deficiency is often treated through oral iron supplements or consumption of an iron-fortified diet, which can modulate luminal iron concentrations in the intestines (Lund et al., 1999) (Carrier et al., 2001) and potentially influence bacterial iron availability and consequent bacterial growth and community structure. We therefore investigated the ecological impact of dietary iron restriction and supplementation on an establishing intestinal microbiota. Dietary iron restriction during community assembly resulted in significant compositional changes frequently associated with a dysbiotic state including decreased microbial richness. Complimentary to our findings, other studies utilizing 16S rRNA gene sequencing have demonstrated that dietary iron restriction also alters the composition of an established intestinal microbiota in rodent models (Werner et al., 2011) (Dostal et al., 2014b) (Pereira et al., 2014). In one study, dietary iron restriction initiated at weaning resulted in compositional changes to the fecal microbiota that

were distinct from the control diet group (Pereira et al., 2014). Consistent with our results, this included a decrease in microbial richness with dietary iron restriction relative to both the baseline community at weaning and the control diet (Pereira et al., 2014). Interestingly, subsequent dietary iron repletion did not fully restore microbial richness or overall community-wide compositional changes (Pereira et al., 2014). In contrast, dietary iron restriction in adult mice with an established microbiota did not alter microbial richness (Werner et al., 2011). Thus limiting intestinal iron availability seems to only impact microbial richness of a developing intestinal microbiota.

Our findings also demonstrate that dietary iron restriction is associated with a reduction in the relative abundances of numerous taxa within the Firmicutes that corresponded with an increase in Enterobacteriaceae. In other rodent studies that utilized 16S rRNA sequencing to characterize the impact of dietary iron restriction on the intestinal microbiota, a change in the relative abundance of Enterobacteriaceae was not reported between the iron deficient and control diets (Werner et al., 2011) (Pereira et al., 2014). An iron-supplemented diet group was not included in these studies. Therefore, our study is the first to our knowledge to assess the impact of dietary iron supplementation on community composition through 16S rRNA sequencing and demonstrate decreased Enterobacteriaceae abundance with iron supplementation. In another rodent study assessing compositional changes by targeted quantitative PCR, dietary iron restriction initiated at weaning resulted in a bloom of Enterobacteriaceae that was reversed with subsequent dietary iron repletion (Dostal et al., 2012a). Decreased Enterobacteriaceae was also observed in infants receiving iron-fortified foods relative to baseline levels (Krebs et al., 2013). In contrast, in infants with a high initial pathogen burden, administration of an iron-fortified diet resulted in a higher relative abundance of *Escherichia* species (Zimmermann et al., 2010) (Jaeggi

et al., 2014). However, a significant increase in the abundance of pathogenic *E. coli* was only observed in infants that received an intermediate iron dose and not in infants that received the highest iron dose (Jaeggi et al., 2014). Increased dietary iron intake in rodents is also associated with an increased relative abundance of short chain fatty acid (SCFA) producers within the Firmicutes phylum and increased intestinal levels of fermentative metabolites including butyrate and proprionate (Dostal et al., 2012a) (Dostal et al., 2014b). Taken together, these findings suggest that dietary iron restriction may perturb the ecological structure of the luminal intestinal community, promoting compositional and functional changes that have been linked to numerous pathological states.

In response to low iron availability, bacteria upregulate genes involved in iron acquisition in order to scavenge iron from the environment. Bacterial taxa such as Enterobacteriaceae encode numerous siderophore-mediated iron transport systems that likely enhance their competitive advantage when iron availability is restricted. Indeed, the relative abundance of endogenous Enterobacteriaceae and predicted genes involved in iron acquisition such as *tonB* were increased with dietary iron restriction in our study. However, the TonB-ExbB-ExbD complex is also involved in the import of vitamin B12 in *E. coli* and other nutrients in other bacteria taxa (Noinaj et al., 2010). Therefore, we cannot conclusively determine whether the predicted increase in the presence of *tonB, exbB* and *exbD* occurs in response to decreased iron availability or other environmental factors. To address this, we deleted *tonB* in a resident intestinal *E. coli* strain and conducted controlled *in vitro* growth competitions with the non-siderophilic intestinal bacterium *E. faecalis*. In contrast to the parental strain, the relative abundance of the *tonB* mutant was decreased when iron availability was restricted, suggesting that TonB-mediated iron acquisition enhances the relative fitness of *E. coli* when iron is limited.

Consistent with our findings, in the presence of a complex community, addition of an iron chelator to an *in vitro* colonic fermentator inoculated with a fecal microbiota results in the expansion of Enterobacteriaceae that corresponded with a reduction in Lachnospiraceae, Ruminococceae and Bacteroidaceae (Dostal et al., 2012b). Similarly, deletion of *tonB* in a probiotic *E. coli* strain reduces its competitive advantage over *Salmonella* in the inflamed intestines when fecal iron concentrations are decreased (Deriu et al., 2013). Thus, decreasing iron availability in the intestines likely provides a fitness advantage for resident bacteria that are more effective at scavenging iron. However, as PiCRUST only predicts the functional potential of a complex microbial community, future studies using metagenomics, transcriptomics and metabolomics are warranted to both confirm the increased presence of iron acquisition genes with dietary iron restriction and to determine if transcription of these systems is upregulated.

One limitation to our study is the exclusion of an experimental group maintained on the iron deficient diet without systemic iron repletion. Werner and colleagues demonstrated that intraperitoneal administration of iron in mice on an iron deficient diet did not significantly impact the composition of the intestinal microbiota (Werner et al., 2011). Moreover, the relative abundances of the majority of bacterial taxa were not significantly altered between the two groups (Werner et al., 2011). Thus, systemic iron repletion has minimal impact on microbial community structure in the intestines and is therefore not a likely significant confounding factor in the low iron diet group in our study.

Intestinal inflammation is associated with compositional changes to the intestinal microbiota including an expansion of Enterobacteriaceae (Lupp et al., 2007) (Arthur et al., 2012) (Winter et al., 2013). Because we observed similar perturbations to the luminal microbiota with dietary iron restriction, we investigated the impact of dietary iron on the development of colitis

in ex-GF *Il10*$^{-/-}$ mice. Interestingly, we observed a bimodal effect of dietary iron on colitis severity, where both dietary iron restriction and supplementation protected against the development of inflammation. In agreement with our observations, Dostal and colleagues reported higher baseline inflammation in the ileum and cecum of rats on a control diet compared to rats receiving an iron deficient or supplemented diet (Dostal et al., 2014b). Dietary iron restriction also prevented the development of immune-mediated ileitis in TNFΔARE mice (Werner et al., 2011). In contrast, increased dietary iron results in exacerbation of chemically induced colitis (Kulnigg and Gasche, 2006) (Chua et al., 2013). However, in many of these studies, dietary iron was administered in high enough amounts to induce iron overloading and therefore may not reflect amounts consumed with iron fortification or oral iron supplements. Indeed, lower doses of daily oral iron supplementation protected against TNBS-induced colitis (Ettreiki, 2012). Administration of an iron-fortified diet in infants with high pathogen burden also resulted in increased fecal markers of inflammation (Jaeggi et al., 2014). However, two other studies demonstrated no impact on dietary iron supplementation on inflammation markers in infants or children with low pathogen burden (Krebs et al., 2013) (Dostal et al., 2014a), suggesting that the initial composition of the microbiota may serve as a prognostic factor for risk of intestinal inflammation with oral iron supplementation.

In *Il10*$^{-/-}$ mice, fecal communities clustered by diet rather than severity of inflammation, suggesting that intestinal iron concentrations had a stronger impact in shaping luminal community structure. Consistent with our findings, Werner and colleagues also demonstrated that diet had a stronger influence on the composition of the intestinal microbiota compared to host genotype (WT versus inflammation-susceptible TNFΔARE) and inflammation severity (Werner et al., 2011). Interestingly, dietary iron restriction in *Il10*$^{-/-}$ mice did not result in the

most severe colitis despite compositional changes to the fecal microbiota frequently associated with inflammation. Moreover, a higher relative abundance of Enterobacteriaceae was not observed in *Il10*$^{-/-}$ mice on the control diet that developed the most severe colitis, suggesting that a more dramatic bloom of Enterobacteriaceae may not correlate with worse inflammation. Together, these observations suggest that the impact of dietary iron on the development of colitis may not be mediated through compositional changes to the luminal microbiota in our model, at least at this time point. However, these findings do not exclude the possibility that dietary iron may impact the course of inflammation by modulating the growth of select resident microbes once disease is initiated. Changes in intestinal iron availability could also alter the function of resident bacteria. Indeed, decreasing iron availability reduces the fermentative activity of the intestinal microbiota (Dostal et al., 2012a) (Dostal et al., 2012b) (Dostal et al., 2014b), a functional change that has been associated with dysbiosis. Moreover, iron also modulates the physiology and proinflammatory potential of adherent-invasive *E. coli*, a functional subset of *E. coli* associated with Crohn's disease (Ellermann et al., 2015). Thus, longitudinal studies investigating the impact of dietary iron on the composition and function of the intestinal microbiota prior to, during, and after the onset of inflammation are warranted to further elucidate the contribution of the intestinal microbiota on iron-mediated effects on colitis. Finally, dietary iron and host iron status can also influence immune function and consequent development of colitis (Werner et al., 2011) (Shanmugam et al., 2014). Indeed, we show that iron can modulate macrophage production of the proinflammatory cytokine IL-12 p40, which correlates with severity of colitis in the *Il10*$^{-/-}$ mouse model (Kim et al., 2005). Thus, in addition to iron-mediated modulation of the intestinal microbiota, the impact of iron on host iron status and immune function also likely contributes to colitis development.

Throughout the first few years of life, the intestinal microbiota undergoes ecological succession and matures to its adult state (Koenig et al., 2011). During this developmental window, the intestinal microbiota is highly prone to environmental disturbances such as antibiotic exposure and malnutrition that significantly impact the composition of the resulting microbial community and can perturb homeostatic physiological processes through adulthood (Cox et al., 2014) (Subramanian et al., 2014) (Nobel et al., 2015). Our study suggests that intestinal iron availability may be an additional environmental factor that modulates community assembly, where decreased intestinal iron availability may delay maturation of the intestinal microbiota. This may be mediated through the creation of an intestinal environment that favors growth of early colonizers with redundant iron acquisition systems such as *E. coli*, thus inhibiting their negative selection. However, as this was not a longitudinal study, future investigations are required to examine the compositional and functional impacts of intestinal iron availability on a developing microbiota, especially given the implications for infants that are at-risk for iron deficiency. Finally, our study demonstrates that colitis severity is reduced with dietary iron supplementation in the absence of distinct compositional changes to the intestinal microbiota, suggesting that iron modulates colitis development through functional changes to the microbiota or direct effects on the host. Given the high prevalence of anemia in individuals with chronic inflammatory diseases such as IBD, the precise mechanisms underlying the effect of iron on colitis development should be explored in future studies.

3.6 Materials and methods

Mice and experimental design. *Il10*$^{-/-}$ and WT 129S6/SvEV mice were maintained in GF conditions at the National Gnotobiotic Rodent Resource Center at UNC-Chapel Hill. Three

groups of adult GF WT mice (n = 8-9, 3 cages per group) and *Il10*$^{-/-}$ mice (n = 4-5, 2-3 cages per group) were transferred to conventional housing. Each group was placed on either an iron deficient diet (<10 ppm iron/kg diet), control diet (35 ppm iron/kg diet) or iron supplemented diet (200 ppm iron/kg diet). The following day, all mice were colonized by oral and rectal swab with fecal slurry obtained from a WT 129S6/SvEV mouse housed in the same facility. After 4 weeks of the dietary interventions, mice were sacrificed and fresh fecal pellets and cecal tissue were collected and processed for 16S rRNA sequencing as previously described (Arthur et al., 2012) (Maharshak et al., 2013). The WT and *Il10*$^{-/-}$ cohorts were run at different times and were therefore colonized with a different donor; thus subsequent 16S rRNA sequencing analyses were run separately for both cohorts. Mice maintained on the iron deficient diet received IP injections of 5 μg/g body weight of dextran iron sulfate (D8517, Sigma). Mice on the control and iron supplemented diets received IP injections of sterile PBS as a vehicle control. A separate cohort of WT and *Il10*$^{-/-}$ animals was used to assess iron content in the feces (Fig. S2). All diets were produced by Harlan and were based on the TD.99397 iron deficient diet and only differed in iron content, which was added in the form of ferrous sulphate and ferric citrate at a 1:1 ratio. All animal protocols were approved by the UNC-Chapel Hill Institutional Animal Care and Use Committee.

Quantification of iron in fecal and liver samples. Iron contents in the liver and feces were measured using atomic absorption spectrophotometry as previously described (Chen et al., 2009) with the following modifications. Briefly, samples were weighed, dessicated in an oven overnight at 90°C and weighed again to obtain the wet and dry sample weights. The samples were digested in 50% HNO_3 and the acid was allowed to evaporate for 24 hours at room

temperature. Samples were diluted in 2% HNO_3 and analyzed by AA spectrophotometry with 2% HNO_3 serving as a blank.

Assessment of colitis and disease activity. At necropsy, cecal, proximal and distal colonic segments were fixed in 10% neutral buffered formalin. Histological inflammation scores (0-4) of cecal, proximal and distal colonic sections were blindly assessed as previously described (Kim et al., 2005). Clinical disease activity (0-4) was assessed at 4 weeks prior to necropsy as previously described (Scheinin et al., 2003). Colonic explant cultures were prepared to assess spontaneous secretion of colonic cytokine production as previously described (Sellon et al., 1998).

Quantitative PCR. Quantitative PCR were performed on fecal DNA to quantify the abundance of 16S rRNA sequences from *E. coli* and from all bacteria using previously reported primer sequences (Maharshak et al., 2013). The Sensifast SYBR No-ROX Kit (Bioline) was utilized with the following PCR conditions: a single hold at 95°C for 2 minutes, followed by 40 cycles at 95°C for 5 seconds, 60°C for 10 seconds and 72°C for 20 seconds. Melting curves were also assessed to ensure specificity of the PCR products.

Bacteria strains and growth conditions. Bacteria strains and plasmids used in this study are listed in Table S1. Bacteria were grown overnight in brain heart infusion (BHI) medium at 37°C without aeration prior to inoculation into experimental conditions: BHI control, BHI with 250 μM of the iron chelator diethylene triamine pentaacetic acid (DTPA; D6518, Sigma), or BHI with 250 μM DTPA and 250 μM ferrous sulfate (I146, Fisher Scientific). Bacterial growth was assessed by spectrophotometry (OD600) and quantitative plating. For dual cultures, selective

media was utilized to distinguish *E. faecalis* (BHI agar with 50 μg/mL kanamycin) and *E. coli* (MacConkey agar) colony forming units. Deletion mutants in *E. coli* were created using the λ-red recombinase system as previously described (Datsenko and Wanner, 2000).

Bacterial RNA isolation and microarray hybridization. *E. coli* NC101 was grown in minimal M9 medium with the indicated concentrations of ferrous sulfate. After 1 hr, aliquots of the culture were collected for RNA isolation. Bacterial RNA was isolated using the RNAeasy isolation kit (Qiagen) according to the manufacturer's instructions. Purified RNA was treated with on-column DNase treatment (Qiagen) and DNA-free DNase treatment (Ambion) according the manufacturer's instructions. RNA samples were prepared for microarray hybridizaion using the Affymetrix *E. coli* Genome 2.0 arrays as previously described (Patwa et al., 2011). Statistical analysis was performed using GeneSpring 7.2 software.

Bone marrow derived macrophage (BMDM) cultures. Bone marrow cells were isolated as previously described (Lutz et al., 1999). Conditioned medium from the murine fibroblast cell line L929 served as a source of M-CSF for macrophage differentiation (Stanley and Heard, 1977). BMDMs were seeded in 24-well plates and maintained in RPMI 1640 medium (Gibco) with 10% heat-inactivated fetal bovine serum (FBS, Gibco) and 1% penicillin/streptomycin/antimycotic (Gibco) at 37°C, 5% CO_2. To assess the impact of iron on BMDM cytokine production, BMDMs were stimulated with heat-killed *E. coli* (MOI=10) following addition of the indicated amounts of ferrous sulphate to the cultures. After 8 hrs, supernatants were collected and stored at -20°C for assessment of cytokine production. BMDM viability was assessed via reduction of the tetrazolium dye, MTT, using spectrophotometry.

Quantification of cytokine production. Commercially available monoclonal anti-mouse IL-12 p40 and interferon gamma (BD Biosciences) capture and detection reagents were utilized to quantify cytokine production by colonic explant cultures, BMDMs and in serum samples by enzyme-linked immunosorbent assay (ELISA) according to the manufacturer's instructions.

Illumina 16S library construction, sequencing and processing. Amplification of the hypervariable V6 region of the 16S rRNA gene via a two-step PCR strategy was performed as previously described (Arthur et al., 2012). Equal amounts of all samples were pooled together and subjected to paired-end Illumina Hi-Seq sequencing. A total of 97,286,872 raw reads were generated for a total of 74 samples. Raw reads were preprocessed as described previously (McCafferty et al., 2013) (Arthur et al., 2014). Briefly, forward and reverse reads were merged if they satisfied having 70 bases overlap with 100% similarity. Reads that were successfully merged were subjected to quality trimming at Q Score 20 followed by length check. Reads shorter than 50 bases were discarded. This resulted in 45,486,399 high quality reads that were incorporated into the subsequent analysis. These reads were then clustered into 1,301 operational taxonomic units (OTUs) using AbundantOTU+ v.0.93b (http://omics.informatics.indiana.edu/AbundantOTU/) (command option "-abundantonly" was used) at 97% similarity incorporating 99.84% of the input sequences. OTUs were checked for chimeric sequences using uchime v. 4.2.40 (http://www.drive5.com/uchime/) (Edgar et al., 2011) utilizing the GOLD database and uchime identified nine OTUs as chimeras. Those nine OTUs were excluded from further analysis. Taxonomy was assigned through the Quantitative Insight into Microbial Ecology (QIIME) (v. 1.8.0) (Caporaso et al., 2010) using uclust consensus taxon

assigner. Finally, we retained OTUs that have ≥ 0.005% of the total number of sequences according to Bokulich and colleauges (Bokulich et al., 2012), resulting in a final dataset that has an average of 608,300 reads per sample (median= 490,000; min= 299,100; max= 1,072,000 reads per sample).

Functional prediction. To predict metagenomic functional content from our 16S rRNA survey, the software package Phylogenetic Investigation of Communities by Reconstruction of Unobserved States (PiCRUST) was used (Langille et al., 2013). Briefly, the same reads that were fed to AbundantOTU+ were used to produce close reference OTUs using QIIME (v. 1.8.0) and GreenGenes dataset (gg_13_5). PiCRUST software was then applied on the resulting biom file to generate KEGG orthologs metagenomic predictions.

Statistical analysis. OTU, phylum, family or KEGG ortholog raw counts were normalized and $\log_{10}$ transformed according to the following formula:

$$\log_{10}\left(\text{raw count} \frac{\text{Number of sequences in sample}}{\text{Average number of sequences per sample}} + 1\right)$$

The normalized and $\log_{10}$ transformed reads were used to produce PCoA plots from Bray-Curtis dissimilarity statistic. Alpha diversity measures (Observed OTU estimate and Shannon diversity index) were calculated after rarefying the raw counts to an even depth equal to the minimum count in all samples examined. We used a mixed linear model utilizing SAS (v. 9.3) software (SAS Institute Inc, Cary, NC) to analyze the data and accounting for possible effects that may arise from co-housing (McCafferty et al., 2013).

The mixed linear model, in which dietary iron level (low, control or high) and source (mucosal or fecal) are fixed effects and cage is a random effect, is formulated as follows:

where Yijkl represents either PCoA axis value, $\log_{10}$ normalized phylum count, $\log_{10}$ normalized family count, $\log_{10}$ normalized KEGG ortholog count or richness value for dietary iron level *i*, source *j*, cage *k* and replicate *l*. D_i.is the effect of the i^{th} dietary iron level. S_j is effect from the j^{th} source. $(SD)_{ij}$ is the interaction effect between dietary iron level *i* and source *j*. $C_{k(i)}$ is the effect from the k^{th} cage that is nested within the i^{th} dietary iron level and ε_{ijkl}εijkl denotes the error associated with measuring Y_{ijkl}Yijkl. We controlled for the false discovery rate (FDR) by correcting the *P*-values using Benjamini and Hochberg (BH) approach (Benjamini and Hochberg, 1995).

For all *in vitro* experiments, *p*-values were calculated using one-way ANOVA with Tukey's multiple comparison post test when 3 or more experimental groups were compared or two-way ANOVA with Bonferroni multiple comparison post test when more than two variables were compared. For all animal experiments, *p*-values were determined using a non-parametric Kruskal-Wallis test.

3.7 Figures

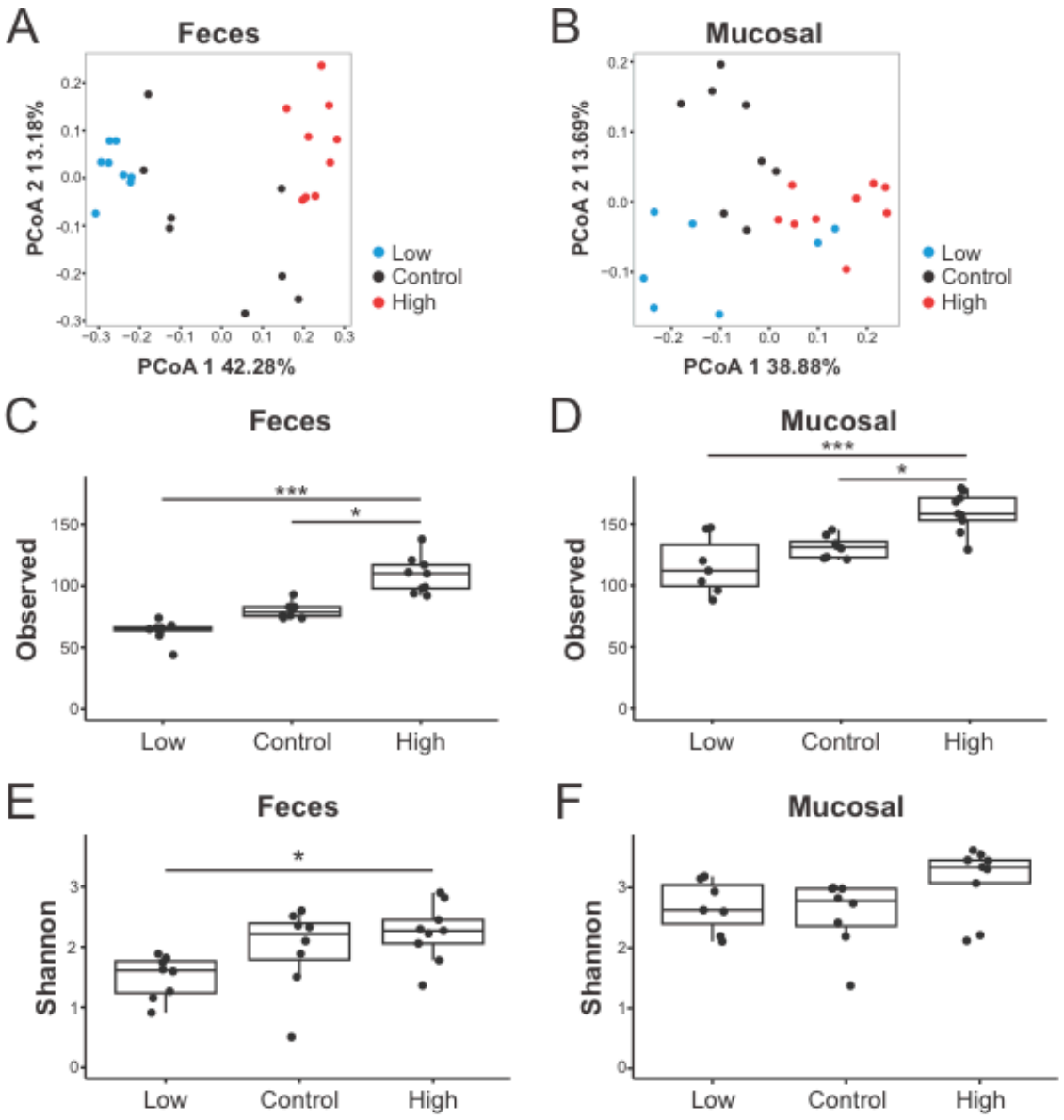

Figure 3.1. Dietary iron alters the structure of the fecal and mucosal microbiota. A+B) Principle coordinate analysis based on Bray-Curtis metrics for the A) fecal and B) mucosal microbiota in ex-GF WT mice maintained on an iron deficient (low), control or iron supplemented (high) diet. Microbial richness as measured by C, D) observed OTUs and E, F) Shannon diversity index for the C, E) fecal and D, F) mucosal microbiota. Each symbol represents an individual mouse, n = 7-9 mice per group. Box and whisker plots show the minimum, first quartile, median, third quartile and maximum values. Comparisons and FDR-corrected p values were determined using a mixed linear model. * $p < 0.05$, *** $p < 0.001$

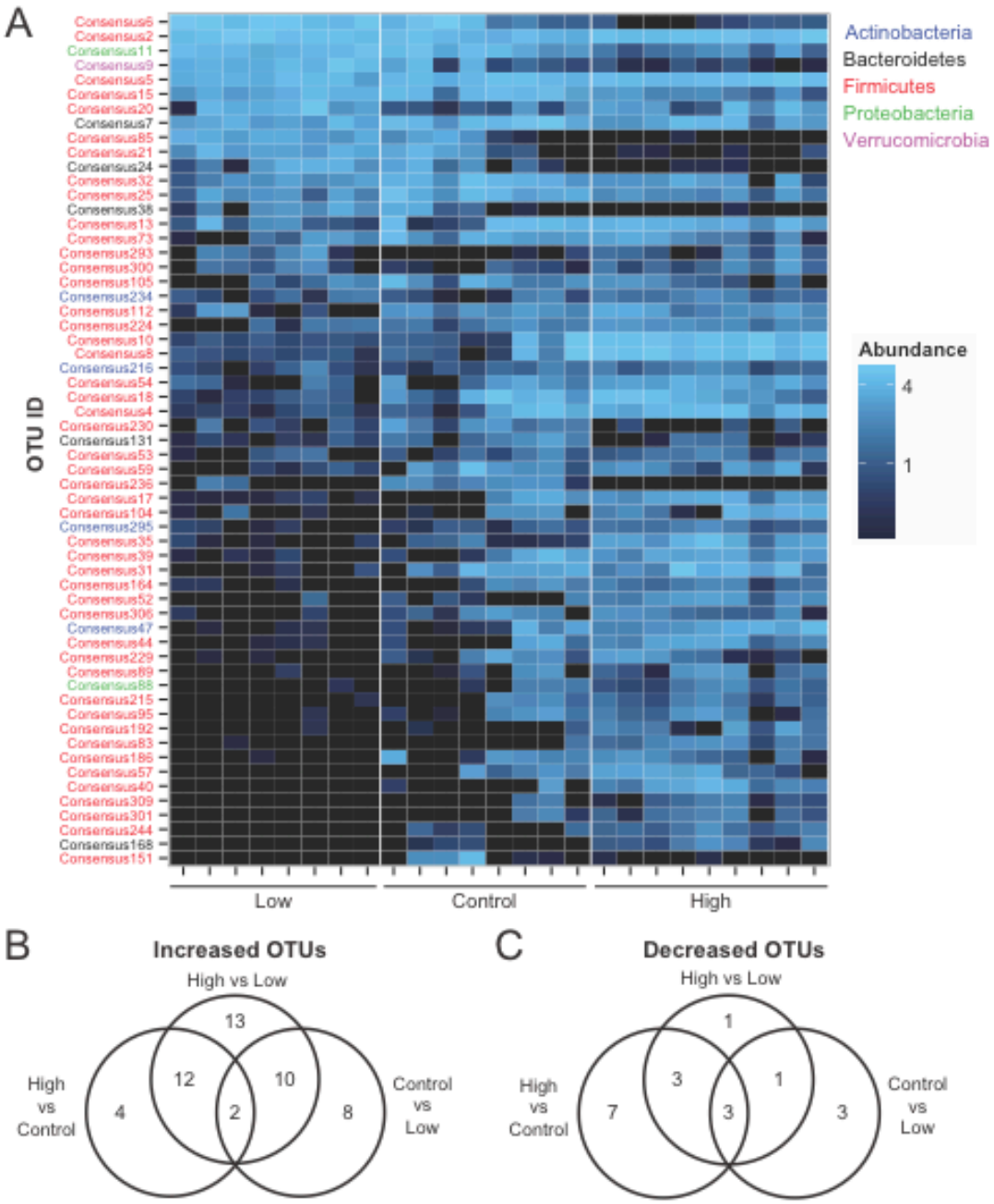

Figure 3.2. Dietary iron enhances the relative fecal abundances of numerous bacterial taxa. A) Heat map of OTUs that are significantly different in abundance (FDR-corrected $p < 0.05$). Each column represents an individual WT mouse. Each row represents individual OTUs, color coded by phylum, that are significantly between at least 2 diet groups as determined using a mixed linear model. The colors of the heat map represent the mean relative abundance (normalized and log transformed) of each OTU. B+C) Venn diagrams of OTUs that are significantly B) increased or C) decreased in relative abundance (FDR-corrected $p < 0.05$) in the feces as determined using a mixed linear model.

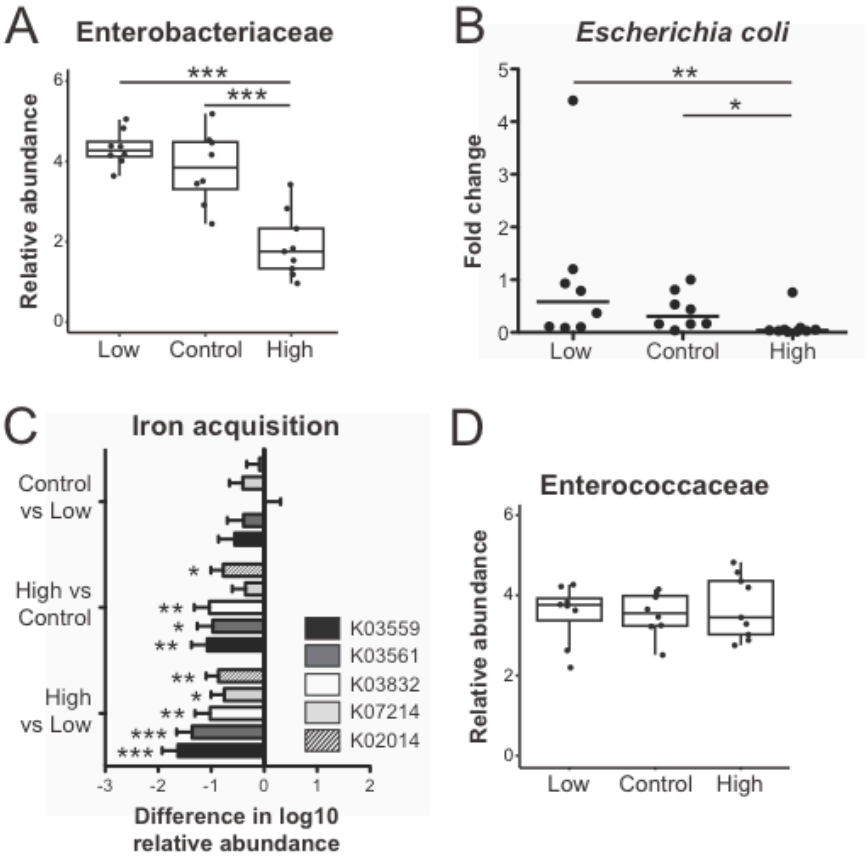

Figure 3.3. Dietary iron restriction promotes a bloom of Enterobacteriaceae and predicted bacterial iron uptake systems. A) Relative fecal abundance of Enterobacteriaceae. B) Abundance of fecal *E. coli* 16S sequences relative to total bacteria 16S sequences as determined by quantitative PCR. Data are presented as the fold change relative to the low iron diet group. Lines are at the medians and *p* values were determined by pairwise comparisons by the Kruskal-Wallis test. C) Differences in the least square means between diet groups of log10 normalized counts of predicted genes involved in iron acquisition as determined by PICRUSt. D) Relative fecal abundance of Enterococcaceae. Each symbol represents an individual mouse, n = 8-9 mice per group. A, D) Box and whisker plots show the minimum, first quartile, median, third quartile and maximum relative abundance. A, C, D) FDR-corrected *p* values were determined using a mixed linear model. * $p < 0.05$, ** $p < 0.01$, *** $p < 0.001$

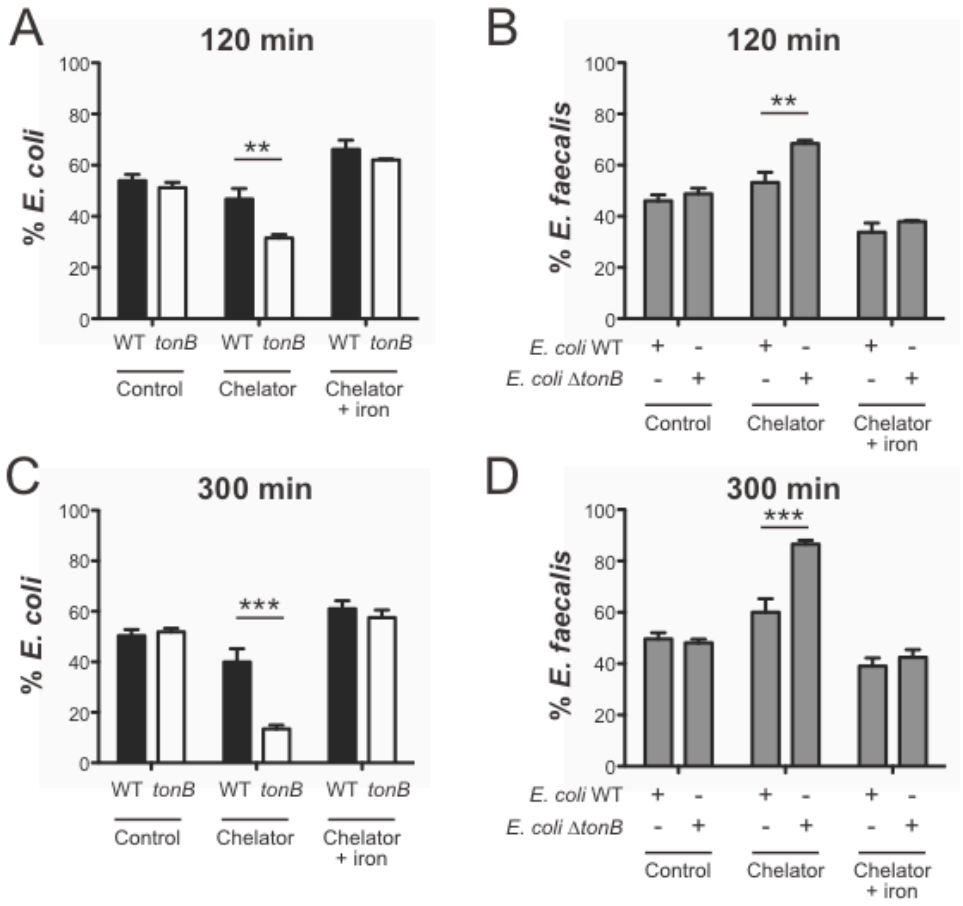

Figure 3.4. TonB-dependent iron acquisition enhances the relative abundance of *E. coli* when iron availability is restricted. *E. coli* WT or the *tonB*-deficient mutant were grown in the presence of *E. faecalis* in rich medium (control), in rich medium with an iron chelator (chelator) or in rich medium with an iron chelator and additional ferrous iron (chelator + iron). Abundance of bacteria was determined by quantitative selective plating. The % abundance of A, C) *E. coli* WT or the *tonB* mutant in the presence of *E. faecalis* and B, D) the % abundance of *E. faecalis* in the presence of *E. coli* WT or the *tonB* mutant after 120 or 300 min of growth. Data are represented as the mean ± SEM of at least three independent experiments. *P* values were determined by two-way ANOVA. ** $p < 0.01$, *** $p < 0.001$

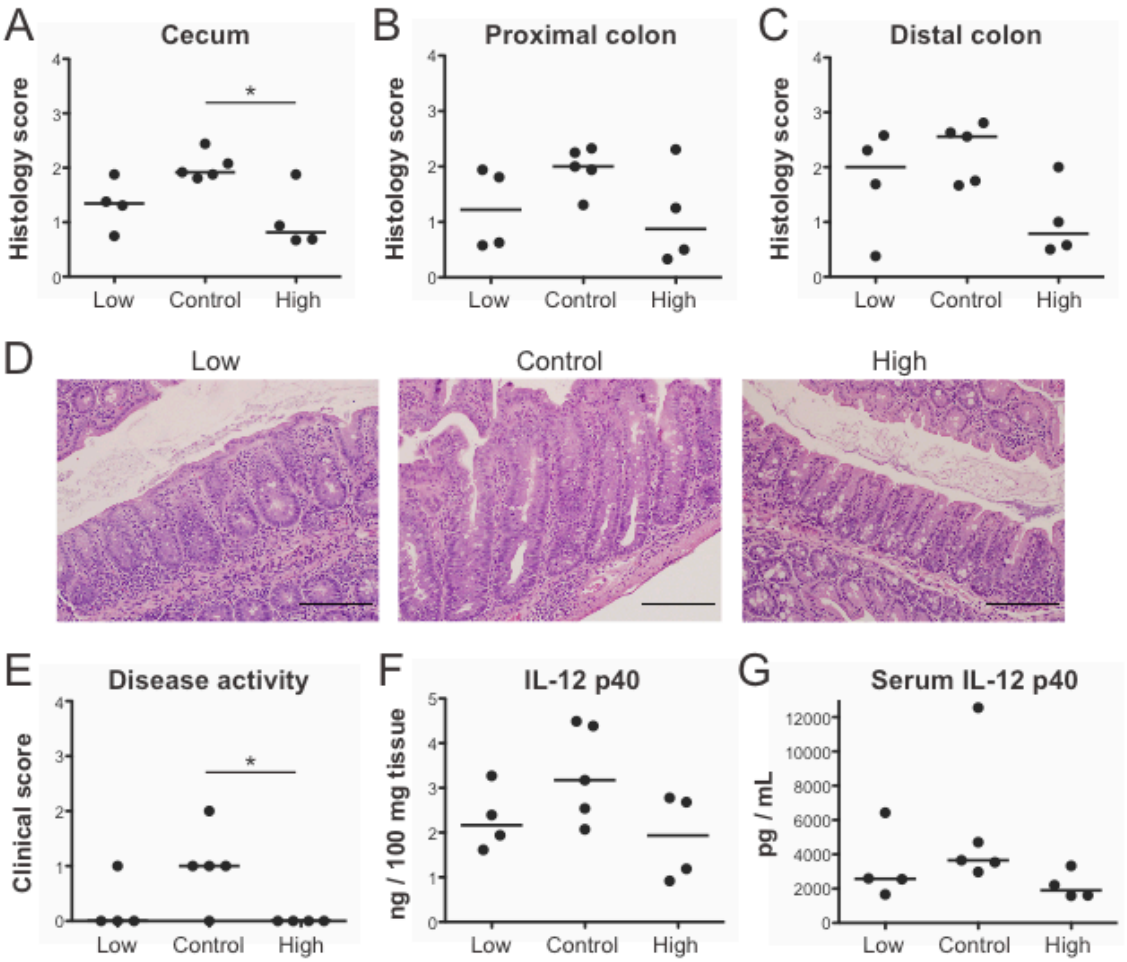

Figure 3.5. Dietary iron impacts the development of colitis in *Il10*$^{-/-}$ mice. Ex-GF *Il10*$^{-/-}$ mice were maintained on an iron deficient (low), control or iron supplemented (high) diet. A-C) Histology scores (0-4) of the A) cecum, B) proximal colon and C) distal colon. D) Representative H&E histology at 200x of the ceca. Scale bar = 20 μm. E) Clinical activity scores (0-4) after 4 weeks. F) Spontaneous secretion of IL-12 p40 by colonic explant cultures. G) Serum IL-12 p40 levels. Each symbol represents an individual mouse, n = 4-5 mice per group. Lines are at the medians. *P* values were determined by pairwise comparisons by the Kruskal-Wallis test. * $p < 0.05$

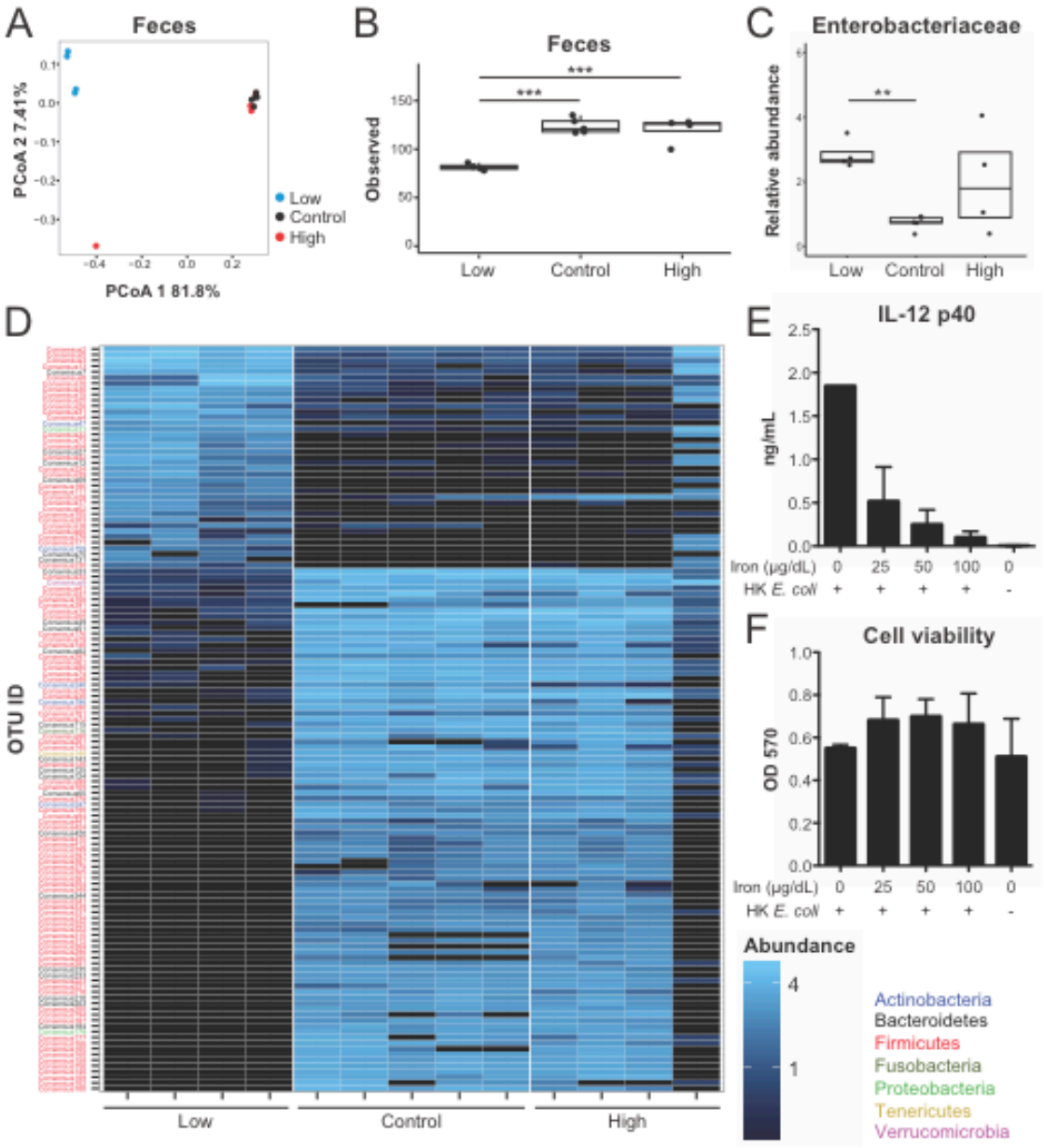

Figure 3.6. Fecal community composition is insensitive to additional dietary iron supplementation in *Il10*$^{-/-}$ mice. A) Principle coordinate analysis based on Bray-Curtis metrics for the fecal microbiota in ex-GF *Il10*$^{-/-}$ mice. B) Microbial richness as measured by observed OTUs. C) Relative fecal abundance of Enterobacteriaceae. B, C) Box and whisker plots show the minimum, first quartile, median, third quartile and maximum relative abundance. Each symbol represents an individual mouse, n = 4-5 mice per group. FDR-corrected p values were determined using a mixed linear model. D) Heat map of OTUs that significantly differ in relative fecal abundance (FDR-corrected $p < 0.05$) as determined using a mixed linear model. Each column represents an individual *Il10*$^{-/-}$ mouse. Each row represents individual OTUs, color coded by phylum. The colors of the heat map represent the mean relative abundance (normalized and log transformed) of each OTU. E) Macrophage production of IL-12 p40 and F) macrophage viability as assessed by the MTT assay after 8 hours. Macrophages were stimulated with heat-

killed *E. coli* and cultured with the indicated concentrations of iron. Data are represented as the mean ± SEM. ** $p < 0.01$, *** $p < 0.001$

3.8 Supplemental Figures

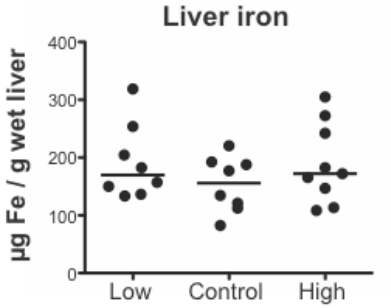

Supplemental Figure 3.1. Liver iron stores in WT mice. Liver iron concentrations were measured in ex-GF WT mice 4 weeks following conventionalization and administration of an iron deficient (low), control or iron supplemented (high) diet. Each symbol represents an individual mouse, n = 8-9 mice per group. Lines are at the medians. P values were determined by pairwise comparisons by the Kruskal-Wallis test.

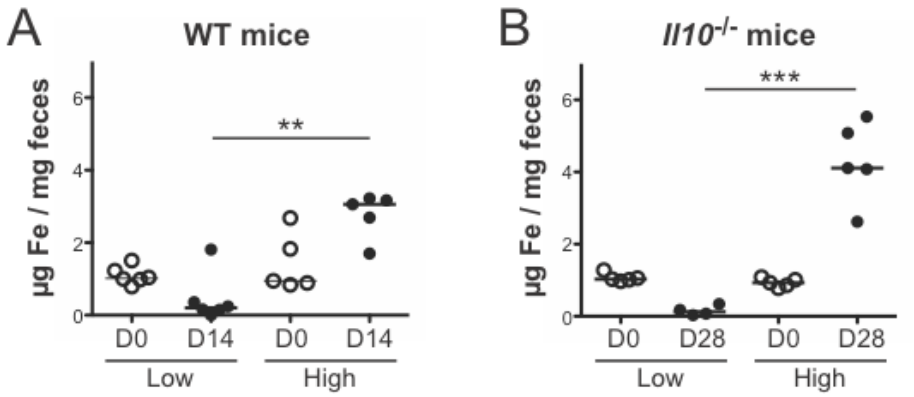

Supplemental Figure 3.2. Dietary iron restriction and supplementation alters fecal iron concentrations. Fecal iron concentrations were measured in A) ex-GF WT mice after 14 days and B) ex-GF *Il10*$^{-/-}$ mice after 28 days following conventionalization and administration of an iron deficient (low), control or iron supplemented (high) diet. Prior to the dietary interventions, mice were maintained on a typical mouse diet. Each symbol represents an individual mouse, n = 5-6 mice per group. Data are represented as μg Fe per mg dried feces. Lines are at the medians. P values were determined by pairwise comparisons by the Kruskal-Wallis test. ** $p < 0.01$, *** $p < 0.001$

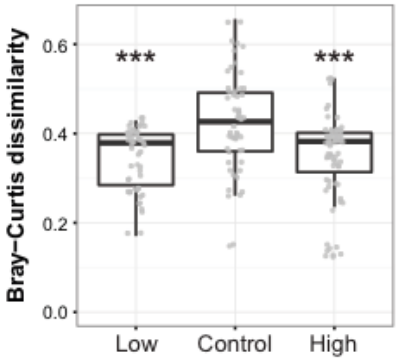

Supplemental Figure 3.3. Distances between WT mice within each diet group. Ex-GF WT mice were maintained on an iron deficient (low), control or iron supplemented (high) diet. Data are represented as pair-wise Bray-Curtis distances between samples within each diet group. Box and whisker plots show the minimum, first quartile, median, third quartile and maximum distance. *P* values were determined using a Student's *t*-test. *** $p < 0.001$ relative to the control diet group.

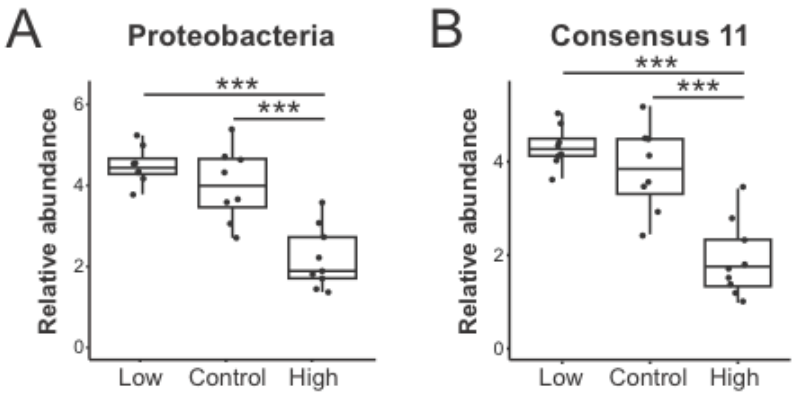

Supplemental Figure 3.4. Dietary iron restriction promotes a bloom of Proteobacteria and Enterobacterioaceae. Relative fecal abundances of A) Proteobacteria and B) Enterobacteriaceae (OTU Consensus 11) in WT mice. Each symbol represents an individual mouse, n = 8-9 mice per group. Box and whisker plots show the minimum, first quartile, median, third quartile and maximum relative abundance. FDR-corrected p values were determined using a mixed linear model. *** $p < 0.001$

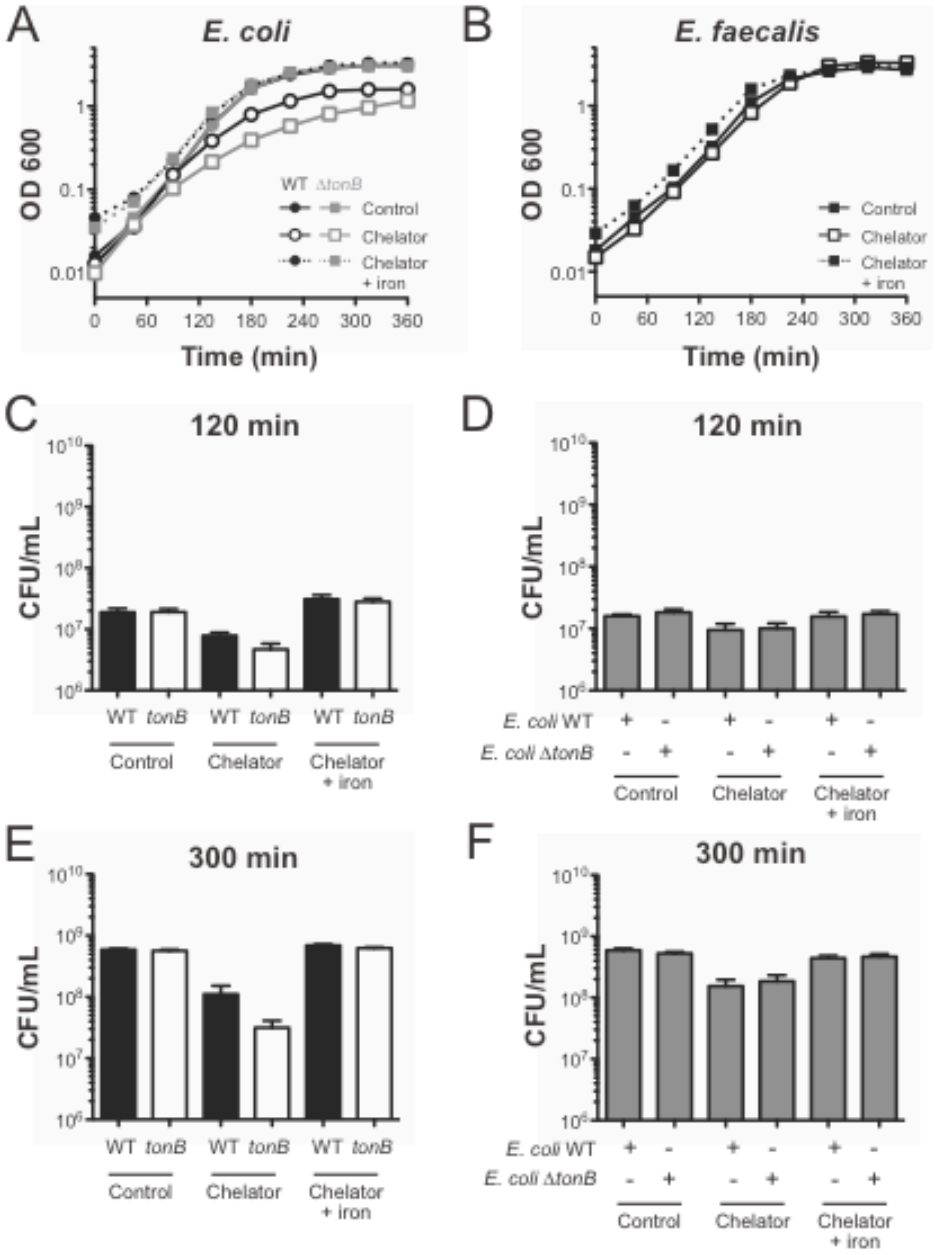

Supplemental Figure 3.5. Growth of *E. faecalis* and the parental and *tonB*-deficient *E. coli* strains in the presence or absence of an iron chelator. A, B) Representative growth curves of A) *E. coli* WT (circles + black lines) or the *tonB*-deficient mutant (squares + grey lines) and B) *E. faecalis* grown in rich medium (control), in rich medium with an iron chelator (chelator) or in rich medium with an iron chelator and additional ferrous iron (chelator + iron). C-F) *E. coli* WT or the *tonB*-deficient mutant was grown in the presence of *E. faecalis*. Abundance of bacteria was determined by quantitative selective plating. The abundance of A, C) *E. coli* WT or the *tonB* mutant in the presence of *E. faecalis* and B, D) the abundance of *E. faecalis* in the presence of *E. coli* WT or the *tonB* mutant after 120 or 300 min of growth. Data are represented as the mean ± SEM of at least three independent experiments.

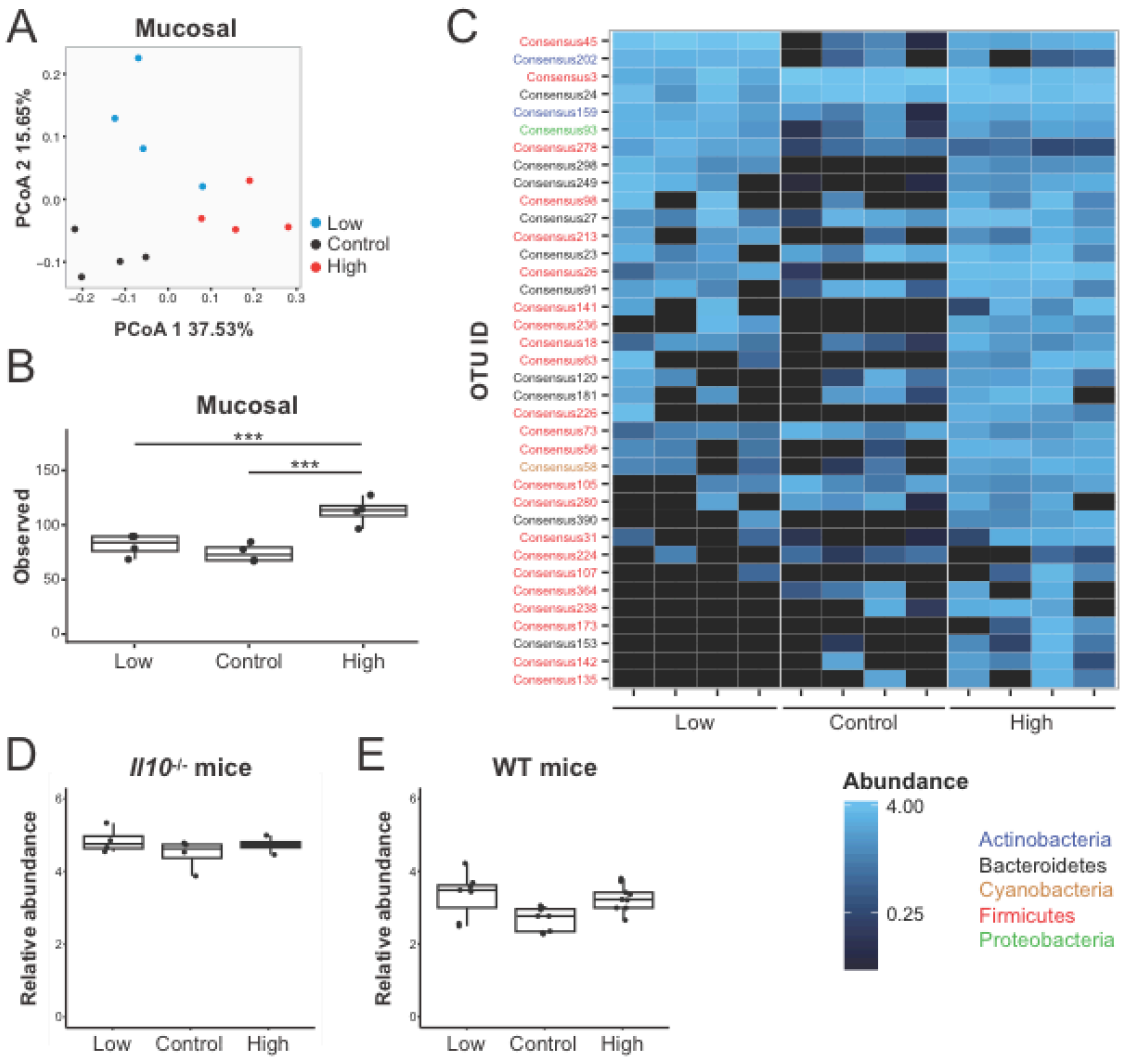

Supplemental Figure 3.6. Compositional changes to the mucosal microbiota in *Il10*$^{-/-}$ mice. A) Principle coordinate analysis based on Bray-Curtis metrics for the mucosal microbiota in ex-GF *Il10*$^{-/-}$ mice maintained on an iron deficient (low), control or iron supplemented (high) diet. B) Microbial richness as measured by observed OTUs. C) Heat map of OTUs that are significantly different in abundance (FDR-corrected $p < 0.05$) as determined using a mixed linear model. Each column represents an individual *Il10*$^{-/-}$ mouse. Each row represents individual OTUs, color coded by phylum. The colors of the heat map represent the mean relative abundance (normalized and log transformed) of each OTU. D, E) Relative mucosal abundance of Enterobacteriaceae in D) *Il10*$^{-/-}$ mice and E) WT mice. Each symbol represents an individual mouse, n = 4-9 mice per group. Box and whisker plots show the minimum, first quartile, median, third quartile and maximum values. Comparisons and FDR-corrected p values were determined using a mixed linear model. *** $p < 0.001$

Strains or plasmids	Description	Reference
Strains		
E. coli NC101	Murine intestinal *E. coli* strain with AIEC characteristics.	Kim 2005
E. coli NC101 Δ*tonB*	NC101 isogenic mutant with *tonB* deleted.	This work
E. faecalis OG1RF	Human oral *E. faecalis* strain	Kim 2005
Plasmids		
pKD46	Plasmid encoding lambda red recombinase.	Datsenko KA 2000
pKD13	Template plasmid for gene deletions using the lambda red recombinase system.	Baba T 2006
pCP20	Plasmid encoding FLP recombinase.	Datsenko KA 2000

Supplemental Table 3.1. Bacterial strains and plasmids used in this study.

	Consensus OTU	Taxonomy	Estimate[A]	FDR *p* value
HIGH VS LOW IRON DIET	Consensus6	Allobaculum spp	-4.44	1.1E-07
	Consensus9	Akkermansia muciniphila	-3.56	5.9E-06
	Consensus85	Allobaculum spp	-3.31	1.1E-07
	Consensus21	Ruminococcus spp	-3.00	9.4E-06
	Consensus24	Bacteroidales	-2.41	3.2E-04
	Consensus11	Enterobacteriaceae	-2.39	2.6E-06
	Consensus38	Parabacteroides spp	-2.00	1.7E-03
	Consensus15	Peptostreptococcaceae	-1.44	5.6E-03
	Consensus5	Lactobacillales	0.74	4.6E-03
	Consensus216	Adlercreutzia spp	0.76	3.0E-02
	Consensus53	Ruminococcus spp	0.97	2.4E-02
	Consensus309	Clostridiales	1.07	3.2E-03
	Consensus295	Coriobacteriaceae	1.31	3.3E-05
	Consensus301	Clostridiales	1.34	9.1E-04
	Consensus88	Sutterella spp	1.38	1.0E-03
	Consensus215	Lachnospiraceae	1.43	3.1E-03
	Consensus168	S24-7	1.47	7.9E-08
	Consensus164	Lachnospiraceae	1.48	1.9E-03
	Consensus229	Clostridiaceae	1.52	3.0E-02
	Consensus224	Lactobacillus spp	1.53	2.0E-04
	Consensus186	Proteiniclasticum spp	1.53	8.3E-03
	Consensus192	Lachnospiraceae	1.56	3.7E-02
	Consensus244	Erysipelotrichaceae	1.57	3.5E-03
	Consensus306	Lactobacillus spp	1.58	5.3E-04
	Consensus89	Oscillospira spp	1.63	3.2E-02
	Consensus59	Clostridiaceae	1.66	1.9E-02
	Consensus95	Oscillospira spp	1.68	2.3E-02
	Consensus112	Enterococcus spp	1.79	2.7E-03
	Consensus83	Lachnospiraceae	1.92	8.6E-04
	Consensus13	Clostridium spp	1.96	1.7E-02
	Consensus104	Staphylococcus spp	2.04	2.1E-02
	Consensus52	Clostridiales	2.33	9.7E-04
	Consensus57	Lactobacillus spp	2.47	2.2E-02
	Consensus54	Streptococcus spp	2.48	2.5E-06
	Consensus17	Clostridiales	2.60	2.6E-05
	Consensus44	Lachnospiraceae	2.63	1.5E-03
	Consensus39	Lachnospiraceae	2.71	5.8E-03
	Consensus40	Ruminococcus gnavus	2.72	4.0E-04
	Consensus18	Clostridium spp	2.83	1.1E-02
	Consensus47	Coriobacteriaceae	2.95	1.3E-04
	Consensus31	Clostridiaceae	3.05	1.4E-03
	Consensus35	Clostridiales	3.07	1.2E-04
	Consensus4	Clostridiales	3.36	1.7E-06
	Consensus10	Allobaculum spp	3.93	1.2E-04
	Consensus8	Allobaculum spp	4.02	1.6E-04

CONTROL VS HIGH IRON DIET	Consensus8	Allobaculum spp	-3.01	4.0E-03
	Consensus10	Allobaculum spp	-2.93	3.4E-03
	Consensus35	Clostridiales	-2.54	1.2E-03
	Consensus40	Ruminococcus gnavus	-2.28	2.7E-03
	Consensus52	Clostridiales	-1.91	6.2E-03
	Consensus83	Lachnospiraceae	-1.74	2.5E-03
	Consensus47	Coriobacteriaceae	-1.66	2.7E-02
	Consensus44	Lachnospiraceae	-1.66	4.5E-02
	Consensus4	Clostridiales	-1.64	1.2E-02
	Consensus17	Clostridiales	-1.56	8.4E-03
	Consensus54	Streptococcus spp	-1.43	3.8E-03
	Consensus168	S24-7	-1.22	2.9E-06
	Consensus293	Lachnospiraceae	-1.13	8.9E-03
	Consensus244	Erysipelotrichaceae	-1.08	4.3E-02
	Consensus300	Lactococcus spp	-1.03	1.2E-02
	Consensus234	Adlercreutzia spp	-0.83	2.9E-02
	Consensus295	Coriobacteriaceae	-0.73	1.6E-02
	Consensus2	Lactobacillus spp	-0.56	2.7E-02
	Consensus7	S24-7	0.97	2.1E-02
	Consensus131	Bacteroides spp	0.99	1.7E-02
	Consensus151	Clostridium bifermentans	1.15	7.5E-03
	Consensus32	Clostridiaceae	1.24	2.7E-02
	Consensus24	Bacteroidales	1.42	3.1E-02
	Consensus85	Allobaculum spp	1.50	7.4E-03
	Consensus25	Clostridiaceae	1.55	8.8E-03
	Consensus21	Ruminococcus spp	1.68	8.7E-03
	Consensus230	Clostridiaceae	1.69	9.4E-05
	Consensus15	Peptostreptococcaceae	1.70	1.2E-03
	Consensus11	Enterobacteriaceae	1.95	7.0E-05
	Consensus236	Streptococcus spp	2.00	7.8E-04
	Consensus6	Allobaculum spp	2.48	1.0E-03
CONTROL VS LOW IRON DIET	Consensus20	Lachnospiraceae	-2.22	3.2E-02
	Consensus9	Akkermansia muciniphila	-2.15	4.3E-03
	Consensus6	Allobaculum spp	-1.96	9.7E-03
	Consensus85	Allobaculum spp	-1.81	1.4E-03
	Consensus21	Ruminococcus spp	-1.31	4.3E-02
	Consensus293	Lachnospiraceae	-1.21	6.0E-03
	Consensus2	Lactobacillus spp	-0.70	7.0E-03
	Consensus224	Lactobacillus spp	0.84	4.0E-02
	Consensus215	Lachnospiraceae	1.00	4.1E-02
	Consensus164	Lachnospiraceae	1.04	3.2E-02
	Consensus54	Streptococcus spp	1.06	3.7E-02
	Consensus131	Bacteroides spp	1.13	7.7E-03
	Consensus151	Clostridium bifermentans	1.24	5.0E-03
	Consensus306	Lactobacillus spp	1.33	3.6E-03
	Consensus230	Clostridiaceae	1.35	1.9E-03
	Consensus32	Clostridiaceae	1.35	1.8E-02
	Consensus25	Clostridiaceae	1.42	1.8E-02

	Consensus112	Enterococcus spp	1.49	1.3E-02
	Consensus229	Clostridiaceae	1.49	3.5E-02
	Consensus105	Clostridiaceae	1.56	9.4E-03
	Consensus186	Proteiniclasticum spp	1.60	7.1E-03
	Consensus236	Streptococcus spp	1.61	6.8E-03
	Consensus73	Clostridium perfringens	1.70	1.4E-02
	Consensus4	Clostridiales	1.72	9.2E-03
	Consensus59	Clostridiaceae	1.83	1.1E-02
	Consensus18	Clostridium spp	2.39	3.5E-02
	Consensus31	Clostridiaceae	2.47	9.5E-03

Supplemental Table 3.2. Changes in relative fecal abundances of bacterial taxa in WT mice. This table lists OTUs that are significantly different in abundance (FDR-corrected $p < 0.05$) in the fecal microbiota of WT mice between at least 2 of the diet groups as determined using a mixed linear model. A = Difference in the least square means of log10 normalized counts of OTUs between the high vs low iron diet (negative = OTU decreased in the high iron diet; positive = OTU increased in the high iron diet), control vs high iron diet (negative = OTU decreased in the control diet; positive = OTU increased in the control diet), or control vs low iron diet (negative = OTU decreased in the control diet; positive = OTU increased in control diet).

Gene Symbol	Fold change			Gene description
	0 vs 5	0 vs 50	5 vs 50	
ybdZ	3.63	17.22	4.75	hypothetical protein
chuT	4.91	11.64	2.37	putative periplasmic binding protein
cirZ	6.46	11.52	1.78	colicin I receptorr; catecholate siderophore receptor CirA
fes	3.36	11.28	3.36	enterobactin/ferric enterobactin esterase
entH	3.35	11.07	3.31	thioesterase required for efficient enterobactin production
c4310	5.96	11.03	1.85	hypothetical protein
chuW	5.00	10.63	2.13	coproporphyrinogen III oxidase
fhuE	7.39	10.46	1.42	ferric-rhodotorulic acid outer membrane transporter
chuA	6.49	10.45	1.61	Outer membrane heme/hemoglobin receptor
fhuF	3.52	10.26	2.92	ferric iron reductase involved in ferric hydroximate transport
entB	3.11	9.85	3.17	2,3-dihydro-2,3-dihydroxybenzoate synthetase; isochorismatase
entE	3.03	8.69	2.87	enterobactin synthase subunit E
entA	2.89	8.40	2.91	2,3-dihydroxybenzoate-2,3-dehydrogenase
sitA	2.85	7.50	2.63	SitA protein
chuX	3.92	7.40	1.89	hypothetical protein; ShuX-like protein
ybiL	5.41	7.39	1.37	catecholate siderophore receptor Fiu
c0670	4.66	7.00	1.50	hypothetical protein
entF	2.93	6.79	2.32	enterobactin synthase subunit F
ycdO	1.77	6.75	3.82	hypothetical protein; inactive ferrous ion transporter EfeUOB
sitC	3.41	6.73	1.97	SitC protein
chuY	3.95	6.73	1.70	hypothetical protein
fes	3.23	6.12	1.89	enterobactin/ferric enterobactin esterase
sitB	2.74	5.45	1.99	SitB protein
ycdB	1.91	5.23	2.74	hypothetical protein
yncE	2.22	4.77	2.15	putative receptor; hypothetical protein
fepB	2.46	4.77	1.93	iron-enterobactin transporter periplasmic binding protein; iron-enterobactin transporter subunit
ycdO	1.78	4.61	2.59	hypothetical protein
c2423	2.85	3.66	1.28	putative AraC type regulator
tonB	1.78	3.63	2.04	transport protein TonB; membrane spanning protein in TonB-ExbB-ExbD transport complex
fhuA	1.49	3.09	2.08	ferrichrome outer membrane transporter
exbB	1.91	2.91	1.52	biopolymer transport protein ExbB; membrane spanning protein in TonB-ExbB-ExbD complex
yqjH	1.66	2.82	1.70	predicted siderophore interacting protein
bfd	1.57	2.55	1.63	bacterioferritin-associated ferredoxin
exbD	1.64	2.53	1.54	biopolymer transport protein ExbD; membrane spanning protein in TonB-ExbB-ExbD complex
pabB	1.11	1.97	1.77	para-aminobenzoate synthase component I; aminodeoxychorismate synthase, subunit I
sufS	1.57	1.90	1.21	bifunctional cysteine desulfurase/selenocysteine lyase; cysteine desulfurase, stimulated by SufE

sodA	1.16	1.56	1.34	superoxide dismutase, Mn
pncA	1.09	1.67	1.54	nicotinamidase/pyrazinamidase
bioB	1.06	1.64	1.55	biotin synthase
mltA	1.17	1.96	1.67	murein transglycosylase A; membrane-bound lytic murein transglycosylase A
yebU	1.02	1.68	1.64	16S rRNA m(5)C1407 methyltransferase, SAM-dependent; rRNA (cytosine-C(5)-)-methyltransferase RsmF
yebT	1.09	1.59	1.47	hypothetical protein
yciR	1.06	1.59	1.51	RNase II stability modulator; cyclic-di-GMP phospho-diesterase; csgD regulator; modulator of Rnase II stability
flk	1.07	1.55	1.45	flagella biosynthesis regulator; predicted flagella assembly protein
holE	1.05	1.55	1.47	DNA polymerase III subunit theta

Supplemental Table 3.3. Microarray results for genes in *E. coli* NC101 upregulated with decreased iron availability. *E. coli* NC101 was cultured in minimal media with 0, 5 or 50 μM added iron for 1 hour. The table below lists genes that are significantly upregulated ≥1.5 fold with decreased iron ($p < 0.1$, pairwise comparisons by one-way ANOVA).

	Consensus OTU	Taxonomy	Estimate[A]	FDR *p* value
HIGH VS LOW IRON DIET	Consensus9	Akkermansia muciniphila	3.64	1.4E-05
	Consensus14	Blautia spp	3.58	3.5E-04
	Consensus30	Lachnospiraceae	3.48	3.9E-04
	Consensus55	Lachnospiraceae	3.00	1.3E-03
	Consensus65	Bacteroides ovatus	2.98	5.2E-04
	Consensus90	Clostridiales	2.92	6.4E-04
	Consensus34	Erysipelotrichaceae	2.91	1.8E-03
	Consensus61	Lachnospiraceae	2.86	3.3E-04
	Consensus72	Lachnospiraceae	2.82	4.7E-04
	Consensus48	Ruminococcaceae	2.79	2.4E-03
	Consensus94	Phascolarctobacterium spp	2.79	4.7E-04
	Consensus109	Coprococcus spp	2.77	1.2E-03
	Consensus79	Lachnospiraceae	2.76	3.2E-03
	Consensus74	Eubacterium dolichum	2.75	1.7E-04
	Consensus49	Bacteroides spp	2.74	3.3E-03
	Consensus99	Eubacterium dolichum	2.70	1.2E-04
	Consensus78	Coprobacillus spp	2.67	4.6E-04
	Consensus80	Lachnospiraceae	2.61	6.8E-03
	Consensus124	Parabacteroides spp	2.58	1.4E-03
	Consensus51	Bacteroides uniformis	2.55	1.4E-03
	Consensus125	Bacteroides spp	2.55	1.1E-03
	Consensus194	Clostridiales	2.55	4.1E-03
	Consensus165	Clostridiales	2.54	2.7E-02
	Consensus169	Ruminococcaceae	2.50	2.8E-03
	Consensus187	Lachnospiraceae	2.48	2.6E-02
	Consensus146	Lachnospiraceae	2.46	7.3E-04
	Consensus160	Ruminococcaceae	2.45	1.4E-03
	Consensus82	Bacteroides fragilis	2.45	8.3E-04
	Consensus144	Acholeplasma spp	2.44	3.2E-04
	Consensus116	Fusobacterium spp	2.43	1.5E-03
	Consensus156	Erysipelotrichaceae	2.42	7.0E-04
	Consensus158	Lachnospiraceae	2.40	1.4E-03
	Consensus221	Ruminococcaceae	2.35	2.3E-03
	Consensus178	Sutterella spp	2.33	8.4E-04
	Consensus143	Bacteroides spp	2.28	1.2E-03
	Consensus184	Barnesiellaceae	2.26	1.0E-03
	Consensus223	Lachnospiraceae	2.26	1.5E-04
	Consensus201	Lachnospiraceae	2.24	7.1E-03
	Consensus33	Bacteroides spp	2.24	1.3E-02
	Consensus200	Lachnospiraceae	2.21	7.3E-04
	Consensus203	Bacteroides ovatus	2.20	9.6E-04
	Consensus96	Blautia spp	2.15	2.5E-03
	Consensus233	Bacteroides spp	2.13	8.3E-04
	Consensus304	Lachnospiraceae	2.13	2.5E-02

	Consensus315	Lachnospiraceae	2.11	2.4E-02
	Consensus210	Bacteroides spp	2.08	8.3E-04
	Consensus176	Lachnospiraceae	2.04	4.8E-04
	Consensus285	Dorea spp	2.04	6.1E-03
	Consensus177	Erysipelotrichaceae	2.00	1.6E-02
	Consensus115	Bacteroides spp	1.98	4.6E-03
	Consensus281	Ruminococcaceae	1.98	3.1E-04
	Consensus126	Clostridiales	1.97	9.0E-04
	Consensus198	Lachnospiraceae	1.97	3.7E-03
	Consensus166	Blautia spp	1.96	9.9E-04
	Consensus247	Eggerthella lenta	1.93	2.0E-03
	Consensus41	Lachnospiraceae	1.92	2.0E-03
	Consensus235	Paraprevotellaceae	1.91	8.4E-04
	Consensus365	Ruminococcaceae	1.89	2.8E-03
	Consensus379	Erysipelotrichaceae	1.89	1.1E-02
	Consensus312	Lachnospiraceae	1.88	1.4E-03
	Consensus322	Ruminococcus gnavus	1.87	2.2E-03
	Consensus100	Lachnospiraceae	1.87	1.5E-03
	Consensus296	Blautia spp	1.85	1.3E-03
	Consensus339	Ruminococcaceae	1.80	1.5E-03
	Consensus361	Lachnospiraceae	1.79	1.8E-03
	Consensus325	Coprococcus spp	1.75	2.0E-03
	Consensus337	Lachnospiraceae	1.74	2.0E-04
	Consensus387	Ruminococcaceae	1.73	1.3E-02
	Consensus415	Lachnospiraceae	1.71	2.0E-03
	Consensus341	Ruminococcaceae	1.69	3.1E-03
	Consensus397	Lachnospiraceae	1.66	1.5E-03
	Consensus291	Blautia producta	1.64	2.6E-02
	Consensus334	Lachnospiraceae	1.62	1.2E-03
	Consensus412	Blautia spp	1.61	3.4E-03
	Consensus344	Barnesiellaceae	1.56	1.5E-03
	Consensus441	Lachnospiraceae	1.55	4.8E-03
	Consensus287	Ruminococcaceae	1.54	2.2E-02
	Consensus399	Blautia spp	1.53	3.5E-03
	Consensus420	Bacteroides spp	1.50	2.7E-03
	Consensus378	Ruminococcus gnavus	1.45	7.7E-03
	Consensus101	Oscillospira spp	1.45	3.2E-02
	Consensus218	Dorea spp	1.38	2.1E-03
	Consensus424	Lachnospiraceae	1.37	2.0E-03
	Consensus349	Ruminococcus spp	1.26	2.7E-02
	Consensus278	Enterococcus spp	-1.06	4.1E-02
	Consensus66	Clostridiaceae	-1.38	4.6E-02
	Consensus263	Peptostreptococcaceae	-1.58	2.1E-02
	Consensus18	Clostridium spp	-1.64	9.2E-03
	Consensus17	Clostridiales	-1.81	1.9E-03
	Consensus12	Bacteroides spp	-1.82	2.5E-03
	Consensus105	Clostridiaceae	-1.93	2.9E-03
	Consensus52	Clostridiales	-1.96	1.2E-02

	Consensus186	Proteiniclasticum spp	-2.02	5.6E-03
	Consensus69	S24-7	-2.07	9.9E-03
	Consensus39	Lachnospiraceae	-2.13	1.8E-03
	Consensus42	Erysipelotrichaceae	-2.16	3.6E-02
	Consensus25	Clostridiaceae	-2.16	4.7E-03
	Consensus32	Clostridiaceae	-2.28	6.2E-04
	Consensus7	S24-7	-2.29	6.4E-03
	Consensus4	Clostridiales	-2.40	2.0E-04
	Consensus15	Peptostreptococcaceae	-2.44	5.9E-05
	Consensus26	Erysipelotrichaceae	-2.46	5.2E-03
	Consensus2	Lactobacillus spp	-2.50	1.7E-03
	Consensus224	Lactobacillus spp	-2.52	2.1E-05
	Consensus36	Clostridiaceae	-2.57	5.8E-03
	Consensus27	S24-7	-2.68	5.8E-03
	Consensus73	Clostridium perfringens	-2.71	1.3E-04
	Consensus10	Allobaculum	-2.72	4.4E-02
	Consensus5	Lactobacillales	-2.73	7.1E-04
	Consensus13	Clostridium spp	-2.88	2.7E-02
	Consensus47	Coriobacteriaceae	-3.00	1.6E-06
	Consensus3	Clostridium perfringens	-3.29	1.5E-05
	Consensus31	Clostridiaceae	-3.32	2.8E-04
CONTROL VS HIGH IRON DIET	Consensus246	Bifidobacterium longum	2.21	1.0E-05
	Consensus102	Lachnospiraceae	2.14	3.2E-02
	Consensus100	Lachnospiraceae	1.89	9.3E-04
	Consensus196	Collinsella spp	1.75	4.6E-03
	Consensus218	Dorea spp	1.62	4.4E-04
	Consensus96	Blautia spp	1.43	2.5E-02
	Consensus126	Clostridiales	1.41	6.6E-03
	Consensus115	Bacteroides spp	1.30	4.0E-02
	Consensus166	Blautia spp	1.28	1.3E-02
	Consensus235	Paraprevotellaceae	0.99	4.0E-02
	Consensus285	Dorea spp	-1.36	5.0E-02
	Consensus28	Anaerotruncus spp	-2.01	5.2E-03
CONTROL VS LOW IRON DIET	Consensus30	Lachnospiraceae	4.10	6.9E-05
	Consensus14	Blautia spp	4.08	7.9E-05
	Consensus48	Ruminococcaceae	3.94	1.2E-04
	Consensus61	Lachnospiraceae	3.81	2.3E-05
	Consensus100	Lachnospiraceae	3.75	4.7E-06
	Consensus72	Lachnospiraceae	3.75	3.7E-05
	Consensus65	Bacteroides ovatus	3.75	5.6E-05
	Consensus34	Erysipelotrichaceae	3.71	2.0E-04
	Consensus51	Bacteroides uniformis	3.71	5.1E-05
	Consensus33	Bacteroides spp	3.70	3.1E-04
	Consensus74	Eubacterium dolichum	3.68	1.3E-05
	Consensus94	Phascolarctobacterium spp	3.62	4.1E-05
	Consensus96	Blautia spp	3.58	3.7E-05
	Consensus80	Lachnospiraceae	3.56	5.5E-04
	Consensus99	Eubacterium dolichum	3.55	1.0E-05

	Consensus49	Bacteroides spp	3.54	3.4E-04
	Consensus82	Bacteroides fragilis	3.51	3.7E-05
	Consensus78	Coprobacillus spp	3.48	4.1E-05
	Consensus79	Lachnospiraceae	3.44	4.6E-04
	Consensus126	Clostridiales	3.38	1.0E-05
	Consensus146	Lachnospiraceae	3.38	4.1E-05
	Consensus125	Bacteroides spp	3.31	9.4E-05
	Consensus156	Erysipelotrichaceae	3.31	4.1E-05
	Consensus115	Bacteroides spp	3.28	6.9E-05
	Consensus143	Bacteroides spp	3.27	4.9E-05
	Consensus116	Fusobacterium spp	3.27	1.0E-04
	Consensus158	Lachnospiraceae	3.25	8.5E-05
	Consensus166	Blautia spp	3.25	1.4E-05
	Consensus144	Acholeplasma spp	3.25	2.3E-05
	Consensus55	Lachnospiraceae	3.22	5.3E-04
	Consensus90	Clostridiales	3.21	2.0E-04
	Consensus160	Ruminococcaceae	3.18	1.2E-04
	Consensus109	Coprococcus spp	3.12	3.2E-04
	Consensus178	Sutterella spp	3.10	5.9E-05
	Consensus200	Lachnospiraceae	3.05	4.1E-05
	Consensus184	Barnesiellaceae	3.03	6.7E-05
	Consensus218	Dorea spp	3.00	3.9E-06
	Consensus124	Parabacteroides spp	2.97	3.3E-04
	Consensus210	Bacteroides spp	2.95	3.8E-05
	Consensus187	Lachnospiraceae	2.92	8.7E-03
	Consensus223	Lachnospiraceae	2.90	1.5E-05
	Consensus235	Paraprevotellaceae	2.89	2.2E-05
	Consensus102	Lachnospiraceae	2.89	3.6E-03
	Consensus9	Akkermansia muciniphila	2.89	4.9E-05
	Consensus176	Lachnospiraceae	2.87	2.2E-05
	Consensus37	Lachnospiraceae	2.84	2.0E-03
	Consensus203	Bacteroides ovatus	2.84	8.5E-05
	Consensus41	Lachnospiraceae	2.83	6.8E-05
	Consensus196	Collinsella spp	2.80	1.4E-04
	Consensus233	Bacteroides spp	2.72	7.8E-05
	Consensus108	Blautia producta	2.71	2.5E-03
	Consensus177	Erysipelotrichaceae	2.63	1.7E-03
	Consensus198	Lachnospiraceae	2.62	3.2E-04
	Consensus145	Blautia spp	2.60	1.4E-03
	Consensus246	Bifidobacterium longum	2.59	3.3E-06
	Consensus140	Lachnospiraceae	2.56	1.8E-03
	Consensus247	Eggerthella lenta	2.45	2.3E-04
	Consensus281	Ruminococcaceae	2.43	4.1E-05
	Consensus296	Blautia spp	2.38	1.2E-04
	Consensus344	Barnesiellaceae	2.36	4.3E-05
	Consensus337	Lachnospiraceae	2.36	1.4E-05
	Consensus221	Ruminococcaceae	2.34	1.7E-03
	Consensus334	Lachnospiraceae	2.32	4.9E-05

	Consensus287	Ruminococcaceae	2.21	1.5E-03
	Consensus169	Ruminococcaceae	2.19	5.0E-03
	Consensus312	Lachnospiraceae	2.19	3.0E-04
	Consensus325	Coprococcus spp	2.18	2.6E-04
	Consensus424	Lachnospiraceae	2.15	4.5E-05
	Consensus349	Ruminococcus spp	2.11	6.0E-04
	Consensus339	Ruminococcaceae	2.05	3.8E-04
	Consensus361	Lachnospiraceae	2.01	5.0E-04
	Consensus399	Blautia spp	2.00	3.4E-04
	Consensus397	Lachnospiraceae	1.99	2.7E-04
	Consensus341	Ruminococcaceae	1.96	7.7E-04
	Consensus420	Bacteroides spp	1.93	2.9E-04
	Consensus378	Ruminococcus gnavus	1.90	8.0E-04
	Consensus322	Ruminococcus gnavus	1.87	1.6E-03
	Consensus412	Blautia spp	1.81	1.1E-03
	Consensus415	Lachnospiraceae	1.80	9.6E-04
	Consensus101	Oscillospira spp	1.69	9.8E-03
	Consensus365	Ruminococcaceae	1.66	4.8E-03
	Consensus354	Clostridiales	1.63	1.1E-02
	Consensus387	Ruminococcaceae	1.62	1.4E-02
	Consensus441	Lachnospiraceae	1.57	3.0E-03
	Consensus131	Bacteroides spp	-1.29	1.4E-02
	Consensus230	Clostridiaceae	-1.33	4.0E-03
	Consensus66	Clostridiaceae	-1.37	4.4E-02
	Consensus75	S24-7	-1.40	4.0E-02
	Consensus159	Coriobacteriaceae	-1.47	1.0E-02
	Consensus171	Lactobacillus spp	-1.50	1.3E-02
	Consensus278	Enterococcus spp	-1.56	2.9E-03
	Consensus263	Peptostreptococcaceae	-1.56	1.9E-02
	Consensus17	Clostridiales	-1.76	1.9E-03
	Consensus105	Clostridiaceae	-1.94	2.0E-03
	Consensus26	Erysipelotrichaceae	-2.01	1.5E-02
	Consensus52	Clostridiales	-2.02	7.2E-03
	Consensus11	Enterobacteriaceae	-2.15	2.5E-03
	Consensus39	Lachnospiraceae	-2.17	1.3E-03
	Consensus4	Clostridiales	-2.18	3.1E-04
	Consensus186	Proteiniclasticum spp	-2.19	2.7E-03
	Consensus111	Proteiniclasticum spp	-2.25	2.9E-02
	Consensus12	Bacteroides spp	-2.25	3.5E-04
	Consensus69	S24-7	-2.34	3.0E-03
	Consensus54	Streptococcus spp	-2.44	3.2E-02
	Consensus224	Lactobacillus spp	-2.48	1.8E-05
	Consensus42	Enterobacteriaceae	-2.64	8.3E-03
	Consensus7	S24-7	-2.69	1.4E-03
	Consensus73	Clostridium perfringens	-2.73	8.0E-05
	Consensus32	Clostridiaceae	-2.75	8.7E-05
	Consensus15	Peptostreptococcaceae	-2.76	1.7E-05
	Consensus27	S24-7	-2.78	3.1E-03

	Consensus25	Clostridiaceae	-2.82	4.7E-04
	Consensus36	Clostridiaceae	-2.83	2.0E-03
	Consensus31	Clostridiaceae	-2.85	7.7E-04
	Consensus10	Allobaculum	-3.01	2.5E-02
	Consensus47	Coriobacteriaceae	-3.02	1.1E-06
	Consensus8	Allobaculum	-3.06	4.5E-02
	Consensus2	Lactobacillus spp	-3.16	2.0E-04
	Consensus3	Clostridium perfringens	-3.35	9.3E-06
	Consensus5	Lactobacillales	-3.44	7.4E-05
	Consensus13	Clostridium spp	-3.65	4.7E-03

Supplemental Table 3.4. Changes in relative fecal abundances of bacterial taxa in *Il10*$^{-/-}$ mice. This table lists OTUs that are significantly different in abundance (FDR-corrected $p < 0.05$) in the fecal microbiota of *Il10*$^{-/-}$ mice between at least 2 of the diet groups as determined using a mixed linear model. A = Difference in the least square means of log10 normalized counts of OTUs between the high vs low iron diet (negative = OTU decreased in the high iron diet; positive = OTU increased in the high iron diet), control vs high iron diet (negative = OTU decreased in the control diet; positive = OTU increased in the control diet), or control vs low iron diet (negative = OTU decreased in the control diet; positive = OTU increased in control diet).

REFERENCES

Abhyankar, A., and Moss, A.C. (2015). Iron Replacement in Patients with Inflammatory Bowel Disease. Inflamm Bowel Dis *21*, 1976–1981.

Adu-Afarwuah, S., Lartey, A., Brown, K.H., Zlotkin, S., Briend, A., and Dewey, K.G. (2008). Home fortification of complementary foods with micronutrient supplements is well accepted and has positive effects on infant iron status in Ghana. American Journal of Clinical Nutrition *87*, 929–938.

Andrews, S.C., Robinson, A.K., and Rodrã guez-Quiã Ones, F. (2003). Bacterial iron homeostasis. FEMS Microbiology Reviews *27*, 215–237.

Arthur, J.C., Perez-Chanona, E., Muhlbauer, M., Tomkovich, S., Uronis, J.M., Fan, T.J., Campbell, B.J., Abujamel, T., Dogan, B., Rogers, A.B., et al. (2012). Intestinal Inflammation Targets Cancer-Inducing Activity of the Microbiota. Science *338*, 120–123.

Arthur, J.C., Gharaibeh, R.Z., Mühlbauer, M., Perez-Chanona, E., Uronis, J.M., McCafferty, J., Fodor, A.A., and Jobin, C. (2014). Microbial genomic analysis reveals the essential role of inflammation in bacteria-induced colorectal cancer. Nature Communications *5*, 4724.

Atarashi, K., Tanoue, T., Oshima, K., Suda, W., Nagano, Y., Nishikawa, H., Fukuda, S., Saito, T., Narushima, S., Hase, K., et al. (2013). Treg induction by a rationally selected mixture of Clostridia strains from the human microbiota. Nature *500*, 232–236.

Balamurugan, R., Mary, R.R., Chittaranjan, S., Jancy, H., Shobana Devi, R., and Ramakrishna, B.S. (2010). Low levels of faecal lactobacilli in women with iron-deficiency anaemia in south India. Br J Nutr *104*, 931–934.

Benjamini, Y., and Hochberg, Y. (1995). Controlling the False Discovery Rate: a Practical and Powerful Approach to Multiple Testing. Journal of the Royal Statistical Society. Series B (Methodological) *57*, 289–300.

Berglund, S., and Domellöf, M. (2014). Meeting iron needs for infants and children. Current Opinion in Clinical Nutrition and Metabolic Care *17*, 267–272.

Bokulich, N.A., Subramanian, S., Faith, J.J., Gevers, D., Gordon, J.I., Knight, R., Mills, D.A., and Caporaso, J.G. (2012). Quality-filtering vastly improves diversity estimates from Illumina amplicon sequencing. Nat Meth *10*, 57–59.

Braun, V., and Hantke, K. (2011). Recent insights into iron import by bacteria. Current Opinion in Chemical Biology *15*, 328–334.

Bryce, G.F., Weller, R., and Brot, N. (1971). Studies on the enzymatic synthesis of 2,3-dihydroxy-N-benzoyl-L-serine in Escherichia coli. Biochemical and Biophysical Research Communications *42*, 871–879.

Caldwell, D.R., and Arcand, C. (1974). Inorganic and metal-organic growth requirements of the genus Bacteroides. J Bacteriol *120*, 322–333.

Caporaso, J.G., Kuczynski, J., Stombaugh, J., Bittinger, K., Bushman, F.D., Costello, E.K., Fierer, N., Peña, A.G., Goodrich, J.K., Gordon, J.I., et al. (2010). QIIME allows analysis of high-throughput community sequencing data. Nat Meth *7*, 335–336.

Carrier, J., Aghdassi, E., Platt, I., Cullen, J., and Allard, J.P. (2001). Effect of oral iron supplementation on oxidative stress and colonic inflammation in rats with induced colitis. Aliment Pharmacol Ther *15*, 1989–1999.

Carvalho, F.A., Koren, O., Goodrich, J.K., Johansson, M.E.V., Nalbantoglu, I., Aitken, J.D., Su, Y., Chassaing, B., Walters, W.A., González, A., et al. (2012). Transient inability to manage proteobacteria promotes chronic gut inflammation in TLR5-deficient mice. Cell Host Microbe *12*, 139–152.

Chen, J., Shen, H., Chen, C., Wang, W., Yu, S., Zhao, M., and Li, M. (2009). The effect of psychological stress on iron absorption in rats. BMC Gastroenterol *9*, 83.

Chua, A.C.G., Klopcic, B.R.S., Ho, D.S., Fu, S.K., Forrest, C.H., Croft, K.D., Olynyk, J.K., Lawrance, I.C., and Trinder, D. (2013). Dietary Iron Enhances Colonic Inflammation and IL-6/IL-11-Stat3 Signaling Promoting Colonic Tumor Development in Mice. PLoS ONE *8*, e78850.

Cox, L.M., Yamanishi, S., Sohn, J., Alekseyenko, A.V., Leung, J.M., Cho, I., Kim, S.G., Li, H., Gao, Z., Mahana, D., et al. (2014). Altering the Intestinal Microbiotaduring a Critical Developmental Window Has Lasting Metabolic Consequences. Cell *158*, 705–721.

Datsenko, K.A., and Wanner, B.L. (2000). One-step inactivation of chromosomal genes in Escherichia coli K-12 using PCR products. Proc Natl Acad Sci USA *97*, 6640–6645.

David, L.A., Maurice, C.F., Carmody, R.N., Gootenberg, D.B., Button, J.E., Wolfe, B.E., Ling, A.V., Devlin, A.S., Varma, Y., Fischbach, M.A., et al. (2013). Diet rapidly and reproducibly alters the human gut microbiome. Nature *505*, 559–563.

Deriu, E., Liu, J.Z., Pezeshki, M., Edwards, R.A., Ochoa, R.J., Contreras, H., Libby, S.J., Fang, F.C., and Raffatellu, M. (2013). Probiotic Bacteria Reduce Salmonella Typhimurium Intestinal Colonization by Competing for Iron. Cell Host Microbe *14*, 26–37.

Devkota, S., Wang, Y., Musch, M.W., Leone, V., Fehlner-Peach, H., Nadimpalli, A., Antonopoulos, D.A., Jabri, B., and Chang, E.B. (2012). Dietary-fat-induced taurocholic acid promotes pathobiont expansion and colitis in Il10−/− mice. Nature.

Dogan, B., Suzuki, H., Herlekar, D., Sartor, R.B., Campbell, B.J., Roberts, C.L., Stewart, K., Scherl, E.J., Araz, Y., Bitar, P.P., et al. (2014). Inflammation-associated adherent-invasive Escherichia coli are enriched in pathways for use of propanediol and iron and M-cell translocation. Inflamm Bowel Dis *20*, 1919–1932.

Domellöf, M., Braegger, C., Campoy, C., Colomb, V., Decsi, T., Fewtrell, M., Hojsak, I.,

Mihatsch, W., Molgaard, C., Shamir, R., et al. (2014). Iron Requirements of Infants and Toddlers. Journal of Pediatric Gastroenterology and Nutrition *58*, 119–129.

Dostal, A., Baumgartner, J., Riesen, N., Chassard, C., Smuts, C.M., Zimmermann, M.B., and Lacroix, C. (2014a). Effects of iron supplementation on dominant bacterial groups in the gut, faecal SCFA and gut inflammation: a randomised, placebo-controlled intervention trial in South African children. Br J Nutr *112*, 547–556.

Dostal, A., Chassard, C., Hilty, F.M., Zimmermann, M.B., Jaeggi, T., Rossi, S., and Lacroix, C. (2012a). Iron depletion and repletion with ferrous sulfate or electrolytic iron modifies the composition and metabolic activity of the gut microbiota in rats. Journal of Nutrition *142*, 271–277.

Dostal, A., Fehlbaum, S., Chassard, C., Zimmermann, M.B., and Lacroix, C. (2012b). Low iron availability in continuous in vitrocolonic fermentations induces strong dysbiosis of the child gut microbial consortium and a decrease in main metabolites. FEMS Microbiol. Ecol. *83*, 161–175.

Dostal, A., Lacroix, C., Pham, V.T., Zimmermann, M.B., Del'homme, C., Bernalier-Donadille, A., and Chassard, C. (2014b). Iron supplementation promotes gut microbiota metabolic activity but not colitis markers in human gut microbiota-associated rats. Br J Nutr *111*, 2135–2145.

Edgar, R.C., Haas, B.J., Clemente, J.C., Quince, C., and Knight, R. (2011). UCHIME improves sensitivity and speed of chimera detection. Bioinformatics *27*, 2194–2200.

Ellermann, M., Huh, E.Y., Liu, B., Carroll, I.M., Tamayo, R., and Sartor, R.B. (2015). Adherent-Invasive Escherichia coli Production of Cellulose Influences Iron-Induced Bacterial Aggregation, Phagocytosis, and Induction of Colitis. Infect Immun *83*, 4068–4080.

Erichsen, K., Ulvik, R.J., Nysaeter, G., Johansen, J., Ostborg, J., Berstad, A., Berge, R.K., and Hausken, T. (2005). Oral ferrous fumarate or intravenous iron sucrose for patients with inflammatory bowel disease. Scand J Gastroenterol *40*, 1058–1065.

Ettreiki, C. (2012). Juvenile ferric iron prevents microbiota dysbiosis and colitis in adult rodents. World J. Gastroenterol. *18*, 2619.

Gera, T., and Sachdev, H.P.S. (2002). Effect of iron supplementation on incidence of infectious illness in children: systematic review. Bmj *325*, 1142.

Hurrell, R., and Egli, I. (2010). Iron bioavailability and dietary reference values. American Journal of Clinical Nutrition *91*, 1461S–1467S.

Imbert, M., and Blondeau, R. (1998). On the iron requirement of lactobacilli grown in chemically defined medium. Curr. Microbiol. *37*, 64–66.

Jaeggi, T., Kortman, G.A.M., Moretti, D., Chassard, C., Holding, P., Dostal, A., Boekhorst, J., Timmerman, H.M., Swinkels, D.W., Tjalsma, H., et al. (2014). Iron fortification adversely affects the gut microbiome, increases pathogen abundance and induces intestinal inflammation in Kenyan infants. Gut.

Kim, S.C., Tonkonogy, S.L., Albright, C.A., Tsang, J., Balish, E.J., Braun, J., Huycke, M.M., and Sartor, R.B. (2005). Variable phenotypes of enterocolitis in interleukin 10-deficient mice monoassociated with two different commensal bacteria. Gastroenterology *128*, 891–906.

Koenig, J.E., Spor, A., Scalfone, N., Fricker, A.D., Stombaugh, J., Knight, R., Angenent, L.T., and Ley, R.E. (2011). Succession of microbial consortia in the developing infant gut microbiome. Proc Natl Acad Sci USA *108 Suppl 1*, 4578–4585.

Krebs, N.F., Sherlock, L.G., Westcott, J., Culbertson, D., Hambidge, K.M., Feazel, L.M., Robertson, C.E., and Frank, D.N. (2013). Effects of Different Complementary Feeding Regimens on Iron Status and Enteric Microbiota in Breastfed Infants. J. Pediatr. *163*, 416–423.e4.

Kulnigg, S., and Gasche, C. (2006). Systematic review: managing anaemia in Crohn's disease. Aliment Pharmacol Ther *24*, 1507–1523.

Langille, M.G.I., Zaneveld, J., Caporaso, J.G., McDonald, D., Knights, D., Reyes, J.A., Clemente, J.C., Burkepile, D.E., Thurber, R.L.V., Knight, R., et al. (2013). nbt.2676. Nature Biotechnology *31*, 814–821.

Letain, T.E., and Postle, K. (1997). TonB protein appears to transduce energy by shuttling between the cytoplasmic membrane and the outer membrane in Escherichia coli. Mol Microbiol *24*, 271–283.

Lund, E.K., Wharf, S.G., Fairweather-Tait, S.J., and Johnson, I.T. (1999). Oral ferrous sulfate supplements increase the free radical-generating capacity of feces from healthy volunteers. Am. J. Clin. Nutr. *69*, 250–255.

Lupp, C., Robertson, M.L., Wickham, M.E., Sekirov, I., Champion, O.L., Gaynor, E.C., and Finlay, B.B. (2007). Host-Mediated Inflammation Disrupts the Intestinal Microbiota and Promotes the Overgrowth of Enterobacteriaceae. Cell Host Microbe *2*, 119–129.

Lutz, M.B., Kukutsch, N., Ogilvie, A.L., Rössner, S., Koch, F., Romani, N., and Schuler, G. (1999). An advanced culture method for generating large quantities of highly pure dendritic cells from mouse bone marrow. J. Immunol. Methods *223*, 77–92.

Maharshak, N., Packey, C.D., Ellermann, M., Manick, S., Siddle, J.P., Huh, E.Y., Plevy, S., Sartor, R.B., and Carroll, I.M. (2013). Altered enteric microbiota ecology in interleukin 10-deficient mice during development and progression of intestinal inflammation. Gut Microbes *4*, 316–324.

Marcelis, J.H., Daas-Slagt, den, H.J., and Hoogkamp-Korstanje, J.A. (1978). Iron requirement and chelator production of staphylococci, Streptococcus faecalis and enterobacteriaceae. Antonie Van Leeuwenhoek *44*, 257–267.

Martinez, C., Antolín, M., Santos, J., Torrejon, A., Casellas, F., Borruel, N., Guarner, F., and Malagelada, J.-R. (2008). Unstable Composition of the Fecal Microbiota in Ulcerative Colitis During Clinical Remission. Am J Gastroenterology *103*, 643–648.

McCafferty, J., hlbauer, M.M.U., Gharaibeh, R.Z., Arthur, J.C., Perez-Chanona, E., Sha, W., Jobin, C., and Fodor, A.A. (2013). Stochastic changes over time and not founder effects drive cage effects in microbial community assembly in a mouse model. *7*, 2116–2125.

McHugh, J.P., Rodríguez-Quinoñes, F., Abdul-Tehrani, H., Svistunenko, D.A., Poole, R.K., Cooper, C.E., and Andrews, S.C. (2003). Global iron-dependent gene regulation in Escherichia coli. A new mechanism for iron homeostasis. J Biol Chem *278*, 29478–29486.

Muegge, B.D., Kuczynski, J., Knights, D., Clemente, J.C., González, A., Fontana, L., Henrissat, B., Knight, R., and Gordon, J.I. (2011). Diet drives convergence in gut microbiome functions across mammalian phylogeny and within humans. Science *332*, 970–974.

Nobel, Y.R., Cox, L.M., Kirigin, F.F., Bokulich, N.A., Yamanishi, S., Teitler, I., Chung, J., Sohn, J., Barber, C.M., Goldfarb, D.S., et al. (2015). Metabolic and metagenomic outcomes from early-life pulsed antibiotic treatment. Nature Communications *6*, 1–15.

Noinaj, N., Guillier, M., Barnard, T.J., and Buchanan, S.K. (2010). TonB-dependent transporters: regulation, structure, and function. Annu Rev Microbiol *64*, 43–60.

Ojeda, P., Bobe, A., Dolan, K., Leone, V., and Martinez, K. (2015). ScienceDirect. J. Nutr. Biochem. 1–10.

Pantoja-Feliciano, I.G., Clemente, J.C., Costello, E.K., Perez, M.E., Blaser, M.J., Knight, R., and Dominguez-Bello, M.G. (2013). Biphasic assembly of the murine intestinal microbiota during early development. Isme J *7*, 1112–1115.

Patwa, L.G., Fan, T.-J., Tchaptchet, S., Liu, Y., Lussier, Y.A., Sartor, R.B., and Hansen, J.J. (2011). Chronic intestinal inflammation induces stress-response genes in commensal Escherichia coli. Gastroenterology *141*, 1842–51.e1–10.

Pereira, D.I.A., Aslam, M.F., Frazer, D.M., Schmidt, A., Walton, G.E., McCartney, A.L., Gibson, G.R., Anderson, G.J., and Powell, J.J. (2014). Dietary iron depletion at weaning imprints low microbiome diversity and this is not recovered with oral nano Fe(III). MicrobiologyOpen *4*, 12–27.

Scheinin, T., Butler, D.M., Salway, F., Scallon, B., and Feldmann, M. (2003). Validation of the interleukin-10 knockout mouse model of colitis: antitumour necrosis factor-antibodies suppress the progression of colitis. Clinical & Experimental Immunology *133*, 38–43.

Sellon, R.K., Tonkonogy, S., Schultz, M., Dieleman, L.A., Grenther, W., Balish, E., Rennick, D.M., and Sartor, R.B. (1998). Resident enteric bacteria are necessary for development of spontaneous colitis and immune system activation in interleukin-10-deficient mice. Infect Immun *66*, 5224–5231.

Seo, S.W., Kim, D., Latif, H., O'Brien, E.J., Szubin, R., and Palsson, B.O. (2014). Deciphering Fur transcriptional regulatory network highlights its complex role beyond iron metabolism in Escherichia coli. Nature Communications *5*, 4910.

Shanmugam, N.K.N., Trebicka, E., Fu, L.L., Shi, H.N., and Cherayil, B.J. (2014). Intestinal Inflammation Modulates Expression of the Iron-Regulating Hormone Hepcidin Depending on Erythropoietic Activity and the Commensal Microbiota. The Journal of Immunology *193*, 1398–1407.

Soofi, S., Cousens, S., Iqbal, S.P., Akhund, T., Khan, J., Ahmed, I., Zaidi, A.K.M., and Bhutta, Z.A. (2013). Effect of provision of daily zinc and iron with several micronutrients on growth and morbidity among young children in Pakistan: a cluster-randomised trial. Lancet *382*, 29–40.

Stanley, E.R., and Heard, P.M. (1977). Factors regulating macrophage production and growth. Purification and some properties of the colony stimulating factor from medium conditioned by mouse L cells. J Biol Chem *252*, 4305–4312.

Subramanian, S., Huq, S., Yatsunenko, T., Haque, R., Mahfuz, M., Alam, M.A., Benezra, A., DeStefano, J., Meier, M.F., Muegge, B.D., et al. (2014). Persistent gut microbiota immaturity in malnourished Bangladeshi children. Nature.

Turnbaugh, P.J., Ley, R.E., Mahowald, M.A., Magrini, V., Mardis, E.R., and Gordon, J.I. (2006). An obesity-associated gut microbiome with increased capacity for energy harvest. Nature *444*, 1027–1031.

Werner, T., Wagner, S.J., Martínez, I., Walter, J., Chang, J.-S., Clavel, T., Kisling, S., Schuemann, K., and Haller, D. (2011). Depletion of luminal iron alters the gut microbiota and prevents Crohn's disease-like ileitis. Gut *60*, 325–333.

Winter, S.E., Winter, M.G., Xavier, M.N., Thiennimitr, P., Poon, V., Keestra, A.M., Laughlin, R.C., Gomez, G., Wu, J., Lawhon, S.D., et al. (2013). Host-Derived Nitrate Boosts Growth of E. coli in the Inflamed Gut. Science *339*, 708–711.

Wu, G.D., Chen, J., Hoffmann, C., Bittinger, K., Chen, Y.-Y., Keilbaugh, S.A., Bewtra, M., Knights, D., Walters, W.A., Knight, R., et al. (2011). Linking long-term dietary patterns with gut microbial enterotypes. Science *334*, 105–108.

Zimmermann, M.B., Chassard, C., Rohner, F., N'Goran, E.K., Nindjin, C., Dostal, A., Utzinger, J., Ghattas, H., Lacroix, C., and Hurrell, R.F. (2010). The effects of iron fortification on the gut microbiota in African children: a randomized controlled trial in Cote d'Ivoire. American Journal of Clinical Nutrition *92*, 1406–1415.

CHAPTER 4

ADHERENT INVASIVE ESCHERICHIA COLI PRODUCTION OF CELLULOSE INFLUENCES IRON-INDUCED BACTERIAL AGGREGATION, PHAGOCYTOSIS AND INDUCTION OF COLITIS[3]

4.1 Personal Contribution to Manuscript

I am the first author on the manuscript entitled "Adherent-invasive *Escherichia coli* production of cellulose influences iron-induced bacterial aggregation, phagocytosis and induction of colitis," published in *Infection and Immunity* in 2015. I contributed to the manuscript by developing the project based on an initial observation of *E. coli* aggregation in response to iron. I created all the mutants utilized in this study. I also conducted all the microbiology, tissue culture, microscopy, animal experiments and data analysis presented in this paper. Finally, I compiled all the figures, wrote the manuscript and revised the manuscript in response to reviewers.

4.2 Overview

Adherent-invasive *Escherichia coli* (AIEC), a functionally distinct subset of resident intestinal *E. coli* associated with Crohn's disease, are characterized by enhanced epithelial adhesion and invasion, survival within macrophages and biofilm formation. Environmental

[3] Melissa Ellermann, Eun Young Huh, Bo Liu, Ian M. Carroll, Rita Tamayo, R. Balfour Sartor. 2015. Adherent-invasive *Escherichia coli* production of cellulose influences iron-induced bacterial aggregation, phagocytosis and induction of colitis. *Infection and Immunity* 83(10):4068-4080.

factors such as iron modulate *E. coli* production of extracellular structures, which in turn influence the formation of multicellular communities such as biofilms and bacterial interactions with host cells. However the physiological and functional responses of AIEC to variable iron availability have not been thoroughly investigated. We therefore characterized the impact of iron on the physiology of the AIEC strain NC101 and subsequent interactions with macrophages. Iron promoted cellulose-dependent aggregation of NC101. Bacterial cells recovered from the aggregates were more susceptible to phagocytosis compared to planktonic cells, which corresponded with decreased macrophage production of the proinflammatory cytokine IL-12 p40. Prevention of aggregate formation through disruption of cellulose production reduced phagocytosis of iron-exposed NC101. In contrast, under iron limiting conditions where NC101 aggregation is not induced, disruption of cellulose production enhanced NC101 phagocytosis and decreased macrophage secretion of IL-12 p40. Finally, abrogation of cellulose production also reduced NC101 induction of colitis when monoassociated in inflammation-prone *Il10*$^{-/-}$ mice. Taken together, our results introduce cellulose as a novel physiological factor that impacts host-bacterial-environmental interactions and alters the proinflammatory potential of AIEC.

4.3 Introduction

Inflammatory bowel diseases (IBD), including Crohn's disease (CD) and ulcerative colitis (UC), comprise a heterogeneous collection of chronic, relapsing immune-mediated disorders. Although the precise etiologies are incompletely understood, accumulating evidence suggests that IBD are the result of inappropriate immune responses toward a subset of resident intestinal microbes and their products in genetically susceptible individuals (Sartor, 2008) (Knights et al., 2013).

The gastrointestinal tract is home to a complex community of microbes referred to as the intestinal microbiota. The development of intestinal inflammation is associated with community-wide changes to the intestinal microbiota, including an expansion in the relative abundance of endogenous *Escherichia coli* in IBD patients (Gevers et al., 2014) and in rodent models of experimental colitis (Arthur et al., 2012) (Winter et al., 2013) (Maharshak et al., 2013). In CD patients, a functionally distinct group of resident enteric *E. coli* known as adherent-invasive *E. coli* (AIEC) are recovered more frequently and in higher quantity from ileal tissue biopsies in comparison to non-CD controls (Darfeuille-Michaud et al., 2004) (Baumgart et al., 2007). In the absence of common identifying genetic determinants (Dogan et al., 2014), AIEC are characterized by their ability to adhere and invade intestinal epithelial cells (Boudeau et al., 1999) and to survive and replicate within macrophages (Glasser et al., 2001). AIEC strains are also moderate to strong *in vitro* biofilm producers (Martinez-Medina et al., 2009). In addition, AIEC strains are capable of inducing and perpetuating intestinal inflammation in various rodent models of experimental colitis, including streptomycin-treated mice (Sartor, 2008; Small et al., 2013), dextran sodium sulfate (DSS) treated mice (Carvalho et al., 2008; Knights et al., 2013), TLR5-deficient mice (Carvalho et al., 2012; Gevers et al., 2014), transgenic CEABAC10 mice (Arthur et al., 2012; Martinez-Medina et al., 2013) and gnotobiotic interleukin-10-deficient (*Il10*$^{-/-}$) mice (Kim et al., 2005; Winter et al., 2013). These functional attributes of AIEC, in conjunction with host factors such as genetic polymorphisms linked to aberrant microbial sensing and clearance (Hugot et al., 2001; Maharshak et al., 2013) (Darfeuille-Michaud et al., 2004; Hampe et al., 2006), potentially enable enhanced mucosal association by AIEC strains (Baumgart et al., 2007; Lapaquette et al., 2010) (Dogan et al., 2014; Sadaghian Sadabad et al., 2014). Together, these characteristics provide the physical opportunity for AIEC strains to

continuously stimulate the mucosal immune system, thus propagating a state of chronic intestinal inflammation.

Macrophages are a key component of host innate immune defense in the intestines, limiting systemic microbial dissemination by destroying potential invaders through phagocytosis, while also sensing and responding to microbial stimuli and informing consequent host immune responses (Boudeau et al., 1999; Steinbach and Plevy, 2014). Through pattern recognition receptors (PRR), macrophages recognize conserved microbial molecular patterns synthesized by resident and pathogenic intestinal bacteria, including extracellular structures such as fimbriae, flagella, lipopolysaccharides and peptidoglycan. Environmental factors such as iron availability influence microbial production of some of these extracellular structures including curli fibrils in *Salmonella enterica* serovar Typhimurium (Glasser et al., 2001; Römling et al., 1998) (Martinez-Medina et al., 2009; White et al., 2008) and type 1 fimbriae in *E. coli* (Wu and Outten, 2009), providing the opportunity for environmental modulation of microbial interactions with macrophages. Indeed, iron impacts *E. coli* interactions with host cells, albeit in contrasting ways. Iron promotes increased internalization of pathogenic *E. coli* by neutrophils (Wise et al., 2002) and intestinal epithelial cells (Alves et al., 2010) (Kortman et al., 2012). In contrast, iron limitation promotes phagocytosis of a non-pathogenic *E. coli* K12 strain by macrophages through decreased expression of the outer membrane protein OmpW (Wu et al., 2013). Extracellular microbial structures that impact interactions with macrophages are also produced within multicellular microbial communities including biofilms and bacterial aggregates. Curli and the exopolysaccharide cellulose are common matrix components present within multicellular structures produced by *S.* Typhimurium and *E. coli* (Römling et al., 2000) (Zogaj et al., 2001) (Serra et al., 2013). Cellulose and/or curli production have also been implicated in modulating

intestinal *E. coli* interactions with epithelial cells (Monteiro et al., 2009) (Wang et al., 2006) and influencing *in vivo* host immune responses to uropathogenic *E. coli* in the urinary tract (Raterman et al., 2013).

Iron is a necessary cofactor for various microbial enzymes and therefore serves as an important micronutrient for most bacteria. In *E. coli,* changes in cytosolic iron concentrations are directly sensed by Fur (Hantke, 2001). When bound to Fe^{2+}, Fur acts as a transcription factor, regulating genes involved in diverse cellular processes such as metabolism, metal acquisition, stress responses, motility and biofilm formation (McHugh et al., 2003) (Seo et al., 2014). Changes in extracellular iron concentrations are also sensed by the membrane-associated kinase BasS, a member of the BasRS two component system (Nagasawa et al., 1993). In reponse to Fe^{3+}, BasRS regulates genes involved in altering the outer membrane landscape of *E. coli* (Wösten et al., 2000) (Ogasawara et al., 2012). Given the importance of iron to microbial growth and function, an integral component of the innate immune response is the secretion of iron scavenging proteins at mucosal surfaces to limit microbial iron availability, a response that is potentiated by inflammation (Raffatellu et al., 2009) (Chassaing et al., 2012).

Studies investigating the impact of iron on *E. coli* physiology and interactions with host cells have been limited to non-pathogenic K12 or pathogenic *E. coli* strains. Consequently, little is known about the impact of iron on the functional attributes of AIEC. Therefore the goal of this study was to characterize how iron impacts the physiology of the AIEC strain NC101 (Patwa et al., 2011) (Dogan et al., 2014) and subsequent interactions with macrophages. Here we show that iron promotes cellulose-dependent aggregation of NC101. Bacterial cells recovered from the aggregates are more susceptible to phagocytosis as prevention of aggregation through disruption of cellulose production reduces macrophage uptake of NC101. Conversely, under iron limiting

conditions where aggregation is not induced, disruption of cellulose production enhanced NC101 phagocytosis and decreased macrophage proinflammatory responses. Abrogation of bacterial cellulose production also delayed onset of colitis in inflammation-prone *Il10*$^{-/-}$ mice monoassociated with NC101. Taken together, our results introduce cellulose as a novel physiological factor that dynamically impacts AIEC-host interactions in the face of changing environmental conditions.

4.4 Results

4.4.1 Iron promotes aggregation of E. coli NC101

Bacterial iron availability varies within the GI tract, likely decreasing towards the mucosal interface with the secretion of host iron-binding proteins, a phenomenon that is potentiated with inflammation (Kortman et al., 2014). However, the physiological responses by AIEC to changes in iron availability have not been well characterized. We therefore investigated the impact of iron on the physiology of *E. coli* NC101, a murine intestinal isolate that exhibits various AIEC characteristics including increased epithelial translocation, enhanced persistence within macrophages and the ability to induce colitis in selectively colonized, inflammation-prone *Il10*$^{-/-}$ mice (Liu et al., 2009) (Kim et al., 2005). When cultured in minimal medium with 5, 10 or 50 μM iron at 37°C, NC101 formed macroscopic aggregates that sediment in culture (Fig. 1A). The proportion of bacterial cells associated with the aggregates significantly increased as the iron concentration increased as assessed by quantitative plating (Fig. S1) and optical density (Fig. 1B). Addition of an iron chelator did not impact NC101 aggregation (Fig. 1C), suggesting that further iron deprivation had no affect on this phenotype. In contrast, the *E. coli* K12 substrain

MG1655 does not form aggregates in response to iron (Fig. S2), indicating that this phenomenon is not universal to all *E. coli* strains.

4.4.2 Cellulose is required for iron-induced aggregation of NC101

The extracellular matrix (ECM) of multicellular structures produced by other *E. coli* strains are composed of proteinaceous components such as fimbriae and curli, exopolysaccharides such as cellulose and/or extracellular DNA (Saldaña et al., 2009) (Hung et al., 2013) (Hadjifrangiskou et al., 2012). The combination of matrix components varies depending on environmental conditions and *E. coli* strain (Hancock et al., 2011). Therefore to determine the extracellular composition of the NC101 aggregates, cellulase, DNase or proteinase was added to the cultures following 2 hours of growth. Addition of cellulase resulted in dispersal of the aggregates (Fig. S3), while DNase and proteinase had no obvious impact (data not shown). This suggests that cellulose is a major extracellular component that contributes to iron-induced aggregation.

Cellulose biosynthesis and structural proteins are encoded by *bcsQABZC* and *bcsEFG* and are required for cellulose production (Zogaj et al., 2001) (Solano et al., 2002) (Serra et al., 2013). However, the presence of *bcs* genes does not necessarily correspond with an ability to produce cellulose. We first assessed whether NC101 is capable of producing cellulose at 37°C utilizing the well-established Calcofluor (CF) binding and red dry and rough (RDAR) colony morphotype assays. In contrast to *E. coli* MG1655 that served as an established negative control (Da Re and Ghigo, 2006), NC101 bound CF indicating the presence of cellulose production (Fig. 2A). Similarly, on Congo red agar, NC101 produced RDAR colonies (Fig. 2B), a colony morphotype that is dependent on cellulose and curli production (Römling et al., 1998) (Zogaj et

al., 2001). To confirm that NC101 is a cellulose producer, an isogenic mutant lacking the *bcsA* gene that encodes the catalytic subunit of cellulose synthase (Omadjela et al., 2013) was created. Deletion of *bcsA* resulted in the loss of CF binding and the production of smooth colonies on Congo red agar (Fig. 2A and 2B). Moreover, the *bcsA* mutant did not form macroscopic aggregates (Fig. 2C and D), confirming that cellulose production is required for iron-induced aggregation of NC101.

Curli are commonly co-expressed with cellulose within RDAR colonies and biofilms (Zogaj et al., 2001) (Bokranz, 2005) (Saldaña et al., 2009). To determine whether curli also contribute to RDAR colony formation in NC101, the *csgA* gene encoding the major subunit of the curli fibrils was disrupted (Olsen et al., 1993). The *csgA* mutant produced pink instead of brown-red textured colonies (Fig. 2B), a phenotype that has been observed in other *csgA*-deficient intestinal *E. coli* (Bokranz, 2005). We also determined whether curli contribute to NC101 aggregation in response to iron. No differences in aggregation were observed between the *cgsA* mutant and NC101, suggesting that curli expression does not significantly contribute to iron-induced aggregate formation (Fig. 2D).

4.4.3 Deletion of fur decreases NC101 aggregation

Given the impact of iron on NC101, we next sought to determine how iron-induced aggregation occurs. In *E. coli*, fluctuations in iron availability can be sensed intracellularly by the transcription factor Fur (Hantke, 2001) or extracellularly by the two-component system BasRS (Hagiwara et al., 2004). To determine whether NC101 aggregation occurs in response to intracellular or extracellular iron, we tested the aggregative abilities of *fur* and *basRS* deletion mutants. In contrast to the parental strain, the *fur* mutant did not form visible aggregates after 2

hours of growth (Fig. 3A and B). This was not the result of a corresponding growth defect with the *fur* mutant at the same time point (Fig. 3D). The aggregates formed by the *fur* mutant after 8 hours were macroscopically smaller compared to the NC101 aggregates (Fig. 3A) with a reduced proportion of bacterial cells associated with the aggregates relative to the whole culture (Fig. 3C). In contrast, deletion of *basRS* did not impact NC101 aggregate formation (Fig. 3B). Taken together, deletion of *fur* limited NC101 aggregation, suggesting that factors promoting iron-induced aggregate formation may be under the Fur modulon.

4.4.4 Decreased aggregation by the fur mutant is not the result of an inability to produce cellulose

Given that iron-induced aggregation of NC101 requires the capacity to produce cellulose, we determined whether cellulose biosynthesis was disrupted in the *fur* mutant as an explanation for its reduced ability to aggregate. We first tested whether cellulose production was unperturbed in the *fur* mutant. Deletion of *fur* did not eliminate CF binding, although the distribution of CF within the inoculum is altered compared to NC101 (Fig. 4A). As growth conditions impact the stimulation of *E. coli* cellulose production, we next determined whether NC101 and the *fur* mutant bind CF when exposed to iron in minimal medium. NC101 microscopic aggregates colocalized with CF (Fig. 4C), confirming that cellulose is a component of the ECM. Although not uniformly observed, single NC101 cells not associated with the aggregates bound CF, suggesting that some planktonic cells produce cellulose. The *fur* mutant also colocalized with CF in the presence of iron, further demonstrating that cellulose production is not abrogated in the mutant strain. Formation of microscopic aggregates by the *fur* mutant was also observed. However, consistent with its decreased ability to form macroscopic aggregates, the microscopic aggregates produced by the *fur* mutant were less frequent and smaller in size compared to

NC101 (Fig. S4). Finally, to determine whether cellulose production is decreased in the *fur* mutant, the extent of CF binding was assessed as a proxy for cellulose production. CF binding in the presence of iron did not differ between NC101 and the *fur* mutant (Fig. 4B). CF binding was also evident for NC101 and the *fur* mutant when grown in minimal medium without iron (Fig. 4B and S5), indicating that cellulose production occurs under iron limiting conditions. Taken together, these data demonstrate that decreased aggregate production by the *fur* mutant is not due to an inability to produce cellulose, suggesting the involvement of other factors in addition to cellulose that promote maximal NC101 aggregation.

4.4.5 NC101 aggregate cells are more susceptible to phagocytosis by macrophages

ECM components produced within microbial multicellular structures potentially alter *E. coli* interactions with macrophages. Given that AIEC are in part characterized by their distinct interactions with macrophages (Glasser et al., 2001), we investigated whether the physiology associated with an aggregative state alters NC101 susceptibility to phagocytosis by macrophages and subsequent intracellular survival. To test this, aggregation of NC101 was induced by growth with iron and cultures containing aggregates were physically dispersed into single cell suspensions and co-cultured with macrophages. NC101 was exposed to iron prior to co-culture with macrophages, as iron availability can also impact macrophage function (Nairz et al., 2010). Under aggregate-inducing conditions, NC101 phagocytosis was significantly enhanced (Fig. 5A). Although the quantity of intracellular NC101 was also increased after 4 and 8 hours, the percent intracellular survival of NC101 was not substantially altered (Fig. 5B). These data demonstrate an association between iron-induced aggregation and increased bacterial uptake by macrophages.

To further explore this association, we physically separated the planktonic and aggregate phases from the same culture and tested whether NC101 cells recovered from the aggregates were more susceptible to phagocytosis. Irrespective of the presence of iron, the extent of internalization of planktonic NC101 remained constant (Fig. 5C). In contrast, a significantly higher amount of aggregate NC101 cells was phagocytosed by macrophages in comparison to planktonic cells from the same culture, suggesting that aggregate NC101 cells are more susceptible to phagocytosis. One explanation for increased phagocytosis of aggregate cells is the incomplete disruption of the aggregates, which could result in more cells entering the macrophage at once. To address this possibility, we investigated whether aggregates of GFP-labeled NC101 were fully dispersed utilizing microscopy. Before physical disruption, the number of aggregates per high-power field was significantly higher when NC101 was cultured with iron (Table S3). After physical disruption, NC101 aggregates were rarely visible microscopically, and importantly, there was no significant difference in the number of NC101 aggregates per field with or without iron. These findings indicate that increased susceptibility of aggregate cells to phagocytosis is not likely due to more bacteria entering the macrophage at once. Instead, these data suggest that the physiology of the individual aggregate cells promotes their phagocytosis.

4.4.6 Cellulose modulates NC101 susceptibility to phagocytosis.

We next sought to identify the physiological factors that mediate enhanced internalization of individual NC101 aggregate cells. Given that cellulose is required for aggregation and deletion of *fur* limits aggregate formation in a cellulose independent manner, we predicted that deletion of *bcsA* or *fur* would reduce macrophage uptake of iron-exposed NC101. As

hypothesized, under aggregate-inducing conditions, macrophage uptake of the *bcsA* and *fur* mutants was significantly decreased in comparison to NC101 (Figs. 6B and S6). However, deletion of *bcsA* or *fur* did not reduce NC101 internalization to levels comparable to non-aggregated NC101, suggesting the involvement of other bacterial factors that contribute to phagocytosis susceptibility of aggregate cells. Conversely, under iron limiting conditions where NC101 aggregation is not induced, the *bcsA* mutant was more susceptible to phagocytosis compared to NC101 (Fig. 6A and S6). This suggests that cellulose may act as an anti-phagocytic factor for non-aggregate NC101 cells. Similar results were also observed with the non-cellulose producing strain MG1655 (Fig. S6). Importantly, the *bcsA* mutant and MG1655 did not form microscopic aggregates (Table S3). Moreover, deletion of *bcsA* did not impact percent survival within macrophages (Fig. S7). Taken together, cellulose disparately modulates NC101 susceptibility to macrophage phagocyotosis by enabling the formation of an aggregative physiological state under iron replete conditions and by potentially acting as an anti-phagocytic factor under iron limiting conditions.

4.4.7 Cellulose alters the proinflammatory potential of NC101

It is unclear how differential phagocytosis of AIEC impacts macrophage proinflammatory responses. As deletion of *bcsA* alters macrophage uptake of NC101, we investigated whether uptake of the *bcsA* mutant also alters macrophage production of p40, the common subunit of the proinflammatory cytokines IL-12 and IL-23. Under non-aggregating conditions (i.e. low iron), production of IL-12 p40 was decreased in macrophages that phagocytosed the *bcsA* mutant (Fig. 6C). Conversely, with increased iron where NC101 aggregation is induced, macrophages that phagocytosed the *bcsA* mutant secreted higher amounts

of IL-12 p40 (Fig. 6D). Deletion of *fur* did not alter IL-12 p40 secretion by the mutant-exposed macrophages, further demonstrating the importance of cellulose in mediating NC101-macrophage interactions. Taken together, these results demonstrate that in addition to impacting NC101 phagocytosis susceptibility, cellulose modulates macrophage production of the proinflammatory cytokine IL-12 p40.

Given the contrasting effects of cellulose on macrophage proinflammatory responses, we next sought to determine how the ability to produce cellulose contributes to the *in vivo* proinflammatory potential of NC101. To investigate this, germ-free *Il10*$^{-/-}$ mice were monoassociated with NC101 or the *bcsA* mutant. AIEC strains such as NC101 uniquely induce colitis when monoassociated in inflammation-susceptible *Il10*$^{-/-}$ mice (Kim et al., 2005), whereas monoassociation of non-AIEC strains including MG1655 (Kim et al., 2008) and Nissle (Schumann et al., 2013) does not induce chronic colitis. Severity of inflammation was assessed by histology and proinflammatory cytokine expression. Monoassociated wild type (WT) mice served as inflammation-resistant controls. After 10 days of colonization, no differences in histological inflammation were observed (Fig. 7B). After 21 days, mice colonized with the parental strain exhibited significantly worse proximal and distal colonic inflammation characterized by increased crypt hyperplasia and leukocytic infiltration into the lamina propria (Fig. 7A and B). By 35 days, pathohistological differences were no longer apparent because severity of inflammation increased in mice colonized with the *bcsA* mutant. Importantly, WT animals colonized with either strain did not exhibit any pathology (Fig. 7C).

We next determined whether differences in histological inflammation at 21 days corresponded with differential expression of proinflammatory cytokines. *Il10*$^{-/-}$ mice monoassociated with NC101 develop colitis that is driven by T-helper (Th)-1 and Th-17

responses, where onset and exacerbation of inflammation is associated with increased production of IL-17, IFN-γ and IL-12 (Kim et al., 2005) (Kim et al., 2007). We therefore determined whether earlier onset of colitis in NC101 colonized mice corresponded with differential expression of *Il17a*, *Ifng* and *Il12b*. Prior to onset of histological inflammation, expression of *Il12b* encoding the p40 subunit was increased in mice colonized with NC101 (Fig. 7D). This was consistent with differences in macrophage production of IL-12 p40 observed *in vitro* in response to NC101 or the *bcsA* mutant under iron limiting conditions. Colonic expression of *Il17a* or *Ifng* did not differ at 10 days (data not shown). At 21 days, coinciding with more severe histopathology, *Il17a* expression was increased in the proximal colon in mice colonized with NC101 (Fig. 7E). In contrast, no significant differences in *Ifng* transcript levels were observed (Fig. S8). Because colitis in NC101 monoassociated *Il10*$^{-/-}$ mice is driven by antigen-specific responses, we also quantified IFN-γ and IL-17 production by unfractionated MLN cells restimulated with the respective bacterial lysates. MLN cells recovered from mice colonized with NC101 produced higher quantities of IL-17 relative to MLN cells isolated from mice colonized with the *bcsA* mutant (Fig. 7F). IFN-γ production by restimulated MLN cells was not significantly different (Fig. S8). Finally, differences in severity of colitis observed at 21 days also corresponded with a 2.4 fold decrease in fecal loads of the *bcsA* mutant (Fig. 8). Cecal luminal densities of the *bcsA* mutant were also consistently decreased relative to NC101, although this was not uniformly observed in the feces. Decreased fecal and cecal concentrations of the *bcsA* mutant relative to the parental strain were likewise observed in WT mice. Taken together, *Il10*$^{-/-}$ mice monoassociated with a cellulose-deficient NC101 mutant exhibited delayed onset of colitis, suggesting that disrupting cellulose production in NC101 reduced its proinflammatory potential in an experimental model of chronic immune-mediated colitis.

4.5 Discussion

Environmental factors such as iron availability that may promote proinflammatory interactions between AIEC, microbes clinically relevant to IBD, and the host have not been well investigated. Therefore the purpose of this study was to characterize how iron impacts the physiology and functional attributes of the AIEC strain NC101. Our findings demonstrate that iron promotes cellulose-dependent aggregation of NC101. Moreover, NC101 aggregate cells are more susceptible to phagocytosis by macrophages. The contribution of cellulose to NC101 phagocytosis susceptibility and consequent macrophage proinflammatory responses changes as iron availability and the physiological state of NC101 is altered, demonstrating a dynamic role for cellulose in modulating host-microbial interactions. Finally, abrogation of cellulose production in NC101 reduced its ability to induce colitis in inflammation-prone *Il10*$^{-/-}$ mice. Taken together, our results demonstrate that cellulose production alters the proinflammatory potential of NC101.

Various environmental factors including temperature and nutrient availability impact multicellular behaviors such as aggregation in *E. coli* and related enteric bacteria (Gerstel and Römling, 2001) (Spurbeck et al., 2012). Interestingly, iron has divergent effects on multicellular behaviors of other *E. coli* functional subtypes including enteroaggregative (Alves et al., 2010), uropathogenic (UPEC) (Hancock et al., 2010) (Rowe et al., 2010) (Depas et al., 2013) and K12 strains (Wu and Outten, 2009). Therefore, given the varying responses of different *E. coli* strains to alterations in iron availability, it is likely that multiple strain-specific mechanisms regulate these responses. Here we show that *fur*-deficient, but not *basRS*-deficient, NC101 exhibited a reduced ability to form aggregates. This suggests that intracellular, rather than extracellular, iron

sensing by NC101 contributes to the induction of this multicellular behavior. This was not the result of an inability of the *fur* mutant to produce cellulose, suggesting that additional factors under the Fur modulon promote maximal NC101 aggregation. Cellulose production by the *fur* mutant may enable its ability to form smaller microscopic aggregates that, compared to NC101, are not macroscopically visible until later in growth. Additionally, the *fur* mutant exhibited a growth defect when grown in minimal medium with iron, which could contribute to decreased aggregate formation. However, this growth defect was only evident during later stages of growth, after aggregate formation had already occurred in the parental strain. Fur has been linked to the regulation of additional multicellular behaviors in UPEC, *E. coli* K12 and other Gram negative bacteria (Banin et al., 2006) (Depas et al., 2013) (Hancock et al., 2010) (Wu et al., 2012) (Seo et al., 2014), demonstrating the importance of iron as an environmental signal in modulating the formation of microbial communities across many bacterial species.

Translocation of microbes and their products across the intestinal epithelial barrier is detected by immune cells including macrophages, where engagement of pattern recognition receptors by microbial products activates signal transduction pathways that promote phagocytosis (Doyle, 2003), microbial killing and production of inflammatory mediators. Assumption of an aggregate physiological state promoted NC101 phagocytosis by macrophages, where NC101 cells recovered from aggregates were more susceptible to phagocytosis compared to planktonic cells. Abrogation of cellulose production prevented aggregation and reduced NC101 susceptibility to phagocytosis under aggregate inducing conditions (i.e. iron exposure). Coinciding with a reduced ability to aggregate, the *fur* mutant was also phagocytosed to a lesser extent despite producing cellulose. Interestingly, increased phagocytosis of iron-exposed (James et al., 1995) (Domingue et al., 1989) or biofilm-associated bacteria has been observed in other

bacterial species (Spiliopoulou et al., 2012) (Daw et al., 2012) and with iron-exposed extraintestinal *E. coli* pathogens (Wise et al., 2002). These results suggest that although cellulose is required for aggregation and presumably the assumption of an aggregate physiological state, other factors contribute to phagocytosis of NC101 aggregate cells.

Under non-aggregate inducing conditions (i.e. low iron) where NC101 aggregation does not occur but cellulose is expressed, deletion of *bcsA* enhanced NC101 susceptibility to phagocytosis. This suggests that in a non-aggregative state, cellulose acts as an antiphagocytic factor, potentially masking bacterial factors that interact with macrophage receptors to promote phagocytosis. Indeed, as no host receptor for cellulose has been identified, it is unlikely that microbial cellulose interacts directly with host cells. This is consistent with the contrasting effects of disrupting cellulose production on NC101 phagocytosis as both microbial iron exposure and the resulting physiological state of NC101 is altered. Thus our study introduces cellulose as a novel factor that modulates interactions between AIEC and macrophages and highlights the complex interplay between bacterial and environmental factors in modulating host-microbial interactions.

Although our investigation demonstrates that cellulose is required for *in vitro* aggregation by NC101 and modulates interactions with macrophages, it is unclear whether NC101 cellulose production and aggregation occurs *in vivo*. In a recent study by Arthur and colleagues, the impact of the inflamed and non-inflamed colonic environments on the NC101 transcriptome was investigated (Arthur et al., 2014). *Bcs* transcripts were detected at 2, 12 and 20 weeks following monoassociation of ex-germ free *Il10*$^{-/-}$ and inflammation-resistant *Il10*$^{-/-}$*rag2*$^{-/-}$ mice, indicating that *bcs* genes are transcribed *in vivo*. However, as cellulose biosynthesis is primarily regulated through allosteric control of cellulose synthase activity (Römling, 2005), presence of *bcs*

transcripts is not conclusive evidence of NC101 cellulose production in the colon. Moreover, current biochemical techniques for assaying the presence of bacterial cellulose *in vitro* are not easily adaptable to the intestinal environment given the presence of plant cellulose and other polysaccharides consisting of glucose monomers.

The contribution of cellulose to the *in vivo* fitness and virulence potential of *E. coli* and related bacteria has only been investigated in UPEC strains in the urinary tract (Raterman et al., 2013) (Larsen et al., 2010) and *S.* Typhimurium when administered intraperitoneally (Pontes et al., 2015). Therefore, to establish whether cellulose contributes to the colitogenicity of AIEC in the GI tract, the severity of colitis was assessed in *Il10*$^{-/-}$ mice monoassociated with NC101 or the cellulose deficient *bcsA* mutant. Onset of colitis was delayed in mice colonized with the cellulose deficient mutant, which corresponded with decreased Th-17-associated immune responses including decreased expression of *Il12b*. This is consistent with our *in vitro* observations demonstrating decreased IL-12 p40 production by macrophages infected with the *bcsA* mutant following exposure to non-aggregate inducing and iron limiting conditions. Reduced macrophage production of IL-12 p40 also corresponded with enhanced phagocytosis of the *bcsA* mutant. Therefore, cellulose may enhance the proinflammatory potential of NC101 by preventing mucosal clearance of NC101 and consequently promoting increased proinflammatory immune responses. However, as deletion of *bcsA* did not completely prevent colitis development and its effects were lost over time, other microbial factors likely contribute to the ability of NC101 to induce colitis. Finally, these results also suggest that iron may be limiting within the inflamed intestines, a finding that has been reported by others (Deriu et al., 2013). However, the precise bioavailability of iron remains unclear, especially as iron concentrations likely vary

throughout the GI tract and depend on other factors including host iron status, inflammation and diet.

Coinciding with decreased inflammation, luminal loads of the *bcsA* mutant were significantly decreased. However, it is unclear whether a 2.4-fold decrease in fecal loads and a 1.8-fold decrease in cecal luminal loads significantly contribute to decreased immune activation in mice colonized with the *bcsA* mutant. Cecal luminal densities of the *bcsA* mutant were also decreased in *Il10*$^{-/-}$ mice prior to evidence of histological inflammation and in noninflamed WT mice. However, this early difference in luminal bacterial loads was not observed in the feces. Therefore, cellulose production may modestly enhance AIEC colonic fitness, which provides a possible additional mechanism for augmenting the proinflammatory potential of NC101. Cellulose provides microbial resistance against a variety of stressors both in the environment (Solano et al., 2002) (Gualdi et al., 2008) (Depas et al., 2013) and within the host (Larsen et al., 2010). For example, deletion of *bcsA* in UPEC enhanced bacterial clearance from the kidneys in a neutrophil-dependent manner (Larsen et al., 2010). Cellulose-dependent multicellular behaviors can also be induced by stressors likely present at mucosal surfaces along the normal and inflamed GI tract including fluctuations in iron availability, peroxide stress and microbial contact with soluble IgA antibodies (Rowe et al., 2010) (Depas et al., 2013) (Amarasinghe et al., 2013). Finally, as intestinal *E. coli* demonstrate a more frequent ability to produce cellulose at 37°C compared to UPEC clinical isolates (Bokranz, 2005), it is tempting to speculate that cellulose may contribute to intestinal fitness of resident intestinal *E.* coli strains.

In the colon, under homeostatic conditions, the mucosal surface is home to a distinct community of bacteria. The composition of the mucosa-associated microbial community is significantly altered in chronic disease states such as CD, which includes an increased abundance

of mucosally-associated resident *E. coli* (Gevers et al., 2014). Host inflammatory responses and intrinsic host genetic defects compromise mucosal and epithelial barrier integrity, enabling enhanced proximity of mucosally-associated bacteria to host cells. Consistent with this, enhanced intestinal tissue AIEC loads, mucosal association and translocation (Martin et al., 2004) (Baumgart et al., 2007) (Carvalho et al., 2012) are correlated with more severe disease in CD and experimental models of colitis. Our study highlights the importance of environmental factors in altering AIEC physiology and subsequent host-microbial interactions and impact on inflammation. Given the lack of identifying genetic loci within AIEC, it would be interesting to investigate whether iron alters the physiological state of other clinical AIEC isolates as a novel functional determinant. Finally future studies are warranted confirming *in vivo* cellulose biosynthesis, and more broadly, assessing the *in vivo* physiological state of AIEC, especially within more defined intestinal niches such as the normal and inflamed mucosa using murine models and clinical mucosal biopsies. This could enable the identification of novel therapeutics that modulate *E. coli* physiology to limit adverse interactions with the underlying mucosa in CD patients and individuals genetically susceptible to CD.

4.6 Materials and methods

Bacterial strains and growth conditions. The bacterial strains and plasmids used in this study are listed in Table S1 in the supplemental material. *E. coli* NC101 was isolated from feces of a wild type mouse as previously described (Kim et al., 2005). Unless otherwise indicated, bacteria from an overnight culture were washed prior to inoculation into the M9 minimal medium with the indicated concentrations of iron as ferrous sulfate (I146, Fisher Scientific). Bacteria were

grown at 250 rpm at 37°C for all experiments. Media was supplemented with 50 μg/mL kanamycin or 100 μg/mL carbenicillin as appropriate.

Construction of isogenic mutant, chromosomally complemented and green fluorescent protein (GFP)-labeled strains. All deletion mutants were created using the *λ-red* recombinase system as previously described (Datsenko and Wanner, 2000). Deletion mutants were chromosomally complemented using the pMCL2868 plasmid (kind gift from M. Chelsea Lane), a mini-Tn7 vector, as previously described (Choi et al., 2005). For GFP-labeled strains, the pEGFP plasmid was transformed into each strain by electroporation. Transformed strains were grown with 100 μg/mL carbenicillin to maintain the plasmid.

Sedimentation assays. Sedimentation assays were performed as previously described (Rowe et al., 2010) with the following modifications. Briefly, bacteria were grown in M9 minimal medium with the indicated concentrations of iron or the iron chelator 2,2-bipyridyl (366-18-7, Alfa Aesar). At the specified time points, cultures were removed from the incubator, and the aggregates were allowed to settle to the bottom of 50-mL conical tubes. An aliquot from the top of the culture (planktonic phase) was taken for optical density quantification by spectrophotometry or quantitative culture. The cultures were then vortexed thoroughly, and the cells were pelleted and washed with phosphate buffered saline (PBS) and passed through a 30-gauge needle to obtain homogenous bacterial suspensions. An aliquot was then taken for quantitative culture or spectrophotometry as a measure of bacterial concentration of the whole culture. The % aggregation was calculated using [(whole culture OD600 - planktonic OD600) / whole culture OD600] x 100. Where indicated, cellulase (from *Aspergillus niger*, C1184, Sigma)

was added to the cultures after 2 hours of growth. The cultures were then vortexed vigorously and incubated for 10 minutes at 37°C.

Assessment of aggregation and CF binding by fluorescence microscopy. GFP-labeled bacteria were grown in M9 minimal medium with the indicated concentrations of iron. For assessing dispersion of the bacterial aggregates prior to the gentamicin protection assays, bacteria aggregates were physically disrupted as described above. When staining with CF, bacteria were cultured with 1% of the Calcofluor White staining solution (18909; Sigma). The cultures were normalized to equivalent optical densities (600 nm). A 5-μL aliquot was spotted onto glass microscope slides in duplicate. Slides were visualized using an Olympus IX71 fluorescence microscope. ImageJ software was utilized to quantify the aggregates, where aggregates were defined as objects in the field that had a pixel intensity threshold of 5 to 215 and pixel size of 201 to infinity. ImageJ software was also utilized to quantify CF binding per cell using the following formula: (mean intensity CF x area CF) / (mean intensity GFP x area GFP). At least 15 high-power fields at 200x magnification per slide were analyzed per experiment. Representative images were taken to demonstrate colocalization of CF with GFP-expressing bacteria at 400x magnification.

Gentamicin protection assays. Bacteria were grown in M9 minimal medium with the indicated concentrations of iron for 2 hours. The cultures were vortexed and washed with PBS to disrupt the aggregates as described above and normalized to equivalent optical densities (600 nm). For experiments using planktonic or aggregate bacterial cells, the aggregates were allowed to settle for 5 minutes to the bottom of the 50-mL conical tubes. The broth phase (top) of the culture was

then collected and cells recovered from this phase were defined as planktonic. The remaining broth phase was removed by aspiration. Aggregates were recovered by resuspension in PBS and were physically disrupted as described above. Gentamicin protection assays were then performed as previous described (Darfeuille-Michaud et al., 2004). Briefly, bone marrow-derived macrophages were seeded in 24-well plates and bacteria were added at a multiplicity of infection (MOI) of 10. After centrifugation for 10 minutes at 228 g, the co-cultures were incubated for 30 minutes in RPMI 1640 medium. Gentamicin-laden medium (RPMI 1640 with 10% FBS and 100 μg/mL gentamicin) was then added to eliminate any remaining extracellular bacteria. The macrophages were lysed with PBS containing 1% Triton X-100 at the indicated time points for enumeration of intracellular bacteria. Intracellular bacteria were quantified by serial dilution plating.

Mice. Germ free *Il10*$^{-/-}$ and wild type mice on the 129S6/SvEV background were originally derived in sterile conditions by hysterectomy at the Gnotobiotic Laboratory (University of Wisconsin, Madison). Mice were maintained in germ free conditions at the National Gnotobiotic Rodent Resource Center at UNC-Chapel Hill. An overnight bacterial culture of *E. coli* NC101 or the *bcsA* mutant was utilized to monoassociate mice via oral and rectal swab as previously described (Kim et al., 2007). Absence of isolator contamination was confirmed by Gram stain and fecal culture. Once monoassociated, fecal and cecal *E. coli* loads were quantified by dilution plating on LB plates as previously described (Patwa et al., 2011). All animal protocols were approved by the UNC-Chapel Hill Institutional Animal Care and Use Committee.

Histological scoring. At necropsy, proximal and distal colonic segments were Swiss rolled and fixed in 10% neutral buffered formalin. Histological inflammation scores (0-4) of proximal and distal colonic sections were blindly assessed as previously described (Kim et al., 2005). Briefly, the scoring system is as follows: 0 = no inflammation; 1 = presence of infiltrating cells within the lamina propria (LP); 2 = epithelial hyperplasia, mild loss of goblet cells and more extensive cellular infiltration within the LP; 3 = marked epithelial hyperplasia, loss of goblet cells, pronounced cellular infiltration within the LP and submucosa ; 4 = ulceration and transmural inflammation. Data are expressed as the composite histology score (0-8), which was calculated by adding the proximal and distal colonic histology scores.

Congo red and Calcofluor (CF) colony morphotypes. A 5-10-μL aliquot of bacteria from an overnight culture in LB broth or after two hours of growth in M9 minimal medium with the indicated concentrations of iron was inoculated onto YESCA agar (10 g/L casamino acids, 1 g/L yeast extract, 20 g/L Bacto agar) with 20 μg/mL Congo red and 10 μg/mL Coommassie blue for the Congo red plates (Da Re and Ghigo, 2006) or onto LB agar with 0.02% CF (Zogaj et al., 2001). CF is a dye that binds cellulose and fluoresces with UV light. Bacteria were grown for 48 hrs at 37°C prior to assessment of colony morphotypes.

Isolation of bone marrow derived macrophages (BMDM). Bone marrow cells were isolated as previously described (Lutz et al., 1999). Conditioned medium from the murine fibroblast cell line L929 served as a source of M-CSF for macrophage differentiation (Stanley and Heard, 1977). During all experiments unless otherwise indicated, bone marrow-derived macrophages

were maintained in RPMI 1640 medium (Gibco) with 10% heat-inactivated fetal bovine serum (FBS, Gibco) and 1% penicillin/streptomycin/antimycotic (Gibco) at 37°C, 5% CO_2.

Mesenteric lymph node (MLN) cultures. MLNs were isolated from *Il10*$^{-/-}$ mice monoassociated with NC101 or the *bcsA* mutant at 21 and 35 days. MLN cultures were prepared as previously described (Patwa et al., 2011). Briefly, MLN cells were plated at a density of 5 x 10^5 per well in quadruplicate in 96-well plates. Cells were cultured in RPMI 1640 medium containing 10% FBS, 2 mM L-glutamine, 1 mM sodium pyruvate, 0.05 mM 2-mercaptoethanol, penicillin (100 U/mL) and streptomycin (100 μg/mL) and were stimulated for 72 hours with NC101 or *bcsA* mutant lysates (10 μg protein/mL) or media control. Culture supernatants were collected and stored at -20°C until cytokine quantification. Bacterial lysates were prepared as previously described (Kim et al., 2005).

Cytokine quantification by enzyme-linked immunosorbent assays (ELISA). Commercially available monoclonal anti-mouse interleukin-17 (IL-17) (R&D Systems), IL-12 p40 (BD Biosciences) and interferon-γ (IFN-γ) (BD Biosciences) capture and detection reagents were utilized to quantify MLN production of IL-17 and IFN-γ and BMM production of IL-12 p40 by ELISA according to the manufacturer's instructions.

Colonic RNA isolation and real-time reverse-transcriptase PCR (RT-PCR). RNA was extracted from proximal colonic tissue using the RNAeasy isolation kit (Qiagen) according to the manufacturer's instructions. Real-time RT-PCR were performed using the Sensifast SYBR No-ROX Kit (Bioline) using the following PCR conditions: a single hold at 95°C for 2 minutes,

followed by 40 cycles at 95°C for 5 seconds, 60°C for 10 seconds and 72°C for 20 seconds. Melting curves were also assessed to ensure specificity of the PCR products. Primers utilized are listed in Table S2.

Statistical analysis. *P*-values were calculated using Student's t-test when 2 experimental groups were compared, one-way ANOVA with Tukey's multiple comparison post test when 3 or more experimental groups were compared, or two-way ANOVA with Bonferroni multiple comparison post test when more than two variables were compared. All enumeration of bacteria by serial dilution and plating was log transformed to normalize the data. For quantification of NC101 aggregates by microscopy, *p*-values were calculated using a non-parametric Kruskal-Wallis test with the Dunn's post test. For all animal experiments, *p*-values were determined using a non-parametric Mann-Whitney test.

4.7 Figures

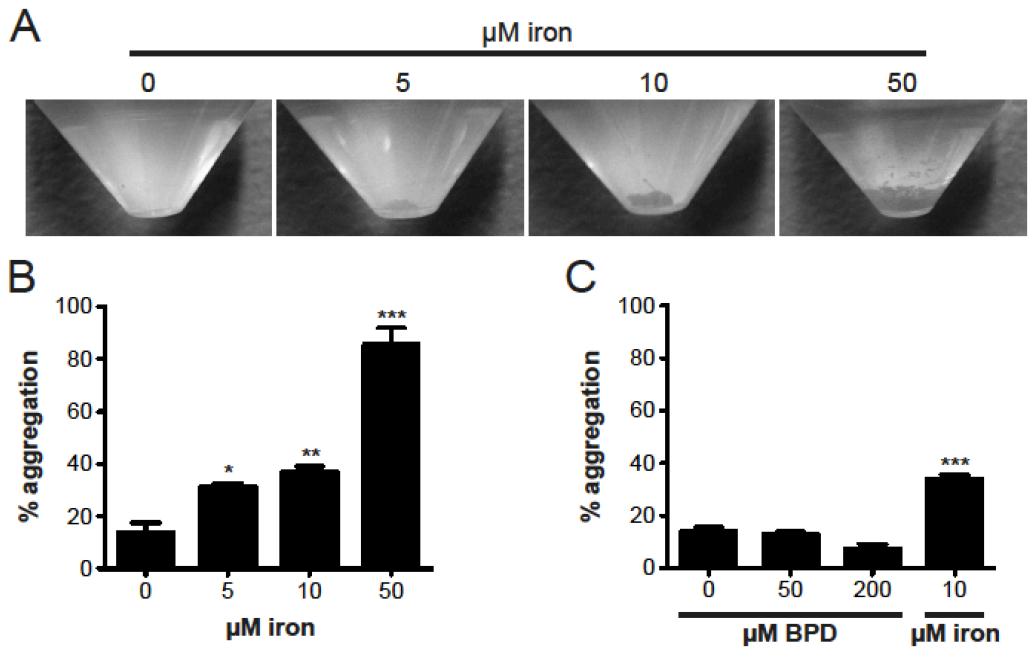

Figure 4.1. Iron promotes aggregation of *E. coli* NC101. (A) Representative images of NC101 aggregates after 2 hours of growth in minimal medium with increasing concentrations of iron. (B, C) Sedimentation assays of NC101 after 2 hours of growth in minimal medium with various concentrations of (B) iron or (C) the iron chelator BPD. Data represent the percent optical density associated with the aggregates relative to the whole culture. All data represent the mean ± SEM of at least 3 independent experiments. Pairwise comparisons by one-way ANOVA. * $p < 0.05$, ** $p < 0.01$, *** $p < 0.001$ compared to the 0 μM condition.

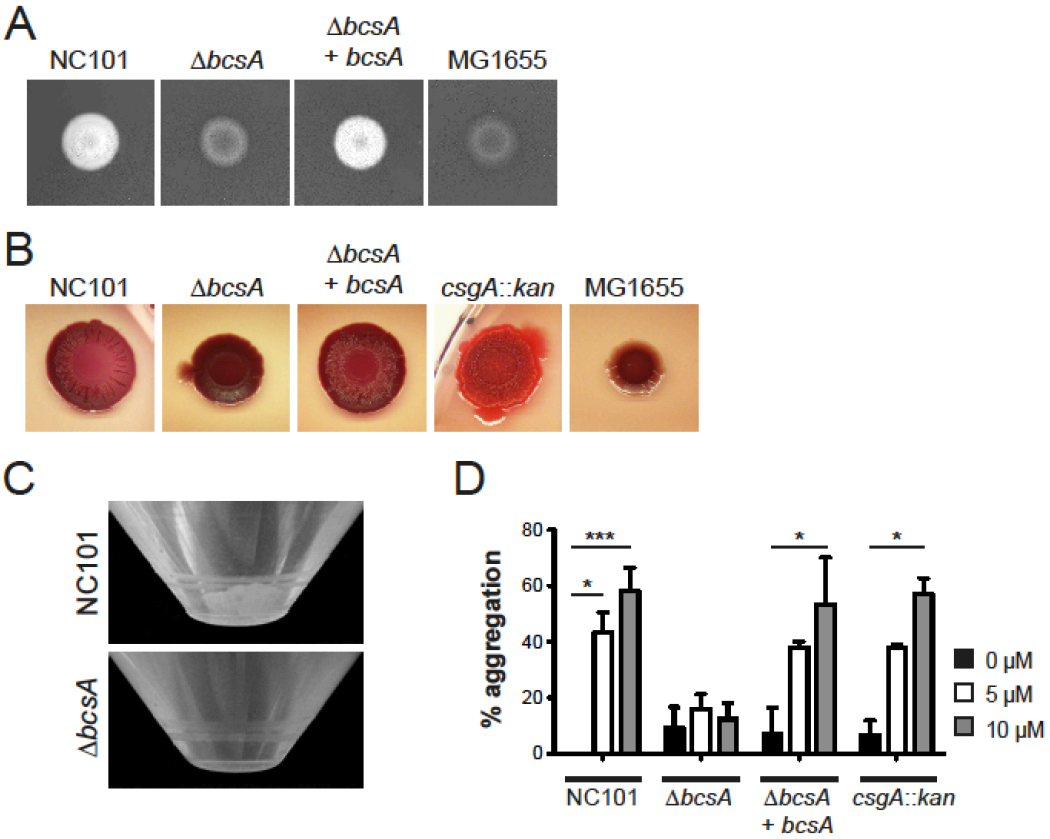

Figure 4.2. Cellulose is required for iron-induced aggregation of NC101. (A, B) Representative colony morphologies of NC101, Δ*bcsA*, Δ*bcsA* + *bcsA* or *csgA*::*kan* on (A) Calcofluor or (B) Congo red agar. *E. coli* MG1655 served as a negative control. (C) Representative images of NC101 and Δ*bcsA* after 2 hours of growth in minimal medium with 10 μM iron. (D) Sedimentation assays of NC101, Δ*bcsA*, Δ*bcsA* + *bcsA* or *csgA*::*kan* after 2 hours of growth in minimal medium with increasing concentrations of iron. Data represent the percent OD600 of the aggregates relative to the whole culture. Data represent the mean ± SEM of three independent experiments. Pairwise comparisons by one-way ANOVA. * $p < 0.05$, *** $p < 0.001$

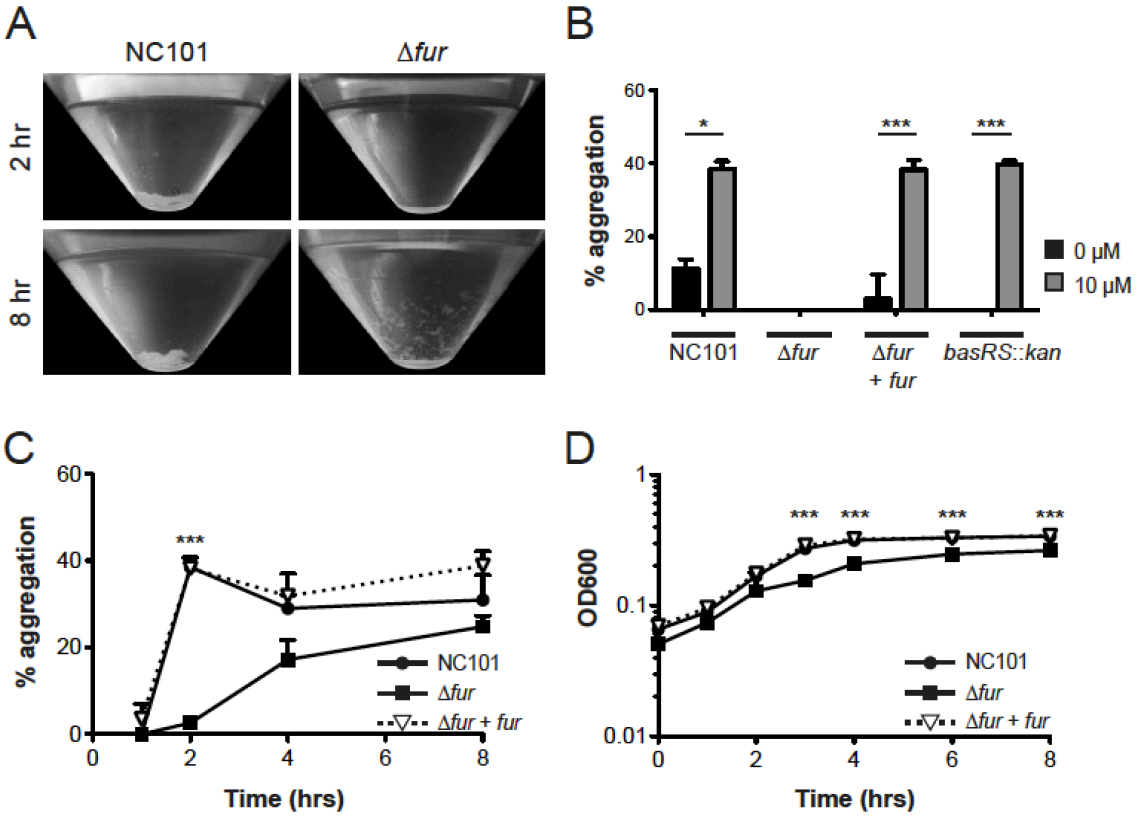

Figure 4.3. Deletion of *fur* in NC101 limits iron-induced aggregation. (A) Representative images of NC101 or Δ*fur* after 2 or 8 hours of growth in minimal medium with 10 μM iron. (B) Sedimentation assays of NC101, Δ*fur*, Δ*fur* + *fur* or *basRS*::*kan* after 2 hours of growth in minimal medium with 0 or 10 μM iron. (C) Time course sedimentation assays and (D) growth curves of NC101, Δ*fur* or Δ*fur* + *fur* in minimal medium with 10 μM iron. Data for all sedimentation assays represent the percent OD600 of the aggregates relative to the whole culture. All data are represented as the mean ± SEM of three independent experiments. Pairwise comparisons by (B) one-way and (C, D) two-way ANOVA. * $p < 0.05$, *** $p < 0.001$

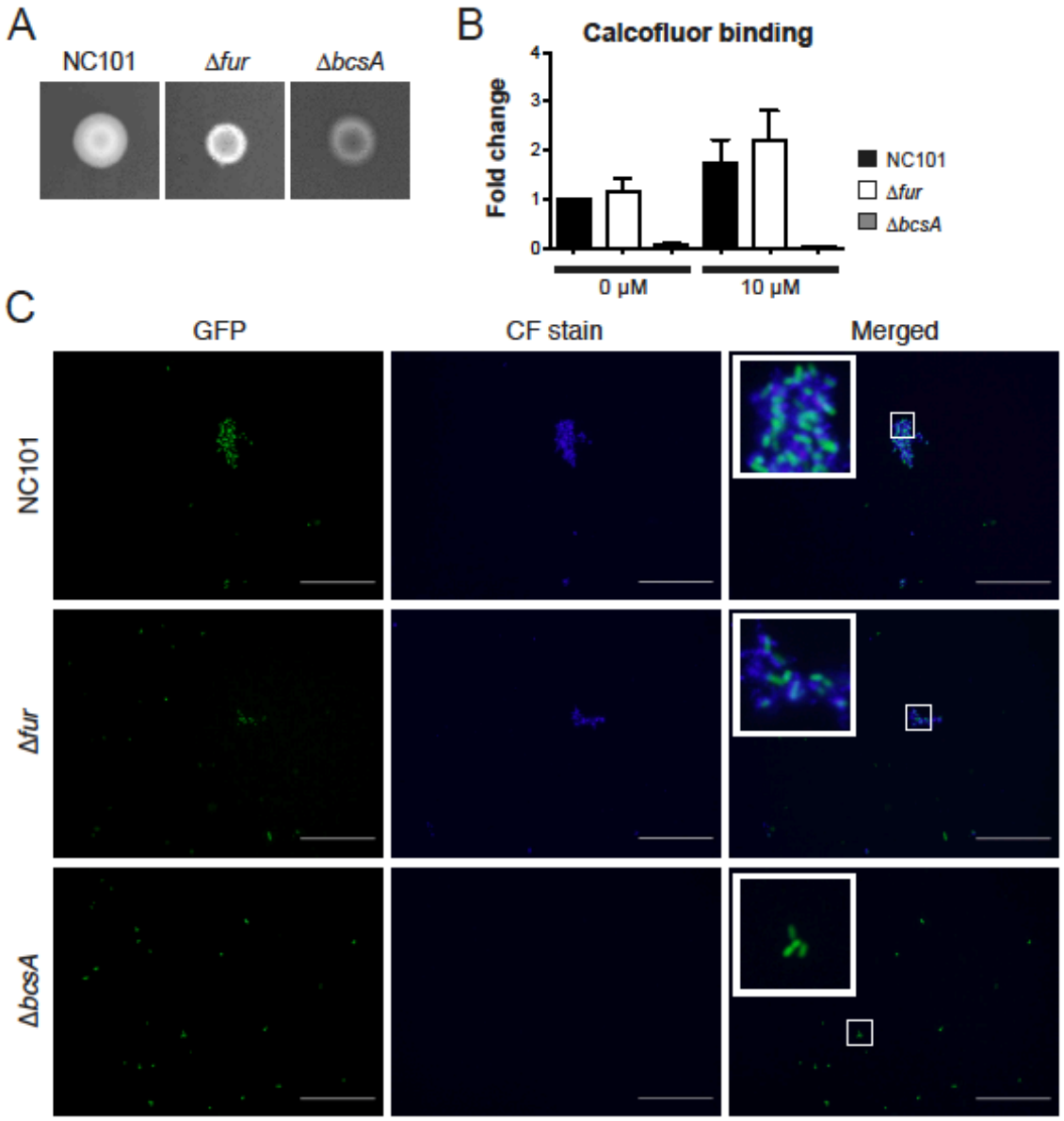

Figure 4.4. Deletion of *fur* does not disrupt NC101 cellulose production. (A) Colony morphologies of NC101, Δ*fur* or Δ*bcsA* on Calcofluor plates. (B) GFP-expressing NC101, Δ*fur* or Δ*bcsA* were grown in minimal medium with 0 or 10 μM iron for 1 hour and stained with Calcofluor. ImageJ software was utilized to calculate mean Calcofluor binding per cell per 200x high-power field. At least 15 fields were analyzed per sample. Data represent the mean ± SEM of three independent experiments relative to the NC101, 0 μM condition. Pairwise comparisons by Kruskal-Wallis. (C) Representative images at 400x of GFP-expressing NC101, Δ*fur* and Δ*bcsA* stained with Calcofluor. Scale bar = 100 μm. Bacteria were grown in minimal medium with 10 μM iron for 1 hour.

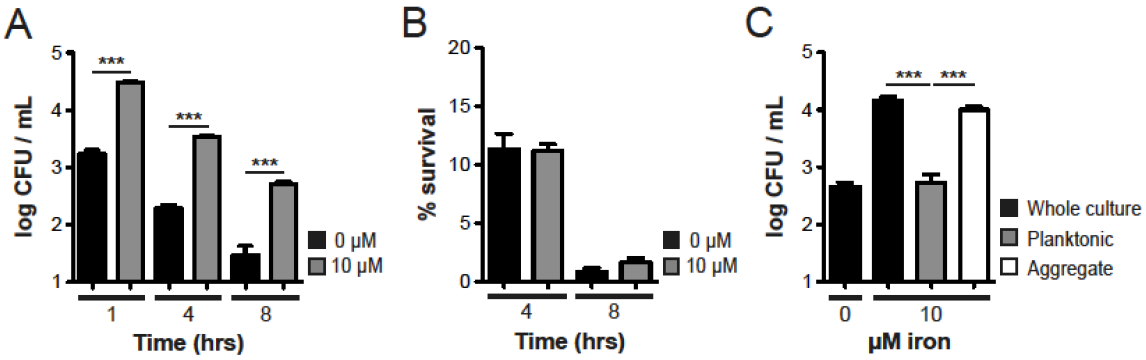

Figure 4.5. NC101 aggregates are more susceptible to phagocytosis. NC101 was grown in minimal medium with 0 or 10 μM iron prior to co-culture with bone marrow-derived macrophages. Following the addition of gentamicin for 30 minutes, intracellular NC101 was quantified after (A) 1 hour as a measure of bacterial uptake and 4 or 8 hours as measures of intracellular survival. (B) 4 to 1 hour and 8 to 1 hour ratios of intracellular NC101 as measures of percent intracellular survival. (C) Planktonic and aggregate fractions of each culture were separated prior to co-culture with macrophages. Intracellular NC101 was quantified after 1 hour. Data are shown as the mean ± SEM of a representative experiment of at least 3 independent experiments with at least 4 technical replicates. Pairwise comparisons by (A, B) t-test and (C) one-way ANOVA. *** $p < 0.001$

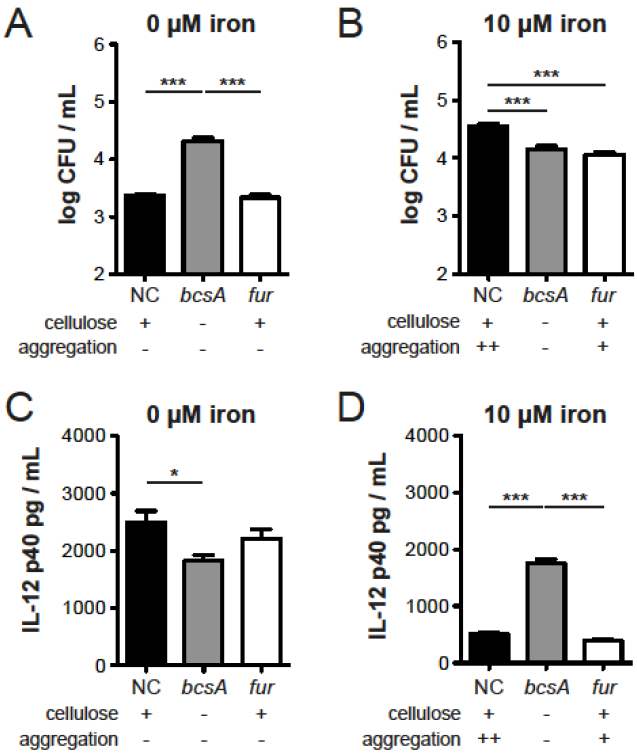

Figure 4.6. Deletion of *bcsA* alters NC101 interactions with macrophages. (A, B) Intracellular NC101, Δ*bcsA* or Δ*fur* after 1 hour co-culture with bone marrow-derived macrophages. (C, D) IL-12 p40 cytokine production by bone marrow-derived macrophages infected with NC101, Δ*bcsA* or Δ*fur* for 8 hours. All bacteria were grown in minimal medium with (A, C) 0 μM or (B, D) 10 μM iron prior to co-culture with macrophages. Data are shown as the mean ± SEM of a representative experiment of 3 independent experiments with at least 4 technical replicates. Pairwise comparisons by one-way ANOVA. * $p < 0.05$, *** $p < 0.001$

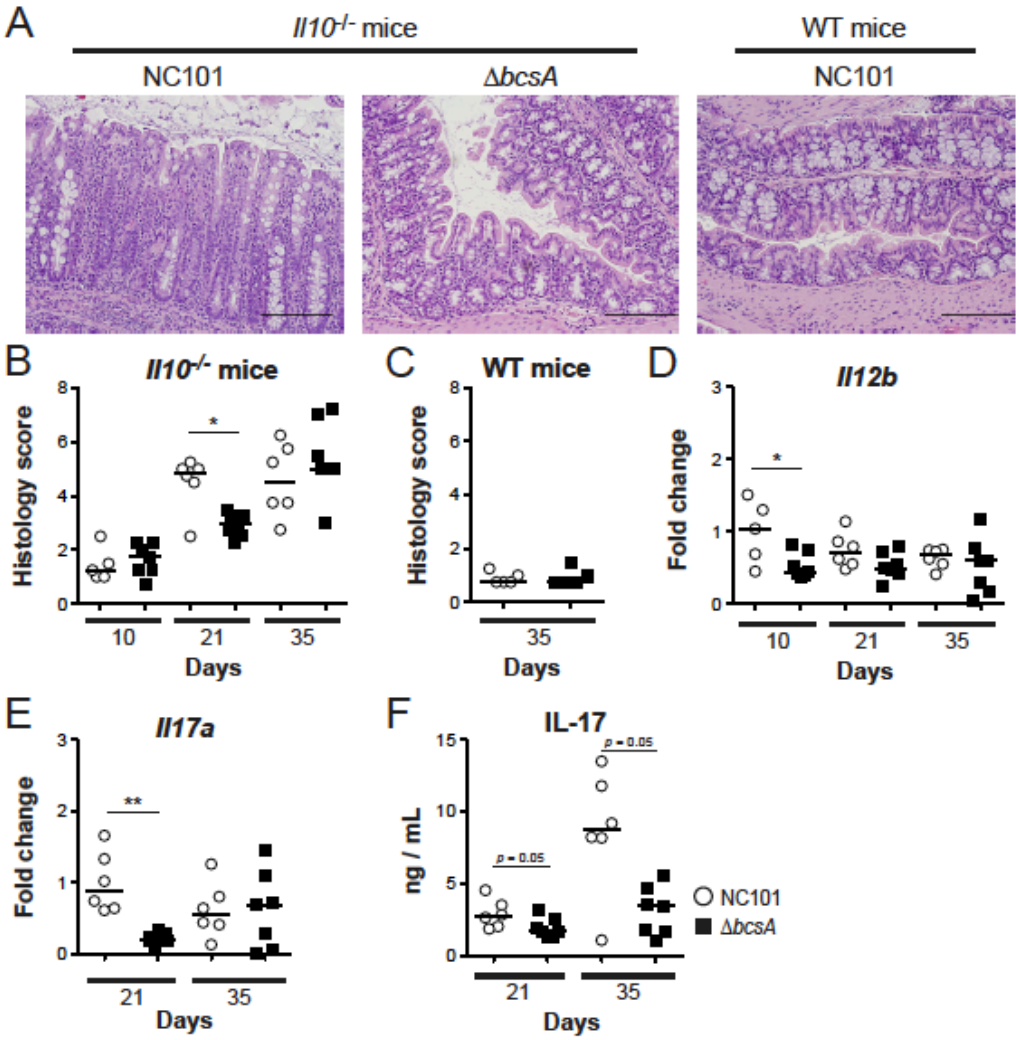

Figure 4.7. Deletion of *bcsA* in NC101 delays onset of colitis in monoassociated *Il10*$^{-/-}$ mice. (A) Representative H&E histology at 200x of the proximal colons of *Il10*$^{-/-}$ or WT mice colonized with NC101 (open circles) or Δ*bcsA* (closed squares) for 21 days. Scale bar = 50 µm. (B, C) Composite proximal and distal colon histology scores (0-8) of B) *Il10*$^{-/-}$ mice or (C) WT mice monoassociated with NC101 or Δ*bcsA*. (D, E) Proximal colon transcript levels of (D) *Il12b* or (E) *Il17a* relative to *Actb* in *Il10*$^{-/-}$ mice monoassociated with NC101 or Δ*bcsA*. Data are expressed as fold change relative to NC101 colonized mice. (F) IL-17 production by unfractionated MLN cells restimulated with the respective bacterial lysates *ex vivo*. MLNs were isolated from *Il10*$^{-/-}$ mice monoassociated with NC101 or Δ*bcsA* for 21 or 35 days. Each symbol represents an individual mouse, n = 5-8 mice per group. Line at median, pairwise comparisons by Mann-Whitney. * $p < 0.05$, ** $p < 0.01$

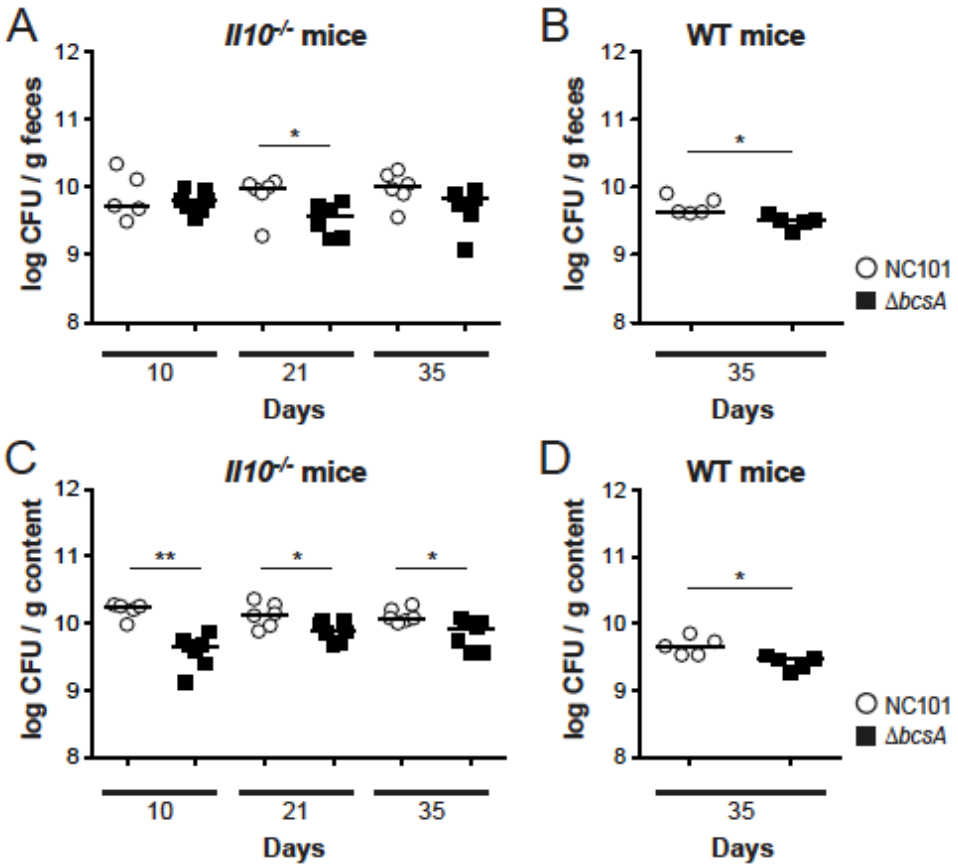

Figure 4.8. Luminal densities of NC101 or the *bcsA* mutant in monoassociated WT or *Il10*$^{-/-}$ mice. Quantitative bacterial culture of feces collected from (A) *Il10*$^{-/-}$ mice or (B) WT mice monoassociated with NC101 (open circles) or Δ*bcsA* (closed squares). Quantitative bacterial culture of cecal content collected from (C) *Il10*$^{-/-}$ mice or (D) WT mice monoassociated with NC101 or Δ*bcsA*. Each symbol represents an individual mouse, n = 5-8 mice per group. Line at median, pairwise comparisons by Mann-Whitney. * $p < 0.05$, ** $p < 0.01$

4.8 Supplemental Figures

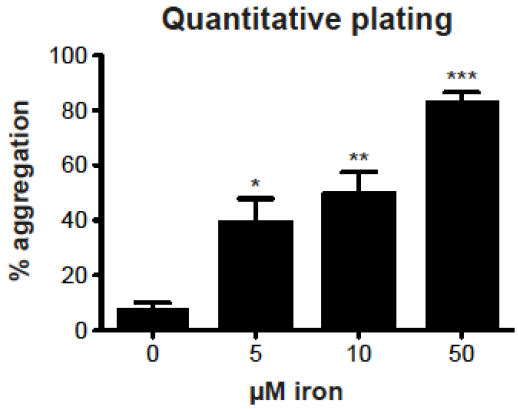

Supplemental Figure 4.1. Iron promotes aggregation of NC101 as assessed by quantitative plating. Sedimentation assays of NC101 after 2 hours of growth in minimal medium with increasing concentrations of iron. Data represent the percent colony forming units associated with the aggregates relative to the whole culture. Data represent the mean ± SEM of at least three independent experiments. Pairwise comparisons by one-way ANOVA. * $p < 0.05$, ** $p < 0.01$, *** $p < 0.001$ compared to the 0 μM condition.

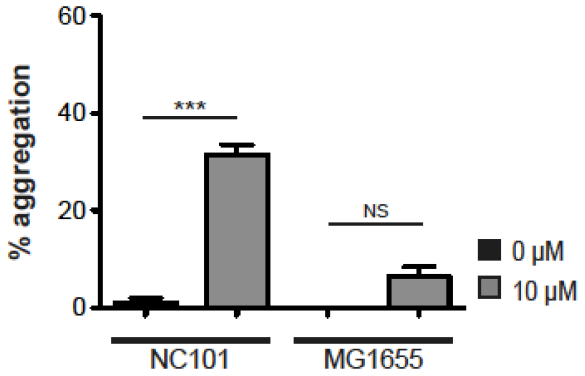

Supplemental Figure 4.2. Iron does not induce aggregation of *E. coli* K12 substrain MG1655. Sedimentation assays of *E. coli* NC101 or MG1655 after 5 hours of growth in minimal medium with 0 or 10 µM iron. Data are represented as the percent OD600 of the aggregates relative to the whole culture. Data represent the mean ± SEM of at least three independent experiments. Pairwise comparisons by one-way ANOVA. *** $p < 0.001$.

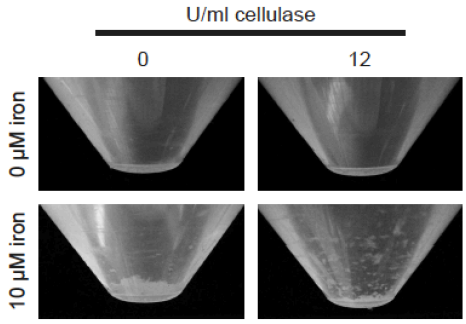

Supplemental Figure 4.3. Addition of cellulase disrupts NC101 aggregates.
Representative images of NC101 after treatment with 12 U/ml cellulase following 2 hours of growth in minimal medium with 0 or 10 µM iron.

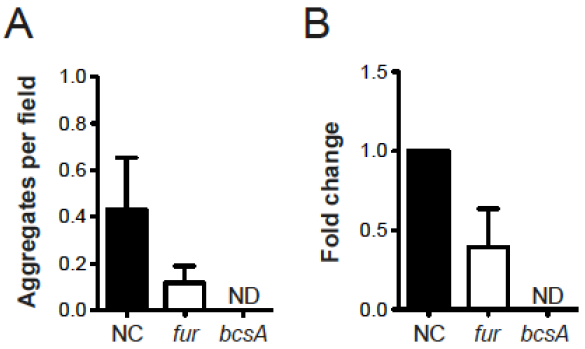

Supplemental Figure 4.4. Deletion of *fur* reduces microscopic aggregation of NC101. GFP-expressing NC101, Δ*fur* or Δ*bcsA* were grown in minimal medium with 10 μM iron for 1 hour. (A) Quantity of microscopic aggregates per 200x high-power field. Data represent the mean ± SEM of three independent experiments. (B) Average pixel size of the microscopic aggregates. Data are expressed as fold change relative to NC101 of three independent experiments. ImageJ software was utilized for these analyses, where at least 15 fields were analyzed per sample per experiment.

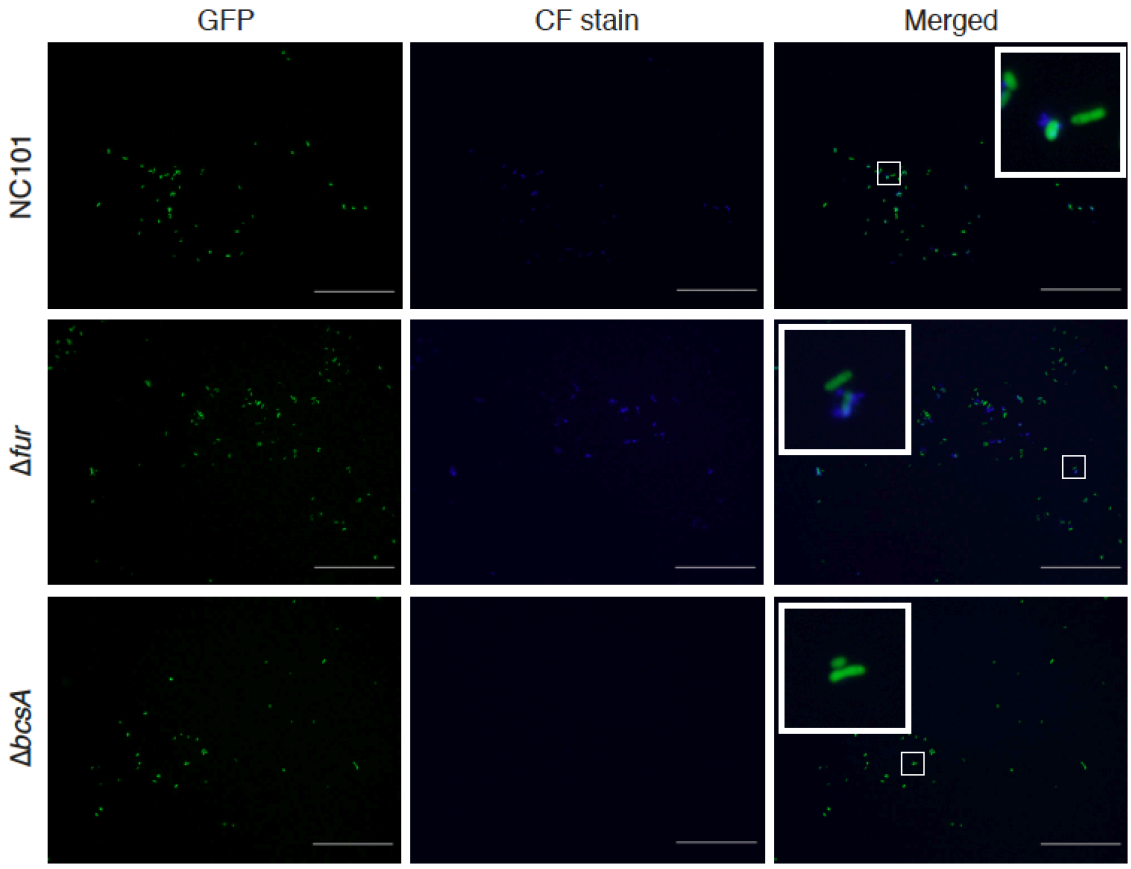

Supplemental Figure 4.5. NC101 produces cellulose under low iron conditions. Representative images at 400x of GFP-expressing NC101, Δ*fur* or Δ*bcsA* stained with Calcofluor. Scale bar = 100 μm. Bacteria were grown in minimal medium for 1 hour.

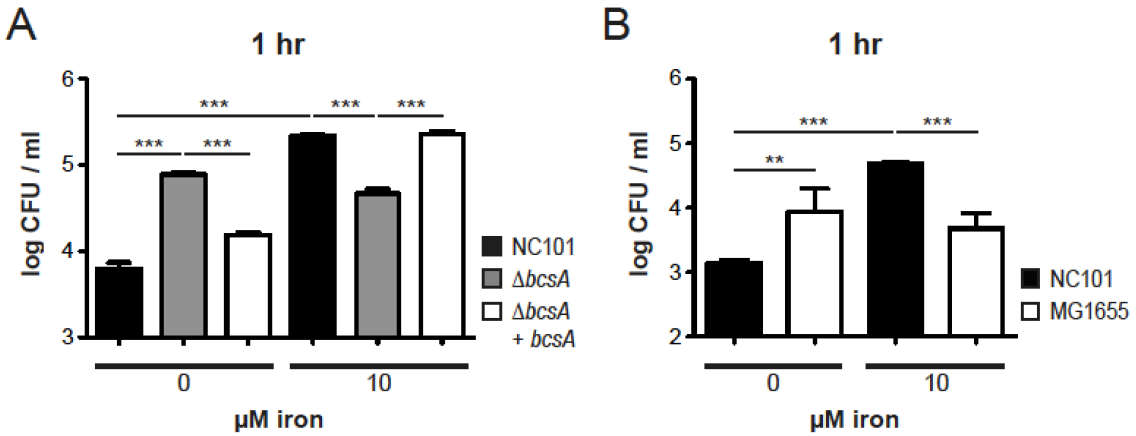

Supplemental Figure 4.6. Phagocytosis of NC101 and MG1655 in the presence and absence of iron. (A) Intracellular NC101, Δ*bcsA* or Δ*bcsA* + *bcsA* after 1 hour co-culture with bone marrow-derived macrophages as a measure of bacterial uptake. (B) Intracellular NC101 or MG1655 after 1 hour co-culture with bone marrow-derived macrophages. All bacteria were grown in minimal medium with 0 or 10 μM iron prior to co-culture with the macrophages. Data are shown as the mean ± SEM of a representative experiment of at least 3 independent experiments with at least 4 technical replicates. Pairwise comparisons by one-way ANOVA. ** $p < 0.01$, *** $p < 0.001$

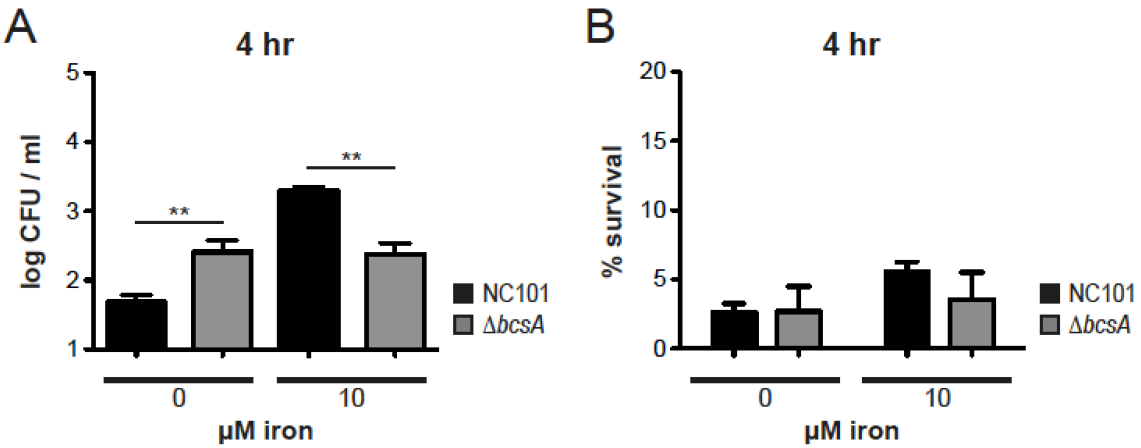

Supplemental Figure 4.7. Deletion of *bcsA* does not impact percent intramacrophagic survival. NC101 or Δ*bcsA* was grown in minimal medium with 0 or 10 μM iron prior to co-culture with bone marrow-derived macrophages. Following the addition of gentamicin, intracellular bacteria were quantified after (A) 4 hours as a measure of intracellular survival. (B) Ratio of 4 to 1 hour intracellular bacteria as a measure of percent intracellular survival. Data are shown as the mean ± SEM of a representative experiment of at least 3 independent experiments with at least 4 technical replicates. Pairwise comparisons by one-way ANOVA. ** $p < 0.01$

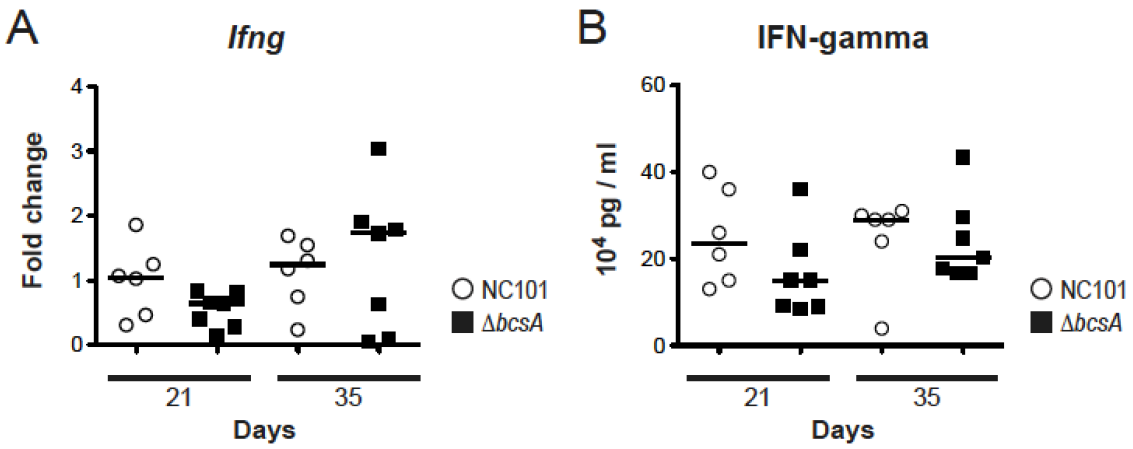

Supplemental Figure 4.8. IFN-γ expression and production did not differ between mice monoassociated with NC101 or the *bcsA* mutant. (A) Proximal colon transcript levels of *Ifng* relative to *Actb* in *Il10*$^{-/-}$ mice monoassociated with NC101 or Δ*bcsA*. Data are expressed as fold change relative to NC101 colonized *Il10*$^{-/-}$ mice at 21 days. (B) IFN-γ production of unfractionated MLN cells restimulated with the respective bacterial lysates *ex vivo*. MLNs were isolated from *Il10*$^{-/-}$ mice monoassociated with NC101 or Δ*bcsA*. Each symbol represents an individual mouse, *n* = 5-8 mice per group. Line at median, pairwise comparisons by Mann-Whitney.

Strains or plasmids	Description	Reference
Strains		
NC101	Murine intestinal *E. coli* strain with AIEC characteristics.	Kim 2005(1)
NC101 Δ*bcsA*	NC101 isogenic mutant with *bcsA* deleted.	This work
NC101 Δ*bcsA* + *bcsA*	NC101 isogenic mutant with *bcsA* deleted that is chromosomally complemented with *bcsA* at the *att7* site.	This work
NC101 *csgA::kan*	NC101 with the kanamycin resistance gene disrupting *csgA*.	This work
NC101 Δ*fur*	NC101 isogenic mutant with *fur* deleted.	This work
NC101 Δ*fur* + *fur*	NC101 isogenic mutant with *fur* deleted that is chromosomally complemented with *fur* at the *att7* site.	This work
NC101 Δ*basRS*	NC101 isogenic mutant with *basRS* deleted.	This work
MG1655	Laboratory *E. coli* K12 strain.	Kim 2008(2)
Plasmids		
pKD46	Plasmid encoding lambda red recombinase.	Datsenko KA 2000(3)
pKD13	Template plasmid for gene deletions using the lambda red recombinase system.	Baba T 2006(4)
pCP20	Plasmid encoding FLP recombinase.	Datsenko KA 2000(3)
pTNS2	Plasmid encoding the *tnsA,B,C* and *D* transposition pathway genes.	Choi KH 2005(5)
pMCL2868-*bcsA*	pMCL2868 harboring the *bcsA* promotor and gene.	This work
pMCL2868-*fur*	pMCL2868 harboring the *fur* promotor and gene.	This work

Supplemental Table 4.1. Bacterial strains and plasmids used in this study.

Name	Sequence (5' to 3')	Reference
KO_bcsA forward	CTGTTAAACTATTCCGGGCTGAAAATGCCAGTCGGGAGTGCATCATGAGTATTCCGGGGATCCGTCGACC	This work
KO_bcsA reverse	AGAATATTTTTCTTTTCATCGCGTTATCATCATTGTTGAGCCAAAACCTGTGTAGGCTGGAGCTGCTTCG	This work
KO_csgA forward	ACGTTAATTTCCATTCGACTTTTAAATCAATCCGATGGGGGTTTTACATGATTCCGGGGATCCGTCGACC	This work
KO_csgA reverse	CGCCCTGTTTCTTTCATACTGATGATGTATTAGTACTGATGAGCGGTCGCTGTAGGCTGGAGCTGCTTCG	This work
KO_fur forward	CACTTCTTCTAATGAAGTGAACCGCTTAGTAACAGGACAGATTCCGCATGATTCCGGGGATCCGTCGACC	This work
KO_fur reverse	GCAGGTTGGCTTTTCTCGTTCAGGCTGGCTTATTTGCCTTCGTGCGCGTGTGTAGGCTGGAGCTGCTTCG	This work
KO_basRS forward	GCTGCGGATGATATTCTGCAAACTTGCAGGAGAGTGAGTGAATGAAAATTATTCCGGGGATCCGTCGACC	This work
KO_basRS reverse	GTGCTGGTGGTCAGCAGCTTTCTTTATATCTGGTTTGCCACGTACTGATCTGTAGGCTGGAGCTGCTTCG	This work
bcsA upstream	TGAAGAGATACTGACGCTGG	This work
bcsA downstream	CGCCTGCGTCATGAAAGAGG	This work
csgA upstream	GCAGAGACAGTCGCAAATGG	This work
csgA downstream	TGTACATATCCCCTTGCTGG	This work
fur upstream	TGGTTTTCATTTAGGCGTGG	This work
fur downstream	AGCTGTAACTCTCGCTTTTC	This work
basRS upstream	ACCTTATTGGGCCTGACTGG	This work
basRS downstream	CTCCTCCAGGTTAACGGAGG	This work
KPN1_bcsA	AAGGTACCATACTGACGCTGGCTAACTG	This work
NOT1_bcsA	AAGCGGCCGCTCCGGTCGGAGGCTTTTGAC	This work
KPN1_fur	AAGGTACCTAACAATATTTGCCAGGGAC	This work
NOT1_fur	AAGCGGCCGCGTTGGCTTTTCTCGTTCAGG	This work
glmS upstream	GATGCTGGTGGCGAAGCTGT	Choi KH 2005(5)
glmS downstream	GATGACGGTTTGTCACATGGA	Choi KH 2005(5)
Il12b forward	CGCAAGAAAGAAAAGATGAAGGAG	This work
Il12b reverse	TTGCATTGGACTTCGGTAGATG	This work
Il17a forward	AACCGTTCCACGTCACCCTGGA	This work
Il17a reverse	TGGTCCAGCTTTCCCTCCGCA	This work
Ifng forward	CTTCCTCATGGCTGTTTCTGG	Arthur JC 2014(6)
Ifng reverse	ACGCTTATGTTGTTGCTGATGG	Arthur JC 2014(6)
ActB	AGCCATGTACGTAGCCATCCAG	Onyiah JC 2013(7)
ActB	TGGCGTGAGGGAGAGCATAG	Onyiah JC 2013(7)

Supplemental Table 4.2. Oligonucleotide primers used in this study.

PRE-AGGREGATE DISPERSAL	0 μM			10 μM		
	NC101	Δ*bcsA*	MG1655	NC101	Δ*bcsA*	MG1655
Aggregates per field	0.18 ± 0.08	0.00 ± 0.00	0.00 ± 0.00	0.95 ± 0.21 ***	0.00 ± 0.00	0.00 ± 0.00
POST-AGGREGATE DISPERSAL	0 μM			10 μM		
	NC101	Δ*bcsA*	MG1655	NC101	Δ*bcsA*	MG1655
Aggregates per field	0.00 ± 0.00	0.00 ± 0.00	0.02 ± 0.00	0.05 ± 0.05	0.00 ± 0.00	0.00 ± 0.00

Supplemental Table 4.3. Quantification of microbial aggregates by microscopy. Quantification of NC101 WT, Δ*bcsA* or MG1655 aggregates per 200x high-power field before and after physical disruption using ImageJ software. At least 15 fields were analyzed per sample. Bacteria were grown in minimal medium with 0 or 10 μM iron for two hours. Data are shown as the mean ± SEM of three independent experiments. *** $p < 0.001$ compared to the NC101, 0 μM condition.

REFERENCES

Alves, J.R., Pereira, A.C.M., Souza, M.C., Costa, S.B., Pinto, A.S., Mattos-Guaraldi, A.L., Hirata-Júnior, R., Rosa, A.C.P., and Asad, L.M.B.O. (2010). Iron-limited condition modulates biofilm formation and interaction with human epithelial cells of enteroaggregative Escherichia coli (EAEC). Journal of Applied Microbiology *108*, 246–255.

Amarasinghe, J.J., D'Hondt, R.E., Waters, C.M., and Mantis, N.J. (2013). Exposure of Salmonella enterica Serovar Typhimurium to a Protective Monoclonal IgA Triggers Exopolysaccharide Production via a Diguanylate Cyclase-Dependent Pathway. Infect Immun *81*, 653–664.

Arthur, J.C., Perez-Chanona, E., Muhlbauer, M., Tomkovich, S., Uronis, J.M., Fan, T.J., Campbell, B.J., Abujamel, T., Dogan, B., Rogers, A.B., et al. (2012). Intestinal Inflammation Targets Cancer-Inducing Activity of the Microbiota. Science *338*, 120–123.

Arthur, J.C., Gharaibeh, R.Z., Mühlbauer, M., Perez-Chanona, E., Uronis, J.M., McCafferty, J., Fodor, A.A., and Jobin, C. (2014). Microbial genomic analysis reveals the essential role of inflammation in bacteria-induced colorectal cancer. Nature Communications *5*, 4724.

Banin, E., Brady, K.M., and Greenberg, E.P. (2006). Chelator-induced dispersal and killing of Pseudomonas aeruginosa cells in a biofilm. Appl Environ Microbiol *72*, 2064–2069.

Baumgart, M., Dogan, B., Rishniw, M., Weitzman, G., Bosworth, B., Yantiss, R., Orsi, R.H., Wiedmann, M., Mcdonough, P., Kim, S.G., et al. (2007). Culture independent analysis of ileal mucosa reveals a selective increase in invasive Escherichia coli of novel phylogeny relative to depletion of Clostridiales in Crohn's disease involving the ileum. Isme J *1*, 403–418.

Bokranz, W. (2005). Expression of cellulose and curli fimbriae by Escherichia coli isolated from the gastrointestinal tract. Journal of Medical Microbiology *54*, 1171–1182.

Boudeau, J., Glasser, A.L., Masseret, E., Joly, B., and Darfeuille-Michaud, A. (1999). Invasive ability of an Escherichia coli strain isolated from the ileal mucosa of a patient with Crohn's disease. Infect Immun *67*, 4499–4509.

Carvalho, F.A., Barnich, N., Sauvanet, P., Darcha, C., Gelot, A., and Darfeuille-Michaud, A. (2008). Crohn's disease-associated Escherichia coli LF82 aggravates colitis in injured mouse colon via signaling by flagellin. Inflamm Bowel Dis *14*, 1051–1060.

Carvalho, F.A., Koren, O., Goodrich, J.K., Johansson, M.E.V., Nalbantoglu, I., Aitken, J.D., Su, Y., Chassaing, B., Walters, W.A., González, A., et al. (2012). Transient inability to manage proteobacteria promotes chronic gut inflammation in TLR5-deficient mice. Cell Host Microbe *12*, 139–152.

Chassaing, B., Srinivasan, G., Delgado, M.A., Young, A.N., Gewirtz, A.T., and Vijay-Kumar, M. (2012). Fecal Lipocalin 2, a Sensitive and Broadly Dynamic Non-Invasive Biomarker for

Intestinal Inflammation. PLoS ONE *7*, e44328.

Choi, K.-H., Gaynor, J.B., White, K.G., Lopez, C., Bosio, C.M., Karkhoff-Schweizer, R.R., and Schweizer, H.P. (2005). A Tn7-based broad-range bacterial cloning and expression system. Nat Meth *2*, 443–448.

Da Re, S., and Ghigo, J.M. (2006). A CsgD-Independent Pathway for Cellulose Production and Biofilm Formation in Escherichia coli. J Bacteriol *188*, 3073–3087.

Darfeuille-Michaud, A., Boudeau, J., Bulois, P., Neut, C., Glasser, A.-L., Barnich, N., Bringer, M.-A., Swidsinski, A., Beaugerie, L., and Colombel, J.-F. (2004). High prevalence of adherent-invasive Escherichia coli associated with ileal mucosa in Crohn's disease. Gastroenterology *127*, 412–421.

Datsenko, K.A., and Wanner, B.L. (2000). One-step inactivation of chromosomal genes in Escherichia coli K-12 using PCR products. Proc Natl Acad Sci USA *97*, 6640–6645.

Daw, K., Baghdayan, A.S., Awasthi, S., and Shankar, N. (2012). Biofilm and planktonic Enterococcus faecalis elicit different responses from host phagocytes in vitro. FEMS Immunol. Med. Microbiol. *65*, 270–282.

Depas, W.H., Hufnagel, D.A., Lee, J.S., Blanco, L.P., Bernstein, H.C., Fisher, S.T., James, G.A., Stewart, P.S., and Chapman, M.R. (2013). Iron induces bimodal population development by Escherichia coli. Proceedings of the National Academy of Sciences *110*, 2629–2634.

Deriu, E., Liu, J.Z., Pezeshki, M., Edwards, R.A., Ochoa, R.J., Contreras, H., Libby, S.J., Fang, F.C., and Raffatellu, M. (2013). Probiotic Bacteria Reduce Salmonella Typhimurium Intestinal Colonization by Competing for Iron. Cell Host Microbe *14*, 26–37.

Dogan, B., Suzuki, H., Herlekar, D., Sartor, R.B., Campbell, B.J., Roberts, C.L., Stewart, K., Scherl, E.J., Araz, Y., Bitar, P.P., et al. (2014). Inflammation-associated adherent-invasive Escherichia coli are enriched in pathways for use of propanediol and iron and M-cell translocation. Inflamm Bowel Dis *20*, 1919–1932.

Domingue, P.A., Lambert, P.A., and Brown, M.R. (1989). Iron depletion alters surface-associated properties of Staphylococcus aureus and its association to human neutrophils in chemiluminescence. FEMS Microbiol Lett *50*, 265–268.

Doyle, S.E. (2003). Toll-like Receptors Induce a Phagocytic Gene Program through p38. J. Exp. Med. *199*, 81–90.

Gerstel, U., and Römling, U. (2001). Oxygen tension and nutrient starvation are major signals that regulate agfD promoter activity and expression of the multicellular morphotype in Salmonella typhimurium. Environmental Microbiology *3*, 638–648.

Gevers, D., Kugathasan, S., Denson, L.A., Vázquez-Baeza, Y., Van Treuren, W., Ren, B., Schwager, E., Knights, D., Song, S.J., Yassour, M., et al. (2014). The Treatment-Naive Microbiome in New-Onset Crohn's Disease. Cell Host Microbe *15*, 382–392.

Glasser, A.L., Boudeau, J., Barnich, N., Perruchot, M.H., Colombel, J.F., and Darfeuille-Michaud, A. (2001). Adherent invasive Escherichia coli strains from patients with Crohn's disease survive and replicate within macrophages without inducing host cell death. Infect Immun *69*, 5529–5537.

Gualdi, L., Tagliabue, L., Bertagnoli, S., Ierano, T., De Castro, C., and Landini, P. (2008). Cellulose modulates biofilm formation by counteracting curli-mediated colonization of solid surfaces in Escherichia coli. Microbiology (Reading, Engl.) *154*, 2017–2024.

Hadjifrangiskou, M., Gu, A.P., Pinkner, J.S., Kostakioti, M., Zhang, E.W., Greene, S.E., and Hultgren, S.J. (2012). Transposon Mutagenesis Identifies Uropathogenic Escherichia coli Biofilm Factors. J Bacteriol *194*, 6195–6205.

Hagiwara, M., Yamashino, T., and Mizuno, T. (2004). A Genome-wide view of the Escherichia coli BasS-BasR two-component system implicated in iron-responses. Biosci. Biotechnol. Biochem. *68*, 1758–1767.

Hampe, J., Franke, A., Rosenstiel, P., Till, A., Teuber, M., Huse, K., Albrecht, M., Mayr, G., La Vega, De, F.M., Briggs, J., et al. (2006). A genome-wide association scan of nonsynonymous SNPs identifies a susceptibility variant for Crohn disease in ATG16L1. Nat. Genet. *39*, 207–211.

Hancock, V., Dahl, M., and Klemm, P. (2010). Abolition of Biofilm Formation in Urinary Tract Escherichia coli and Klebsiella Isolates by Metal Interference through Competition for Fur. Appl Environ Microbiol *76*, 3836–3841.

Hancock, V., Witsø, I.L., and Klemm, P. (2011). Biofilm formation as a function of adhesin, growth medium, substratum and strain type. Int J Med Microbiol *301*, 570–576.

Hantke, K. (2001). Iron and metal regulation in bacteria. Current Opinion in Microbiology *4*, 172–177.

Hugot, J.P., Chamaillard, M., Zouali, H., Lesage, S., Cézard, J.P., Belaiche, J., Almer, S., Tysk, C., O'Morain, C.A., Gassull, M., et al. (2001). Association of NOD2 leucine-rich repeat variants with susceptibility to Crohn's disease. Nature *411*, 599–603.

Hung, C., Zhou, Y., Pinkner, J.S., Dodson, K.W., Crowley, J.R., Heuser, J., Chapman, M.R., Hadjifrangiskou, M., Henderson, J.P., and Hultgren, S.J. (2013). Escherichia coli Biofilms Have an Organized and Complex Extracellular Matrix Structure. mBio *4*, e00645–13–e00645–13.

James, B.W., Mauchline, W.S., Fitzgeorge, R.B., Dennis, P.J., and Keevil, C.W. (1995). Influence of iron-limited continuous culture on physiology and virulence of Legionella pneumophila. Infect Immun *63*, 4224–4230.

Kim, S.C., Tonkonogy, S.L., Albright, C.A., Tsang, J., Balish, E.J., Braun, J., Huycke, M.M., and Sartor, R.B. (2005). Variable phenotypes of enterocolitis in interleukin 10-deficient mice monoassociated with two different commensal bacteria. Gastroenterology *128*, 891–906.

Kim, S.C., Tonkonogy, S.L., Jarvis, H.W., Darfeuille-Michaud, A., and Sartor, R.B. (2008).

Escherichia coli Strains Differentially Induce Colitis in IL-10 Gene Deficient Mice. Gastroenterology *134*, A–23.

Kim, S.C., Tonkonogy, S.L., Karrasch, T., Jobin, C., and Sartor, R.B. (2007). Dual-association of gnotobiotic IL-10-/- mice with 2 nonpathogenic commensal bacteria induces aggressive pancolitis. Inflamm Bowel Dis *13*, 1457–1466.

Knights, D., Lassen, K.G., and Xavier, R.J. (2013). Advances in inflammatory bowel disease pathogenesis: linking host genetics and the microbiome. Gut *62*, 1505–1510.

Kortman, G.A.M., Boleij, A., Swinkels, D.W., and Tjalsma, H. (2012). Iron Availability Increases the Pathogenic Potential of Salmonella Typhimurium and Other Enteric Pathogens at the Intestinal Epithelial Interface. PLoS ONE *7*, e29968.

Kortman, G.A.M., Raffatellu, M., Swinkels, D.W., and Tjalsma, H. (2014). Nutritional iron turned inside out: intestinal stress from a gut microbial perspective. FEMS Microbiology Reviews.

Lapaquette, P., Glasser, A.-L., Huett, A., Xavier, R.J., and Darfeuille-Michaud, A. (2010). Crohn's disease-associated adherent-invasive E. coli are selectively favoured by impaired autophagy to replicate intracellularly. Cell. Microbiol. *12*, 99–113.

Larsen, S., Bendtzen, K., and Nielsen, O.H. (2010). Extraintestinal manifestations of inflammatory bowel disease: Epidemiology, diagnosis, and management. Ann Med *42*, 97–114.

Liu, B., Schmitz, J.M., Holt, L.C., Jarvis, W., Bringer, M.-A.S., Kim, S.C., Darfeuille-Michaud, A., and Sartor, R.B. (2009). Increased Intracellular Survival of E. coli NC101 Within Macrophages May Contribute to Its Ability to Induce Colitis. Gastroenterology *136*, A–704–704.

Lutz, M.B., Kukutsch, N., Ogilvie, A.L., Rössner, S., Koch, F., Romani, N., and Schuler, G. (1999). An advanced culture method for generating large quantities of highly pure dendritic cells from mouse bone marrow. J. Immunol. Methods *223*, 77–92.

Maharshak, N., Packey, C.D., Ellermann, M., Manick, S., Siddle, J.P., Huh, E.Y., Plevy, S., Sartor, R.B., and Carroll, I.M. (2013). Altered enteric microbiota ecology in interleukin 10-deficient mice during development and progression of intestinal inflammation. Gut Microbes *4*, 316–324.

Martin, H.M., Campbell, B.J., Hart, C.A., Mpofu, C., Nayar, M., Singh, R., Englyst, H., Williams, H.F., and Rhodes, J.M. (2004). Enhanced Escherichia coli adherence and invasion in Crohn's disease and colon cancer. Gastroenterology *127*, 80–93.

Martinez-Medina, M., Denizot, J., Dreux, N., Robin, F., Billard, E., Bonnet, R., Darfeuille-Michaud, A., and Barnich, N. (2013). Western diet induces dysbiosis with increased E coli in CEABAC10 mice, alters host barrier function favouring AIEC colonisation. Gut *63*, 116–124.

Martinez-Medina, M., Naves, P., Blanco, J., Aldeguer, X., Blanco, J.E., Blanco, M., Ponte, C., Soriano, F., Darfeuille-Michaud, A., and Garcia-Gil, L.J. (2009). Biofilm formation as a novel

phenotypic feature of adherent-invasive Escherichia coli (AIEC). BMC Microbiol. *9*, 202.

McHugh, J.P., Rodríguez-Quinoñes, F., Abdul-Tehrani, H., Svistunenko, D.A., Poole, R.K., Cooper, C.E., and Andrews, S.C. (2003). Global iron-dependent gene regulation in Escherichia coli. A new mechanism for iron homeostasis. J Biol Chem *278*, 29478–29486.

Monteiro, C., Saxena, I., Wang, X., Kader, A., Bokranz, W., Simm, R., Nobles, D., Chromek, M., Brauner, A., Brown, R.M., Jr, et al. (2009). Characterization of cellulose production in Escherichia coliNissle 1917 and its biological consequences. Environmental Microbiology *11*, 1105–1116.

Nagasawa, S., Ishige, K., and Mizuno, T. (1993). Novel members of the two-component signal transduction genes in Escherichia coli. J. Biochem. *114*, 350–357.

Nairz, M., Schroll, A., Sonnweber, T., and Weiss, G. (2010). The struggle for iron - a metal at the host-pathogen interface. Cell. Microbiol. *12*, 1691–1702.

Ogasawara, H., Shinohara, S., Yamamoto, K., and Ishihama, A. (2012). Novel regulation targets of the metal-response BasS-BasR two-component system of Escherichia coli. Microbiology (Reading, Engl.) *158*, 1482–1492.

Olsen, A., Arnqvist, A., Hammar, M., Sukupolvi, S., and Normark, S. (1993). The RpoS sigma factor relieves H-NS-mediated transcriptional repression of csgA, the subunit gene of fibronectin-binding curli in Escherichia coli. Mol Microbiol *7*, 523–536.

Omadjela, O., Narahari, A., Strumillo, J., Mélida, H., Mazur, O., Bulone, V., and Zimmer, J. (2013). BcsA and BcsB form the catalytically active core of bacterial cellulose synthase sufficient for in vitro cellulose synthesis. Proceedings of the National Academy of Sciences *110*, 17856–17861.

Patwa, L.G., Fan, T.-J., Tchaptchet, S., Liu, Y., Lussier, Y.A., Sartor, R.B., and Hansen, J.J. (2011). Chronic intestinal inflammation induces stress-response genes in commensal Escherichia coli. Gastroenterology *141*, 1842–51.e1–10.

Pontes, M.H., Lee, E.-J., Choi, J., and Groisman, E.A. (2015). Salmonella promotes virulence by repressing cellulose production. Proceedings of the National Academy of Sciences *112*, 5183–5188.

Raffatellu, M., George, M.D., Akiyama, Y., Hornsby, M.J., Nuccio, S.-P., Paixao, T.A., Butler, B.P., Chu, H., Santos, R.L., Berger, T., et al. (2009). Lipocalin-2 resistance confers an advantage to Salmonella enterica serotype Typhimurium for growth and survival in the inflamed intestine. Cell Host Microbe *5*, 476–486.

Raterman, E.L., Shapiro, D.D., Stevens, D.J., Schwartz, K.J., and Welch, R.A. (2013). Genetic analysis of the role of yfiR in the ability of Escherichia coli CFT073 to control cellular cyclic dimeric GMP levels and to persist in the urinary tract. Infect Immun *81*, 3089–3098.

Rowe, M.C., Withers, H.L., and Swift, S. (2010). Uropathogenic Escherichia coli forms biofilm

aggregates under iron restriction that disperse upon the supply of iron. FEMS Microbiol Lett *307*, 102–109.

Römling, U. (2005). Characterization of the rdar morphotype, a multicellular behaviour in Enterobacteriaceae. CMLS, Cell. Mol. Life Sci. *62*, 1234–1246.

Römling, U., Rohde, M., Olsen, A., Normark, S., and Reinköster, J. (2000). AgfD, the checkpoint of multicellular and aggregative behaviour in Salmonella typhimurium regulates at least two independent pathways. Mol Microbiol *36*, 10–23.

Römling, U., Sierralta, W.D., Eriksson, K., and Normark, S. (1998). Multicellular and aggregative behaviour of Salmonella typhimurium strains is controlled by mutations in the agfD promoter. Mol Microbiol *28*, 249–264.

Sadaghian Sadabad, M., Regeling, A., de Goffau, M.C., Blokzijl, T., Weersma, R.K., Penders, J., Faber, K.N., Harmsen, H.J.M., and Dijkstra, G. (2014). The ATG16L1-T300A allele impairs clearance of pathosymbionts in the inflamed ileal mucosa of Crohn's disease patients. Gut.

Saldaña, Z., Xicohtencatl-Cortes, J., Avelino, F., Phillips, A.D., Kaper, J.B., Puente, J.L., and Girón, J.A. (2009). Synergistic role of curli and cellulose in cell adherence and biofilm formation of attaching and effacing Escherichia coliand identification of Fis as a negative regulator of curli. Environmental Microbiology *11*, 992–1006.

Sartor, R.B. (2008). Microbial influences in inflammatory bowel diseases. Gastroenterology *134*, 577–594.

Schumann, S., Alpert, C., Engst, W., Klopfleisch, R., Loh, G., Bleich, A., and Blaut, M. (2013). Mild gut inflammation modulates the proteome of intestinal Escherichia coli. Environmental Microbiology *16*, 2966–2979.

Seo, S.W., Kim, D., Latif, H., O'Brien, E.J., Szubin, R., and Palsson, B.O. (2014). Deciphering Fur transcriptional regulatory network highlights its complex role beyond iron metabolism in Escherichia coli. Nature Communications *5*, 4910.

Serra, D.O., Richter, A.M., and Hengge, R. (2013). Cellulose as an architectural element in spatially structured Escherichia coli biofilms. J Bacteriol *195*, 5540–5554.

Small, C.-L.N., Reid-Yu, S.A., McPhee, J.B., and Coombes, B.K. (2013). Persistent infection with Crohn's disease-associated adherent-invasive Escherichia coli leads to chronic inflammation and intestinal fibrosis. Nature Communications *4*, 1957.

Solano, C., García, B., Valle, J., Berasain, C., Ghigo, J.-M., Gamazo, C., and Lasa, I. (2002). Genetic analysis of Salmonella enteritidis biofilm formation: critical role of cellulose. Mol Microbiol *43*, 793–808.

Spiliopoulou, A.I., Kolonitsiou, F., Krevvata, M.I., Leontsinidis, M., Wilkinson, T.S., Mack, D., and Anastassiou, E.D. (2012). Bacterial adhesion, intracellular survival and cytokine induction upon stimulation of mononuclear cells with planktonic or biofilm phase Staphylococcus

epidermidis. FEMS Microbiol Lett *330*, 56–65.

Spurbeck, R.R., Tarrien, R.J., and Mobley, H.L.T. (2012). Enzymatically active and inactive phosphodiesterases and diguanylate cyclases are involved in regulation of Motility or sessility in Escherichia coli CFT073. mBio *3*.

Stanley, E.R., and Heard, P.M. (1977). Factors regulating macrophage production and growth. Purification and some properties of the colony stimulating factor from medium conditioned by mouse L cells. J Biol Chem *252*, 4305–4312.

Steinbach, E.C., and Plevy, S.E. (2014). The Role of Macrophages and Dendritic Cells in the Initiation of Inflammation in IBD. Inflamm Bowel Dis *20*, 166–175.

Wang, X., Rochon, M., Lamprokostopoulou, A., Lünsdorf, H., Nimtz, M., and Römling, U. (2006). Impact of biofilm matrix components on interaction of commensal Escherichia coli with the gastrointestinal cell line HT-29. CMLS, Cell. Mol. Life Sci. *63*, 2352–2363.

White, A.P., Gibson, D.L., Grassl, G.A., Kay, W.W., Finlay, B.B., Vallance, B.A., and Surette, M.G. (2008). Aggregation via the Red, Dry, and Rough Morphotype Is Not a Virulence Adaptation in Salmonella enterica Serovar Typhimurium. Infect Immun *76*, 1048–1058.

Winter, S.E., Winter, M.G., Xavier, M.N., Thiennimitr, P., Poon, V., Keestra, A.M., Laughlin, R.C., Gomez, G., Wu, J., Lawhon, S.D., et al. (2013). Host-Derived Nitrate Boosts Growth of E. coli in the Inflamed Gut. Science *339*, 708–711.

Wise, A.J., Hogan, J.S., Cannon, V.B., and Smith, K.L. (2002). Phagocytosis and serum susceptibility of Escherichia coil cultured in iron-deplete and iron-replete media. J Dairy Sci *85*, 1454–1459.

Wösten, M.M., Kox, L.F., Chamnongpol, S., Soncini, F.C., and Groisman, E.A. (2000). A signal transduction system that responds to extracellular iron. Cell *103*, 113–125.

Wu, C.C., Lin, C.T., Cheng, W.Y., Huang, C.J., Wang, Z.C., and Peng, H.L. (2012). Fur-dependent MrkHI regulation of type 3 fimbriae in Klebsiella pneumoniae CG43. Microbiology (Reading, Engl.) *158*, 1045–1056.

Wu, X.-B., Tian, L.-H., Zou, H.-J., Wang, C.-Y., Yu, Z.-Q., Tang, C.-H., Zhao, F.-K., and Pan, J.-Y. (2013). Outer membrane protein OmpW of Escherichia coli is required for resistance to phagocytosis. Research in Microbiologoy *164*, 848–855.

Wu, Y., and Outten, F.W. (2009). IscR Controls Iron-Dependent Biofilm Formation in Escherichia coli by Regulating Type I Fimbria Expression. J Bacteriol *191*, 1248–1257.

Zogaj, X., Nimtz, M., Rohde, M., Bokranz, W., and Römling, U. (2001). The multicellular morphotypes of Salmonella typhimurium and Escherichia coli produce cellulose as the second component of the extracellular matrix. Mol Microbiol *39*, 1452–1463.

CHAPTER 5

CONCLUSIONS AND FUTURE PERSPECTIVES

5.1 Overview

IBD are chronic, intestinal, immune-mediated inflammatory disorders that are the result of inappropriate immune responses to a subset of resident enteric bacteria and their products (Sartor, 2008). Although the etiology is incompletely understood, complex interactions between genetics, environmental factors, and the intestinal microbiota are thought to contribute to the development and perpetuation of these diseases. Current IBD therapies such as immunosuppressive drugs can result in adverse side effects and are ineffective at inducing complete remission for many patients. Thus the development of safer and more effective treatment options are clearly needed.

IDA is one of the most common complications experienced by IBD patients (Kulnigg and Gasche, 2006). Oral iron supplementation can be effective in treating IDA and is often the first choice of treatment because of its convenience and low cost (Rizvi and Schoen, 2011) (Hwang et al., 2012). However, disease exacerbation has been reported in some IBD patients receiving oral iron supplementation (Erichsen et al., 2005b) (de Silva et al., 2005), although this has not been consistently reported in all clinical studies (Schröder et al., 2005) (Erichsen et al., 2005a) (Lee et al., 2012). Moreover, increased dietary iron consumption has been correlated with more severe histopathology and disease development in some rodent models of experimental colitis (Kulnigg

and Gasche, 2006) (Werner et al., 2011) (Chua et al., 2013). One hypothesis to explain how iron may exacerbate intestinal inflammation is through the increased production of ROS as a byproduct of the Fenton reaction. However, some resident enteric bacteria such as AIEC drive and perpetuate intestinal inflammation in genetically susceptible hosts (Kim et al., 2005) (Carvalho et al., 2009) (Carvalho et al., 2012). Moreover, iron is a limiting nutrient for the growth of many bacterial taxa and can also impact bacterial physiology and function (Andrews et al., 2003). Thus changing intestinal iron concentrations through dietary manipulations can conceivably modulate the composition and proinflammatory potential of the intestinal microbiota as a second putative mechanism for influencing colitis development. We therefore investigated how iron modulates the ecological structure of the intestinal microbiota and alters the physiology and proinflammatory potential of AIEC, a distinct functional pathotype of enteric resident *E. coli* associated with CD (Darfeuille-Michaud et al., 2004) (Martin et al., 2004) (Sasaki et al., 2007).

In inflammation-resistant WT mice, decreasing luminal iron concentrations during community assembly resulted in compositional changes to the intestinal microbiota consistent with a dysbiotic state, including decreased microbial richness and a bloom in the siderophilic resident bacterium *E. coli*. Indeed, we observed similar compositional changes in inflammation-susceptible *Il10*$^{-/-}$ mice during the development of intestinal inflammation in the absence of dietary iron interventions. When iron availability was restricted *in vitro*, inactivation of siderophore-mediated iron transport in an AIEC strain, *E. coli* NC101, reduced its relative fitness when grown in competition with a non-siderophilic intestinal bacterium. Thus encoding numerous iron acquisition systems may provide AIEC and other resident *E. coli* a competitive advantage when iron availability is limiting and may also explain the *in vivo* enrichment of *E. coli* with dietary iron restriction.

Because intestinal inflammation is associated with a relative expansion of *E. coli*, we also investigated the impact of dietary iron on colitis development in inflammation-prone *Il10*$^{-/-}$ mice. Although dietary iron supplementation limited colitis development in *Il10*$^{-/-}$ mice, this was not associated with distinct compositional changes to the luminal microbiota in comparison to mice on the control diet that developed the most severe colitis. However, differences in inflammation severity between the two diet groups were associated with minor compositional changes to the mucosal microbiota. Thus, the impact of iron on the mucosal community may contribute to the protective effect of dietary iron supplementation, especially given its closer proximity to the intestinal epithelial barrier and underlying mucosal immune system. Finally, our findings do not exclude the possibility that iron supplementation functionally alters the intestinal microbiota in a manner that limits colitis development. Indeed, utilizing the AIEC strain NC101 as a model organism, we demonstrated that iron promoted cellulose-dependent aggregation of NC101, which corresponded with an enhanced susceptibility to macrophage phagocytosis and reduced induction of macrophage proinflammatory cytokine production. Conversely, when bacterial iron availability was restricted, cellulose-positive NC101 exhibited increased resistance against phagocytosis while also promoting macrophage production of IL-12 p40. Abrogation of cellulose production also delayed NC101 induction of colitis in monoassociated *Il10*$^{-/-}$ mice and was associated with decreased colonic expression of IL-12, therefore suggesting that cellulose enhances the proinflammatory potential of NC101 in this model. Taken together, our findings suggest that decreasing microbial iron availability may enhance the proinflammatory potential of the intestinal microbiota and highlight the complex interplay between host, microbial and environmental factors in the development of IBD.

5.2 Longitudinal and long-term effects of dietary iron interventions

Our results demonstrate that dietary iron restriction and supplementation during community assembly alters the composition of the resulting intestinal microbiota. Specifically, dietary iron restriction during this developmental window seems to constrain maturation of the intestinal microbiota as indicated by decreased microbial richness and increased Proteobacteria compared to developing communities exposed to higher amounts of iron. However, the compositional impact of dietary iron to the intestinal microbiota was assessed at a single time point in adult ex-GF mice. Thus, longitudinal studies characterizing the impact of intestinal iron availability during community assembly in young mice following weaning need to be performed. Additionally, given that dietary macromolecules can rapidly impact the composition of the microbiota (David et al., 2013) (Carmody et al., 2015), it would be interesting to investigate how rapidly dietary iron interventions affects both a developing and an established microbiota and whether these changes are reproducible with consecutive periods of dietary iron restriction and repletion within the same host. Interestingly, Pereira and colleagues demonstrated that following a 4-week period of dietary iron restriction that was initiated at weaning, community composition was only partially restored through iron repletion after 4 weeks (Pereira et al., 2014). However, repletion was accomplished through administration of a diet that contained iron concentrations comparable to a control diet (Pereira et al., 2014). Thus it is remains to be determined whether repletion with an iron fortified diet can revert the microbial community to its original state following a period of dietary iron restriction.

Recent studies have highlighted the importance of an early microbiota developmental window to the health and physiology of the host through adulthood (Cox et al., 2014) (Subramanian et al., 2014) (Nobel et al., 2015). For example, early life exposure to antibiotics

not only perturbs the establishing community, but also results in negative metabolic consequences that are evident through adulthood (Cox et al., 2014). Therefore, because dietary iron restriction also appears to be a disruptive selective force for the developing microbiota, it would be worth investigating whether such early-life compositional changes result in long-lasting repercussions for the adult host. Indeed, recent studies have implicated the intestinal microbiota in modulating host iron status in colitic *Il10*$^{-/-}$ mice and IEC iron homeostasis in WT mice (Shanmugam et al., 2014) (Deschemin et al., 2015). Moreover, dietary iron restriction decreases fermentative metabolites such as butyrate in the intestines that have been shown to modulate numerous host processes including immune function (Waldecker et al., 2008) (Dostal et al., 2012a) (Berndt et al., 2012) (Smith et al., 2013) (Dostal et al., 2014). Together, this supports the possibility that iron-mediated effects on the microbiota may modulate certain aspects of host physiology and susceptibility to colitis development, effects that may endure through adulthood.

We also demonstrated that dietary iron supplementation during community assembly limits the development of colitis in *Il10*$^{-/-}$ mice. However, as onset of IBD also occurs in adults when the intestinal microbiota has already been established, it would be interesting to assess the impact of dietary iron interventions on colitis susceptibility in adult *Il10*$^{-/-}$ mice with a mature microbiota. Moreover, as only one time point was assessed for colitis severity, future studies will need to determine whether protection against colitis in mice receiving iron-fortified diets is prolonged or whether onset of disease is simply delayed.

Finally, to our knowledge, the impact of dietary iron interventions initiated after the onset of immune-mediated intestinal inflammation has not been assessed in rodent models. This is a clinically important avenue to explore given that IBD patients with active disease may also be

iron deficient. Moreover, dietary iron restriction seems to have a greater impact on the developing microbiota that is both compositionally unstable and more vulnerable to environmental disturbances (Koenig et al., 2011) (Cox et al., 2014). Similarly, because the inflammation-associated microbiota is also unstable (Martinez et al., 2008) and may be more prone to environmental perturbations such as changes in iron availability, assessing the impact of dietary iron interventions on the microbiota after inflammation has developed is an important future direction. Interestingly, in contrast to our findings, dietary iron supplementation in hosts with initial high pathogen burden, including enteric pathogens belonging to the Enterobacteriaceae family, was associated with enhanced fecal markers of inflammation and further promoted a bloom of both endogenous and pathogenic Enterobacteriaceae in infants (Jaeggi et al., 2014). Thus, the impact of dietary iron supplementation on both community composition and inflammation susceptibility may also be dependent on the initial state of the intestinal microbiota and is worth delineating in future studies. In the context of IBD, this could ultimately lead to the identification of prognostic fecal markers that could be utilized in the clinic to identify patients who are at risk for disease relapse or exacerbation in response to oral iron supplementation.

5.3 The functional impact of iron on the intestinal microbiome

The composition of the intestinal microbiota exhibits high interindividual variability (Costello et al., 2009), which is likely affected by host genetics, long-term dietary patterns, environmental factors and stochastic influences. Thus, in addition to differences in experimental design, the high interindividual variability of the intestinal microbiota may in part explain the lack of consistent compositional changes observed in response to dietary iron restriction or

supplementation between different rodent studies. Indeed even within the same housing facility, in contrast to WT mice, we show that the composition of the fecal microbiota in *Il10*$^{-/-}$ mice is insensitive to additional dietary iron supplementation, suggesting that host genetics may influence the impact of dietary iron supplementation on the microbiota. Consistent with these observations, high interindividual variability was also reported in infant studies examining the impact of dietary iron supplementation on the fecal microbiota (Krebs et al., 2013) (Jaeggi et al., 2014). Thus, using metabolomics and meta-transcriptomics to assess community-wide functional alterations may identify more conserved changes in response to dietary iron interventions. Indeed, when measuring targeted SCFAs, Dostal and colleagues showed that increasing bacterial iron availability enhances the production of propionate and butyrate by the intestinal community in two different rodent models and when using an *in vitro* colonic fermentation model (Dostal et al., 2012a) (Dostal et al., 2012b) (Dostal et al., 2014). Moreover, shifts in the intestinal microbiome have been reported in the absence of significant compositional changes (McNulty et al., 2011), further highlighting the importance of conducting metabolomic or transcriptomic microbiome studies in response to dietary iron. Community-wide functional changes may also explain how dietary iron supplementation limited colitis development in *Il10*$^{-/-}$ mice in the absence of significant compositional changes to the luminal microbiota. Finally, the functional profiles of the human intestinal microbiota are more similar between individuals compared to compositional profiles (Lozupone et al., 2012) and may therefore be more sensitive in detecting consistent alterations in response to specific diets or pathological states. Thus, investigating the functional impact of dietary iron interventions could provide a more definitive answer regarding the important clinical concern over the safety of oral iron supplementation within specific population subsets including IBD patients.

5.4 The redundancy of iron acquisition in AIEC

AIEC strains encode redundant pathways for acquiring iron including siderophore biosynthetic and transport systems, heme iron importers and ferrous iron permeases (Andrews et al., 2003) (Dogan et al., 2014). This heavy genomic investment in iron acquisition may confer AIEC and other endogenous *E. coli* a fitness advantage within the intestinal environment. Indeed, iron acquisition through the ferrous iron permease FeoB is required for colonization of the intestines by an *E. coli* K12 strain (Stojiljkovic et al., 1993). We and others have also shown that decreasing intestinal iron availability promotes a bloom of endogenous Enterobacteriaceae including *E. coli* (Dostal et al., 2012a). Similarly, in the inflamed environment where iron availability is likely decreased (Deriu et al., 2013), both probiotic and pathogenic members of the Enterobacteriaceae family rely on iron acquisition systems to outcompete other members of the community and to thrive within this intestinal environment (Deriu et al., 2013) (Behnsen et al., 2014). Given that AIEC strains are recovered in higher abundance from CD patients compared to non-CD controls (Martin et al., 2004), it is tempting to speculate that encoding numerous iron acquisition systems contributes to AIEC fitness within the inflamed environment, a hypothesis that warrants further exploration.

The GI tract is home to a heterogeneous collection of potential microbial niches, where distinct bacterial communities reside within the lumen, the mucosa, and longitudinally along the GI tract (Zoetendal et al., 2002) (Eckburg et al., 2005) (Zhang et al., 2014). Availability of nutrients such as iron likely varies throughout the intestines (Kortman et al., 2014) and may therefore serve as a selective force in shaping community dynamics within each site. Gradients of bacterial iron availability likely exist within the intestines, where maximal iron concentrations

are likely found in the lumen and decreases towards the mucosa as a result of host iron binding proteins present within mucosal secretions (Kortman et al., 2014). Thus encoding numerous ways to acquire iron may provide AIEC strains the ability to thrive within distinct intestinal microenvironments. Consistent with this idea, in an UPEC strain, maximal production of specific siderophores depends on several environmental factors including pH, oxygenation and availability of other nutrients (Valdebenito et al., 2006). Each iron acquisition system may therefore uniquely maximize AIEC fitness within a specific microenvironment, while also providing resilience in the face of changing environmental conditions such as the development of inflammation. Thus, it would be interesting to investigate the contribution of each iron acquisition system to the fitness of AIEC within specific microenvironments in both the inflamed and non-inflamed intestines. More broadly, quantifying the expression of iron acquisition genes within specific intestinal niches in conjunction with defining their contribution to *E. coli* fitness may serve as an indicator for the spatial bioavailability of iron for *E. coli* along the GI tract.

AIEC strains may also encode diverse iron acquisition systems as a means to sense and functionally adapt to their local environment. Genes involved in scavenging iron are transcriptionally upregulated when intracellular iron concentrations are decreased, a cellular state that is sensed by the transcription factor Fur (Andrews et al., 2003). Given the likely variability of bacterial iron availability within the intestines, it is possible that AIEC may utilize Fur to sense its location within the intestines (i.e. lumen versus mucosa) and adapt accordingly to its microenvironment. Indeed, in addition to iron acquisition genes, Fur regulates the expression of genes involved in diverse physiological processes including biofilm formation and motility (McHugh et al., 2003) (Seo et al., 2014). This provides a transcriptional mechanism by which sensing of the local environment by Fur can lead to the modulation of AIEC physiology, function

and subsequent host-microbial interactions. Indeed, we show that Fur is required for maximal aggregation of an AIEC strain in response to iron, which in turn impacts AIEC susceptibility to phagocytosis. Finally, as each iron acquisition system in *E. coli* may be preferentially expressed under specific environmental conditions (Valdebenito et al., 2006), the regulation of these systems is likely complex and involves other factors in addition to Fur. For example, there is evidence that in addition to its role in chelating ferric iron from the external environment, the yersiniabactin-iron complex may also exhibit signaling capabilities in *Yersinia spp.* through interactions with transcriptional regulators like YbtA (Perry and Fetherston, 2011). These additional signaling inputs may further refine the ability of AIEC to sense its local environment and enable more finely tuned physiological and functional responses within a specific intestinal microenvironment.

5.5 AIEC cellulose production in the intestines

Cellulose is an exopolysaccharide produced by some *E. coli* strains as part of the ECM within multicellular communities including biofilms and bacterial aggregates (Bokranz, 2005) (Saldaña et al., 2009) (Serra et al., 2013) (Depas et al., 2013). Definitively demonstrating cellulose production within the intestines by *E. coli* or other Enterobacteriaceae family members is challenging because of the mechanism by which cellulose production is regulated and because of its biochemical structure. Measuring protein or transcript levels of bacterial cellulose synthase (BcsA) or other genes within the *bcs* operon is not meaningful given the post-translational regulation of bacterial cellulose production. Biochemical approaches on the other hand rely on hydrolysis of cellulose and detection of glucose monomers using mass spectrometry (Zogaj et al., 2001) (Bokranz, 2005). Using this same approach to detect bacterial cellulose production in

intestinal samples is difficult because of the presence of plant cellulose in the diet, which is chemically indistinguishable from bacterial cellulose. Utilizing the Calcofluor fluorochrome to detect cellulose-positive bacteria in intestinal samples poses a similar issue as Calcofluor can also intercalate plant cellulose and other complex polysaccharides likely present in the lumen. Thus, most studies to date have relied on cellulose-deficient mutants to interrogate the contribution of cellulose production to *in vivo* fitness and virulence potential of Enterobacteriaceae family members. Nonetheless, using confocal microscopy, Pontes and colleagues have recently shown that *Salmonella* biosynthesis of cellulose occurs within the phagolysosome of a macrophage cell line (Pontes et al., 2015). This is the first study to our knowledge that has demonstrated cellulose production by Enterobacteriaceae when interacting with host cells and provides direct evidence that bacterial cellulose production occurs within host environments.

Our study is the first to our knowledge to investigate the contribution of cellulose production to the proinflammatory potential of resident *E. coli* within the intestinal environment. We demonstrate that abrogating cellulose production in the AIEC strain NC101 delays onset of colitis when monoassociated in *Il10*$^{-/-}$ mice. However, the precise mechanism by which NC101 cellulose production enhances colitis induction in this model remains to be elucidated. Our *in vitro* work suggests that under iron limiting conditions, cellulose may provide NC101 resistance against mucosal clearance by macrophages while also promoting enhanced production of the Th-1/Th-17-associated proinflammatory cytokine IL-12 p40. However, future studies will need to confirm this putative mechanism *in vivo.* Consistent with our findings, in an UTI model of infection, abrogation of cellulose production also reduced UPEC resistance against neutrophils *in vivo* (Kai-Larsen et al., 2010). Given that extrusion of neutrophils into the lumen occurs as part

of the innate immune response and has been shown to contain resident Enterobacteriaceae within the lumen during enteric infection (Molloy et al., 2013), it is tempting to speculate that cellulose production may also protect AIEC against the antimicrobial responses of neutrophils. Finally, as our *in vivo* studies were conducted in monoassociated mice, an important future direction will be to determine whether AIEC cellulose production impacts the development of colitis in the presence of a complex microbial community.

More broadly, cellulose may also enhance the ability of intestinal *E. coli* strains to adapt to distinct microenvironments by adopting a different physiological state in response to specific environmental stimuli. Cellulose production is post-transcriptionally regulated by c-di-GMP and intracellular concentrations of this second bacterial messenger in *E. coli* is modulated through the enzymatic activities of numerous putative DGCs and PDEs (Spurbeck et al., 2012). This provides the potential for distinct environmental stimuli to modulate cellulose production through transcriptional regulation of these enzymes. For example, expression of *adrA,* which encodes a DGC that is required for cellulose production in many *Salmonella* and *E. coli* strains, is positively regulated by the transcription factor CsgD (Römling et al., 2000) (Zogaj et al., 2001) (García et al., 2004). The *csgD* locus is directly downstream of a congested promoter region that serves as a signaling node for numerous transcription factors (Prigent-Combaret et al., 2001) (Gerstel et al., 2003). Indeed, oxygenation and nutrient availability have been shown to modulate the expression of CsgD and consequent cellulose-dependent multicellular behaviors (Gerstel and Römling, 2001), therefore demonstrating that distinct environmental stimuli can modulate bacterial physiology in a cellulose-dependent manner.

Interestingly, cellulose production at the physiological temperature of 37°C is more common in fecal rather than uropathogenic *E. coli* isolates (Bokranz, 2005), suggesting that

resident intestinal *E. coli* may synthesize cellulose within the intestinal environment. Moreover, environmental stimuli likely present in the intestines, such as peroxide stress and IgA monoclonal antibodies, have been shown to stimulate cellulose production and cellulose-dependent multicellular behaviors in Enterobacteriaceae (Amarasinghe et al., 2013) (Depas et al., 2013), suggesting that cellulose production may confer a fitness advantage in the gut. Thus, it would be interesting to determine whether cellulose production is more common in AIEC versus non-AIEC intestinal strains and to identify the environmental factors such as iron availability that stimulate cellulose production and cellulose-dependent behaviors such as aggregation in other AIEC isolates. Such studies could also provide mechanistic insight for how cellulose may modulate host-bacterial interactions and the proinflammatory potential of AIEC strains.

5.6 Conclusion

Epidemiological studies have correlated dietary factors with increased risk for disease development, exacerbation and relapse in IBD patients. Iron is of particular interest because of the clinical concern of disease exacerbation with oral iron supplementation. Moreover, iron can selectively modulate the growth, physiology and function of numerous bacterial taxa. Our findings demonstrate that iron profoundly impacts the ecological structure of the intestinal microbiota. Iron also modulates the physiology and proinflammatory potential of AIEC, demonstrating the importance of identifying functional alterations to the intestinal microbiota that potentially compromise its symbiotic relationship with the host. Taken together, these studies contribute towards our understanding of how dietary factors and local bacterial nutrient availability modulates host-microbial interactions and could ultimately lead to the identification of novel antimicrobial targets for IBD.

REFERENCES

Amarasinghe, J.J., D'Hondt, R.E., Waters, C.M., and Mantis, N.J. (2013). Exposure of Salmonella enterica Serovar Typhimurium to a Protective Monoclonal IgA Triggers Exopolysaccharide Production via a Diguanylate Cyclase-Dependent Pathway. Infect Immun *81*, 653–664.

Andrews, S.C., Robinson, A.K., and Rodrã guez-Quiã Ones, F. (2003). Bacterial iron homeostasis. FEMS Microbiology Reviews *27*, 215–237.

Behnsen, J., Jellbauer, S., Wong, C.P., Edwards, R.A., George, M.D., Ouyang, W., and Raffatellu, M. (2014). The Cytokine IL-22 Promotes Pathogen Colonization by Suppressing Related Commensal Bacteria. Immunity *40*, 262–273.

Berndt, B.E., Zhang, M., Owyang, S.Y., Cole, T.S., Wang, T.W., Luther, J., Veniaminova, N.A., Merchant, J.L., Chen, C.C., Huffnagle, G.B., et al. (2012). Butyrate increases IL-23 production by stimulated dendritic cells. AJP: Gastrointestinal and Liver Physiology *303*, G1384–G1392.

Bokranz, W. (2005). Expression of cellulose and curli fimbriae by Escherichia coli isolated from the gastrointestinal tract. Journal of Medical Microbiology *54*, 1171–1182.

Carmody, R.N., Gerber, G.K., Luevano, J.M., Jr, Gatti, D.M., Somes, L., Svenson, K.L., and Turnbaugh, P.J. (2015). Diet Dominates Host Genotypein Shaping the Murine Gut Microbiota. Cell Host Microbe *17*, 72–84.

Carvalho, F.A., Barnich, N., Sivignon, A., Darcha, C., Chan, C.H.F., Stanners, C.P., and Darfeuille-Michaud, A. (2009). Crohn's disease adherent-invasive Escherichia coli colonize and induce strong gut inflammation in transgenic mice expressing human CEACAM. J. Exp. Med. *206*, 2179–2189.

Carvalho, F.A., Koren, O., Goodrich, J.K., Johansson, M.E.V., Nalbantoglu, I., Aitken, J.D., Su, Y., Chassaing, B., Walters, W.A., González, A., et al. (2012). Transient inability to manage proteobacteria promotes chronic gut inflammation in TLR5-deficient mice. Cell Host Microbe *12*, 139–152.

Chua, A.C.G., Klopcic, B.R.S., Ho, D.S., Fu, S.K., Forrest, C.H., Croft, K.D., Olynyk, J.K., Lawrance, I.C., and Trinder, D. (2013). Dietary Iron Enhances Colonic Inflammation and IL-6/IL-11-Stat3 Signaling Promoting Colonic Tumor Development in Mice. PLoS ONE *8*, e78850.

Costello, E.K., Lauber, C.L., Hamady, M., Fierer, N., Gordon, J.I., and Knight, R. (2009). Bacterial community variation in human body habitats across space and time. Science *326*, 1694–1697.

Cox, L.M., Yamanishi, S., Sohn, J., Alekseyenko, A.V., Leung, J.M., Cho, I., Kim, S.G., Li, H., Gao, Z., Mahana, D., et al. (2014). Altering the Intestinal Microbiotaduring a Critical Developmental Window Has Lasting Metabolic Consequences. Cell *158*, 705–721.

Darfeuille-Michaud, A., Boudeau, J., Bulois, P., Neut, C., Glasser, A.-L., Barnich, N., Bringer, M.-A., Swidsinski, A., Beaugerie, L., and Colombel, J.-F. (2004). High prevalence of adherent-invasive Escherichia coli associated with ileal mucosa in Crohn's disease. Gastroenterology *127*, 412–421.

David, L.A., Maurice, C.F., Carmody, R.N., Gootenberg, D.B., Button, J.E., Wolfe, B.E., Ling, A.V., Devlin, A.S., Varma, Y., Fischbach, M.A., et al. (2013). Diet rapidly and reproducibly alters the human gut microbiome. Nature *505*, 559–563.

de Silva, A.D., Tsironi, E., Feakins, R.M., and Rampton, D.S. (2005). Efficacy and tolerability of oral iron therapy in inflammatory bowel disease: a prospective, comparative trial. Aliment Pharmacol Ther *22*, 1097–1105.

Depas, W.H., Hufnagel, D.A., Lee, J.S., Blanco, L.P., Bernstein, H.C., Fisher, S.T., James, G.A., Stewart, P.S., and Chapman, M.R. (2013). Iron induces bimodal population development by Escherichia coli. Proceedings of the National Academy of Sciences *110*, 2629–2634.

Deriu, E., Liu, J.Z., Pezeshki, M., Edwards, R.A., Ochoa, R.J., Contreras, H., Libby, S.J., Fang, F.C., and Raffatellu, M. (2013). Probiotic Bacteria Reduce Salmonella Typhimurium Intestinal Colonization by Competing for Iron. Cell Host Microbe *14*, 26–37.

Deschemin, J.C., Noordine, M.L., Remot, A., Willemetz, A., Afif, C., Canonne-Hergaux, F., Langella, P., Karim, Z., Vaulont, S., Thomas, M., et al. (2015). The microbiota shifts the iron sensing of intestinal cells. The FASEB Journal.

Dogan, B., Suzuki, H., Herlekar, D., Sartor, R.B., Campbell, B.J., Roberts, C.L., Stewart, K., Scherl, E.J., Araz, Y., Bitar, P.P., et al. (2014). Inflammation-associated adherent-invasive Escherichia coli are enriched in pathways for use of propanediol and iron and M-cell translocation. Inflamm Bowel Dis *20*, 1919–1932.

Dostal, A., Chassard, C., Hilty, F.M., Zimmermann, M.B., Jaeggi, T., Rossi, S., and Lacroix, C. (2012a). Iron depletion and repletion with ferrous sulfate or electrolytic iron modifies the composition and metabolic activity of the gut microbiota in rats. Journal of Nutrition *142*, 271–277.

Dostal, A., Fehlbaum, S., Chassard, C., Zimmermann, M.B., and Lacroix, C. (2012b). Low iron availability in continuous in vitrocolonic fermentations induces strong dysbiosis of the child gut microbial consortium and a decrease in main metabolites. FEMS Microbiol. Ecol. *83*, 161–175.

Dostal, A., Lacroix, C., Pham, V.T., Zimmermann, M.B., Del'homme, C., Bernalier-Donadille, A., and Chassard, C. (2014). Iron supplementation promotes gut microbiota metabolic activity but not colitis markers in human gut microbiota-associated rats. Br J Nutr *111*, 2135–2145.

Eckburg, P.B., Bik, E.M., Bernstein, C.N., Purdom, E., Dethlefsen, L., Sargent, M., Gill, S.R., Nelson, K.E., and Relman, D.A. (2005). Diversity of the human intestinal microbial flora. Science *308*, 1635–1638.

Erichsen, K., Ulvik, R.J., Grimstad, T., Berstad, A., Berge, R.K., and Hausken, T. (2005a).

Effects of ferrous sulphate and non-ionic iron-polymaltose complex on markers of oxidative tissue damage in patients with inflammatory bowel disease. Aliment Pharmacol Ther *22*, 831–838.

Erichsen, K., Ulvik, R.J., Nysaeter, G., Johansen, J., Ostborg, J., Berstad, A., Berge, R.K., and Hausken, T. (2005b). Oral ferrous fumarate or intravenous iron sucrose for patients with inflammatory bowel disease. Scand J Gastroenterol *40*, 1058–1065.

García, B., Latasa, C., Solano, C., Portillo, F.G.-D., Gamazo, C., and Lasa, I. (2004). Role of the GGDEF protein family in Salmonella cellulose biosynthesis and biofilm formation. Mol Microbiol *54*, 264–277.

Gerstel, U., and Römling, U. (2001). Oxygen tension and nutrient starvation are major signals that regulate agfD promoter activity and expression of the multicellular morphotype in Salmonella typhimurium. Environmental Microbiology *3*, 638–648.

Gerstel, U., Park, C., and Römling, U. (2003). Complex regulation of csgD promoter activity by global regulatory proteins. Mol Microbiol *49*, 639–654.

Hwang, C., Ross, V., and Mahadevan, U. (2012). Micronutrient deficiencies in inflammatory bowel disease: From A to zinc. Inflamm Bowel Dis *18*, 1961–1981.

Jaeggi, T., Kortman, G.A.M., Moretti, D., Chassard, C., Holding, P., Dostal, A., Boekhorst, J., Timmerman, H.M., Swinkels, D.W., Tjalsma, H., et al. (2014). Iron fortification adversely affects the gut microbiome, increases pathogen abundance and induces intestinal inflammation in Kenyan infants. Gut.

Kai-Larsen, Y., Lüthje, P., Chromek, M., Peters, V., Wang, X., Holm, Å., Kádas, L., Hedlund, K.-O., Johansson, J., Chapman, M.R., et al. (2010). Uropathogenic Escherichia coli Modulates Immune Responses and Its Curli Fimbriae Interact with the Antimicrobial Peptide LL-37. PLoS Pathog. *6*, e1001010.

Kim, S.C., Tonkonogy, S.L., Albright, C.A., Tsang, J., Balish, E.J., Braun, J., Huycke, M.M., and Sartor, R.B. (2005). Variable phenotypes of enterocolitis in interleukin 10-deficient mice monoassociated with two different commensal bacteria. Gastroenterology *128*, 891–906.

Koenig, J.E., Spor, A., Scalfone, N., Fricker, A.D., Stombaugh, J., Knight, R., Angenent, L.T., and Ley, R.E. (2011). Succession of microbial consortia in the developing infant gut microbiome. Proc Natl Acad Sci USA *108 Suppl 1*, 4578–4585.

Kortman, G.A.M., Raffatellu, M., Swinkels, D.W., and Tjalsma, H. (2014). Nutritional iron turned inside out: intestinal stress from a gut microbial perspective. FEMS Microbiology Reviews.

Krebs, N.F., Sherlock, L.G., Westcott, J., Culbertson, D., Hambidge, K.M., Feazel, L.M., Robertson, C.E., and Frank, D.N. (2013). Effects of Different Complementary Feeding Regimens on Iron Status and Enteric Microbiota in Breastfed Infants. J. Pediatr. *163*, 416–423.e4.

Kulnigg, S., and Gasche, C. (2006). Systematic review: managing anaemia in Crohn's disease. Aliment Pharmacol Ther *24*, 1507–1523.

Lee, T.W., Kolber, M.R., Fedorak, R.N., and van Zanten, S.V. (2012). Iron replacement therapy in inflammatory bowel disease patients with iron deficiency anemia: A systematic review and meta-analysis. Journal of Crohn's and Colitis *6*, 267–275.

Lozupone, C.A., Stombaugh, J.I., Gordon, J.I., Jansson, J.K., and Knight, R. (2012). Diversity, stability and resilience of the human gut microbiota. Nature *489*, 220–230.

Martin, H.M., Campbell, B.J., Hart, C.A., Mpofu, C., Nayar, M., Singh, R., Englyst, H., Williams, H.F., and Rhodes, J.M. (2004). Enhanced Escherichia coli adherence and invasion in Crohn's disease and colon cancer. Gastroenterology *127*, 80–93.

Martinez, C., Antolín, M., Santos, J., Torrejon, A., Casellas, F., Borruel, N., Guarner, F., and Malagelada, J.-R. (2008). Unstable Composition of the Fecal Microbiota in Ulcerative Colitis During Clinical Remission. Am J Gastroenterology *103*, 643–648.

McHugh, J.P., Rodríguez-Quinoñes, F., Abdul-Tehrani, H., Svistunenko, D.A., Poole, R.K., Cooper, C.E., and Andrews, S.C. (2003). Global iron-dependent gene regulation in Escherichia coli. A new mechanism for iron homeostasis. J Biol Chem *278*, 29478–29486.

McNulty, N.P., Yatsunenko, T., Hsiao, A., Faith, J.J., Muegge, B.D., Goodman, A.L., Henrissat, B., Oozeer, R., Cools-Portier, S., Gobert, G., et al. (2011). The Impact of a Consortium of Fermented Milk Strains on the Gut Microbiome of Gnotobiotic Mice and Monozygotic Twins. Sci Transl Med *3*, 106ra106–106ra106.

Molloy, M.J., Grainger, J.R., Bouladoux, N., Hand, T.W., Koo, L.Y., Naik, S., Quinones, M., Dzutsev, A.K., Gao, J.-L., Trinchieri, G., et al. (2013). Intraluminal Containment of Commensal Outgrowth in the Gut during Infection-Induced Dysbiosis. Cell Host Microbe *14*, 318–328.

Nobel, Y.R., Cox, L.M., Kirigin, F.F., Bokulich, N.A., Yamanishi, S., Teitler, I., Chung, J., Sohn, J., Barber, C.M., Goldfarb, D.S., et al. (2015). Metabolic and metagenomic outcomes from early-life pulsed antibiotic treatment. Nature Communications *6*, 1–15.

Pereira, D.I.A., Aslam, M.F., Frazer, D.M., Schmidt, A., Walton, G.E., McCartney, A.L., Gibson, G.R., Anderson, G.J., and Powell, J.J. (2014). Dietary iron depletion at weaning imprints low microbiome diversity and this is not recovered with oral nano Fe(III). Microbiology Open *4*, 12–27.

Perry, R.D., and Fetherston, J.D. (2011). Yersiniabactin iron uptake: mechanisms and role in Yersinia pestis pathogenesis. Microbes and Infection *13*, 808–817.

Pontes, M.H., Lee, E.-J., Choi, J., and Groisman, E.A. (2015). Salmonella promotes virulence by repressing cellulose production. Proceedings of the National Academy of Sciences *112*, 5183–5188.

Prigent-Combaret, C., Brombacher, E., Vidal, O., Ambert, A., Lejeune, P., Landini, P., and

Dorel, C. (2001). Complex regulatory network controls initial adhesion and biofilm formation in Escherichia coli via regulation of the csgD gene. J Bacteriol *183*, 7213–7223.

Rizvi, S., and Schoen, R.E. (2011). Supplementation with oral vs. intravenous iron for anemia with IBD or gastrointestinal bleeding: is oral iron getting a bad rap? Am J Gastroenterology *106*, 1872–1879.

Römling, U., Rohde, M., Olsen, A., Normark, S., and Reinköster, J. (2000). AgfD, the checkpoint of multicellular and aggregative behaviour in Salmonella typhimurium regulates at least two independent pathways. Mol Microbiol *36*, 10–23.

Saldaña, Z., Xicohtencatl-Cortes, J., Avelino, F., Phillips, A.D., Kaper, J.B., Puente, J.L., and Girón, J.A. (2009). Synergistic role of curli and cellulose in cell adherence and biofilm formation of attaching and effacing Escherichia coliand identification of Fis as a negative regulator of curli. Environmental Microbiology *11*, 992–1006.

Sartor, R.B. (2008). Microbial influences in inflammatory bowel diseases. Gastroenterology *134*, 577–594.

Sasaki, M., Sitaraman, S.V., Babbin, B.A., Gerner-Smidt, P., Ribot, E.M., Garrett, N., Alpern, J.A., Akyildiz, A., Theiss, A.L., Nusrat, A., et al. (2007). Invasive Escherichia coli are a feature of Crohn's disease. Lab. Invest. *87*, 1042–1054.

Schröder, O., Mickisch, O., Seidler, U., de Weerth, A., Dignass, A.U., Herfarth, H., Reinshagen, M., Schreiber, S., Junge, U., Schrott, M., et al. (2005). Intravenous iron sucrose versus oral iron supplementation for the treatment of iron deficiency anemia in patients with inflammatory bowel disease--a randomized, controlled, open-label, multicenter study. Am J Gastroenterology *100*, 2503–2509.

Seo, S.W., Kim, D., Latif, H., O'Brien, E.J., Szubin, R., and Palsson, B.O. (2014). Deciphering Fur transcriptional regulatory network highlights its complex role beyond iron metabolism in Escherichia coli. Nature Communications *5*, 4910.

Serra, D.O., Richter, A.M., and Hengge, R. (2013). Cellulose as an architectural element in spatially structured Escherichia coli biofilms. J Bacteriol *195*, 5540–5554.

Shanmugam, N.K.N., Trebicka, E., Fu, L.L., Shi, H.N., and Cherayil, B.J. (2014). Intestinal Inflammation Modulates Expression of the Iron-Regulating Hormone Hepcidin Depending on Erythropoietic Activity and the Commensal Microbiota. The Journal of Immunology *193*, 1398–1407.

Smith, P.M., Howitt, M.R., Panikov, N., Michaud, M., Gallini, C.A., Bohlooly-Y, M., Glickman, J.N., and Garrett, W.S. (2013). The Microbial Metabolites, Short-Chain Fatty Acids, Regulate Colonic Treg Cell Homeostasis. Science *341*, 569–573.

Spurbeck, R.R., Tarrien, R.J., and Mobley, H.L.T. (2012). Enzymatically active and inactive phosphodiesterases and diguanylate cyclases are involved in regulation of Motility or sessility in Escherichia coli CFT073. mBio *3*.

Stojiljkovic, I., Cobeljic, M., and Hantke, K. (1993). Escherichia coli K-12 ferrous iron uptake mutants are impaired in their ability to colonize the mouse intestine. FEMS Microbiol Lett *108*, 111–115.

Subramanian, S., Huq, S., Yatsunenko, T., Haque, R., Mahfuz, M., Alam, M.A., Benezra, A., DeStefano, J., Meier, M.F., Muegge, B.D., et al. (2014). Persistent gut microbiota immaturity in malnourished Bangladeshi children. Nature.

Valdebenito, M., Crumbliss, A.L., Winkelmann, G., and Hantke, K. (2006). Environmental factors influence the production of enterobactin, salmochelin, aerobactin, and yersiniabactin in Escherichia coli strain Nissle 1917. Int J Med Microbiol *296*, 513–520.

Waldecker, M., Kautenburger, T., Daumann, H., Busch, C., and Schrenk, D. (2008). Inhibition of histone-deacetylase activity by short-chain fatty acids and some polyphenol metabolites formed in the colon. J. Nutr. Biochem. *19*, 587–593.

Werner, T., Wagner, S.J., Martínez, I., Walter, J., Chang, J.-S., Clavel, T., Kisling, S., Schuemann, K., and Haller, D. (2011). Depletion of luminal iron alters the gut microbiota and prevents Crohn's disease-like ileitis. Gut *60*, 325–333.

Zhang, Z., Geng, J., Tang, X., Fan, H., Xu, J., Wen, X., Ma, Z.S., and Shi, P. (2014). Spatial heterogeneity and co-occurrence patterns of human mucosal-associated intestinal microbiota. Isme J *8*, 881–893.

Zoetendal, E.G., Wright, von, A., Vilpponen-Salmela, T., Ben-Amor, K., Akkermans, A.D.L., and de Vos, W.M. (2002). Mucosa-Associated Bacteria in the Human Gastrointestinal Tract Are Uniformly Distributed along the Colon and Differ from the Community Recovered from Feces. Appl Environ Microbiol *68*, 3401–3407.

Zogaj, X., Nimtz, M., Rohde, M., Bokranz, W., and Römling, U. (2001). The multicellular morphotypes of Salmonella typhimurium and Escherichia coli produce cellulose as the second component of the extracellular matrix. Mol Microbiol *39*, 1452–1463.